2007

Chemical differences of atherosclerotic plaques in native and bypass human coronary arteries and diseased and non-diseased human aortas

Samuel Jean Washington
Louisiana State University and Agricultural and Mechanical College, swashi1@lsu.edu

CHEMICAL DIFFERENCES OF ATHEROSCLEROTIC PLAQUES IN NATIVE AND BYPASS HUMAN CORONARY ARTERIES AND DISEASED AND NON-DISEASED HUMAN AORTAS

A Dissertation

Submitted to the Graduate Faculty of the
Louisiana State University and
Agriculture and Mechanical College
in partial fulfillment of the
requirements for the degree of
Doctor of Philosophy

in

The Department of Chemistry

By
Samuel Jean Washington
B.S. Northeast Louisiana University, 1973
M.S. University of Nebraska-Lincoln, 1978
May 2007

DEDICATION

I want to dedicate this work to my patient and loving wife, Louella. You gave me constant encouragement to accomplish the one goal that I have desired for over thirty years. You consistently reminded me of how faith works and to continually walk in that realm. Acquiring knowledge has no age or boundaries and life is too short not to make the most of it. Thank you Lou, you have been a blessing to me in this life.

ACKNOWLEDGEMENTS

The author wishes to thank **Dr. Isiah Warner** for his guidance and mentoring in attempting an advanced degree, **Dr. Patrick Limbach** for not giving up on me despite his decision to explore other opportunities, and **Dr. James Robinson** for his patience and encouragement.

Special thanks to my parents, **Shelton and Lillian Blunt**, for the wisdom and prayers that never let me quit and to my 14 siblings for all their support.

Thanks to all my friends and associates at the Center for Energy and Environmental Studies at Southern University. I would also to thank **Dr. Paul Turner** and **Dr. Michael Stubblefield** for their support and for giving me the opportunity to complete this study.

I would like to thank **Dr. Jack Losso** for all his assistance in understanding protein separations. Additional thanks and appreciation to **Dr. Sayo Fakayode, Dr. Mark Lowry**, **Dr. Kristin Fletcher**, **Dr. Xiadong Huang,** and **Dr. Larry Sallans** for all the technical assistance provided.

I would like to express my gratitude to all my friends in the **Warner Research Group**. Despite being a graduate student, they have shown me respect that I did not deserve.

Finally, I would like to give thanks to my wife **Louella Washington** and my children **Erin**, **Chadwick**, **Elliott**, and **Darrien** for their love, patience, and understanding.

TABLE OF CONTENTS

LIST OF TABLES

LIST OF FIGURES

Figure **Page**

LIST OF ABBREVIATIONS

ABBREVIATIONS	NAME
HPLC	high performance liquid chromatography
RP-HPLC	reverse phase high performance liquid chromatography
SDS	sodium dodecylsufate
SDS-PAGE	sodium dodecylsulfate polyacrylamide gel electrophoresis
ACN	acetonitrile
TRIS	tris[hydroxymethyl]aminoethane
APCI	atmospheric pressure chemical ionization
MS	mass spectrometry
ESI-MS	electrospray ionization mass spectrometry
TOF	time-of-flight
MALDI-TOF	matrix assisted laser desorption ionization time-of-flight
LTQ- FTICR- MS	linear quadrupole ion trap Fourier transform ion cyclotron resonance mass spectrometer
IEF	isoelectric focusing
IPG	immobiline pH gradient
SMC	smooth muscle cells
PCA	principle component analysis
DTT	dithiothreotol
CHAPS	3-[(3cholamidopropyl)dimethyl-ammonio]-1 propanesulfonate
ASB-14	amidosulfobetaine-14
CA	carrier ampholyte

TERMINOLOGY

Acyl CoA cholesterol acytransferase (ACAT)
The enzyme that esterifies cholesterol for storage.

Adventitia
The outer layer of a blood vessel composed of collagenous and elastic fiber.

Aorta
The main blood vessel that carries oxygenated blood away from the heart to the body.

Atheroma
An abnormal fatty deposit in an artery.

Arteriosclerosis
A chronic disease characterized by abnormal thickening and hardening of the arterial walls with resulting loss of elasticity.

Atherosclerosis
Atheromatous deposit and fibrosis of the inner layer of the arteries.

Artery
Blood vessels that transport oxygen-poor but, pulmonary blood away from the body towards the heart.

Calcification
Deposition of calcium in the arterial wall.

Cardiovascular disease
Disease of the heart and blood vessels

Cholesterol
A steroid alcohol that functions to regulate membrane fluidity and is a precursor in various metabolic pathways a constituent of LDL and is a major cause of arteriosclerosis.

CyDye 3
1-(5-carboxypentyl)-1`-propylindocarbocyanine halide N-hydroxy-succinimidyl ester

CyDye 5
1-(5-carboxypentyl)-1´-methylindodicarbocyanine halide N-hydroxy-succinimidyl ester

Embolism
The sudden obstruction of a blood vessel by an abnormal particle (as a bubble) circulating in the blood.

Endoplasmic Reticulum
A folded membranous compartment with the cytoplasm responsible for various cellular tasks. It functions in lipid synthesis and enzymes of numerous pathways of intermediate metabolism are located at its surface.

Endothelium
Cells that constitute the interface of the blood and vessel walls.

Fatty Streak
Flat or slightly elevated lesions that contain intracellular and extracellular lipids in intima. They are found in the early stages of atherosclerosis.

High Density Lipoprotein
A lipoprotein that functions to scavenger excess cholesterol from tissue cells and transport it to the liver to be excreted as bile salts.

Intima
Inner most layer of tissue in a blood vessel consisting of endothelial layers backed by connective tissue and elastic tissue.

Ischemia
Loss of blood to tissues due to obstruction of inflow of arterial blood usually resulting in stroke.

Lecithin
Any of several waxy hygroscopic phospholipids found animal and plants having antioxidant properties.

Lecithin:cholesterol acyltransferase
An enzyme secreted from the liver that esterifies cholesterol in plasma from cholesterol and the acyl group on phosphatidylcholine

Lesions
Change in the structure of arterial wall due to injury or disease.

Low Density Lipoprotein
A lipoprotein that distributes cholesterol from the liver to other tissues.

Macrophage
Large scavenger cell present in connective tissue and other organs and tissues.

Matrix gamma carboxyglutamic acid protein
The protein controls the formation and the restoration of bone. It is a Vitamin K dependent protein and has a strong affinity for calcium binding and can be crystallized in the form of hydroxyapatite.

Media
The middle coat of the wall of a blood or lymph vessel containing circular muscle fiber.

Myocardial infarction
Death of the middle musculature wall of the heart due to circulatory occlusion.

Osteonectin
A protein that plays a role in mineralization of covalently bound bone

Osteopontin
OPN is an acidic protein, with several Asp or Glu residues, which exhibit a high amino acid homology between species. The protein is associated wit mineralized ions and contains calcium or hydroxypatite binding site.

Soft plaque
Smooth and fatty deposits, sometimes call amorphous plaque.

Stroke
Loss of consciousness, sensation, and voluntary motions caused by rupture or obstruction (clot) of an artery in the brain

Thrombosis
The formation or presence of a blood clot within a blood vessel during life.

ABSTRACT

Cardiovascular disease, primarily atherosclerosis involves a number of distinct processes that are associated with plaque development. The use of differential gel electrophoresis to determine differences between proteins produced in native and bypass coronary arteries from the same heart has been studied. The analytical techniques presented in this study to characterize plaque samples include two dimensional gel electrophoresis, sodium dodecylsulfate polyacrylamide gel electrophoresis, mass spectrometry, differential gel electrophoresis, and high performance liquid chromatography.

An overview of the stages involved in atherosclerosis and the theories implicated in the manifestation of atherosclerosis was presented. A design study using the Box Behnken method was used to optimize the components in lysis buffer to solubilize the membrane proteins present in the intima in atherosclerotic plaques. The number of proteins located as spots in the gel were optimized in this study.

The isolation and characterization of proteins in intima and media extracts of diseased aortas were separated using two dimensional gel electrophoresis followed by excision of gel spots and tryptic digestion to peptides. Mass analysis (MS and MS/MS) of the digested peptides with a linear quadrupole trap Fourier transform ion cyclotron resonance mass spectrometer was used to determine the amino acid sequences.

Protein extracts of normal and diseased aortas and native and bypass arteries were analyzed using differential gel electrophoresis system. Cydye 3 (1-(5-carboxypentyl)-1`-propylindocarbocyanine halide N-hydroxy-succinimidyl ester) and Cydye 5 (1-(5-carboxypentyl)-1´-methylindodicarbocyanine halide N-hydroxy-succinimidyl ester) are

fluorescent dyes used in our study to identify differentially expressed proteins of interest in the same gel using matrix assisted laser desorption ionization time-of-flight mass spectrometry. Several proteins in normal and diseased tissues were identified

A study of the separation and quantification of cholesterol and cholesteryl esters was performed using reverse phase high performance liquid chromatograph interfaced with atmospheric pressure chemical ionization probe that was introduced into a quadrupole mass analyzer. Thirty-five samples were analyzed by principal component analysis that produced two distinct age groups based on age. In addition, a disease severity index was generated from the data. This study concluded that age and low disease severity index were indicators of the atherogenic states of the extracts analyzed.

CHAPTER 1

INTRODUCTION

1.1 Background on Atherosclerosis

Cardiovascular disease continues to be one of the major causes of death in developed countries despite recent advances in understanding the risk factors associated with heart diseases [1-3]. Cardiovascular disease or ischemic heart disease in the United States is among the highest in the world and has been reported to be 5 times higher than in Japan [4]. It should be noted that atherosclerosis, the pathogenic degenerative form of the disease is less prevalent in Central and South America, Africa, and Asia in particular [4]. Atherosclerosis accounts for approximately half of deaths and serious morbidity in the Western world with 20 to 25% due specifically to myocardial infarction in the United States [4].

Atherosclerosis involves many complications including ischemic heart disease, myocardial infarction, stroke, and gangrene of the extremities. Ischemic heart disease is the predominant source of death. Its occurrence in the United States and other Western countries rose progressively from the turn of the century to a peak in the late 1960's. However it has since fallen by more than 30 % [4]. The present mortality rate is around 26%. Numerous disparities have been found geographically and racially for incidences of this disease. For example, in Sweden the mortality from ischemic heart disease is eightfold higher than in Japan.

The prevalence and severity of the disease can be attributed to risk factors that have been identified by a number of studies of well defined groups (Table 1.1) [5]. The two notably comprehensive studies are the Framingham (Massachusetts) Study and the Multiple Risk Factor Intervention Trial [6]. From these studies, it was concluded that the factors that are not modifiable include age, sex, and genetics.

Table 1.1 – Risk factors for atherosclerosis [4]

Major	
Uncontrollable	***Controllable with lifestyle modifications***
Increasing age	Obesity
Male gender	Physical Activity
Family history	Stress ("type A" personality)
Genetic abnormalities	Postmenopausal estrogen deficiency
	High carbohydrate intake
Potentially Controllable	
Hyperlipidemia	Alcohol
Hypertension	Lipoprotein-A
Cigarettes smoking	Hardened (trans) unsaturated fat intake
Diabetes	*Chlamydia pneumoniae*

Age is a dominant nonmodifiable factor in atherosclerosis with an increase in the death rate that rises with each decade of life [7]. The question of aging is seldom investigated as the dominant variable in arterial tissue in preparation for later intrusion by atheroma. Time ordered incremental thickening of the intimal layer, begins before age 20 or around the cessation of puberty. Tracy [8] has provided two conclusions in this regard. The first influence of age is on the evolution of fibro plastic arteriosclerosis which was summarized in the formula:

$$F = \beta A^2 (1-\alpha A); \qquad (1.1)$$

where F is a quantitative measure of fibro plastic arteriosclerosis, and A is age in years. The coefficients β and α are empirical parameters that serve to transform the effects of time, A in the morphological consequences, F. These parameters are reported to vary between groups of subjects such as between men and women and between nations, such that aging is not viewed as identical in every group. The second conclusion from Tracey [8] is that intrusion of atheroma is also stated to be governed by another formula, i.e.

$$W = bF - a \qquad (1.2)$$

where $W>0$ marks the higher probability of atheroma and $W<0$ is indicative of a low probability. The empirical parameters, a and b, can be influenced by fatty deposits (i.e. "fatty streaks"),

arterial size, and some other factors. Underlying views have been reported in numerous scientific investigations on the concept of intimal thickening with regards to aging and the onset of atherosclerosis [9-14].

Sex or gender is reported as another risk factor for the onset of cardiovascular disease. Males are much more prone to atherosclerosis and its consequence than females. Complications from atherosclerosis are uncommon in premenstrual woman, unless they are predisposed by diabetes, hyperlipidemia, or severe hypertension. Post menopausal incidences of atherosclerosis increases, possibly due to a decrease in natural estrogen levels and equalizes by the seventh to eighth decade [4].

Genetics play another key role in the propensity of atherosclerosis. This relates to familial clustering of other risk factors such as hypertension or diabetes, and less commonly involving hereditary genetic derangement in lipoprotein metabolism from excessively high blood lipid levels, such as familial hypercholesterolemia [4]. Other controllable risk factors responsive to change are hyperlipidemia, hypertension, cigarette smoking, and diabetes mellitus.

1.1.1 Pathogenesis of Atherosclerosis

The "responses to injury theory" was formulated in an attempt to explain the molecular and cellular events leading to lesion formation [15]. The inflammatory response to the endothelial injury is normally a protective one, however prolonged and excessive. The more excessive time interval causes an inflammatory fibroproliferative response causing the disease. Numerous pathophysiologic processes have been postulated as specific cellular and molecular responses to an inflammatory disease such as atherosclerosis. Several theories have been postulated to explain inflammatory responses to atherosclerosis. Ross et al. [16] proposed a

response to injury theory accounting for the most prominent initiation of the disease. Endothelial denudation was proposed as the first step in this process.

The actual cause of endothelial injury is uncertain. However, experimental inducements suggest several factors including hemodynamic forces, immune complex deposition, irradiation, and chemically induced intimal thickening [17]. Specific causes are unknown, although speculation is that culprits include circulatory physiologic imbalances induced by smoking, homocysteine, viruses, and other infectious agents such as herpes and chlamydia. Two main factors reported to act in concert in the progression of atherosclerosis are hemodynamic disturbances and the adverse effects of hypercholesterolemia. Hemodynamic effects produce plaques at ostia of vessels arising from aorta, branch points, and additional points along the vessel walls where disturbed patterns are predominant [17]. Disturbed areas produce turbulent blood flow and low stress which are prone to atherosclerotic events; however, smooth laminar flow protects vessel injury.

It has been reported that laminar flow blocks inflammation that mediates or causes endothelial dysfunction and protects against the development of lesions [17, 18]. Additionally, when nonlaminar flow is prevalent, the production of leukocyte adhesion molecules occurs which have been observed to augment wall stresses and promote arterial smooth muscle cells that bind and retain lipoprotein particles [19]. These particles facilitate oxidative modification of the protein inflammatory responses at sites of lesion formation [20].

When normal endothelium is present, leukocytes exhibit poor adhesion; however inflammation causes adhesive expression that binds to various receptor sites on leukocytes. Several adhesive molecules such as selectins with rolling interactions induce inflamed endothelium. Cytokines, secreted by cells in the immune sytem, provide cellular movement to

leukocytes causing migration into the intima. Epidemiological studies have implicated basal cytokines such as interleukin-6 (IL-6), tumor necrosis factor (TNFα) , cell adhesion molecules as (intercellular adhesion molecule-1 (ICAM-1), P selectin, and E selectin as well as down stream reactants as C-reactive protein (CRP), fibrinogen, and serum amyloid A [21, 22-31].

1.1.2 Inflammation and Oxidized Lipoprotein

Lipids have been implicated as one of the primary agents causing atherosclerosis [32]. This class of compounds was studied with animal models producing various inflammatory responses as progression of the disease occurs [32]. Oxidized low density lipoproteins (LDL) are known to be retained in the intima by covalently binding to proteins such as glycoproteins [32-35]. Examples of proteins present in the lipid fraction of specific oxidative processes have been elucidated [36]. Modification of lipids or hydrophobic fatty acid proteins promotes induction of adhesive molecules and other cells that trigger immune responses creating macrophages in vascular cell walls. Experimental evidence points to oxidation of the LDL hypothesis promoting atherosclerosis in plaques; however it still remains unproven. The majority of evidence of LDL oxidation stems from in vitro studies of cell cultures by treatment with transition metals [36]. An LDL oxidative product from the reaction with hypochlorus acid has been proven to be present in human atherosclerotic plaques [36].

A primary risk factor which is known to predispose to heart disease is the elevated level of cholesterol in human plasma [36]. When allowed to accumulate over a period of time, cholesterol contributes to the development of atherosclerotic plaques where fatty acids deposit onto the lining of the inner surface of coronary arteries. Cholesterol exists in plasma lipoproteins both as free sterol and as cholesterol esters. Low density lipoprotein (LDL) contains more cholesterol than five other LDL classes [36]. Cholesterol and its esters comprise two thirds of

the total plasma cholesterol with greater than 40% of the LDL particle attributed to these two sterols. The actual LDL particle contains a single molecule of apoprotein B-100 (Mr=513,000) as its primary protein component. Since cholesterol is primarily synthesized in the liver, the LDL plays a key role in delivering cholesterol to other tissues in the body [36]. A key to understanding the role of LDL and cholesterol homeostasis and the prevalent condition of atherosclerosis relies on understanding the mechanism of cholesterol cellular uptake. The findings of Brown et al. demonstrated that cholesterol uptake by cells is a receptor mediated process and the receptors are themselves regulated [37].

To understand the relationship between cholesterol levels and atherogenesis, the mechanism for cholesterol uptake from LDL to cells is required. Cholesterol esters present hydrophobicity problems when transversing the cell membrane. Brown and Goldstein [37] suggested that cholesterol is taken into the cells through the action of a specific LDL receptor. This receptor was found to be clustered in a structure called a coated pit, or invagination whose abundant protein is clathrin. In a mediated process called endocytosis, a large molecule such as LDL is taken into the cell. LDL thus binds to its receptor, through recognition of the B-100 apoprotein by the receptor. The cellular plasma membrane fuses in the vicinity of the LDL receptor complex and the coated pits are endocytotic vesicles. Lysozymes interact due to their hydrolytic properties and the LDL apoprotein becomes hydrolyzed to amino acids and the cholesterol esters which later under hydrolysis produces free cholesterol. The receptor becomes recycled back to the plasma membrane where additional LDL can be picked up.

Cholesterol is present in the endoplasmic reticulum where it is adjusted by: 1) reducing HMG-CoA; 2) Enhances acyl-CoA: cholesterol acyltransferase (ACAT) production with similar

increases in cholesterol esters; 3) It decreases mRNA at the LDL site. Cholesterol will not be absorbed into the cell if the LDL receptor is reduced thus cholesterol content is increased [36].

Studies of gene cloning and DNA sequence have identified four mutations that affect the LDL receptor [38, 39]. First, are mutations leading to insufficient receptor synthesis. When these receptors are synthesized, a second mutation occurs when no migration is seen from the endoplasmic reticulum to the Golgi complex. A third mutation occurs when the synthesized LDL receptor fails to bind LDL. A final mutation may occur at the cell surface that has bound LDL receptors but no clustering in the coated pits occurs, preventing endocytosis.

As is evident, lipoproteins play a major contribution in the atherogenetic process in three different ways. First, these macromolecules are the main carriers of lipid and phospholipids modified in the vessel wall. Second, lipoproteins are the main transporters of dietary fats which serve as raw materials for membrane synthesis which affects the lubricity of the membrane and its function. Third these also serve as precursors of lipid secondary messengers with activitiy. The function of lipoprotein also serves as mediators of cellular modulations that are associated with atherogenesis.

Additional evidence suggests LDL as the principal agent of atherosclerosis can be based on five criteria. One of the most compelling evidence can be observed from the genetic elevation of LDL that is a consequence of a mutation from the receptor gene [40]. Homozygous familial hypercholesterolemia points to LDL at the prototype of an atherogenic lipoprotein [40]. Mutations for animal models such as the bovine affects the structure of apoprotein B and LDL so that its clearance from the plasma can be directly associated with the development of atherosclerosis [41]. There exists a well documented correlation between plasma and concentration of low density lipoprotein and the risk of atherosclerosis as well as cardiovascular

disease [42]. Atherosclerosis can be induced in various animal models that indicate a strong correlation with the levels of plasma LDL concentrations [43]. The presences of reporters of LDL apoprotein B, the protein of LDL and cholesterol ester, in human and animal atherosclerotic plaques reveal additional roles of the protein in the disease. LDL–like entities have been extracted from plaques [43]. In addition, the LDL influences the cells in various ways to facilitate the evolution of plaques.

1.1.3 Development of Atherosclerotic Plaques

A number of distinct processes are associated with plaque development: lipid accumulation, inflammation, cell proliferation, cell death, and thrombosis. Some of the molecular events underlying each of these processes and the stimuli for these events have been identified [44]. However many other processes require clarification. Atherosclerosis is the result of accumulation of numerous components in the coronary arteries, resulting in the formation of plaque deposits. It is a passive progressive disease characterized by the accumulation of lipids and fibrous elements in the large arteries. Lipids from the lipoprotein component are influenced by the monocytes [44] that liberate growth factors causing the proliferation of smooth muscle cells. When the endothelial cell becomes permeable, macromolecules such as LDL which have been modified as macrophage scavengers and other receptors are loaded with lipid and foam cells [45]. The foams cells deteriorate and stored lipids or other sterols become trapped. Fibrous plaques become evident due to accumulation of lipids, mostly cholesterol and cholesterol esters and smooth muscle cells. Lesions develop from this complicated process which may be expressed as fatty streaks or complicated [46]. Variability of lesions has led to classification of these lesions based on the American Heart Association Study [47, 48]. These classifications are depicted in Table 1.2. Such lesions are described from initial

fatty streaks to complicated lesions based on the advancement and severity of the disease [49]. Plaques may exhibit different degrees of stability and rupture capability causing myocardial infarction or stokes. The composition of the plaques is of importance in pathological studies of composition and vulnerability of plaques. Plaque rupture often occurs at the lesion edges that contain foam cells.

Table 1.2. American Heart Association classification of human atherosclerotic lesions [4]

Nomenclature and main histology	**Description of disease progression**	**Sequences in Progression**
Type I (initial) lesion	Macrophage foam cells	I
Type II (fatty streak)	Lesions and lipid accumulation	II
Type III (intermediate)lesion	Excellular lipid pools	III
Type IV (atheroma) lesion	Atheroma lesions lipid pools	IV
Type V (fibroatheroma) lesion	Lipid core and fibrotic layers, calcification	V
Type VI (complicated)lesion	Thrombus and complicated lesions	VI

The early lesions of atherosclerosis consist of sub endothelial accumulations of cholesterol-engorged macrophages, often referred as foam cells. In humans, such fatty streak lesions can usually be found in the aorta in the second decade and coronary arteries in the second decade and the cerebral arteries in the third or fourth decades. Due to differences in blood flow dynamics, there are preferred sites of lesion formation within the arteries. Fatty streaks are not clinically significant, but they do accumulate as a result of lipid-rich necrotic debris and smooth muscle cells. Plaques that develop are complex, with calcification, ulceration at the luminal surface, and hemorrhage from small vessel walls. Although advanced lesions can grow sufficiently large to

block blood flow, the most important clinical complication is an acute occlusion due to the formation of a thrombus or blood clot, resulting in myocardial infarction or stroke.

Stary et al. [48] presented evidence that atherosclerosis causes lesions that are isolated in large and medium sized arteries, the brain, the heart, and legs. This process occurs during childhood and involves macrophages that develop into foam cells that are deposited within the junction of the tunica intima and tunica media layers of the artery during the first week of life. Foam cells further progress into a fibrous atheroma beginning at about 30 years of age. A further association has been suggested between the endothelial cells and the macrophage. This suggestion has later developed into the "response to injury" hypothesis.

Proteins play a major role in the development of atherosclerosis; however, they act in concert with fats in the pathogenesis of the disease [36,48]. Fats are insoluble products complexed in saturated and unsaturated forms as triglycerides and cholesterol. Fats are transported between the intestine, liver, and peripheral plasma in the form of soluble complexes called lipoproteins. The name of the lipid with which fat is associated is apoprotein. The lipoprotein circulates in spherical particles that consist of an envelope of phospholipid and apoprotein with a lipid core. Lipoproteins can be differentiated by density, configuration, and electrophoretic mobility into chylomicrons, very low-density lipoproteins (VLDL), low density lipoproteins (LDL), intermediate density lipoproteins (IDL), and high density lipoproteins (HDL).¨ The major characteristics of proteins that are involved in the metabolic pathway of cholesterol and their proatherogenic composition are given in Tables 1.3 and 1.4.

On the cellular surface, LDL undergoes oxidation in the presence of free radicals in addition to interactions with metal ions such as copper. The macrophages and monocytes

consume the oxidized LDL and forms fatty streaks and lesions. These precursors often result in the formation of plaque in the arteries, the final degenerative form of atherosclerosis.

Table 1.3 Properties of major human plasma lipoprotein classes [35]

	Chylomicron	**VLDL**	**IDL**	**LDL**	**HDL**
Density	< 0.95	0.95-1.006	1.006 -1.019	1.019 -1.063	1.063-1.210
Components (% dry weight					
Protein	2	8	15	22	40-55
Triacyglycerol	86	55	31	6	4
Free Cholesterol	2	7	7	8	4
Cholesterol esters	3	12	23	42	12-20
Phospholipids	7	18	22	22	25-30
Apoprotein composition	A-I,A-II,B-48,C-I,C-II, C-III	B-100, C-I, C-II,C-III,E	B-100, C-I,C-II,C-III,E	B-100	A-I, A-II,C-I,C-II,C-III,D,E

VLDL=very low-density lipoprotein
IDL = intermediate-density lipoprotein
LDL = low-density lipoprotein
HDL = high-density protein
LCAT = lecithin: cholesterol acyltransferase
LPL = lipoprotein lipase

Table 1.4 Apoproteins of the human plasma lipoproteins [35]

Apoprotein	**Molecular Weight**	**Characteristics**
A-I	28,300	Major protein in HDL; activates LCAT
A-II	17,400	Major protein in HDL
B-48	241,000	Found in chylomicrons
B-100	513,000	Major protein in LDL
C-I	7,000	Found in chylomicrons; activated LCAT and LPL
C-II	10,000	Found in VLDL; activates LPL
C-III	9,300	Found in chylomicrons, VLDL,HDL, inhibits LPL
D	35,000	HDL protein, cholesterol ester transfer protein
E	33,000	Found in VLDL,LDL,HDL

1.1.4 Vascular Calcification

Vascular calcification is observed in the progression of atherosclerosis that has been regarded as a passive unregulated degenerative process [49]. However, the concept of ossification has been recently documented [50, 51]. The process of ossification that is normally

observed in bone mineral formation can be found in arterial walls. Similar bone formation regulators and bone structural proteins are expressed in atherosclerotic plaques including bone morphogenetic protein -2 (BMP-2), osteopontin, matrix γ carboxyglutamic acid protein (MGP), and osteoprotegerin [49].

Vascular calicification was first reported by Anderson who found matrix vesicles from osteogenesis in human calcified aortas [52]. Giachelli [53] later proved similar expressions at the molecular level of bone matrix proteins in vascular smooth muscle. Expression of osteogenic factors was also found by Bostrom [54] and Shanahan [55] in cultured vascular cells. Cultures of vascular smooth cell express bone proteins in the presence of alkaline phosphatase [56]. Several cells in the process have been implicated including macrophages, mass cells and vascular smooth muscle cells are involved in the atherosclerotic intimal calcification [57]. TNF- α is released as macrophage that respond to oxidized LDL and vascular smooth muscle cells differentiate into osteoblasts, alkaline phosphatase expression and mineralization. Mast cells as extracellular tryptase initiate calcification by an unknown mechanism and are often observed at sites of some calcium deposits. These cells are known to release cytokines which release tumor necrosis factor (TNF) α and interleukin-1 [58, 59]. Calcification of vascular cells is similar to SMC's and has osteoblastic characteristics forming calcifying nodules in vitro. Several types of cells may be categorized. Pericytes possess microvascular smooth muscle phenotypic characteristics [60].They form high nodules that mineralize with hydroxyapatite and express MGP through osteogenic differentiation with calcified matrix. The abundance of microvessels facilitates avenues that contribute to arterial calcification [61]. Vascular dendritic cells also contribute to the calcification as demonstrated in the expression of S-100 [62]. These cells are apparent in aortocoronary saphenous vein bypass grafts.

Molecular mediators are proteins that are notably responsible for arterial calcification. BMP 1-7 [63] are growth factors that share homology with tissue derived growth factor Beta and belong to the same family of proteins. BMP-2 and BMP-4 induce osteoblast differentiation and tissue events that are required for bone formation. MGP (matrix GLa protein) is a class of proteins that has approximately 14KDa mass units that is formed in vascular smooth muscle cells and the intima by macrophages and endothelial cells [64]. It contains 5 gamma carboxyglutamic acid residues which are derived from the action of gamma carboxylase using Vitamin K. Although GLa proteins are not confined to the vessel tissues, a common origin is shared with the γ carboxylation pathway of these proteins. Only Gla residues are the site for binding hydroxyapatite. This pathway is illustrated in Figure 1.1. Table 1.5 illustrates various Gla containing proteins and their tissue localization. The role of MGP is not directly observed, but in

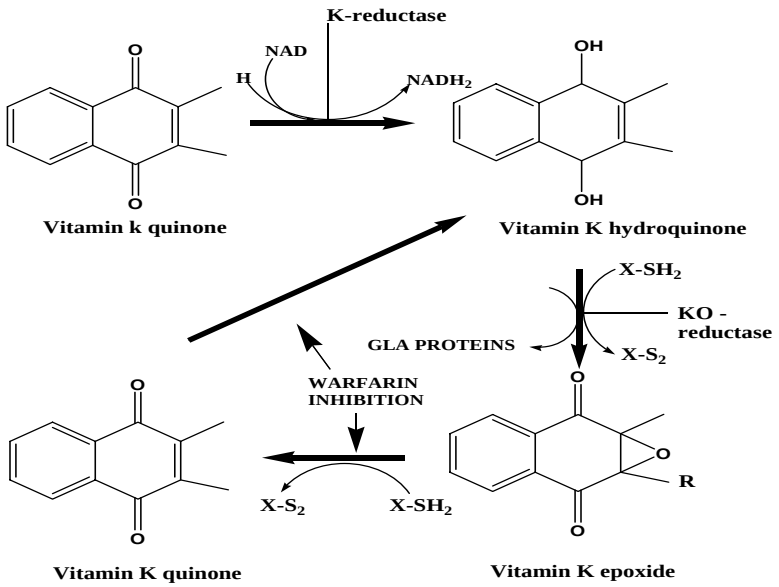

Figure 1.1. Metabolic pathway of the generation of gamma carboxy glutamic acid proteins in the Vitamin K process. Warfarin inhibits the process causing calcification

Table 1.5 Glutamic acid proteins and their tissue location [65]

PROTEIN	FUNCTION	Immunochemical Detection	IN ARTERY?
MGP	Ca-inhibitor	Antibody Unavailable	Yes
BGP	Ca-inhibitor	Antibody	Yes
PGP	Ca-inhibitor	Antibody	Yes
Prothrombin*	Coagulation	Antibody	Yes
Factor VII*	Coagulation	Antibody	Unknown
Factor IX*	Coagulation	Antibody	Unknown
Factor X*	Coagulation	Antibody	Unknown
Factor Z	Coagulation	Antibody	Unknown
Protein C*	Anticoagulation	Antibody	Unknown
PRGP1	Unknown	Unknown	Unknown
PRGP2	Unknown	Unknown	Unknown

null mouse studies it is a potent inhibitor of vascular calcification particularly hydroxyapatite [65-67]. It has been implicated in numerous studies; however it also inhibits the effects of BMP-2. The antagonistic effects of MGP as well as MGP mRNA can be seen by oxidative stress and medications such as warfarin and diphenylhydantoin. When the ability to generate vitamin K in the reduced form is minimized or the ability to use vitamin KH2 co-factor, arterial calcification and osteoporosis occurs. Other antagonists and regulators of MGP and MGP mRNA production include retinoic acid [68], vitamin D3, growth factors [69, 70], and apoptosis [71, 72].

Fatty streaks that have been studied containing microzones of calcification predominantly located in the musculoelastic layer of the intima. Bobrystev et al. [73] examined the development of atherosclerotic lesions and the presence of calcified deposits formed due to physiochemical processes. A major observation produced evidence that the calcification process

was a result of a preexisting structural base of unesterified cholesterol in extracellular matrices or altered elastin fibres. Association of calcification deposit with elastin fibres, collagen fibres, lipid vesicles as well as unesterifed cholesterol was also studied. Osteopontin and osteonectin are two proteins noted by Hirota et al. that involve physiochemical and pathological calcification [74]. Insitu hybridization and immunohistochemistry indicated that levels of osteopontin mRNA expression increased plaque formation and macrophages. The atheromatous plaques were determined to be positive for osteopontin.

1.2 Research Goals and Objectives

In this study, the goal is to elucidate differences in the structure and molecular weight of the proteins that are associated with the atherosclerotic plaques from native and bypass arteries from the same heart. To this end, analytical techniques that will be used in the separation and identification of proteins found in plaque samples extracted from the intima and media layers of the vessels include: 1) SDS PAGE, 2) high pressure liquid chromatography, 3) 2-D gel electrophoresis, 4) matrix assisted laser desorption ionization mass spectrometry, and 5) electrospray ionization coupled to a quadrupole mass spectrometer. The first objectives in the research will optimize the extraction and separation aspects of the proteins in the tissue samples. The second objective will involve the analysis and characterization of crude protein extracts using mass spectrometry.

The samples, acquired from Louisiana State University Health Science Center – Department of Pathology, contain tissues including arterial membranes and muscular material. The separation of these components from the arteries is somewhat difficult due to the size of the artery including some plaque material during the dissecting procedure. Extraction of the intima layer of the inner wall using organics is well suited for fats including triglycerides, cholesterol

and its esters. However, proteins present a more difficult problem due to their hydrophobic and hydrophilic properties. This fact is compounded by the fact that some proteins are known to denature in the presence of organics. Therefore, the method for protein extraction will be conducted in aqueous medium in the presence of phosphate buffer saline or a similar buffer at a pH of 7.4. Liquid nitrogen is commonly used both to keep the proteins from denaturing due to temperature and various effects of proteases. This was shown to be effective in grinding the crude samples prior to extraction.

The widely accepted protocol for separating proteins is typically by the use of SDS polyacrylamide gel electrophoresis. Achieving optimum separation and gel performance is important in this study because it will be necessary to monitor differences in protein composition between two arteries. Once the proteins are loaded on the gel and separation occurs, excision of the proteins from the gel is necessary. This is followed by further extractions to remove the proteins from the gels. The efficiency of this method is low and quite often in gel digestion is used in the identification of proteins. To improve recovery, addition of detergents such as Tween 20 or sodium dodecylsulfate, may be needed. Additionally, different volatile organics have been used. The procedures for protein removal from gels are vital from the standpoint of ensuring that the detection limits of the mass spectrometer have been exceeded. The most common technique for mass detection of proteins is the use of MALDI- time of flight (TOF) mass spectrometers.

In order to determine extraction efficiency, MALDI TOF has been used initially to monitor the extract for proteins with high molecular weights (>25 kilodaltons) typical lipoprotein masses. Protein masses of this magnitude have not been achieved at this point; therefore additional methods must be evaluated to enhance this procedure.

1.3 Analytical Techniques Used in this Study

1.3.1 Sodium Dodecylsulfate Polyacrylamide Gel Electrophoresis (SDS-PAGE)

British workers measured the mobilities of inorganic ions using gel media. Consden et al. [75] first used gels specific for protein separations. Later Smithies used starch as a medium that produced larger gains in resolution. The first introduction of synthetic polyacrylamide as a technique for active molecular size separations was conducted by Reymond [76]. Alternative procedures by Ornstein [77] and Davis [78] devised methods for gels consisting of disc gels that resulted in narrow protein zones. Maizel and collaborators [79] discovered the widely used method for molecular size distribution analysis with sodium dodecylsulfate polyacrylamide gel electrophoresis (SDS-PAGE). The physio-chemical basis of the concept is based on the mobility of a protein that is proportional to its charges in a small charge range [80]. Historically, higher charges produce reduced mobility's with further enhancement of the charge, the mobility reach a limiting value. Analysis of protein molecules is possible with additional increases in charge. SDS is an anionic detergent or surfactant that has an effect on the protein size analysis when it is hydrophobically bound to the protein reversibly. The limit in mobility of the complex has been shown to be a linear decreasing function of the logarithm of its molecular weight.

SDS-PAGE employs three fundamental properties of proteins: size, net charge and its relative hydrophobicity [81]. During the electrophoretic process, a particle with an electric charge Q is forced through a viscous medium (liquid or gel) by the action of an electric field with a potential gradient E. The frictional resistance f must be overcome to migrate through the supporting medium while the driving is acting on the moving particle. This mathematical phenomenon is related by the equation below:

$$QE=f \tag{1.3}$$

In solution, the resistance obeys Stoke's law:

$$f = 6\pi r v \eta \qquad (1.4)$$

where r equals the particle radius, v its velocity and η the viscosity of the medium. The behavior in gels is more complex as a function of pore size and particle size.

The mobility of an analyte during electrophoresis m of a particle is defined by

$$m = d/tE = v/E = Q/f \qquad (1.5)$$

where d represents the migration distance of the particle in time t.

As the particle migrates through the medium a potential gradient or field strength is observed that corresponds to the ratio of current density J, to the specific conductivity χ as follows :

$$E = J/\chi \qquad (1.6)$$

When a particle migrates through the gel, its velocity is given by

$$v = Em = mJ/\chi \qquad (1.7)$$

where J equals current density and χ equals specific conductivity.

The ionic strength of monovalent or divalent buffers affects the mobility of the ionic species. Analytes with high migration velocities have low ionic strengths with little heat evolution where as high ionic strength buffers lead to slower migration velocities. Heat generation is enhanced despite sharper zones. The equation for ionic strength is represented as:

$$\mu = \tfrac{1}{2} \sum_{i=1}^{i=n} c_i z_i \qquad (1.8)$$

where c_i is the molar concentration of a single ionic species and z_i is the charge of the species in a solution with n ions.

As previously discussed, SDS-PAGE is composed of polyacrylamide gels that are synthesized using the following reactions:

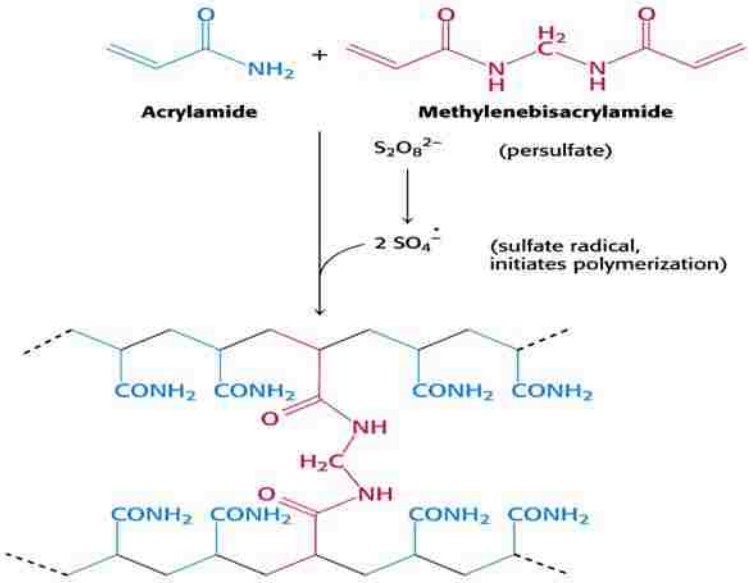

Figure1.2. Polymerization of acrylamide for protein separations

The acrylamide monomer is reacted with NN methylene bisacrylamide in the presence of tetramethylethylenediamine (TEMED) to yield the corresponding polymer. The polymerization is free radical base catalyzed with ammonium persulfate and TEMED. The polymer provides advantages over other media support by: 1) free charge state that is free of electroendosmotic flow effects on the components, 2) it is a clear gel that is suitable for densitometry measurements and 3) the method is versatile in pore size distribution that can be controlled by changing the monomer and the comonomer concentrations.

Proteins are amphoteric compounds in which their net charge is determined by the medium in which they are suspended. When the protein solution is at a pH above its protein isoelectric point, the protein bears a net negative charge and will migrate towards the anode in an electric field. For solutions at pH below its isoelectric point, the protein is positively charged and migrates towards the cathode. Proteins are separated based the solution pH under both

native and denaturing conditions. The most widely used method for analyzing mixtures of proteins is sodium dodecylsulfate polyacrylamide gel electrophoresis (SDS-PAGE). In this technique, proteins are reacted with the anionic detergent SDS (or sodium lauryl sulfate) to form negatively charged complexes [82]. The aqueous detergent solution forms globular micelles composed of 70-80 molecules with the dodecyl hydrocarbon moiety in the core and the sulfate head groups in the hydrophilic shell. When SDS and protein interact, complexes form that resembles necklace-like structures composed of proteins micelles connected by flexible polypeptide segments [83]. These structures result in large amounts of SDS incorporated into the SDS-protein complex in a ratio of approximately 1.4g / SDS g protein. Under non-denaturing conditions, the electrophoretic separation of proteins is determined by both size and charge of the molecules. During the non-denaturing process, the charge of the protein is determined by size and charge of the molecules. However, the SDS masks the charge of the protein and the anionic moieties have a roughly constant net negative charge per unit mass. Reduction of disulphide bonds is necessary to adopt the protein to the random coil configuration necessary for separation by size using either 2-mercaptoethanol or dithiothreitol (DTT). The charge of the micelle is thus negative so that the separation is now determined by molecular weight. The commonly used protocol for proteins is described by Laemmli [84].

Experimentally, a slab gel base on the Laemmli process consists of two types of gels, a stacker gel and a resolving gel. The usual method denatures the protein with SDS followed by complete denaturation by heat and disulfide breakage by a reducing agent such as β mercaptoethanol. The proteins are placed into wells in the stacker and under buffering conditions using TRIS: glycine: SDS mixture under an applied voltage. The proteins migrate

through the stacker gel to the resolving gel where separation occurs. For running native proteins, neither SDS nor the heating of the protein mixture are used.

The molecular weight distribution of the proteins in a gel may be resolved by changing the effective size of the media. The effective pore size of the gel is an inverse function of total monomer concentration (%T and C) which is the sum of the concentration of the monomer and cross linking material. In practice the lower the concentrations of the gel, the smaller the proteins that are entrained. Increases in molecular weight are observed from the top of the gels as the protein migrates downward. The porosities of the polyacrylamide developed by Raymond and Nikimichi [85], Toombs [85], Rodbard and Chrambach [86], and Righeti et al. [87] are predicted by the following equations:

1. $p = K' d / C^{1/2}$ (1.9)

2. $p = K' d / C + K''$ (1.10)

3. $p = 1 / C^{1/3}$ (1.11)

4. $p = 140.7 \times C^{-07}$ (1.12)

where p is the mean porosity, d is the distance migrated, c is the concentration and K is a constant.

Gel electrophoresis determines proteins and nucleic acid molecular weight based on the comparison of migration distances by a single gel concentration or a pore size gradient. This technique has the capability of measuring both size and net surface charge densities. A procedure by Ferguson [Ferguson 88-91] directly correlates the mobility values or relative mobility R_f to the migration distance of the analyte to the migration distance of a dye or a marker with a tracking dye or silver stain. This protocol is based on the plot of log mobility vs the gel concentration that is often expressed as percent T. These plots are very useful for molecular

determination and to quantitatively determine the maximum resolution between two components and the optimal gel concentration for best separation.

1.3.2 Visualization of SDS PAGE

Visualization of proteins in polyacrylamide gel and electroblot mainly rely on noncovalent interactions. Rabilloud [93] enhanced the availability of these interactions. In noncovalent interactions which are generally reversible, staining methods are used that are compatible with proteins as well as a variety of proteomic applications. This staining use gels or blots directly. The visualization techniques that are noncovalently bound to proteins may be categorized in three areas: organic dyes such as Coomassie brilliant blue [94,95], fluorescent probes such as Sypro dyes or Nile red based on fluorescent detection[96] and metal ion binding such as negative and positive staining with zinc imidazole. Silver staining of gels is commonly used for gel visualization [93, 97, and 98]. The advantages of using this procedure is due to its low sensitivity in nanogram range which is 50 to 100 times more sensitive than the Coomassie blue, ten times more than the colloidal blue, and at least twice as sensitive as the negative staining zinc / imidazole method.

1.3.3 Two Dimensional Gel Electrophoresis (2DE)

Two dimensional electrophoresis (2DE) is another tool for separating complex mixtures of proteins into many components. When proteins are in an electric field, they migrate at a rate that is dependent on their conformation, size, and electric charge. In 2DE, the use of size and charge allow high resolution separation of proteins. This technique was first described by O'Farrell and Klose [99] in 1975. The original separation technique was performed in carrier ampholyte containing polyacrylamide gels cast in narrow tubes. The first-dimension step allows separation by isoelectric focusing, based on charge. The second-dimension step, SDS

polyacrylamide gel electrophoresis (SDS-PAGE), separates proteins according to their molecular weights. Isoelectric focusing separates proteins based on their isoelectric points (pI). Proteins can possess positive, negative or zero net charge depending on the pH of the environment resulting in amphoteric properties. The sum of the negative and positive charges of the amino acid side chains along with the amino and carboxyl termini a net charge can be determined on the molecule. The isoelectric point occurs at the specific pH that produces a net charge of zero. When proteins produce a positive charge, the pH value lies below the respective pI. Additionally, a negative charge results when the pH value is above its pI. If the net charge of a protein is plotted against the pH, the observed isoelectric exists when the net charge intersects the abscissa or a net charge of zero.

Proteins in a pH gradient using the IEF technique under an electric field move to the position where its net charge is zero. The protein will migrate towards the cathode with a positive charge. A negative charge is observed when the protein migrates towards the anode and becomes less charged as it reaches a net charge of zero. Carrier ampholytes generate pH gradients originally cast in tubes [99]. These ampholytes are small soluble, amphoteric molecules possessing high buffering capacities near their pI's. Hundreds of polymeric species exist at various pI's over a range of pH units. The carrier ampholyte with the lowest pI (most negative charge) moves toward the anode and the ampholyte with the highest pI (more positive charge) moves towards the cathode. Other carrier ampholytes will align between the two pH extremes according to their pI's and buffer environment.

Despite the unique properties of carrier ampholytes, several limitations are observed: 1) batch to batch variations, 2) instability and tendency to drift, and 3) low mechanically stability causing bending or breakage of the rods. The limitations of the carrier ampholyte lead to

development of an alternative technique for pH gradient formulations. Bjellqvist et al. [100] developed immobilized pH gradients or IPG that are covalently incorporated consisting of an acidic and a buffering group in a polyacrylamide gel with it is cast. As polymerization occurs, the acrylamide portions of the buffers are copolymerized along with the acrylamide and bisacrylamide monomers to form the corresponding gel [85]. A pH gradient formed similar to pouring a polyacrylamide slab gel. However instead of two solutions of different % T, the two solutions contain acidic and basic mixtures of acrylamido buffers that are cast onto a plastic backing. Prior isoelectric focusing, the gel strips must be rehydrated in solutions that are comparable to the separation without compromising protein solubilities. Immobilised pH gradients in the first dimension also have advantages over carrier ampholyte-based separations. The cathodic drifts that are apparent in ampholyte based separations are eliminated due to the pH gradient covalently fixed within the gels allowing a broader pH range for separations. Additionally, this provides for the separation of more highly acidic and highly basic proteins. The IPG possess a higher load capacity for proteins than the carrier ampholytes [101]. Reproducibility of the IPG strips that are well characterized eliminates batch to batch variability. Others advantages include reduction of preparation time, prevention of stretching , breaking, ease of handling and samples can be applied to the gel strips during gel rehydration [102,103]. The normal pH range of 3.5-10 is used in protein separations; however other immobiline ranges are possible.

Separation and resolution of complex biological samples depends on the appropriate preparation of the tissues prior to IEF [82]. The proteins in the sample must remain in solution during the entire process and devoid of interfering analytes such as salts. To assure protein solubility, various agents are employed in the sample preparation step.

The solubilization of proteins is important in high resolution in separations in 2D gel electrophoresis [104]. This process breaks down interactions between the substances to be analyzed and interfering substances as well as preventing reaggregation during the sample preparation. Analytical techniques used in protein chemistry are important and proteins to be analyzed must be 1) extracted from the biological sample; 2) freed from any substances interfering with the technique or other processes; 3) and must remain in solution during the entire separation process. To provide a suitable environment for proteins for electrophoresis some knowledge of the cohesive forces maintaining the macromolecular structure of the biological complexes and the interactions with other molecules is necessary. There are numerous forces that are attributed to protein cohesion and interactions with other molecules. These factors include disulfide bonds, hydrogen bonding, and electrostatic interactions. Other forces related to protein-protein interactions are charge-dipole, dipole-dipole, Van der Waals, and hydrophobic forces. The lateral chain of apolar amino acid (L, V, I, F, W, Y) are examples of specific cores in the proteins which are responsible for protein-protein interactions and binding of lipids and other apolar molecules to proteins.

Numerous interfering substances as nonprotein substances may be present in biological extracts for separation by gel electrophoresis. Such impurities can interfere with the separation aspect and subsequent visualization. These impurities can cause problems by increasing the conductivity in the first dimension and reduce IEF effectiveness. These substances can accumulate at the anode or cathode or within the strip causing streaking either vertically or horizontally on the final SDS separation in the second dimension. The contaminates can be removed by a variety of precipitation techniques that require resuspension in a salt free medium. Guy et al. [105] used trichloroacetic acid as the method of precipitation and organics such as

acetone [106], ethanol or a mixture of chloroform and methanol [107] were shown to be equally as effective. Dialysis has been proven to be another to remove impurities such as salts from the protein extract particularly those with lower molecular weights. Some devices are capable of concentrating and dialyzing the sample (ie vacuum dialysers, or centrifugeable devices) [108]. However, the major problems that exist in these devices are due to loss of proteins by adsorption onto the membrane of losses due to diffusion through the membrane for low molecular weight proteins [104]. In some cases, the problems can be minimized by denaturing detergents, thereby reducing the effects of absorption to the membrane. Often caution must be taken in the presence of detergents with micelles that are large enough in molecular weight that can be retained onto the membrane.

Deoxyribonucleic (DNA) and ribonucleic (RNA) acids in high concentrations can result in poor focusing in the acidic region of the IEF gel. Additionally, high background can be seen when using silver staining techniques for visualizing the gels. DNA increases the viscosity of samples that may by too high to be effective. Nucleases can be used to mitigate the problems encountered with these contaminants. Blomberg and others [109] accomplished this by the addition of one-tenth volume of a solution containing 1 mg/ml DNase I, 0.25 mg/ml RNase A, and 50 mM $MgCl_2$ to the protein samples followed by incubation on ice.

Lipids are also present interferences with respect to IEF depending on their supramolecular structure by binding to proteins usually lipid carriers when they exist as monomers. The binding alters the characteristics used for the electrophoretic separation and often gives rise to artifactual heterogeneity [109]. Supramolecular assemblies of lipids (membranes and vesicles) produce more severe problems during electrophoresis. Resolution to this problem can minimized using detergents to disrupt the membranes, solubilize the lipids,

delipidate and solubilize the proteins bound to the membranes or vesicles. Others techniques require organic solvent precipitation for the removal of salts or lipids. Organic solvents such methylene chloride, acetone, hexane, isopropanol and methanol are effective in minimizing the presence of lipids however these solvents can cause denaturation of most proteins.

Uncharged polysaccharides pose problems due to their large molecule weights which, cause the molecules to clog the pores in polyacrylamide gels. These entities can be removed using ultracentrifugation or selective precipitation with trichloroacetic acid, ammonium sulfate, phenol ammonium acetate [110], or dyes [111,112] and resolubilization of the protein pellet.

Proteolysis from cell lysis liberates proteases that contribute to the degradation of proteins. These proteases must be inhibited during sample preparation. Denaturants as urea are usually effective, but some proteases retain activity. Some protease inhibitors are needed in additional to denaturing variants. Phenylmethylsulfonyl fluoride and aminoethybensenesulfonyl fluoride irreversibly inhibits serine and cysteine proteases [82]. Ethylenediaminetetraacetic acid (EDTA) with the ability to chelates metal ions inhibits metalloproteinases. Peptide proteases such as leupeptin, pepstatin, aprotinin, and bestatin are active against different classes or proteases in micromolar concentrations.

Protein samples properly treated for the interfering substances mentioned above must be fully solubilized, disaggregated, denatured, and reduced prior to IEF processing. To achieve optimum separation, samples for 2D electrophoresis must contain a neutral chaotrope, usually urea or a mixture of urea derivatives, a neutral or zwitterionic detergent, and a reductant that is capable of reducing protein disulfide bonds to sulfhydryls and maintaining their reduced stated during electrophoresis.

Chaotropes such as urea are used in 2D electrophoresis in concentrations of 7M to 9M as a denaturing agent. Rabilloud et al. [113] has shown that urea and thiourea used in combinations can effective in solubilizing proteins particularly those associated with membranes. Optimal ratios of the two may differ depending on the samples [114]. The use of thiourea may result in disturbances and loss in resolution in the acidic range of pH 3-5 in IEF separations due to possible impurities in the commercial preparations.

Detergents are also effective to completely solublize proteins. Nonionic detergents that are used for this procedure are Triton X-100 or Nonidet P-40 as well as the use of zwitterionic detergents as cholamidosulfobetaines as (3-[3-cholamidopropyl) dimethylammonio]-1-propane sulfonate (CHAPS) and CHAPSO [115]. Alkylsulfobetaine detergents as SB 3-10 [116] are often used but are less effective due to their limited solubility in urea solutions. Such reagents that require lower concentrations of urea and thiourea reduces the effective solubilization of the proteins. Amidoalkylsulfobetaines have been developed that are highly soluble in urea and thiourea solutions and are amenable to proteins that present solubility problems; however, many of these are not available commercially [117]. SDS has been the reagent of choice for denaturing in electrophoresis; however it cannot be used as the sole agent for IEF although rapid solubilization and extraction are demonstrated.

Reductions of the disulfide bonds provide greater susceptibility for solubilization. This is performed by exposing disulfide bonds. 2-mercaptoethanol was normally used to reduce samples for 2D electrophoresis, but has been largely replaced by the sulfhydryl reductant dithiothreitol (DTT) and dithioerythritol (DTE) usually effective at lower concentrations and higher purity. The 2-mercaptoethanol introduces unwanted keratins despite stringent commercial processing.

The first dimension of isoelectric focusing (IEF) requires complete protein solubility as they are subjected to an electric field in which they migrate to their respective isoelectric point (pI). By definition, the pI is state of lowest possible net charge and thus lowest solubility in aqueous media. The protein studies in this study are mainly membrane proteins that involve the intima and media and diseases that are associated with them. Many integral membranes proteins tend to be hydrophobic with large masses > 100 kilodaltons. Two major problems exist in the preparation of membrane proteins for 2DE. First, detergent compatibility with IEF is necessary for effectively extracting membrane proteins. Second, protein solubility must be maintained throughout IPG loading doing first dimension separation. SDS although normally used in one – dimensional separation, is incompatible with IEF due to the charged head. Extracts of proteins that are solubilized with SDS must undergo solvent or acid precipitation, removing or reducing SDS or lipids. These processes may result in significant loss or modification of proteins during precipitation. Optimization of extraction conditions by altering buffers, choatropes, and detergents demonstrate reliability in achieving high resolution maps of membrane proteins. An array of proteins spots result that assigns molecular weight and pH based on an x and y coordinate system. Thousands of proteins can be separated using this method.

The protein extract must be aliquoted into a rehydration buffer containing urea, DTT and the immobilized pH gradient (IPG) buffer. The mixture is absorbed into a dry strip containing IPG gel with a same pH gradient contained in the rehydration buffer. The strip is placed into a focusing cup and voltage up to 8000 can be applied for effective separation. Further treatment of the strip is necessary to prevent oxidation of the sulfhydryl groups using DTT. Residual DTT must be reacted using iodoacetamide. Second dimension gel electrophoresis follows by applying the dry strip directly to the gel and performing electrophoresis in the presence of running buffers

usually containing TRIS-glycine with SDS for denaturing purposes. Detection of proteins is performed using similar staining methods as previously discussed depending on the types of molecules and compatibility with mass spectrometry. An illustration of the 2D gel electrophoretic process can be summarized in Figure 1.3.

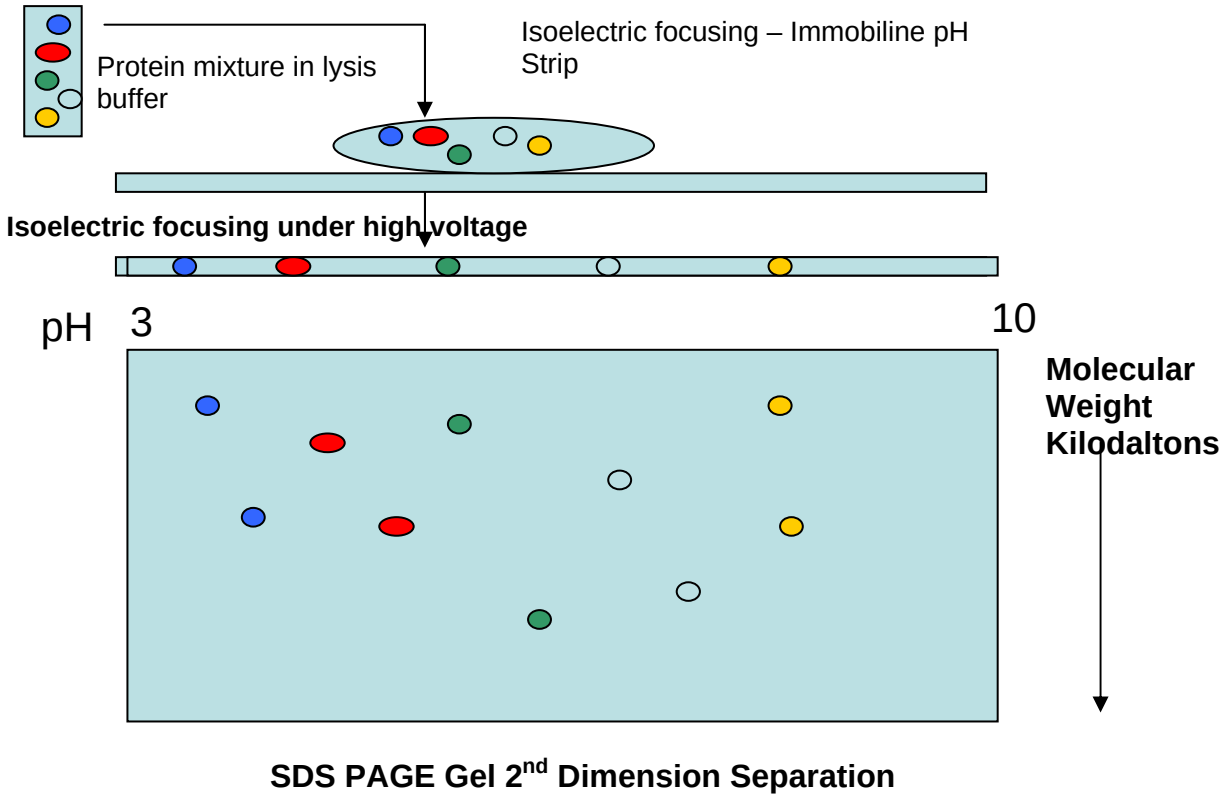

Figure 1.3 2D Illustration of 2DE gel electrophoresis and the separation of proteins using SDS-PAGE

Numerous advances have been employed for 2D electrophoresis proteomic technologies to characterize proteins expressed by an organism or tissue. Advances in pretreatment of samples for solubilization, denaturation, and reduction provide many aspects of the technology. Although entire genomes for many species known, the actual identification of proteins is low for 2D analysis. Databases are constantly being updated to produce protein maps of diseased and nondiseased states of tissues and cells. In addition, post translational modifications of proteins,

such as phosphorylation and glycosylation, are being added to global databases. A major complement to the area of protein identification and one of the main tools for sequencing the separated entities has become the rapid advancement of mass spectrometry of biological compounds.

1.3.4 Mass Spectrometry

One of the most versatile and comprehensive tools used by chemists and biochemists for the ultrahigh detection, sensitivity, and high molecular weight specificity has been mass spectrometry [118]. The mass spectrometry was initially conceptualized by Sir Joseph J. Thomson [119] in 1897 through his cathode ray tube experiments in which he measured the mass-to-charge ratio of the positively charged kanal ray particles when passing the collimated beam through crossed electric and magnetic fields. The actual work credited to the concept of mass spectrometry was conducted on the analysis of positive rays with a parabola mass spectrograph. The field continued with the discovery of new isotopes and determination of their relative abundances and exact masses.

The uniqueness of mass spectrometry as an analytical tool is due to the several unique capabilities [120]. The analytical technique determines the molecular mass and structure of fragment ions. It also provides for ultra high detection sensitivities in the attomole and zeptomole ranges. The analytical technique can be used for a variety of analytes that includes volatile or nonvolatile, polar or nonpolar, as well as solid, liquid, or gaseous materials

Mass spectrometry measures the masses of individual analytes that are converted into molecules in the gas phase ionic species capable of being manipulated by their motions and can be detected. The energy that is generated during the ionization process promotes fragmentation with the exception of soft ionization processes as electrospray and matrix assisted laser

desorption ionization. The mass analyzer is required to separate the molecular ions and their fragments according to their mass to charge ratios. The current used to generate the masses is detected by a suitable detector and a mass spectrum is displayed. The ions that are generated must move freely without collision or interactions so that a high vacuum is necessary [120]. Originally, mass spectrometers were restricted to small thermostable compounds due to lack of effective techniques to ionize and transfer ionized molecules from condensed phase into the gas phase without excessive fragmentation of molecular ions of intact bimolecular [121].

Proteomics involves the systematic analysis of all the proteins in a tissue or cell which has mass spectrometry as the central strategy for identification and amino sequencing. Mass spectrometers typically consist of an ion source, mass analyzer, and a detector that registers the ions mass to charge (m/z) ratio. Two ionization techniques that are commonly used to volatilize and ionize proteins and peptides for mass spectrometric analyses are matrix assisted laser desorption ionization (MALDI) and electrospray ionization (ESI) [122].

1.3.4.1 Matrix Assisted Laser Desorption Ionization (MALDI)

MALDI was first introduced in 1988 [123] and has become a popular tool for peptides, proteins, and other biomolecules such as oligonucleotides, carbohydrates, natural products, and lipids. MALDI is advantageous for the analysis of biomolecules due to its nondestructive vaporization and ionization of both large and small biomolecules. In this analysis the analyte is first co-crystallized with a large molar excess of matrix compound that normally consists of a UV absorbing weak organic acid that is irradiated with a pulsed UV laser and results in the vaporization of the matrix that carries the analyte with it. The matrix absorbs the energy from the laser source and serves and a proton donor and receptor which ultimately ionizes the analyte in both positive and negative ionization modes [124]. MALDI technique mixes the analyte with

a suitable matrix compound in ratios ranging from 1000 to 10,000 times molar excess in an organic solvent which upon evaporation co-crystallization occurs. The crystallized surface is exposed to an ultraviolet laser devices such as Nd-YAG laser (Yttrium-aluminum-garnet-crystals doped with neodymium) for pulse durations of about 5-15 ns and at wave lengths of 266 or 355 nm or a N_2 –laser at a wavelength of 337 nm with a pulse duration of 1-5 ns, in a high vacuum ion source. The matrix typically absorbs the energy from the laser, ionizes and then dissociates. A solid phase change to a supercompressed gas and the ions assume a charge that protonates the analyte (Figure1.4) [125-127].

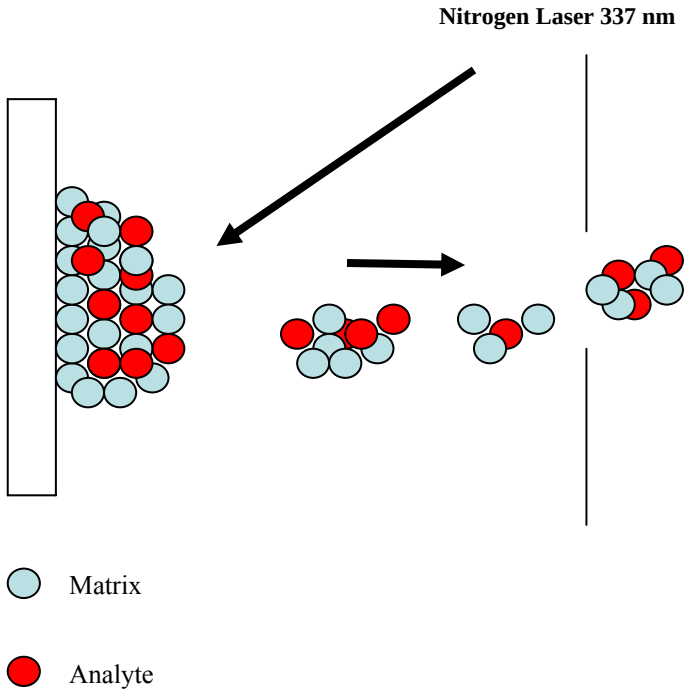

Figure 1.4 Matrix assisted laser desorption ionization concept producing gaseous phase ions with a nitrogen laser

1.3.4.2 Electrospray Ionization

Electrospray ionization is a soft ionization technique applicable to a large array of compounds present in liquid. It is beneficial in the analysis and characterization of biomolecules and their noncovalent interactions. This technique is unique due to its capability to interface with high performance liquid chromatography, capillary electrophoresis [128] and numerous other separation techniques [129]. ESI draws on its popular use due to continuous-flow operation, tolerance to different types of solvents (such as acetonitrile, methanol, water, etc), variability of flow rates, and the unique characteristic of generating intact multiply charged ions of fragile chemical and biological analytes. The use of this technique occurs as an atmospheric pressure ionization process.

Electrospray is a technique that allows the transfer of solution phase ions to the gas phase. Ions in electrospray may be singly or multiply charged inorganic ions, (2) the alkaline earth ions; (3) singly and doubly charged transition metal ions; (4) anions of inorganic and organic acids;(5) singly and multiply charged protonated organic bases; and (6) singly and multiply deprotonated organic acids or organophosphates [130]. Solvents may include polar solvents such as water, methanol, or ethanol and aprotic solvents such as acetone, acetonitrile, and dimethyl sulfoxide [130].

The first ESI experiments generated gas phase ions from electrically charged liquids droplets resulting from electrospraying the solution of an analyte at atmospheric pressure [131]. Fenn and co-workers [132] further established the technique to mass spectrometry. Additional efforts were used in the developed in the use of ESIMS for biomolecules in which the

biopolymers with a mass range of over 100 kDa was determined with mass accuracies of >.01% [133-135].

The electrospray ionization process has various designs and operations for the analysis of peptides and proteins; however the most basic design is illustrated in Figure 1.6. In the ionization process of peptides, a solution of an acidic aqueous media containing the peptide or protein is sprayed or aspirated through a small diameter needle. A high voltage, usually at a maximum of 4 kilovolts, is applied to this needle that produces what is termed a Taylor cone from which droplets of the solution are emitted. As the ions drift downfield towards the meniscus of the liquid, negative ions move towards the center away from the surface. During these conditions, the mutual repulsion between the positive ions at the surface overcomes the surface tension of the liquid causing the surface to expand allowing the ions to move downfield. The cone emerges as a fine jet mist which breaks up into small charged droplets. Protons emanating from the acidic and the peptides produce positive charges that are attracted towards the plate from the instrument [136].

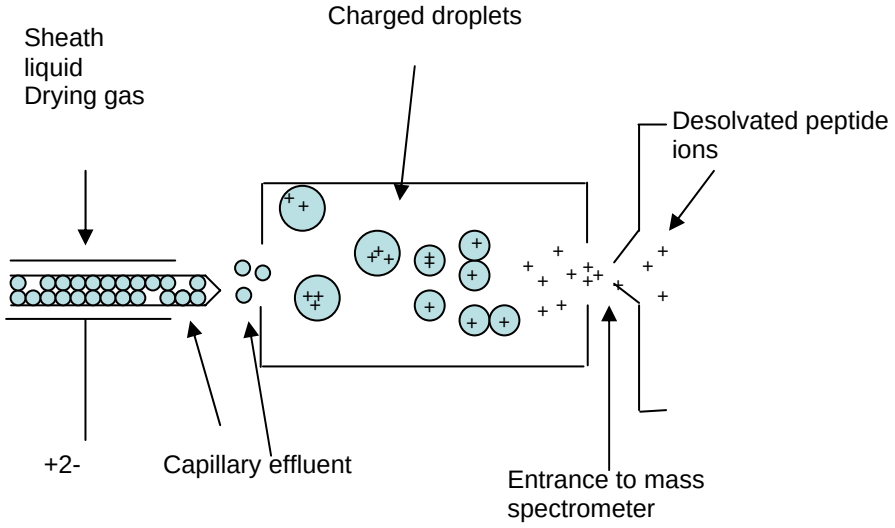

Figure 1.5 Electrospray ionization process demonstration of charged droplets generation of gaseous desolvated peptides

Pfeifer and Hendricks [137] have applied equations to predict the dependence of the current, radius and the charge of the droplets. As droplets are produced by the solvent and charged ionic species, a reduction in the number of aspirated analytes is observed due to solvent evaporation under atmospheric conditions under constant charge. The energy needed for the elimination of some of the molecules is provided by the thermal energy of the air. The charges of the droplets are constant as a consequence of the emission of ions from the solution in the gas phase and are highly endogeric [137].

The radius R of the droplet is decreased at a constant charge q that leads to an increase in the electrostatic repulsion of the charges at the surface until the droplets reach the Rayleigh stability limit [130]:

$$q = 8\pi (\varepsilon_0 \gamma R^3)^{1/2} \qquad (1.15)$$

where :

q = the charge of the droplet

ε = permittivity of the vacuum

γ = surface tension of solvent

R = radius of droplets produced

The equation provides the conditions at which the electrostatic repulsion equals the force due to the surface tension that holds the droplets together. The instability of the charged droplets occurs as the radius and charge are satisfied. The droplets undergo fission at a point close to the Rayleigh limit and smaller droplets are ejected. The time for droplet with radius R_0 and charge to reach a certain size R_1 is estimated with the use of expression providing the rate of solvent evaporation for small droplets involved. This phenomenon is solvent dependent so that when volatile solvents such as methanol, water, and acetonitrile are used the droplets are a few

micrometers of less in diameter and leads to a dependence of the radius of the droplet radius on the time t:

$$R = R_0 - (\alpha \upsilon p^o M/4\rho R_g T)\, t \qquad (1.16)$$

where:

υ = the average thermal velocity of the solvent vapor

p^o = the saturation vapor pressure of the solvent at the temperature of the droplet

M = molar mass of the solvent molecule

ρ = density of solvent

R_g = gas constant

T = temperature of droplet

α = condensation coefficient of solvent

1.3.4.5 Time-of-Flight Mass Analyzer (TOF)

The mass analyzer most often coupled to the MALDI is the time-of-flight mass spectrometer. As ions are generated in the ion source under a single electric field a constant kinetic energy can obtained and passes a drift region at a certain time. The kinetic energy of the ions is given by:

$$KE = mv^2/2 \text{ and} \qquad (1.17)$$

$$KE = zeV_s \qquad (1.18)$$

Thus, the equation then can be given as:

$$mv^2/2 = zeV_s \qquad (1.19)$$

Where m is the mass of the ion, v is the velocity, z is the unit of charge, e is the charge of a proton, and V_s is the accelerating voltage.

The time required to drift through the flight tube can described as:

$$t = d/v \quad (1.20)$$

where t denotes the time, d is the flight distance and v is the velocity.

Replacing v by the value in 3.1 gives:

$$t^2 = m / z\ (d^2/V_s e) \quad (1.21)$$

The relationship indicates that the m/z (mass to charge) can be calculated from a measurement of t^2 provided the term in parenthesis is constant. The mass range in the linear time of flight instrument can be calculated from the above equation and in theory has no mass limit making the method suitable for soft ionization of biomolecules [138].

Linear TOF instruments have been regarded as low resolution techniques due to the spread of velocities of the ions that are ejected from the target. The resolution can be defined in the equation:

$$R = m / \Delta m = t/2\Delta t \quad (1.22)$$

where m is the difference in mass between the m and m+1 peaks and the Δt is the width of an ion packet of constant mass.

Additionally, large background peaks arise for the products from unimolecular decay in the flight tube. The resolution can be improved by using an electrostatic mirror in a reflectron mass analyzer. The initial kinetic energy dispersion of ions can be compensated by using the reflectron. The relationship of the flight times in the reflectron can be defined as:

$$t = (m/2eV)^{1/2}[L_1 + L_2 + 4d] \quad (1.23)$$

where L_1 and L_2 are the lengths of the drift regions and d is the distance the ion traveled in the reflectron mirror. Figure 1.6 illustrates the differences between the two modes of MALDI instrumentation. The majority of information in the field of proteomics provided by MALDI-

TOF analysis results from proteins excised gel bands or spots that are subjected to reduction, alkylation, and finally enzymatic digestin with trypsin. The peptides must be effectively digested and extracted from the polyacrylamide matris of 2DE.

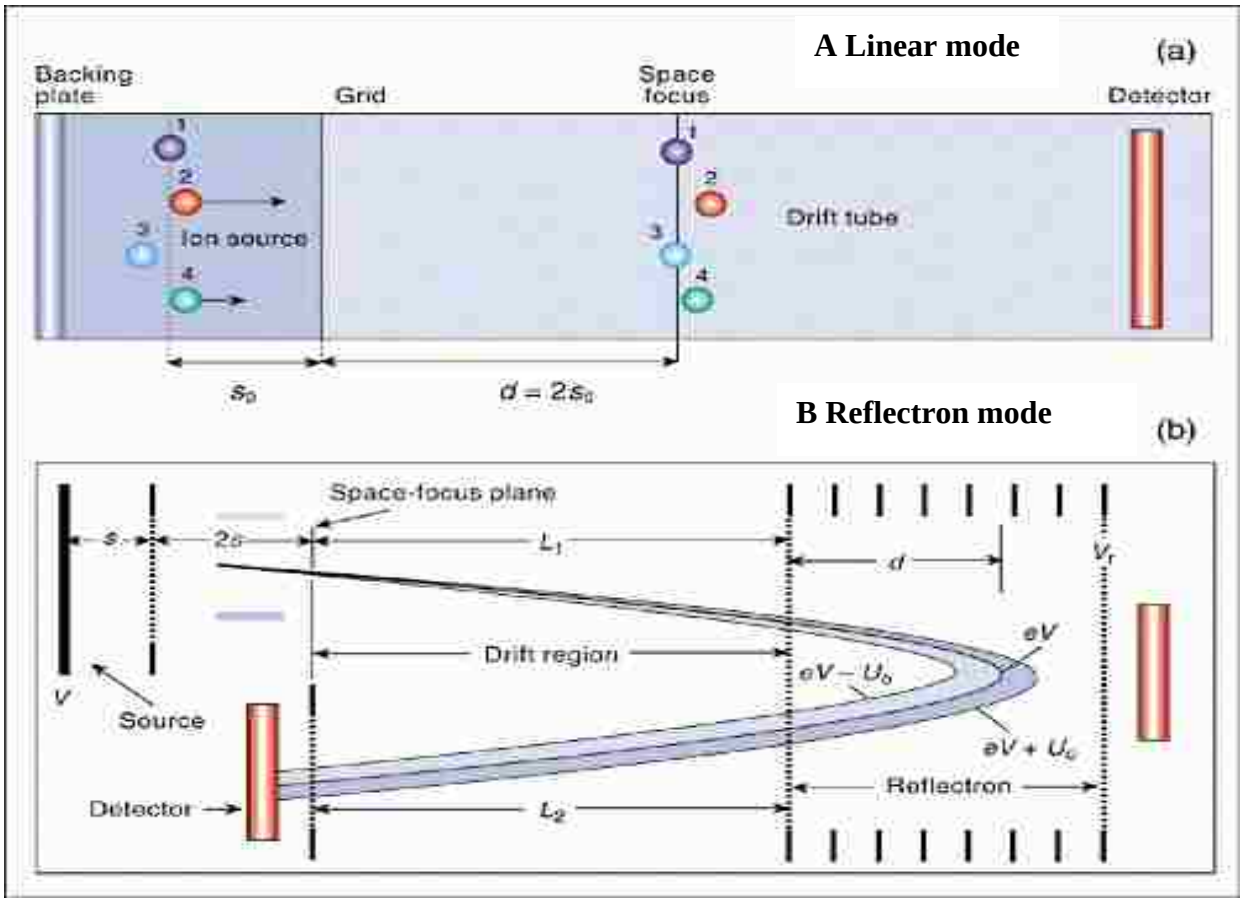

Figure 1.6 Time-of-flight mass analyzer. A) Linear mode B) Reflectron mode

Trypsin, the main protease used in the digested process is present in the gel at concentrations significantly below the Michaelis constant of the enzyme. Other proteases commonly used in proteomics are listed in Table 5. Peptide masses obtained in the initial elucidation of the molecular structure of the protein may consist of average masses; however, for high mass accuracy, monoisotopic masses are needed.

Table 1.6 Methods of enzyme cleavages of proteins for proteomics

Method of Protein Cleavage	**Site of Cleavage**	**Exception**	**pH Range**
Trypsin	C-Terminus of Lysine and Arginine	Proline	7-8
Endoproteinase Glu-C (V8-DE)	C-Terminus of Glutamic and Aspartic Acid	Proline	4-8
Chymotrypsin	C-Terminus of F.Y,W,L,I,V,M	Proline	7.5-8.5
Endoproteinase Lysine-C	C-Terminus of Lysine	Proline	8.5-8.8
Arginine-C	C-Terminus of Arginine	Proline	7.5-8.5
Elastase	Non Specific C-Terminus of G.A,S,V,L,I		8-8.5
Pepsin	C-Terminus F.L.E		2-4
Pronase	Any Peptide		7-8

Peptide masses acquired through tryptic digest for MALDI-MS require the use of highly developed databases containing amino acid sequences or peptide finger print matching to achieve positive identification of the proteins of interest. Algorithms [139-141] for the identification of proteins by mass spectrometry data is matched to a database. Using this method, a mass fingerprint of the peptides is obtained and compared to the expected tryptic peptide masses for each entry in the database. The resulting proteins can be ranked according to the number of peptide matches and scoring algorithms which considers the mass accuracy and the percentage of the protein sequence covered calculates a level of confidence of the match [142]. High mass

accuracy (10 to 50 ppm) with at least five peptide masses as a rule is needed for positive protein matches and 15% of the protein sequence coverage for an unambiguous identification. One drawback of using peptide mass fingerprinting occurs when protein mixtures are found in one spot. The mixture is converted to peptides and adds to the complexity of identifying proteins.

1.3.4.6 Quadrupole Mass Analyzer

The quadrupole mass analyzer is one of the most widely used mass spectrometer that separates masses of analytes based on electric field parameters. Ion trajectories are the basis in which the quadrupole operate and are controlled by a set of time-dependent forces generated by the application of direct and radiofrequency potentials to a set of electrodes. The quadrupole is two dimensional field device consisting of four rods aligned parallel arranged in a square array. A field is created in the rods by connecting opposite pairs. As ions are injected from one in the direction of the quadrupoles (z direction), those with very narrow m/z ranges produce stable ranges and their motion is confined with the field defined by the electrode. These ions are detected; however, unstable ions are not due to trajectories in the quadrupoles.

The field induced by the quadrupole is supplied by a direct current potential U and a superimposed radiofrequency (rf) potential V cos ωt (U-V cosωt) to one pair of rods (where ω is the angular frequency related to the frequency *f,* in hertz, by $\omega = 2\pi f$, V the amplitude of rf voltage, and t the time). The rods at the opposing end possess the opposite dc potential (-U) and rf potential with the same magnitude but out of phase by 180º (-U-Vcosωt). An oscillating field is created such that the potential at any given point within the rods is given by:

$$\Phi (x,y) = \Phi\, x^2 - y^2 / r^2_0 \qquad (1.24)$$

where Φ_0, is the applied potential that is equal to U-Vcosωt, r_0 the inscribed radius located between the rods and x and y represents the distances from the center of the field.

1.3.4.7 Ion Trap Mass Analyzer

Ion trap (IT) mass spectrometers are used in the detection of biomolecules; however the principle of analysis varies from the beam-type instruments. The quadrupole ion trap is a three dimensional analogue of the linear quadrupole mass filter [143]. Ions are in the presence of forces induced by an applied RF field that is applied in three directions. The ions in the trap have no degrees of freedom and are trapped within the three ring electrode and two end cap electrodes of hyperbolic cross sections. IT actually store and manipulate ions in time rather than space with central electrodes at two ends. At one of the end cap electrode, a small opening gated allows electron beams to enter the trap. This can produce in situ ionization of the sample molecules. The other cap electrode usually has perforations through which ions escape for detection [129]. The ions contained in the trap are stable in the r and z direction whose exact position is depicted by the Mathieu stability diagram. The motion of the ions in the r and z directions may be described in by the solutions of the Mathieu equation below:

$$a_z = -2ar = -16zU/m(r^2 + 2z^2)\omega^2 \quad (1.25)$$

$$q_z = -2q_z = 8zV/m(r^2 + 2z^2)\omega^2 \quad (1.26)$$

where a_z and q_z represent the Mathieu parameters, U the dc potential, V the rf potential applied between the ring and end cap electrodes, ω is the angular frequency. The radial stability of the ions in the trap is expressed by az and qz and must be maintained at the same time with the stability in the z direction. The optimum operation of the trap requires that the ions initial conditions of the ion are favorable by using a helium buffer gas to remove kinetic energy form the ions and cause them to exist in the central core of the trap. To obtain mass spectra the quadrupole is operated in an unstable scan mode condition by increasing the amplitude V of the applied rf that move the ions in the q_z direction until the boundaries are reached to give a value

of q_z = .908. When this region of instability is reached, the kinetic energy of the ions and z direction excursions increase resulting in the ions leaving the trap in the end-cap electrode where the detector is located. The mass analysis of the trap can be obtained by rearranging the Mathieu parameter q_z that can be represented by the following equation:

$$m/z = 8V / q_z (r2 + 2z2)\omega^2 \qquad (1.27)$$

Application of appropriate dc and rf voltages to the electrodes produces ions of a broad m/z range that are trapped with in the boundaries of the electrodes.

IT possesses the capability of providing multiple stages of MS with high sensitivity and fast data acquisition. The mass analyzers allow high throughput; however limited resolution anad low ion trapping results in mass measurements that lack mass accuracy [144]. Ion traps allow isolation of only one ion species while ejecting others from the trap. The ion can fragment by collisional induced dissociation and be detected or multiple fragmentations can be performed without the need for multiple analyzers.

Traditional quadrupole ion traps are widely used for proteomics; however their developmental use for the identification of cellular proteomes is limited. This limitation is due to the complexity of samples in the proteomes analysis where thousands of proteins and peptides may be eluted. A slow scan rate and limited ion capacity and trapping efficiency is observed. [145].

To enhance the capability of the quadrupole ion trap mass analyzer, a novel design was introduced by Schartz [145]. The linear quadrupole trap or 2D trap is composed of a quadrupole with four hyperbolic cross-sectional rods giving it linear features. Ions in the LIT are trapped in an axial fashion as opposed to central trapping in the 3D trap. Linear ion traps (LIT) higher trapping capacities expand the dynamic range and the overall sensitivity of 3-D traps. The LIT

have an optional slow scanning function that increases resolution and a multiple stage sequential MS/MS capability in which fragment ions are isolated and further fragmented. This is useful for the analysis of post translational modifications such as phosphorylation [146]. The utility and performance of the 2D ion trap mass spectrometer in proteomic analyses has been compared by Mayya [147] and Blackler [148]. The 2D trap is operated analogous to the ion trap however several advantages can be observed with respect to performance characteristics [146]. The linear quadrupole has no rf field in the ion injection axis for the ions to overcome before entering the trap improving the trapping efficiency. The linear configuration of the mass analyzer provides a larger volume improves the overall ion capacity before space charge effects can be achieved. The increased ion capacity is enhanced by the ability of the trap to eject ions radially on each side as opposed to the axial direction. Two detectors can be used resulting in a two-fold increase in detection efficiency.

1.3.4.8 Fourier Transform Ion Cyclotron Resonance Mass Analyzer

The quantitative identification of proteins in low part per million ranges can be achieved using the Fourier Transform ion cyclotron resonance mass spectrometer. Fourier transform resonance mass spectrometry (FTICRMS / FTMS) is a unique mass analyzer due to its capability for high mass, high resolution, and multiple detectors. Advantages can be observed in high mass accuracy, multistage tandem mass spectrometry, and ability to trap ions for extended periods of time. The analyzers can be useful for ion molecule reaction as well as structure elucidation studies [129].

The principle of ion cyclotron resonance involves several techniques occurring in the same region of space and time. The steps involve ionization, mass analysis, and detection. The takes place in a 1.0 centimeter cell that is placed in a strong magnetic field. Ions are constrained

by a magnetic and electric field. Ions placed in a magnetic field will precess at a frequency (ω_c) that is characteristic of its m/z values. The ions move in circular orbits defined by equations 1.28 and 1.29 describe the time to complete a single revolution. The cyclotron frequency, number of revolutions per second can be given by Equation 1.30:

$$t = 2\pi r / \upsilon \quad (1.28)$$

$$t = 2\pi m / z\beta \quad (1.29)$$

$$\omega_c = z\,\beta / 2\pi m \quad (1.30)$$

where t denotes the time, r is the radius, m is the mass of the ions, and ω is the cyclotron frequency which is the number of revolutions per second.

1.4 References

(1) Ross, R. *Nature* **1993**, 362, 801-809.

(2) Ross, R. *New Eng. J. Med.* **1999,** 340, 115-126.

(3) Ross, R. *New Eng. J. Med.* **1993,** 314, 488-500.

(4) Kumar, V.; Abbas, A.; Fausto, N.; Blood Vessels. In *Robbins and Cotran Pathologic Basis of Disease*, 7th ed.; Elsevier Saunders: Philadelphia, PA, **2005**; pp 511-553.

(5) Ross, R. *New Eng J Med*. **1976,** 295, 420-425.

(6) Kannel, W.B., Wilson, P.W.F. *Med. Clin. North America* 79, 951.

(7) Tracy, R.; Introduction to the Sequestration Hypothesis. In *The Role of Aging in Atherosclerosis: The sequestration hypothesis;* Kluwer Academic: Norwell, MA, **2003**; pp.1 – 11.

(8) Tracy, R. *The American Journal of Forensic Medicine and Pathology,* **1984**, 5 (1), 15-18.

(9) Chavoz, E.I.; Repin V.S.; Orekhov, A.N.; Anotov, A.S.; Preobrazhensky, S.N.; Soboleva, E.L.; Smirnov, V.N. *Atheroscl. Rev.* **1986**, 14, 7-60.

(10) Committee on Vascular Lesions of the Council on Arteriosclerosis, American American Heart Association *Arterscl. Thromb.***1992**, 12, 120-134.

(11) Committee on Vascular Lesions of the Council on Arteriosclerosis, American Heart Association, *Arterioscl. Thromb.* **1994**, 14, 840-856.

(12) Davies, M.J.; Richardson, P.D.; Woolf, N.; Mann Jr., D.R. *Br Heart J.* **1993,** 69, 377-81.

(13) Dock, W. *JAMA* **1946**, 131, 875 – 878.

(14) Dohi, Y.; Kojima, M.; Sato, K.; Luscher, T.F.; *Drugs and Aging*, **1995** 7, 278-291.

(15) Raines, R.; Ross, R. *The Journal of Nutrition* 1995, 125, 3.

(16) Ross, R.; New *Eng J Med*. **1999**, 340(2) 115-126

(17) Gimbrone, M.A. Jr.; Topper, J.N.; Nagel, T.; Anderson, K.R.; Garcia-Cardenna, G. *Ann NY Acad Sci* **2000,** 902, 239.

(18) Berk, B.C.; Abe, J.I; Mir, W.; Surapisitchat, J.; Yan, C. Ann *NY Acad Sci.* **2001**, 947, 93.

(19) Nagel, T.; Resnick, N.; Atkinson, W.T. *J Clinical Investigation* **1994**, 94,885-891

(20) Lee, R.T.; Yamamoto, C.; Feng, Y.; Potter-Perigo, S.; Briggs, W.H.; Landschulz, K.T.; Turi, T.G.; Thompson, J.F.; Libby, P.; Wight, T.N. *J Biol Chem,* **2001**, 276, 13847-13651.

(21) Ridker, P.M.; Hennekens, C.H.; Buring, J.E.; Rafia, N. *New Eng J Med.* **2000**, 342, 836-843.

(22) Ridker, P.M.; Rifal, N.; Stampfer, M.J.; Hennekens, C.H. *Circulation* **2000**, 101, 1767-1772.

(23) Harris, T.B.; Ferrucci, L.; Tracy, R.P.; Corti, M.C.; Wachholder, S.; Ettinger Jr., W.H; Heimovitz, H.; Cohen, H.J.; Wallace, R. *.Am J. Med.* **1999**, 106,506-512.

(24) Ridker.P.M.; Rifai, N.; Pfeffer, M.; Sacks, F; Lepage, S. *Circulation.* **2000** 101, 2149-2153.

(25) Ridker, P.M.; Cushman, M.; Stampfer, M.J.; Tracy, R.P.; Hennekens, C.H. *New Eng J Med.* **1997**, 336, 973-979.

(26) Haaverkate, F.; Thompson, S.G.; Pyke, S.D.; Gallimore, J.R.; Pepys, MB. *Lancet* **1997,**349, 462-466.

(27) Kuller, L.H.; Tracy, R.P.; Shaten, J.; Meilahn, E.N. *Am J Epidemiol.* **1996**, 144, 537-547.

(28) Tracy, R.P.; Lemaitre, R.N.; Psaty, B.M.; Ives, D.G.; Evans, R.W.; Cushman, M.; Meilahn, E.N.; Kuller, L.H. *Arterioscler Thromb Vasc Biol.* **1997**, 17,1121-1127.

(29) Ridker, P.M.; Buring, J.E.; Shih, J.; Matias, M.; Hennekens, C.H. *Circulation* **1998**, 98,731-733.

(30) Danesh, J.; Whincup, P.; Walker, M.; Lennon, L.;Thomson, A.; Appleby, P.; Gallimore, J.R.; Pepys, M.B. *BMJ,* **2000**,321,199-204.

(31) Koenig, W.; Sund, M.; Frohlich,M.; Fischer, H.G.; Lowel, H.; Doring, A.; Hutchinson, W.L.; Pepys, M.B. *Circulation* **1999**, 99,237-242.

(32) Libby, P.; Ridker, P.M.; Maseri, A. *Circulation* **2002**, 105, 1135–1143

(33) Berlinger, J.; Leitinger, N.; Watson, A.; Huber, J.; Fogelman, A.; Navab, M.; *Thromb Haemost.* **1997**, 78,195-199.

(34) Williams, K.J.; Tabas, I. *Curr Opin Lipidol.* **1998**, 9, 471-474.

(35) Witzum, J.L.; Berlinger, J.A. *Curr Opin Lipidol,* **1998**, 9,441-448

(36) Mathew, C.K.; van Holde, K.E.; Ahern, K.G.; Lipid Metabolism I: Fatty Acids, Triacylglycerols and Lipoproteins. Biochemistry, 3rd ed., Robin Hedyen: San Francisco, CA, 2**000**, pp 626-666.

(37) Brown, M.; Goldstein, J.L. *Science* **1986**, 232, 34-47.

(38) Steinberg, D.S. *J. Biol Chem.* **1997**, 272, 20963-20966.

(39) Goldstein, J.L.; Brown, M.S. *Ann. Rev. Biochem*. **1977**, 46, 897-930.

(40) Rapaz, J.J.; Hasler-Rapacz, J.; Taylor, K.M.; Checovich, W.J.; Atttie, A.D. *Science* **1986**, 234, 1573-1577.

(41) Lipid Research Clinics Program: The Lipid Research Clinics Coronary Primary Prevention Trial Results II, *J. Am. Med .Assoc.* **1984**, 251, 365-374.

(42) Wissler, R.W. *Ann N.Y. Acad. Sci.* **1968**, 149, 907-922.

(43) Territo, M.; Berliner, J.A.; Fogelman *J. Clin Invest* **1984**, 74, 2279-2284

(44) Steinberg, D.; Parthasarathy, S.; Carew, J.; Khoo, J.C.; Witzum; J.L.; *New Engl J. Med*. **1989**, 320 ,915-924.

(45) Lusis, Aldons J. *Nature* **2000**, 7,233-241.

(46) Stary, H.C.; Blankenhorn, D.H.; Chandler, A.B.; Glagov, S.; Insull, W. Jr.; Richardson, M.; Rosenfield, M.E.; Schaffer, S.A.; Schwartz, C.J.; Wagner, W.D. *Circulation* **1992**, 85, No.1, 391-405.

(47) Stary, H.C.; Chandler, A.B.; Glagov, S.; Guyton, J.R.; Insull, W. Jr ; Rosenfield, M.E.; Schaffer, S.A.; Schwartz, C.J.; Wagner, W.D.; Wissler, R.W. *Arterioscler Thromb.* **1994**, 14, 840-856.

(48) Stary, H.C.; Dinsmore, R.E.; Fuster, V.; Glagov, S.; Insull, W.Jr; Rosenfield, M. E.; Schaffer, S.A.; Schwartz, C.J.; Wagner, W.D.; Wissler, R.W. *Arterioscler. Thromb.* **1995**, 15, 1512-1531.

(49) Abedin, M.; Tintut, Y.; Demer, L. *Arterioscler..Thromb..Vasc..Biol.* **2004**; 24, 1161-1170.

(50) Demer, L.L.; Watson, K.E.; Bostrom, K. *Trends in Cardiovasc Med.,* **1994**, 4, 45-49.

(51) Otto, C.M.; Kuusisto, J.; Reichenbach, D.D.; Gown, O.; O'Brien, K.D. *Circulation* **1994**, 90, 844-853.

(52) Anderson, HC; McGregor, D.H.; Tanimura, A. *Proc. Soc. Exp. Biol. Med.* **1983**, 172, 173-177.

(53) Giachelli, C.; Bae, N.; Lombardi, D.; Majesky, M.; Schwartz, S. *Biochem. Biophys. Res. Commun.* **1991**, 177, 867-873.

(54) Bostrom, K., Watson, K.E., Horn, S., Wortham, C., Herman, I.M., Demer, L.L., *J Clin Invest* **1993**, 91, 1800-1809.

(55) Shanahan, C.M., Cary, N.r., Metcalfe, J.C., Weissberg, P.L. *J. Clin. Inves.t* **1994**, 93, 2393-2402.

(56) Shioi, A.; Nishizawa, Y.; Jono, S.; Koyama, H.; Hosoi, M.; Mori; H. *Arterio. Thromb. Vasc. Biol.* **1995**, 15, 2003-2009.

(57) Jeziorska, M.; McCollum, C.; Wooley, D.E. *J. Pathol.* **1998**, 185, 10-17.

(58) Frangogiannis, N.G.; Lindsey, M.L.; Michael, L.H.; Youker, K.A.; Bressler, R.B.; Mendoza, L.H.; Spengler, R.N.; Smith, C.W.; Entman, M.L. *Circulation* **1998,** 98:699-710.

(59) Tetlow, L.C. *Ann Rhem Dis* **1995**, 54,896-903.

(60) Shepro, D. *FASEB J.* **1993**, 1031-1038.

(61) Kumamoto, M. *Hum. Pathol.* **1995**, 26, 450-456.

(62) Bobryshev, Y.V.; Lord, R.S.A. *Acta. Histo. Chem. Cytochem.* **1995**, 28, 371-380.

(63) Wozney, J.M., et al. *Science* **1988**, 242, 1528-1534.

(64) Wallin, R.; Cain, D.; Sane D.C., *Thromb. Haemost.* **1999**, 82, 1764-1767.

(65) Shanahan, C.M.; Proudfoot, D.; Farzaneh-Far, A.; Weissberg, P.L. *Critical Rev Eurkary Gene Express*, **1998**, 8, 3&4, 357 -375.

(66) Fraser, J.D.; Price, P.A. *J. Biol. Chem.* **1998**, 263, 11033-11036.

(67) Shanahan, C.M.; Weissberg, P.L.; Metcalf, J.C. *Circ. Res.* **1993**, 73,193-204.

(68) Candela, M.L.; Price, P.A. *Endocrinology* **1992**, 130,102-108.

(69) Barone, L.M.; Owen, T.A.; Tassinari, M.S.; Bortell, R.;Stein,G.S.; Lian, J.B. *J. Cell. Biochem* **1991**, 46, 351-365.

(70) Barone, L.M.; Aronow, M.A.; Tassinari, M.S.; Conlon, D.; Canalis, E.; Stein,G.S.; Lian, B. *J. Cell. Physiol.* **1994**, 160, 255-264.

(71) Baudet, C.; Perret, E.; Delpech, B.; Kaghad, M.; Brachet, P.; Wion, D.; Caput, D. *Cell Death. Diff.* **1998**, 5,116-125.

(72) Briehl, M.M., Miesfeld, R.L.M. *Endocrinol*. **1991**, 5, 1318-1388

(73) Bobryshev, Y.V.; Lord, R.S.A.; Warren, B. *Atherosclerosis,* **1995**, 118, 119-21

(74) Hirota, S., Asada, H., Kohn, K., Tsukamoto, Y., Ito, A., Yoshkawa, K., Xu, Z., Numura, S., Kitamura, Y. *J. Invest. Dermatol*. **1995**, 105, 138-142.

(75) Consden, R.; Gordon, A.H.; Martin, A.J.P. *Biochem. J.* **1946**, 40, 33

(76) Smithies, O. *Biochem. J.* **1955**, 61,629.

(77) Ornstein, L. *Ann.N.Y.Acad Sci.,* **1964,** 121,321.

(78) Davis, B.J. *Ann. N.Y. Acad Sci*., **1964**, 121,404.

(79) Maizel, J.V.; Fundamental Techniques in Virology, Academic Press

(80) Colin, F.S.; Whittaker, M. eds. *Basic theory of electrophoresis: definitions, terminology and comparison of the basic techniques* ; Electrophoretic Techniques **1969**,1-25.

(81) Raymond, S.; Nakamichi, M. *Anal. Biochem* **1962**, 3, 23.

(82) Simpson, R., SDS PAGE of Proteins. In *Proteins and Proteomics A Laboratory Manual*. Cold Springs Harbor Laboratory Press, Cold Spring Harbor, NY, p. 52.

(83) Ibel, K.; May, R.P.; Kirschner, K.; Szadkowski, H.; Mascher, E.; Lurdahl, P. *Eur. J. Biochem.* **1990**, 190, 311-318.

(84) Laemmli, U.K. *Nature*, **1970**, 227, 680-685.

(85) Toombs, M.P. *Biochem. J.* **1965,** 96,119.

(86) Rodbard, D.; Chrambach, A. *Proc. Nat. Acad, Sci. USA,* **1970,** 65,970.

(87) Righetti.P.G.; Brost, B.C.; Snyder, R.S. J. *Biochem. Biophys. Methods* **1981**, 4, 347.

(88) Chrambach, A. The Practice of Quantitative Gel Electrophoresis, VCH, Weinheim. **1965**, 1.

(89) Allen, R.C.; Graves, G.M. *Biotechnology* **1990,** 8, 1288.

(90) Chrambach, A., Rodbard, D. *Science,* **1971**, 172,440.

(91) Ferguson, K.A. *Metabolism* **1964,** 13,985.

(92) Rodbard, D.; Chrambach, A.; Allen R.C.; Maurer, H.R. (eds) Electrophoresis and Isoelectric Focusing on Polyacrylamide Gel, de Gruyter, Berlin, **1974**, 28.

(93) Rabilloud, T. *Anal. Chem.* **2000,** 72, 48A-55A.

(94) Neuhoff, V.; Arold, N.; Taube, D.; Ehradt, W. *Electrophoresis*, **1988**, 9, 255-262.

(95) Neuhoff, V.; Stamm, R.; Pardowitz, I.; Arold, N.; Ehrhardt, W.; Taube, D. *Electrophoresis*, **1990**, 11, 101-117.

(96) Patton, W.F. *Electrophoresis* **2000**, 21, 1123-1144.

(97) Riboullard, T.; Vuillard, L.; Gilly, C.; Lawrence, J.J. *Cell. Mol. Biol.* **1994b**, 40, 57-75.

(98) Schevchenko, A.; Wilm, M; Vorm, O.; Mann, M. *Anal Chem* **1996**, 68, 850-858.

(99) O'Farrell, P.H. *J. Biol. Chem*. **1975**, 250, 4007-4021.

(100) Bjellqvist, B.; Ek, K.; Righetti, P.G.; Gianazza, E., Gorg, A. Westermeier, R.; Postel, W.; *J. Biochem. Biophys. Methods* **1982**, 6, 317-339.

(101) Bjellqvist, B.; Sanchez, J.C.; Pasquali, C.; Ravier, F.; Paquet, N.; Frutiger, S.; Hughes, G.J.; Hochstrasser, D. *Electrohoresis*, **1993**, 14, 1375-1378.

(102) Robilloud, T.; Valette, C.; Lawrence, J.J. *Electrophoresis*, **1994**, 15, 1552-1558.

(103) Sanchez, J.C.; Rouge, V.; Pisteur, M.; Ravier, F.; Tonella, L.; Moosmayer, M.; Wilkins, M.R.; Hochstrasser, D.F. *Electrophoresis*, **1997**, 18, 324-327.

(104) Robilloud, T. *Electrophoresis*, **1996**, 17,813-829.

(105) Guy, G.R.;Philip, R.; Tan, Y.H. *Electrophoresis*, **1994**, 15, 417-440.

(106) Flengsrud, R.; Kobro, G. *Anal. Biochem.,* **1989**,177,33-36.

(107) Taylor, R.S.; Wu, C.C.; Hays, L.G.; Eng, J.K.; Yates, J.R.; Howell, K.E. *Electophoresis*, **2000**, 3441-3459.

(108) Manabe, T.; Hayama, E.; Okuyama, T. **1982**, 28,824-827.

(109) Blomberg, A.; Blomberg, L.; Norbeck, J.; Fey, S.J.; Larsen, P.M.; Larsen, M.; Roepstorff, P.; Degand, H.; Boutry, M.; Posch, A.; Gorg. A. *Electrophoresis*, **1995**, 16, 1935-1945.

(110) Hurkman, W.J.; Tanaka, C. *Plant Physiol*. **1986**, 81,802-806.

(111) Marshall, T.; Williams, K.M. *Electrophoresis*, **1992**, 13,887-888.

(112) Marshall, T.; Abbott, N.J.; Fox, P.; Williams, K.M. *Electrophoresis* **1995**, 16, 28-31.

(113) Rabilloud, T.; Adessi, C.; Giraudel, A.; Lunardi, J. *Electrophoresis*, **1997**, 18, 307 -316.

(114) Musante, L.; Candiano, G.; Ghiggeri, G.M. *J. Chromatogr*. **1997**,705, 351-356.

(115) Perdew, G.H.; Schaup, H.W.; Selivonchick, D.P. *Anal. Biochem*. **1983**, 135,453-455.

(116) Molloy, M.P.; Herbert, B.R.; Walsh, B.J.; Tyler, M.I.; Traini, M.; Sanchez, J.; Hochstrasser, D.F.; William, K.L.; Gooley, A.A. *Electrophoresis*, **1998**, 19, 837-844.

(117) Santoni, V.; Rabilloud, T.; Doumas, P.; Rouquie, D.; Mansion, M.; Kieffer, S.; Garin, J.; Rossignol, M. *Electrophoresis*, **2000**, 20,705-711.

(118) Dass, C. In *Principles and Practice of Biological Spectrometry;* Desiderio, D.M., Nibbering, N.M.M. Eds. Wiley-Interscience Series on Mass Spectrometry; A John Wiley & Sons Inc. New York, **2001**; Chapters 1-5.

(119) Thomson, J.J. *Philos. Mag.* **1897**, 44,293.

(120) Melov, M.E.; Grovshkov, H.R.; Udseth, H.R.; Anderson, G.A.; Smith, R.D. *Anal Chem.*, **2000**, 72, 2271-2279.

(121) Aebersold, R. *Science*, **2006**, 312,312-317.

(122) Aebersold, R., Mann, M. *Nature* **2003**, 422, 198-207.

(123) Karas, M.; Hillenkamp, F. *Anal. Chem.* **1988**, 60, 259-280.

(124) Lewis, J.K., Wei, j., Siuzdak, G., Encyc of Anal Chem. R.A., Meyers ed. John Wiley and Sons, Inc. New York, NY pp 1-14.

(125) Bakhtur, R., Tse, F.L.S. *Mutagenesis*, **2000**, 15, 5,415-430.

(126) Jespersen, P.K.; Neissen, W.M.A.; Tjaden, U.R.; van der Greef, J. *Rapid Comm Mass Spectrom*. **1998**, 33, 1088-1093.

(127) Hillenkamp, F.; Karas, M.; Beavis, R.C.; Chait, B.T. *Anal. Chem.* **1991**, 63, 1193A-1203A.

(128) Garcia, F.; Henion, J.D. *Anal. Chem.* **1992,** 64, 985-990.

(129) Dass, C., Ionization Methods. In Principles and Practices in Biological Mass Spectrometry Desiderio, D.M., Nibbering, N.M.M., Eds. John Wiley and Sons, Inc., New York, NY **2001**, pp 37-38.

(130) Cole, R.B. Fundamental Aspects of Electrospray Ionization. In *Electrospray Ionization Mass Spectrometry, Fundamentals, Instrumentation, and Applications.* Richard Cole Ed. **1997**, John Wiley and Sons, Inc. New York, NY p.6.

(131) Dole, M.; Mack, L.L.; Hines, R.L. *J. Chem. Phys.* **1968**, 49, 2240-2249.

(132) Yamashito, M.; Fenn, J.B. *J. Phys. Chem*. **1984**, 88, 4671 – 4675.

(133) Fenn, J.B.; Mann, M.; Meng, C.K.; Wong, S.F.; Whitehouse, C.M. *Science*, **1989**, 246, 64 -71.

(134) Fenn, J.B.; Mann, M.; Meng, C.K.; Wong, S.F.; Whitehouse, C.M. *Mass Spectrom Rev*, **1990**, 9, 37-70.

(135) Smith, R.D.; Loo, J.A.; Ogorzalek, R.R.; Busman, M.; Udseth, H.R. *Mass Spectrom. Rev.* **1991**, 10, 359- 451.

(136) Kinter, M., Sherman, N.E., Fundamental Mass Spectrometry, In *Protein Sequencing and*

Identification Using Tandem Mass Spectrometry, Desiderio, D.M., Nibbering, N.M.M., John Wiley and Sons, Inc. New York, NY **2000**, p.32.

(137) Pfiefer, R.J.; Hendricks, C.D. *AIAA, J.* **1968**, 6, 496.

(138) De Hoffman, E.; Charette, J.; Stroobant, V. Mass Analyzers, In Mass Spectrometry Principles and Applications, John Wiley and Sons, Inc. New York, NY, **1996**, p. 60.

(139) Cotter, R.J.; Time-of-Flight Mass Spectrometry. In Time-of- Flight Mass Spectrometry, Cotter, R.J., Ed. American Chemical Society, Washington, DC **1994**, pp 16-48.

(140) Berndt, P., Hobohm, U., Lagen, H., *Electrophoresis,* **1999,** 20, 3521-3526.

(141) Perkins, D.N.; Pappin, D.J.; Creasy, D.M.; Cotterell, J.S. *Electrophoresis **1999,*** 20, 3551-3567.

(142) Eriksson, J.; Chait, B.T.; Fenyo, D.; *Anal Chem* **2000**, 72, 999-1005.

(143) Mann, M.; Hendrickson, R.C.; Pandey, A. *Ann. Rev. Biochem.* **2001**, 70, 437-73.

(144) Riter, L.S.; Gooding, K.M.; Hodge, B.D.; Julian Jr., R.K. *Proteomics,* **2006,** 6, 1735-40.

(145) Schwartz, J.C.; Senko, M.W.; Syka, J.E.P.; *J. Am. Soc. Mass Spectrom.* **2002,** 13,659-669.

(146) Peterman, S.M.; Dufresne, C.P.; Horning, S.; *J.Biomole Tech.* **2005,** 16, 112-124.

(147) Mayya, V.; Rezaul, K.; Cong, Y.S.; Han, D. *Mol. Cell Proteomics*, **2005,** 4(2), 214-233.

(148) Blackler, A.R.; Klammer, A.A.; MacCoss, M.J.; Wu, C.C.; *Anal. Chem.* **2006,** 78, 1337-44.

CHAPTER 2
OPTIMIZATION OF MEMBRANE PROTEIN SOLUBILIZATION IN HUMAN AORTAS USING TWO DIMENSIONAL GEL ELECTROPHORESIS

2.1 Introduction

Proteomics is defined as the analysis of protein mixtures that are derived from tissues, cells or other matrixes of complex extracts from animals or plants that contain differences in the protein expression or modifications [1]. It encompasses large scale studies of gene expression at the proteome level in areas such as protein function, characterization of post translational modifications, protein interactions and protein analysis. The detection of proteins that may be markers for numerous diseases are studied using this technique followed by mass spectrometry. Three areas best describe this technique: (1) protein microcharacterization for identification of proteins and their post translational modification; (2) comparison of differential expression proteomics in a wide range of diseases; (3) and studies of protein-protein interactions and post translational modifications [1-3].

The separation of proteins from their native environment such as in tissues, cells, or plasma presents a challenge especially when the isolation and analysis of each component is the goal of the investigation. One of the most widely used methods for isolating and characterizing protein for the tissues lysates is two dimensional gel electrophoresis. Proteins migrate in an electric field at a rate that is dependent on their conformation, size, and electric charge. O'Farrell and J. Klose used the latter of these characteristics to separate proteins in the first dimension, isoelectric focusing based on their charge [4]. The second dimension for the separation is according to molecular weight using sodium dodecyl sulfate polyacrylamide gel electrophoresis [4, 5]. The proteins are displayed as spots on *x*- and *y*-coordinates rather than

bands in one dimensional separation. As a result of this technique, thousands of proteins can be resolved that permits identification when combined further with mass spectrometry.

Isoelectric focusing method developed by O'Farrell [4] depended on carrier ampholytes generated pH gradients in polyacrylamide tube gels. The carrier ampholytes consisted of small amphoteric molecules possessing high buffering capacity near their isoelectric points (pI) [6]. When a voltage is applied, the carrier ampholytes will align according to their pI's. The buffering capacity results in a continuous pH gradient across the gel. The isoelectric point of protein is defined as the pH value at which the protein exhibits a net zero charge. At pH values above the pI, a protein carries a net negative charge and carries a net positive charge at pH values below the pI. When proteins are placed in a pH gradient under an electric field, they migrate to the pH value where no net charge occurs which is the pI for the molecule. The use of carrier ampholytes is limited for several reasons including batch to batch variability, instability with tendencies to cause drifting towards the cathode with time, and the difficulty in working with soft acrylamide gels in tubes [6].

The development of immobilized pH gradients (IPG) for isoelectric focusing by Bjellqvist et al. [7] incorporated acrylamido buffers into a polyacrylamide gel at the time it is cast. The polymer is placed onto a plastic backing and then placed onto strips with various pH gradients. The pH range used for most studies is usually from 3-10; however, narrower ranges are available depending on the range of the analytes.

Our study is aimed at the investigation of the separation and differentiation of proteins that are components of thoracic aortas in diseased and nondiseased states. The pathogenesis of atherosclerosis occurs in the membrane lining the vessels that carry the blood supply to the heart. The membranes affected by the disease in the coronary artery and aortas are the intima, the

media, and the adventita. The site of disease or plaque formation for atherosclerosis is predominantly located in the intimal membrane. When extensive thrombosis or plaques are formed the intima and media are indistinguishable. The membrane proteins, which are components of the two diseased tissues, are highly hydrophobic and present solubility problems in IPG dry strips. Overcoming these barriers require an analysis of proteins solubility and methods that disaggregate the molecules for inclusion into the polyacrylamide gels.

To achieve solubilization of membrane proteins in addition to high resolution on polyacrylamide gels, disruption of molecular interactions is necessary to obtain single polypeptides that are essential throughout the separation process. Proteins fold by covalent and noncovalent interactions in their native state. Molecular interactions through covalent linkages of cysteine residues are the strongest while weaker forces or noncovalent forces consist of Van der Waals forces such as hydrogen bonding, ionic bonds, and other hydrophobic interactions [8]. Complete solubility of proteins for isoelectric focusing (IEF) must be achieved by disaggregation, denaturation, and reduction.

During the denaturation process, sodium dodecylsulfate (SDS) disrupts hydrogen bonding, blocks hydrophobic interactions, and partially unfolds the protein and eliminates secondary and tertiary structures. The process of using SDS in gel electrophoresis is performed by heating the sample in concentrations of 2% (w/v) or higher in the presence of 2-mercaptoethanol. The use of SDS however is limited in IEF in the first dimension. As the solubilization process occurs, simultaneous goals that must be achieved are: breaking macromolecular interactions to yield separate polypeptide chains, preventing artefactual modifications of the polypeptides during the solubilization medium, removal of substances that may interfere with 2DE and maintaining the protein in solution during the entire process [10].

Many compounds that bind to proteins and interfere with the electrophoretic process must be eliminated if their amounts exceed a critical interference threshold. These compounds include salts, lipids, polysaccharides and nucleic acids [10]. Salts are disruptive in the electrophoresis of proteins by producing joule heating as they migrate through the pH gradient and accumulate at both the cathode and electrode. The accumulation produces high conductivity zones that depend on the quantity of salts in the sample. Low electric fields are present due to high conductivity and voltage drops. Protein focusing is affected and appears as streaks interfering with resolution. Detergents in 2DE must have a zero net charge and must be either nonionic or zwitterionic. Ionic detergents such as SDS can be tolerated in the initial solubilisation; however, lower amounts are necessary for effective separation during IEF. SDS must be diluted with nonionic or zwitterionic surfactant to reduce its final concentration to approximately 0.25%. The reduction of SDS for tolerable IEF similarly reduces the amount of protein loading and increases losses for separation.

Reagents to overcome restrictive uses of SDS were developed that proved to be amenable to 2D separation for protein solubilization. The alternative process involved a multiple approach to protein solubility with chaotropes, surfactants, reducing agents and alkylating agents [6]. Urea is a choice of chaotrope that is commonly used as a replacement for SDS in concentrations range of 7-9M. Thiourea at a concentration of 2M is also used in combination with urea to enhance the solubility of membrane proteins. Several detergents have proven to be effective but the most common nonionic detergent use is (3-[3-cholamidopropyl)dimethylammonio]-1-propane sulfonate) (CHAPS). Detergents are useful in 2DE to prevent hydrophobic interactions between the hydrophobic protein domains as well as avoiding loss of proteins due to aggregation and precipitation [7]. The more commonly used ionic detergents for protein solubilization include Triton X-100, Nonidet P-40, dodecyl maltoside and some phosphines. Those detergents that are

more effective for hydrophobic membranes proteins are CHAPS, sulfobetaines as SB-10 or ASB-14 which show compatibility with urea and thiourea.

A reducing agent for disulfide bonds and prevention of reoxidation is a critical step in the preparation for IEF. The agents are necessary for cleavage of intra and intermolecular disulfide bonds that promotes complete unfolding of the protein. The more commonly used reductants for IEF are dithiothretol and dithioerythritol. The choice however is predominantly sample specific [8].

The most efficient techniques of 2DE may be achieved by optimizing each component in the extraction or sampled preparation steps. Our study was focused on the methods of optimization of the choatrope, detergent, and the reductant as well as the use of IPG buffer for solubilization of highly membrane protein for maximum spot detection in the gels. Few systematic studies were found that reported the concentrations of the critical ingredients for protein solubilization in biological components. The use of Taguchi method is well known in the development of industrial processes and recently in the life sciences [9, 10]

To find the optimal and most robust conditions for 2DE a designed study was conducted similar to the Taguchi method in the characterization of proteins that were bound to chromatin at defined stages of the cell cycle in cell free extracts derived from Xenopus eggs [11]. The use of tissue from a heterogeneous surface of human aortas or arteries would be irreproducible since areas that are diseased and nondiseased exist. It was necessary, by physical means, to mix the entire intimal surfaces to study the effectiveness of the solubilization process as well as produce a homogeneous matrix.

The performance of 2DE depends on the ability of proteins to become solubilized during tissue interaction with the lysis buffer. The combination of the lysis buffer concentrations is

extensive in the literature for optimum solubilization. However, there are no defined or systematic studies that address the optimum concentrations of the critical ingredients because the use of conventional methods is time consuming and investigation of one variables at a time is labor intensive and costly. There are methods particularly in industry that address multi-parametric matrices. One method is the Taguchi method that has been used for decades in the optimization of industrial processes [11]. These methods have found wide use in the biological sciences [9, 10, 12].

2.2 Research Goals and Objectives

This study investigate the influence of four variables such as IPG buffer (v/v), CHAPS (wt/v), ASB-14 (wt/v), and DTT (wt/v) at three concentration levels on membrane protein solubility using experimental design. To obtain all interactions including optimum conditions various experimental designs must be examined with emphasis on number of experiments, time constraint, and cost. The full factorial design using four variables with at three levels enables one to study the all the main effect and interactions, however, the number of experiments needed is 3^4 or 81 experiments. This exceeds the quantity, time and labor permitted for the use of the aorta and artery samples. A fraction factorial would allow the study of a reduced number of main effects from the full factorial design depending on the confounding pattern of the design. Deciding the interactions are of importance for optimum responses may not produce the optimum conditions. The Plackett Burmann designs enable the study of the main effects and may be used only for screening purposes. Central Composite experimental design is typically used to study the variables at 5 levels and can be used to investigate both the main as well as interaction effect of variables on the response. The Box-Behnken experimental design is used for optimization purposes for one or several responses with 3 to 6 design variables at three levels

(low, center, and high). The use of Box-Behnken design for the optimization involving the investigation of biological samples such as human aorta is prefereable because of the limited samples and the cost of analysis. Therefore, we used a Box-Behnken design for the optimization of lysis buffer for membrane protein solubilization of human aorta samples. The number of experiments in a Box Behnken design remains fixed based on a certain number of variables. For our study, four variables are to be monitored and three levels which gives a total of 27 runs to complete the optimization. With constraints of time of experiments, cost, and limited sample quantity per subject, the Box-Behnken gives the desired information for the biological system studied.

2.3 Experimental

2.3.1 Materials and Reagents

Urea, glycerol, glycine, thiourea, ASB -14, iodoacetamide, and Sigma Markers (for molecular standards) and guanidium hydrochloride were purchased from Sigma Aldrich Corp (St. Louis, MO USA). All of the reagents were of the highest purity and when available specified electrophoresis grade. Sodium dodecyl sulfate (SDS) was obtained from BioRad (San Diego, CA USA) for electrophoresis.

Tris(hydroxymethyl)aminomethane (TRIS) was obtained form Invitrogen (San Diego, CA USA). 3-[(3-Cholamidopropyl)dimethyl-ammonio]-1-propanesulfonate (CHAPS was purchased for Calbiochem (San CA USA). Dithiothreitol was obtained from Fluka Biochemika (Sigma Aldrich, St Louis, MO USA). Trichloroacetic acid was purchased from Fisher Scientific (Rockville MD, USA). The immobiline pH gradient dry strips, immobiline pH gradient buffer pH 3-10 NL and mineral oil, and Drystreak were obtained from GE Healthcare Inc. (Piscataway,

New Jersey USA). The colloidal blue coomassie blue stain was obtained from Invitrogen (CA USA). Methanol (HPLC grade) was obtained from EMD Chemical (City USA).

Isoelectric focusing was performed using an Ettan IPGphor unit (GE Healthcare, Piscataway, NJ USA. The gel electrophoresis in the second dimension was conducted using a BioRad Criterion electrophoresis unit with a Powerset 1000. The gels were 12 % polyacrylamide that were precast and purchased from BioRad (San Diego, CA USA).

2.3.2 Methods

Thoracic aortas and arteries from human hearts were obtained from Louisiana State University Health Science Center in New Orleans, Louisiana. The samples were frozen immediately with dry ice and stored at -70ºC until dissection. During the extraction procedure, the tissue was allowed to thaw to room temperature. The intima membrane from normal and diseased tissue was carefully removed from the media and adventitia. Approximately 250 to 350 mg of tissue was isolated then placed in liquid nitrogen and ground with a mortar and pestle into a powder. The powder was placed in lysis buffer composed of 7M urea, 2M thiourea, 2M guanidium hydrochloride with the other reagents varied according to the parameters from the design study. The temperature of the lysis was maintained at 4ºC and precaution was taken to prevent the urea containing solution not to exceed 30ºC. Tissue extract was homogenized with a Tarazen Homogeniser for 1 minute followed by sonication at 4ºC for 4 minutes. The mixture was centrifuged at 12,000 x g for 20 minutes at 20ºC in an Eppendorf 540 microcentrifuge. The supernatant was maintained at < 20ºC until the precipitation steps.

The procedure for precipitation of the cell lysates was used for optimal protein recovery and accurate assays. Acetone used in this procedure was prechilled and stored at -20ºC and kept on dry ice during the entire experimental procedure. Solutions of supernatant, acetone and

trichloroacetic acid were mixed in 1:8:1 ratio by volume. The mixture was allowed to precipitate at -20ºC for 1 hr and centrifuged at 11,500 rpm (18,000 x g) for 15 minutes at 4ºC in a microcentrifuge.

The supernatant was then discarded and washed with 1 milliliter of cold acetone followed by centrifugation at 11,500 rpm for 15 minutes at 4ºC. The supernatant was discarded and the protein pellet was dissolved in the appropriate volume of rehydration buffer containing 7M urea, 2M thiourea, 12 µl IPG buffer, 12 µl destreak reagent and 7 mg dithiothreotol. The sample was allowed to sit at room temperature for 1 hour while vortexing intermittently every ten minutes. Following protein pellet solubilization, the sample was placed in Eppendorf microcentrifuge tubes and centrifuged at 14,000 rpm for 10 minutes at room temperature. The supernatant was removed and stored at -70ºC until ready for use.

2.3.2.1 Rehydration Buffer

The selection of rehydration solution depends on the protein solubility requirement. The rehydration buffer was composed of 7M urea, 2M thiourea, 12 µl IPG buffer (pH range 3-10), 7 mg DTT, 12 µl Destreak solution, 20 µl 1% bromophenol solution. Approximately 60 µl of tissue extract was mixed carefully with 160 µl rehydration buffer without causing air entrainment. The solution was pipetted evenly into an 11 cm ceramic strip holder covering the entire length. The immobiline dry strip was carefully removed from the cover foil starting with the anodic end (+ end). Using forceps, the immobiline drystrip gel was lowered gel side down and the anodic end (+) of the strip directed toward the pointed end of the ceramic holder. With the acidic end, the strip was lowered and slide back and forth along the surface of the solution, tilting the strip holder slightly to ensure complete wetting of the gel surface. The cathodic end was lowered in the channel making sure that the gel contacts the strip holder electrodes at each

end. It is important not to allow air bubble entrainment under the strip to prevent oxidation during isoelectric focusing. The strip is overlayed with immobiline drystrip cover fluid to minimize evaporation and thus prevent urea crystallization. Cover fluid was pippetted dropwise at one end of the holder, then at the other end until the entire gel is sufficiently covered. The strip holder is covered with the plastic holder cover with pressure blocks on the underside so that good contact is made as the gel swells. The holder was placed onto the Ettan IPGphor II (GE Healthcare) platform for the rehydration protocol. The following summarizes the rehydration and focusing conditions:

IEF (Isoelectric Focusing) Conditions:

Rehydraton: 12:00 Hr at 20° C

IEF Params: 50μA/Strip at 20° C

Step 1: Step 500V 500 Vhr

Step 2: Grad 1000V 700 Vhr

Step 3: Grad 6000V 7000 Vhr

Step 4: Grad 6000V 4000 Vhr

Total Volt Hours: ≈12,000

2.3.2.2 Equilibration of Immobiline Dry Strips

Following the isoelectric focusing step, equilibration was performed immediately prior to the second-dimension run. The strip was placed in a horizontal position with the gel side up into an equilibration solution consisting of 6M urea, 75 mM Tris-HCl, pH 8.8, glycerol (30%), 100 mg of DTT to preserve the fully reduced state of denatured, unalkylated proteins and sodium dodecylsulfate (1%). The SDS denatures the protein and forms negatively charged protein SDS complexes. The drystrip was allowed to mix for 15 minutes at room temperature on a solution

rocker. Iodoacetamide (250 mg) was added to a second equilibration solution without DTT and the dry strip submerged in a horizontal position with the gel side up and shaken for an additional 15 minutes. The iodoacetamide was introduced in the second equilibration buffer to minimize unwanted reactions of cysteine residues especially during the analysis using mass spectrometry.

2.3.2.3 Second Dimension Sodium Dodecylsulfate Polyacrylamide Gel Electrophoresis

The second dimension protocol separates the proteins from the dry strip by molecular weight. The drip strip gel was equilibrated in an electrophoresis solution of 1% SDS buffer to lubricate it. A precast slab gel from BioRad for the Criterion Gel System was used with a 12.5% acrylamide concentration specially used for IPG gels. With a plastic ruler or thin forceps, the immobiline drystrip is gently pushed between the glass plates of the slab gel, ensuring that the plastic backing on the strip was placed against the longer plate. The drystrip was carefully inspected to ensure that no air bubbles are trapped between the strip and the slab gel surface or between the gel backing and the glass plate. Additionally, the the drystrip and the slab gel were cargfully connected at all points without any gaps. The drystrip was then sealed with a solution of 1% agarose to prevent the possibility of floating or moving in the electrophoresis buffer. Molecular weight markers were added to the well position on the slab gel.

The slab gel was placed into a BioRad Criterion gel electrophoresis unit followed by the addition of the running buffer. The running buffer was made by adding 30 gram of TRIS and 144 grams of glycine, and 10 grams of SDS into one liter of ultra pure 18 mohms water. This mixture is a 10X running buffer stock solution. A 1x solution was prepared and added to the appropriate chamber containing the slab gel ensuring that the liquid buffer contacts the electrodes. A setting of 200 volts was applied to the gel for 1 hour or until the bromophenol blue tracking solution migrates the full length of the gel.

After the completion of the electrophoresis run, the gel was carefully removed from the glass plates and washed three times with ultra pure deionized water. Between 50 to 100 ml of colloidal commassie blue staining solution was added to the gel and the solution was shaken on a rocker for maximum of 12 hours. The staining solution was removed and the gel was carefully washed with ultra pure deionised water. Destaining with water is continued until the background of the gel is clear and protein spots can be distinguished.

2.3.2.4 Design Study Parameters

The lysis buffer normally consists of chaoatropes, urea and thiourea, detergent(s), and reducing agent(s) and carrier ampholytes [13-15]. The range of formulations for the lysis buffer used contains 7M urea, 2M thiourea that is normally reported to give the best 2D images with the immobilized pH gradient. Guanidium hydrochloride was added to the mixture to enhance the removal of proteins in atherosclerotic plaques. The use of this reagent may be restricted because of its ionic nature and must be removed prior to applications to the IPG dry strips. A Box-Behnken design was used to simultaneously investigate the effects of the design variables (lysis buffer composition in this study) on the response (membrane protein solubility as indicated by the number of spot). The variables used for the optimization study with the Box- Behnken design consist of IPG buffer (v/v), CHAPS (w/v), DTT (w/v), and ASB-14 (wt/v). Each variable was investigated at three different levels; IPG buffer (5, 12.5, 20µl); CHAPS (10, 25, 40 mg); ASB-14 (4, 10, 16 mg); and DTT (20, 60, 100 mM). The experimental design and multivariate data analysis was performed using chemometric software, The Unsrambler (Camo, Corvallis, OR, USA, version 9.1.2). A summary of the levels of variables and number of experimental runs using the Box-Behnken design is shown in Table 2.1.

Table 2.1. Levels and range of the design variables for Box Behnken

Experiment No	Immobiline pH Gradient Buffer (µl/ml)	CHAPS (mg/ml)	ASB-14 (mg/ml)	DTT (mM)
1	20	25	10	100
2	12.5	25	10	60
3	20	25	4	60
4	12.5	10	10	100
5	12.5	40	10	60
6	12.5	25	16	20
7	12.5	40	10	20
8	5	25	16	60
9	12.5	25	16	100
10	5	40	10	60
11	5	25	10	20
12	12.5	40	4	60
13	20	40	10	60
14	12.5	25	10	60
15	5	25	4	60
16	12.5	25	4	100
17	12.5	25	16	60
18	12.5	10	4	60
19	5	25	10	100
20	12.5	10	10	20
21	12.5	25	10	60
22	5	25	16	60
23	12.5	10	16	60
24	5	10	16	60
25	20	10	10	60
26	20	25	10	20
27	12.5	25	4	20

The focusing of the sample onto the IPG strip (3-10 pH) was conducted at similar parameters for all experiments with the rehydration step run time maintained at 12 hours without any voltage applied. The entire focusing steps were performed in the ceramic sample cups. Following the rehydration step, the current for each strip was set at 50 uA per strip. A fast ramping step was necessary to increase the voltage to 500V to achieve 500 Vhrs for the initial stage. This step was followed by a gradient step to 1000V to obtain 700 Vhrs. The next gradient

steps were set to 6000V to obtain a total of 7000Vhr. A final gradient setting of 6000V was conducted to give 4000 Vhr for this step interval with the total volt-hours for the experimental runs set for 12,000 volt hours. Although variations in the IPG buffer normally require longer ramp times, it was held constant to maintain consistency in the design study. The total value of volt-hours was based on the manufacturer's suggestions for the strip length used.

Following IEF, the gel strip was prepared for SDS-PAGE by two additional preparative steps. The IPG strip was equilibrated with SDS buffer and DTT, the reductant, to prevent reoxidation. This step was followed by alkylation with iodoacetamide to alkylate cysteine residues and prevent their modification during and after SDS-PAGE. Variable alkylation can cause substantial artefactual spots on 2D gels [16-17]. Excess DTT contributes to streaking in the final gel, causing a decrease in the resolution of protein spots. An additional precipitation step composed of an acetone / trichloroacetic acid wash was necessary to remove undesirable salts, lipids, and nucleic acids that contribute to streaking and reduced resolution of protein spots.

Dithiothreitol or DTT, a commonly used reductant for 2DE, was compared to the other variables in the study. The breaking of disulfide bonds in proteins is accomplished by an equilibrium displacement process using a large excess of free thiols. Simple alkyl thiols are too volatile causing some problems in maintaining a certain concentration and possess an unpleasant odor. Much less volatile thiols are frequently used in biological applications such as β mercaptoethanol, dithioerythiol or dithiothreitol [19]. These thiols are used in high concentrations to ensure maximum displacement of the thiol-disulfide equilibrium that favors the thiol form of the protein [19]. Since the intramolecular, cyclic condensation produced during oxidation of DTT or DTE the equilibrium is driven more efficiently toward the reduction of the protein [19]. Because of this reaction, the reductant can be used at a lower concentration

(100mM or less). The drawbacks of these chemicals is due to dissolved oxygen that reoxizides the thiols into disulfides, consuming the free thiols.

2.4 Results and Discussion

The results of the number of spot obtained under various experimental conditions of lysis composition are shown in Figure 2.1. From Figure 2.1, it was apparent that lysis buffer composition has significant influence on the membrane protein solubility and the number of spot counts in 2D gel electrophoresis. The minimum number of spots (7) was obtained in experiment number 5 which corresponds to IPG , CHAPS, ASB – 14 and DTT concentrations of 12.5ul / mL, 40mg / ml, 10mg / mL, and 60mM respectively, in lysis buffer. The low number of spot count at this condition was an indication of low or poor membrane protein solubility at this lysis buffer composition. However, the maximum spot count of 130 was obtained in experimental run 23 containing lysis buffer composition of 12.5 µl / ml IPG buffer, 10 mg / ml CHAPS, 16 mg/ ml ASB – 14, and 60 mM DTT. Therefore, the optimum lysis buffer composition for protein solubilzation is at experiment 23.

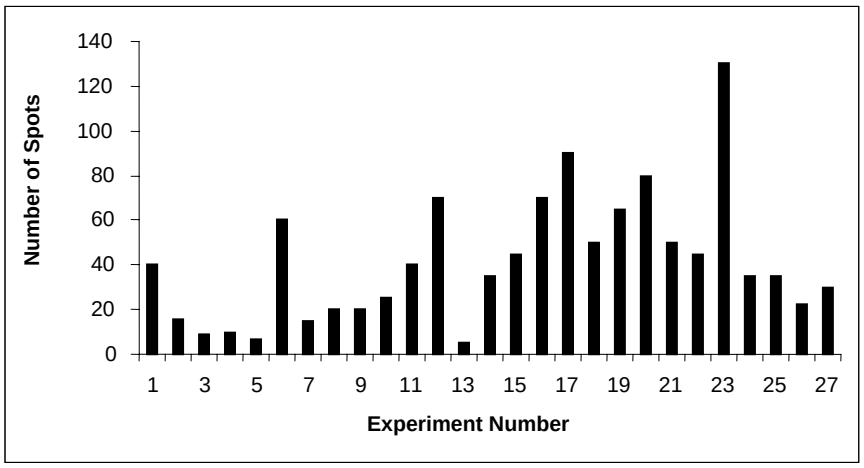

Figure 2.1 Bar plots of spot counts from gels from various conditions in the Box Behnken design study. The lowest spot count resulted from run conditions in run 5 and maximum in run 23.

Figure 2.2 is a surface response plot showing the influence of DTT concentration and CHAP concentration on the number of spots resolved on the 12% polyacryamide gel. Generally, high protein solubility (high spot count) was obtained at low CHAPS concentration in the lysis buffer. Higher protein solubility can be achieved at CHAPS concentration range of 10 to 25 mg/ml with optimal protein solubility at 10 mg/ml. In addition, the optimum condition for protein solubilization was obtained for lysis buffer containing DTT concentration of 60 mM. Low DTT concentration at 60 mM gave the best conditions to achieve high spot counts.

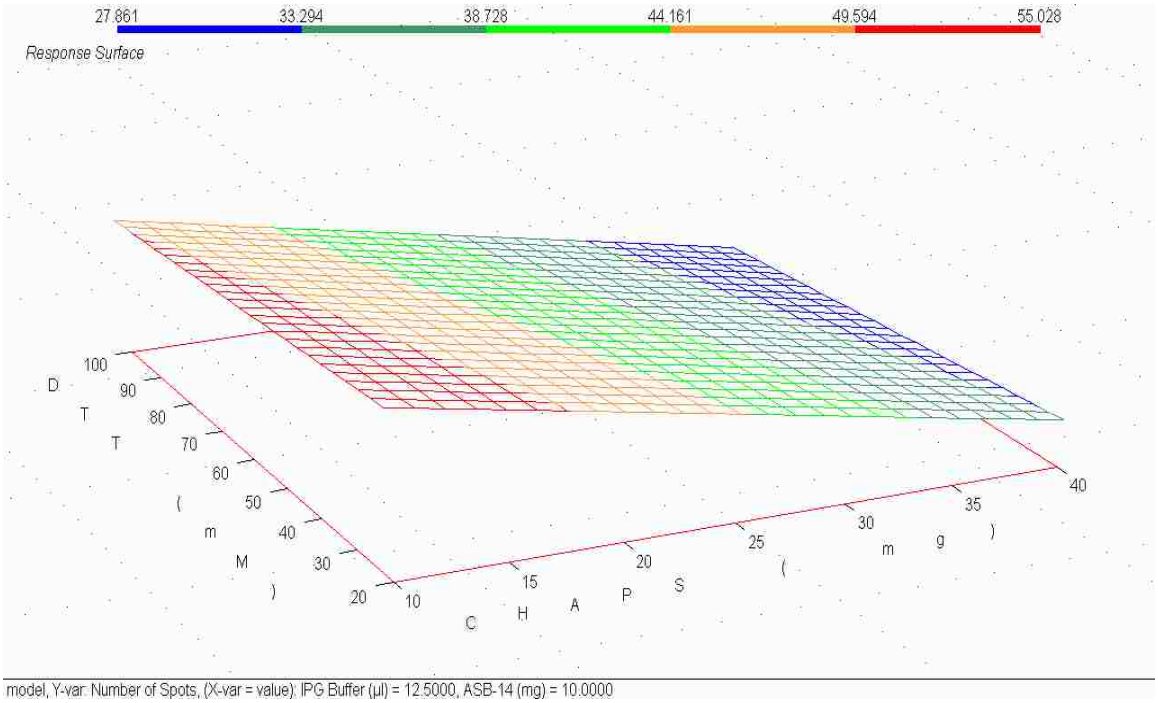

Figure 2.2 Surface response plot showing the influence of DTT and CHAPS concentration on the number of spots. Low DTT concentration at 60mM gave the best conditions for high spot count

The influence of the ASB-14 and IPG buffer concentration on the spot count response is shown in Figure 2.3. The concentration of ASB – 14 with the optimal range for the highest protein spot count was found to be from 14 to 16 mg/mL, with optimum conditions at ASB-14 concentration of 16 mg/L. High protein solubility was obtained in a lysis buffer containing IPG

buffer in the range of 5- 10 µL, with actual optimal condition for protein solubilization obtained at lysis buffer containing at 12.5 µL/ m/l of IPG.

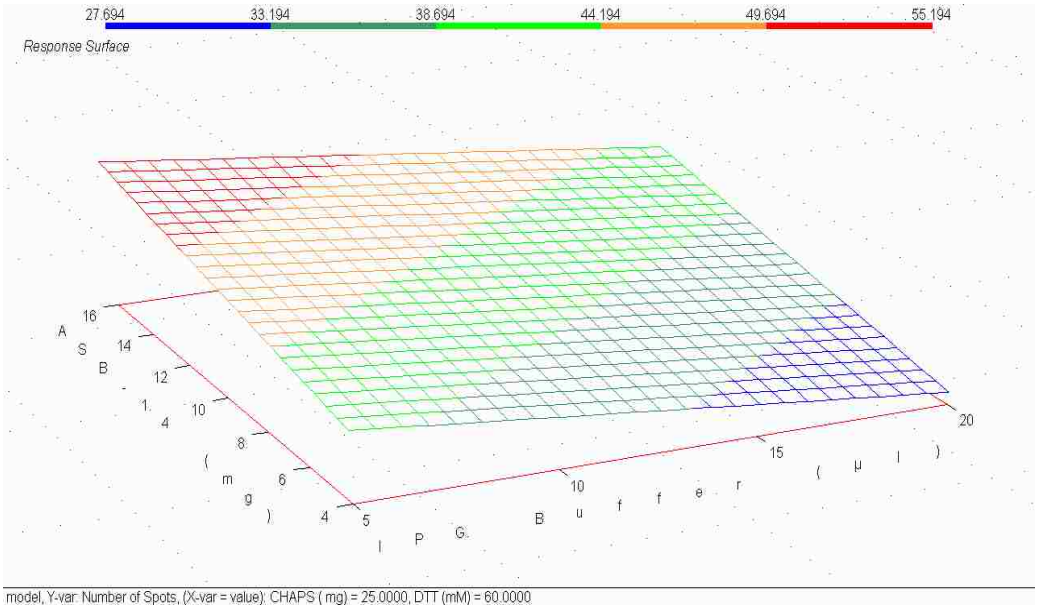

Figure 2.3 Surface response plot of ASB – 14 and IPG concentration on the number of spots. The highest spot count was obtained in the buffer range 5-10 µL and ASB-14 range 14-16 mg//ml.

The SDS-PAGE images of the second dimensional analysis of experiment 5 and 23, where the minimum and maximum spot counts were obtained from the experimental design were shown in Figure 2.4 and Figure 2.5, respectively. Experimental conditions for minimum spot counts produce horizontal streaking. These streaks are due to salts or imbalances in the lysis buffer and are the main causes of poor resolution in gels. In contrast, Figure 2.5 illlustrates the best conditions for the experimental design with the spot resolution greatly improves although some horizontal steaking is evident. In addition, the use of experimental design at optimum condition increased the number of spot from 96 to 134 (34% increase) compared to when we initially optimized the lysis buffer composition using the traditional method involving optimizing one variable at a time.

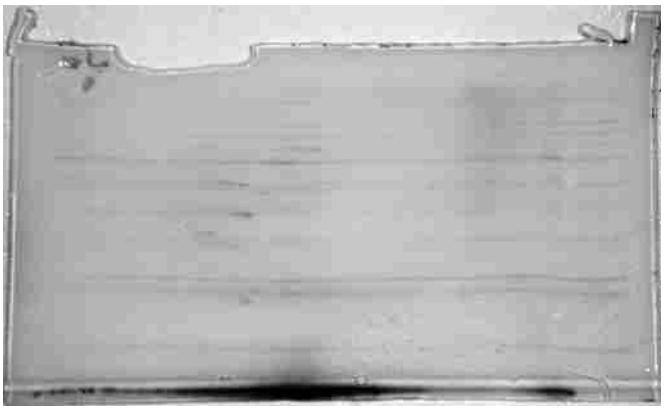

Figure 2.4. 2DE image of experimental run 5 of Box Behnken design. Polyacrylamide concentration = 12 % with TRIS/ Glycine buffer with 2% SDS added. The IEF focusing totaled 12,000 volt-hours. The gel image illustrated the lowest number of protein spots.

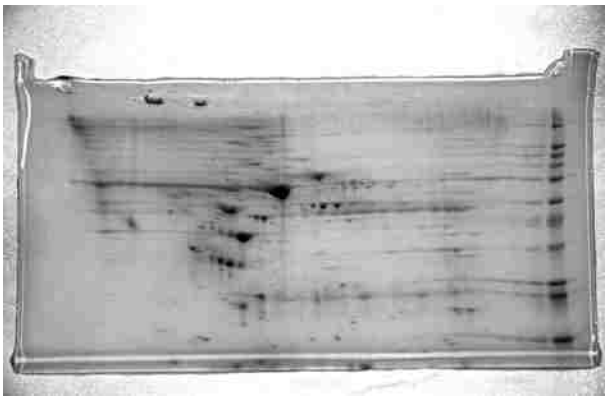

Figure 2.5 2DE image of experimental run 23 of Box Behnken design. Polyacrylamide concentration = 12 % with TRIS/ Glycine running buffer with 2% SDS added. The IEF focusing totaled 12,000 volt-hours. The gel image illustrates the maximum protein spots.

2.5. Reproducibility and Validation of the Design Method

The use of biological tissues for experimental design studies must be homogeneous enough to discern changes that are not due to changes in the compositions of the tissue. Intima tissues may contain various degrees of the diseased state, but physically mixing in liquid nitrogen to powdered homogeneous samples was achieved.

To further test the validity of the optimum conditions for membrane protein solubility obtained from the Box Behnken study on intima samples for diseased and nondiseased tissue, extractions using another different and independent thoracic aorta tissue samples were performed. In addition, analysis of another aorta samples were used to evaluate and investigate the results of the optimum trends on random samples. In order to assess the differences in the extent of atherosclerosis in the tissue we selected areas that were described as normal or non-diseased and those with complicated plaque or thrombus (diseased) for analysis. Based on these criteria, tissue samples were characterized as diseased high and low while nondiseased samples were described as nondiseased high and low. The high and low designation describes the maximum and minimum spot count conditions respectively from the experimental design study. The reproducibility studies were conducted using thoracic aorta tissue excised from a 56 year old female. Dissection and extraction procedures followed the previous described protocol in experimental section. The extractions of the samples were performed at the lysis buffer composition where the minimum and maximum number of spot count was obtained from Box-Benhken design (expt., 5 and 23, respectively in Table 2.1). The IEF experimental runs were conducted in triplicate for all extracted protein samples.

The results of the number of spot count obtained for the diseased and non-diseased aorta samples are shown in Table 2.2. Our study confirms that when the optimum conditions were applied in diseased tissues an increase in spot counts were observed. In non diseased tissues, similarly, increases in the spot count were obtained when these parameters were used.

Table 2.2. Reproducibility Studies of Diseased and Non- Diseased Aorta Extracts

	Diseased Tissue	Diseased Tissue	Non-Diseased Tissue	Non-Diseased Tissue
Run Number	Non-Optimum	Optimum	Non-Optimum	Optimum
1	14	22	27	40
2	12	35	30	35
3	13	26	31	38
Average No of Spots	13	28	29	38
Standard Deviation	1	7	2	3

Typical polyacrylamide images of the parameters obtained at low and optimum spot counts from the reproducibility study for diseased and non-diseased samples are illustrated in Figures 2.6 and 2.7, respectively. The studies confirmed the validity of the design as well as the reproducibility results. Horizontal and vertical streaking was minimized, enhancing the resolution of individual spots for further analysis and identification of proteins by in-gel digestion with trypsin and mass spectrometry. Peptide mass fingerprinting or LC/MS/MS for *denovo* sequencing with tandem mass spectrometry can be used for positive identification of proteins found in the various plaques. Proteins can be compared for increase or decrease in expressions between the disease and nondiseased tissue extracts.

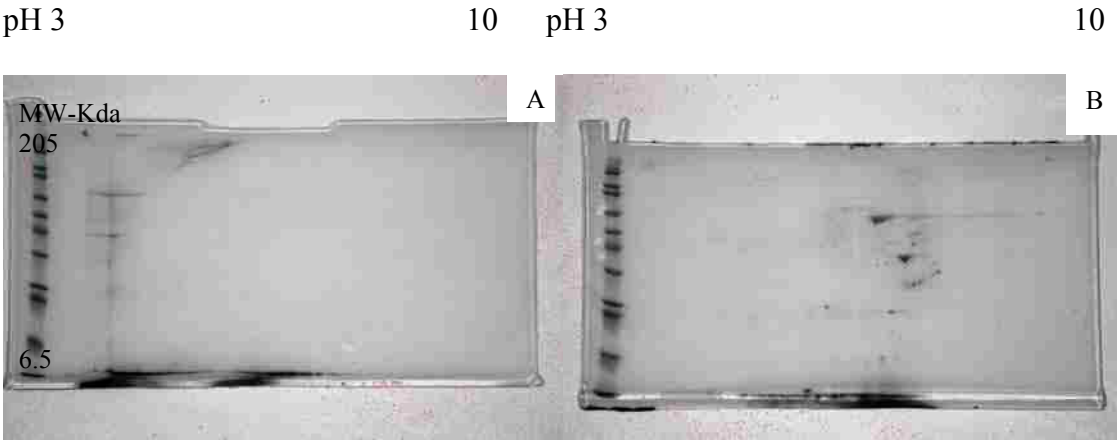

Figure 2.6. Comparison of Nondiseased tissues from Box Behken optimization parameters A) Low spot count; 12.5ul IPG buffer: 40mg/ml CHAPS:10mg/ml ASB-14:60 mM DTT; B) High spot count; 20 uL IPG buffer : 10 mg/ml CHAPS : 10 g/ml ASB-14 : 60 mM DTT. Polyacrylamide concentration = 12 % with TRIS/ Glycine running buffer with 2% SDS added. The IEF focusing totaled 12,000 volt-hours.

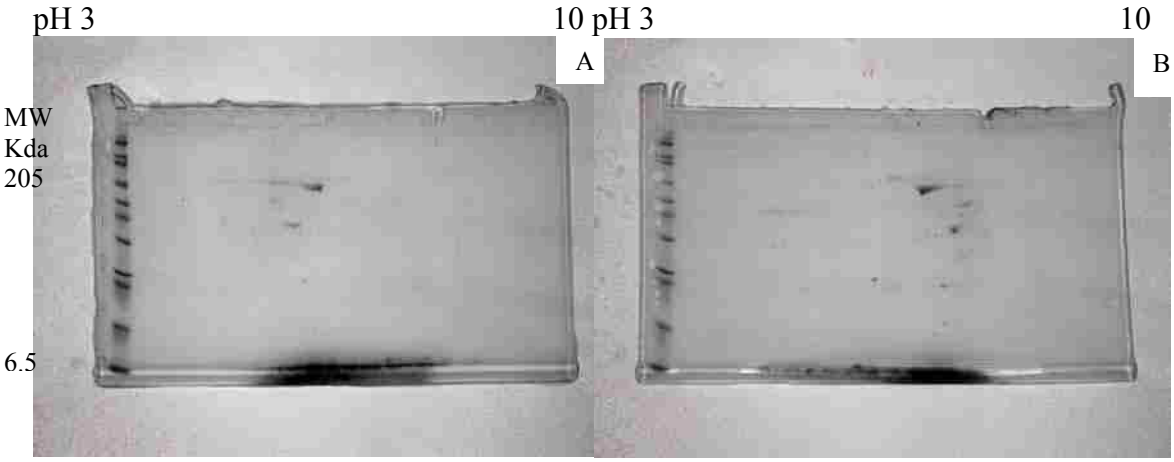

Figure 2.7. Comparison of Diseased tissues from Box Behken optimization parameters A) Low spot count; 12.5ul IPG buffer: 40mg/ml CHAPS: 10mg/ml ASB-14:60 mM DTT; B) High spot count; 20 uL IPG buffer : 10 mg/ml CHAPS : 10 g/ml ASB-14 : 60 mM DTT. Polyacrylamide concentration = 12 % with TRIS/ Glycine running buffer with 2% SDS added. The IEF focusing totaled 12,000 volt-hours.

The data validates the use of the optimum conditions with the standard deviation within acceptable ranges for biological samples of varying degrees of diseased states. The data will be

used to evaluate larger gel formats for higher protein concentrations that can be analyzed with 2DE.

2.6 Conclusions

This study successfully used a Box Behken experimental design to optimize the composition of four key components, IPG buffer, CHAPS, ASB-14 and DTT, in the lysis buffer for the membrane protein solubilization. Tissues for the normal and diseased intima of thoracic aortas extracted using lysis buffer in IEF with IPG drystrips. This method for optimal spot count (protein solubilization) reduced the number of experiments when compared to classical approaches that require additional time and material cost. The method was found to be highly reproducible with high potential in solubilization of wide range of highly hydrophobic membrane protein in human and animal samples. This approach will further utilized for the elucidation of proteins expressed in the formation of atherosclerosis.

2.7 References

(1) Hoeben, A.; Landuyt, B.; Botrus, G.; De Boeck Guetens, G.; Highly van Oosterom, A.T.; deBruijn, E.A. *Analytica Chimica Acta* **2006**, 564, 19-33

(2) Mohr, S.; Leikauf, G.D.; Keith, G.; Rihn, B.H. *J Clin. Oncol.* **2002**,3165-3175

(3) Petricoin, E.F.; Liotta, A.L. *J. Nutr.* **2003**, 133,2476S-2484S

(4) O'Farrell, P.H. *J. Biol. Chem.***1975**, 250, 4007-4921

(5) Klose, J. *Humanangenetik*, **1975**, 26,231-243.

(6) Simpson, R; Preparative Two-dimensional Gel Electrophoresis with Immobilized pH Gradients. In *Proteins and Proteomics, a Laboratory Manual,* Stochaj. W.R., Berkel-Man, T., Laird, N., Cold Springs Harbor Laboratory Press: Cold Harbor, NY **2003**; pp 143-219.

(7) Bjellqvist, B.; Ek, K.; Rightetti, P. G.; Gianazza, E.; Gorg, A.; Westermeier, R.; Postel, W. *J. Biochem Biophys Methods* **1995**, 6: 317-339.

(8) Rabilloud, T. *Electrophoresis*, **1996**, 17,813-829.

(9) Getz, E.B.; Xiao, M.; Chakfabarty, T., Cooke, R.; Selvin, P. R. *Anal. Biochem.* **1999**, 273, 73-80.

(10) Rabilloud, T.; Chevallet, M. Solubilization of Proteins in Two- Dimensional Electrophoresis. In *Proteome Research: Two Dimensional Gel Electeophoresis and Identification Methods*. Rabilloud, T., Ed. Springer Verlag Berlin Heidelberg, New York, NY **2000**, pp 9-29.

(11) Jeney, C.; Dobaoy, O.; Lengley, A.; Adam, E.; Nasz, I. *J. Immunol. Methods.* **1999**, 223, 137-146.

(12) Burch, G.J., Ferguson, C.H., Cartwright, G., Kwong, F.Y., *Biochem Soc Trans* **1995**, 23, 1075.

(13) Guennadi, A.K.; Porter, I.M.; Blow, J.J.; Swedlow, J.R. *Proteome Science* **2004**, 2,6, 1-12.

(14) Cobb, B.D.; Clarkson, J.M. *Nucleic Acids Res*. **1994**, 22, 3801-3805

(15) Shaw,M.M.; Riederer,B.M. *Proteomics* **2003**, 3, 1408-1417]

(16) Molloy, M.P.; Herbert, B.R.; Walsh, B.J.; Tyler, M.I.; Traini, M.; Sanchez, J.C.; Hochstrasser, D.F.; Williams, K.L., Gooley, A.A. *Electrophoresis* **1998**, 19,837-844.

(17) Molloy, M.P. *Anal. Biochem.* **2000**, 280, 1-10.

(18) Herbert, B.; Galvani, M.; Hamdan, M.; Olivieri, E.; MacCarthy, J.; Perdersen, S.; Righetti, P.G. *Electrophoresis* **2001**, 22, 2046-2057.

(19) Galvanic, M.; Hamdan, M.; Herbert, B.; Righetti, P.G. *Electrophoresis* **2001**, 22, 2058-2065.

CHAPTER 3

ISOLATION AND CHARACTERIZATION OF PROTEINS FROM ATHEROSCLEROTIC PLAQUES USING TWO DIMENSIONAL GEL ELECTROPHORESIS AND MASS SPECTROMETRY

3.1 Introduction

Cardiovascular disease, primarily atherosclerosis, causes 1/3 of all deaths in the United States annually [1-3]. A number of distinct processes are associated with plaque development: lipid accumulation, inflammation, cell proliferation, cell death, and thrombosis. Some of the molecular events underlying each of these processes and the stimuli for these events have been identified; however, much remains to be clarified [4]. Atherosclerosis is the result of accumulation of numerous components in the coronary arteries, resulting in the formation of plaque deposits. It is a passive progressive disease characterized by the accumulation of lipids and fibrous elements in the large arteries [5]. The early lesions of atherosclerosis consist of sub endothelial accumulations of cholesterol-engorged macrophages, known as foam cells. In humans, such fatty streak lesions can usually be found in the aorta and coronary arteries in the second decade and the cerebral arteries in the third or fourth decades. Because of differences in blood flow dynamics, there are preferred sites of lesion formation within the arteries. Fatty streaks are not clinically significant, but they are the accumulation of lipid-rich necrotic debris and smooth muscle cells. Plaques that develop from these fatty streaks are complex, with calcification, ulceration at the luminal surface, and hemorrhage from small vessel wall. Although advanced lesions can grow sufficiently large to block blood flow, the most important clinical complication is an acute occlusion due to the formation of a thrombus or blood clot, resulting in myocardial infarction or stroke [6]. A comparison of the complex processes in normal and major cardiac events of a diseased artery is illustrated in Figure 3.1. The major

pathological events in atherosclerosis are contained in two distinct areas: media-tunica and within subdomains of plaques within the intimal layer of the artery or aortas.

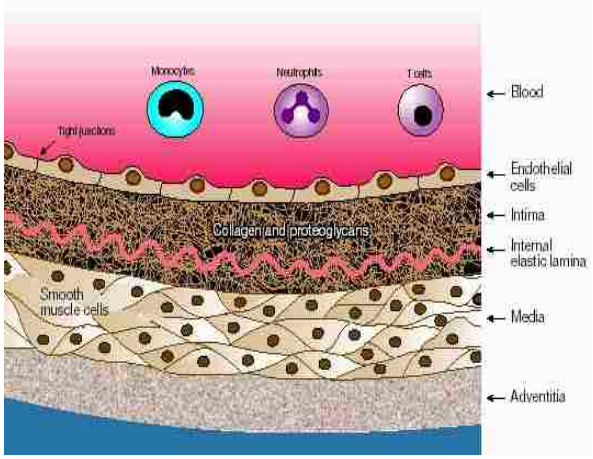

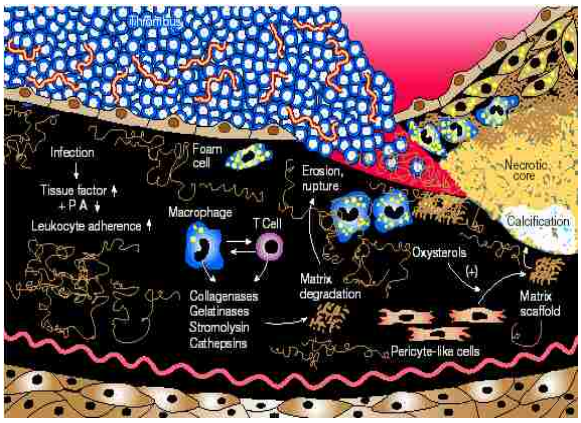

Normal Artery Artery with Complicated Plaques

Figure 3.1 Comparison between a normal vessel and a vessel in the diseases state. [6]

Because the plaques are of heterogeneous cellular composition, a proteomic analysis of most lesions is difficult. Researchers have surgically excised various segments of normal and diseased arteries and cultured the cells invitro in protein-free medium. The secreted proteins from both cultures were extracted and analyzed for biological variations. Proteins from 2D gel electrophoresis were displayed as spots and were compared to cultured regions from both normal and diseased areas [7]. These findings showed that the more complicated the lesions, the higher the number of secreted proteins which suggested the production of specific proteins relating to the complexity of the atherosclerotic lesions. Plaques may grow to obstruct the lumen and potentially causing peripheral vascular disease. When this occurs, intima and media become indistinguishable and proteins may not be specific to the area determined to be the site of inflammation [8].

A proteomic assessment of the analysis of intima and media proteins has been developed in this study using a combination of techniques, including two-dimensional gel electrophoresis, image analysis, and mass spectrometry [9]. Proteomics has been used to study protein expression in tissues, cells, or fluids [10]. Other studies have documented the use of this technique for analysis of protein expression in various stages during the formation of atherosclerotic plaques [11-14].

Mass spectrometry is the most commonly used method for the analysis of gel-separated proteins and is the fundamental technology for proteomics replacing Edman degradation for the identification of proteins. The use of "soft ionization" techniques, matrix-assisted laser desorption / ionization (MALDI) and electrospray ionization (ESI) have been shown to be superior in the analysis of biomolecules. The coupling of the time-of-flight mass analyzer to a MALDI source is widely used in the identification of proteins from peptide mass fingerprinting with database searches [15]. The approach is sensitive and user friendly for a variety of biological fields involving processing of peptides from digestion with trypsin [16]. The peptides masses from the mass spectrometer are fingerprints of protein cleavages by the protease. The theoretical sequences of these masses are available from databases accessed through Web search engines [17-23].

Electrospray ionization technique employed in this study is an atmospheric pressure ionization that is coupled to a mass spectrometer for the characterization of biomolecules and associated noncovalent interactions in the gas phase [24]. The interfacing of ESI to high performance liquid chromatography has a broad spectrum of uses in the biological field. ESIMS uses continuous flow operation, variable solvents, and a wide range of flow rates including nano flows for small volume analytes.

ESI-MS generates intact multiple charged ions of proteins and other biological compounds, reducing the harsh ionization found in other processes. The method was first introduced by Dole and co-workers for the generation of gas phase ions from electrically charged liquid droplets produced by electrospraying an analyte solution at atmospheric pressure. The coupling of ESI to mass spectrometry was accomplished by Fenn and co-workers [25] and later developed for the analysis of biological molecules by Fenn et al.[26,27], Henion[28], and Smith [29].

HPLC-MS has become the most widely useful analytical tool for numerous applications such as qualitative and quantitative analysis of complex mixtures of biochemical, inorganic, and organic compounds [24]. HPLC analysis is accomplished by placing an analyte of interest on a column containing an appropriate stationary phase. The analytes are differentially partitioned on the sorbent matrix. Separation occurs by elution from a stream of liquid mobile phase. The more commonly used technique for biological compounds w the reverse phase (RP) mode of HPLC. The stationary phase consists of a nonpolar matrix and the polar phase is a polar solvent. RP-HPLC involves the interaction between the nonpolar hydrocarbonaceous matrix in the stationary phase and the hydrophobic group of the biomolecules. A UV-Visible detector system is used to quantitate the separation of the analytes in the mobile phase.

The RP-HPLC mobile phase is connected to the ESI ionization source prior to mass analysis. The ESI source consists of numerous designs, but typically the liquid mobile phase flows continuously through a stainless steel capillary at 2 to 5 µl/min. However, lower flows nL/min to µl/min is used for nano flow operation. A potential is usually 3-4 kV is usually placed on the tip of the capillary and the walls of the atmospheric pressure region or the counter electrode. Nitrogen is normally used as the sheath gas heated to aid in the evaporation of the

solvent from the charged droplets containing the analytes. The ionization of the droplets is comprised of 3 processes: droplet formation, droplet shrinkage, and gas ion formation with electrostatic forces applied causing the liquid to emerge from the capillary as a jet in the shape of a Taylor cone [30]. Two theories have been accounted to explain the mechanism of the formation of gas phase ion from the charged droplets: the charge residue model and the ion desorption model [31].

In peptide ion fragmentation in MS/MS cleavages of the bonds between the carbonyl oxygen and the amide nitrogen forms “y” ions and “b” ions. The y ion fragmentation occurs when the positively charged of the peptide fragment is retained on the C – terminus of the original peptide ion. Alternatively, the b-ion fragmentation is the retention of the charge on the N-terminal portion of the original peptide ion.

3.2 Research Goals and Objectives

Our studies are focused on the identification of proteins from the intima and media of tissue extracts of atherosclerotic plaques. To optimize the separation of as many proteins in the tissue as possible including membrane and highly alkaline proteins, sodium dodecylsulfate was employed with carrier ampholytes (pH 3.5 – 10) ran with 12.5% polyacrylamide gels glass tubes. The purpose of this approach was to provide a template to separate and isolate as many proteins as possible from the tissue. In this work, the use of a hybrid linear trap / Fourier transform ion cyclotron resonance (ICR) mass spectrometer was selected to perform protein sequencing using the bottom-up approach. The hybrid system was used for the characterization of proteins from 2D gels digested with trypsin. Further separation of the peptides was achieved by fast reverse phase high performance liquid chromatography with nanospray capability directed into the linear quardrupole trap Fourier transform ion cyclotron resonance (LTQ-FTICR) mass spectrometer.

The benefit of the linear trap was seen in the ion accumulation and activation prior to detection in the ICR cell that produced an increase in the scan rate [32]. An increase in the duty cycle allowed for data-dependent mass analysis of coeluting peptides that increased peptide coverage without increasing the length of the gradient length [32].

3.3 Experimental

3.3.1 Materials and Reagents

Urea, thiourea, SB 3-10, dithiothreitol, β-mercaptoethanol, nuclease inhibitors, acetonitrile, ammonium bicarbonate, dithiothreitol, trifluoroacetic acid, and iodoacetamide were obtained from Sigma Aldrich Corporation (St Louis, MO USA). Sigma Marker protein standards were obtained from Sigma Aldrich Corporation (St Louis, MO USA). All of the reagents were of the highest purity and when available specified electrophoresis grade.

Sodium dodecylsulfate was obtained from EM Scientific (Cherry Hill, NJ USA). Polyacrylamide gels (10%) and agarose were obtained from BioRad (San Diego, CA USA). Tris(hydroxymethyl)aminomethane (TRIS) was obtained from Invitrogen (San Diego, CA USA). 3-[(Cholamidopropyl)dimethyl-ammonio]-1-propanesulfonate (CHAPS) and protease inhibitors were obtained from Calbiochem (San Diego, CA USA). Ampholines (pH 3.5-10) were obtained from GE Healthcare (Piscataway, NJ USA). Ziptips was obtained from Millipore (Billerica, MA USA). Formic acid was obtained from Fisher Scientific (Waltham, MA USA).

3.3.2 Methods

Human thoracic aortas stored at -70ºC were thawed in an ice bath. The tissue of interest was dissected with a sterile scalpel then place in 50 ml centrifuged tubes. The samples of intima and media were refrozen in dry ice for homogenization. The samples were homogenized in 3 ml of osmotic buffer containing 10x nuclease stock and protease inhibitor. 400 µl of the above

sample was then diluted with 400 μL sodium dodecylsulfate (SDS) buffer that was heated to boiling without β- mercaptoethanol. The sample was heated in boiling water for five minutes followed by protein determination using a BCA assay (Pierce Chemical). The samples were then diluted with SDS buffer or IPG buffer to determine the effectiveness of either in protein separation on the gel. The SDS buffer samples were then diluted to 5.0 mg/ml containing SDS buffer with β- mercaptoethanol. The other sample was diluted with 5.0 mg/ml IPG buffer. The composition of the IPG buffer included: 7M urea, 2M thiourea, 30 mM TRIS buffer at pH 7.3, 4% CHAPS, and 1% SB 3-10.

Two dimensional electrophoresis was performed using the method of O' Farrell [33]. Isoelectric focusing (IEF) was performed in glass tubes of inner diameter 3.0 mm using 2.0% pH 3.5 – 10 ampholines for 20,000 volt-hours. 50 ng of IEF standard, tropomyosin, was added to each sample. The protein migrates as a doublet with lower polypeptide spot of molecular weight of 33,000 and isoelectric point of 5.2; an arrow on the stained gel marks its position. The enclosed tube gel pH gradient plot for this set of ampholines was determined with a surface pH electrode.

Following equilibration for 10 minutes in buffer containing 10% glycerol, 50 mM dithiothreitol, 2.3% SDS and 0.0625 M TRIS, pH 6.8, each tube gel was sealed to the top of a stacking gel of 10% acrylamide slab gel (1.0 mm thick). SDS slab gel electrophoresis was conducted for 4 hours at 12.5 mA / gel. The following protein standards in 0.5% agarose were added to the slab gel in a well as the tube gel was sealed to the slab gel: myosin (220,000), phophorylase A (94,000), catalase (60,000), actin (43,000), carbonic anhydrase (29,000) and lysozyme (14,000). The standards appeared as bands on the basic edge of the Coomassie Blue stains. The gels were dried between sheets of cellophane paper with acid end to the left.

The gel spots were excised used a clean razor blade. Necessary precautions were taken in handling the samples to prevent contamination particularly with keratins. The protocol used was based on in-gel protocols. The following solutions were prepared : 25 mM ammonium bicarbonate 100 mg / 50 ml, 25 mM ammonium bicarbonate in 50% acetonitrile / water, 50% acetronitrile / 5% formic acid and 12 ng/ µl trypsin (modified and freshly diluted) in 25 mm ammonium bicarbonate. Each excised gel spot was destained three times for 10 minutes with a solution containing 200 µl of 25 mM ammonium bicarbonate / 50% acetonitrile. The gel solution was vortexed intermittently to enhance color removal. The resulting solution from each extraction was discarded. The procedure was repeated until the gels began to shrink and became white. The gel pieces were further reduced with fresh solutions of 10 mM dithiothreotol in 25 mM ammonium bicarbonate (1.5 mg /ml). The DTT was added to cover the pieces followed by vortexing and spinning for 1 minute. The samples were incubated in a water bath at 56ºC for 45 minutes and allowed to cool to room temperature, then centrifuged. The solution was discarded and immediately 55 mM iodoacetamide in 25 mM ammonium bicarbonate was added to cover the gel pieces. This mixture was incubated at room temperature in the dark for 45 minutes followed by removal of the supernatant. Gel pieces were washed with 100 µl of ammonium bicarbonate then vortexed for 10 minutes and centrifuged for 2 minutes followed by removal of the supernatant. The gel pieces were dehydrated with 100 µl of 50% 25mM ammonium bicarbonate / acetonitrile. This solution was then vortcxed and centrifuged for 2 minutes with the resulting supernatant discarded. This procedure was repeated for a second time. The gel pieces were placed in a speed vacuum centrifuge for 20 minutes and dried prior to digestion. A solution of trypsin (12 ng / ml) in ammonium bicarbonate was added to cover the gel pieces and incubated on ice for 45 minutes. If the gel pieces absorb the solution, additional liquid was used.

This solution was incubated overnight at 37º C. The solution was acidified with 10 µl of 2 % trifluoroacetic acid in water for 2 minutes. This supernatant was removed and placed in a clean microcentrifuge tube. To the gel pieces, 30 ul of 50% acetonitrile / 5% formic acid was added followed by sonication for 20 to 30 minutes. The gel pieces were centrifuged for 5 minutes and the supernatant combined with the previous solution. The process was repeated and all supernatants combined. The extracts were vortexed, centrifuged for 2 minutes and placed in a speed vacuum to reduce the volume of peptides to 10 µl. An additional cleanup step may be used with C18 Ziptip (Eppendorf) when analyzing low levels of peptides. Peptides were eluted from the Ziptips using an elution buffer composed of 50% acetonitrile / 0.1% trifluoroacetic acid. The final solution was pumped through a micro high performance liquid chromatography system as described below.

3.3.3 Instrumental Analysis

The peptides from the tryptic digest were diluted with 0.1% trifluoroacetic acid (10:1 v/v) and loaded on a C18 Biobasic 75µm x 10 cm reverse phase column (New Objective) equipped with a 15 µm picofrit tip for electrospray applications. A 2 µl aliquot was injected into a mobile phase a flow rate of 200 nL/ min using a Surveyor Liquid Chromatographic System (Thermo Electron, San Jose, CA). The solvent system consisted of a binary system composed of A) 95:5:0.1 water:acetonitrile: formic acid (%) (v/v) and B) 5:95:0.1 water: acetonitrile: formic acid (%) (v/v). A gradient flow was used with solvent A pumped at 90% for 5 minutes and decreasing to 50% in 60 minutes. The final gradient was pumped from 50% A to 20% in 17 minutes then finally increased to 90% gradient for 28 minutes.

The mass spectrometry experiments were performed using a linear quadrupole trap (LTQ) Fourier transform ion cyclotron mass spectrometer (FT) (Thermo Electron, Bremen,

Germany) equipped with an open-ended cylindrical cell controlled by LTQ Tune 1.0. Detection in the linear trap and the ICR cell was controlled by Xcalibur software increasing the duty cycle of the analysis. Parallel data acquisition of MS and MS/MS can be acquired simultaneously. The acquired resolution settings for MS and MS/MS scans were 100000 for MS data and 25,000 for product ions.

Database searching of the full scans of the MS/MS spectral data was performed using the Bioworks version 3.2 suite of programs (Thermo Electron San Jose, CA USA). The spectra information for the Bioworks database was downloaded from the National Center for Biotechnology Information (NCBI) website (http://www.ncbi.nlm.ih.gov/blast/db/fasta). A mass tolerance for precursor was set at 1 Da. The files in the Bioworks software were filtered according to cross-correlation scores as a function of charge states to increase the confidence limits. The Xcorr values for the determination of acceptable peptide matches were 1.5 for precursor ions with a charge of one, 2.0 for fragments from doubly charged ions, and 2.5 for triply charged ions. The full scan spectral analysis was searched for sequence coverage using Swiss Prot (uniprot_trembl_human.fasta). The SEQUEST database was used for peptide peak assignments. SEQUEST is primarily to determine if MS/MS peptides are matches for the amino acid sequences for the precursor ion. The proteins in the database are subjected to tryptic digestion and the program generates a master of peptides for comparison to the MS/MS scans. Theoretical MS/MS spectrum are generated and comparison against the selected peptides. A correlation score is calculated for each match between the MS/Ms scan and the theoretical spectra. The best peptide matches are reported from this data. Post translational modifications of peptides such as phosphorylation of serine, threonine, tyrosine were considered in using the SEQUEST algorithm to determine the peptide masses of the ions from MS/MS analysis.

3.4 Results and Discussions

The tissue of thoracic aortas for cadavers from a 57 year old female and an 80 year old male were dissected from the adventitia. Samples of intima, intima /media, and media were isolated from each and homogenized with nuclease and protease inhibitors. Boiling both sets of tissues with SDS for 5 minutes was necessary to maximize solubility of proteins including lipids usually formed as a consequence of atherosclerosis leading to foam cells and to plaque formation. 100 µl of sample containing 500 µg of protein was loaded on the SDS polyacrylamide gels for protein identification. Two different buffer systems were studied to compare the effectiveness of buffers on the solubility of proteins. One method used buffers compatible with immobiline pH gradient drystrips composed of 7M urea, 2M thiourea, 30 mM TRIS pH 7.3, 4% CHAPS and 1% SB 3-10. The other method used SDS Boiling buffer containing β-mercaptoethanol. The gels were stained with Coomassie Blue and imaged with a 1-D Kodak Logic Imaging System. Table 3.1 lists the samples in this study.

Table 3.1. Summary of tissue extracts of atherosclerotic plaques from thoracic aortas

Gel Identification	Sample No.	Tube Buffer	Quantity Loaded (µL)	Quantity Loaded (µg)	Staining Method
LF210-01	80 year old intima	IPG	100	500	Coomassie
LF210-02	57 year old intima	IPG	100	500	Coomassie
LF210-03	57 year old media	IPG	100	500	Coomassie
LF210-04	80 year old media/intima	IPG	100	500	Coomassie
LF210-05	80 year old intima	SDS	100	500	Coomassie
LF210-06	57 year old intima	SDS	100	500	Coomassie
LF210-07	57 year old media	SDS	100	500	Coomassie
LF210-08	80 year old media/intima	SDS	100	500	Coomassie

100 µl of tissue extracts for the various membranes from the aortas was loaded on the tube gels containing 500 µg of protein as determined by the Bradford assay. The gel images of the SDS PAGE extracts of plaques from various areas in the aorta are illustrated in Figures 3.2-3.9.

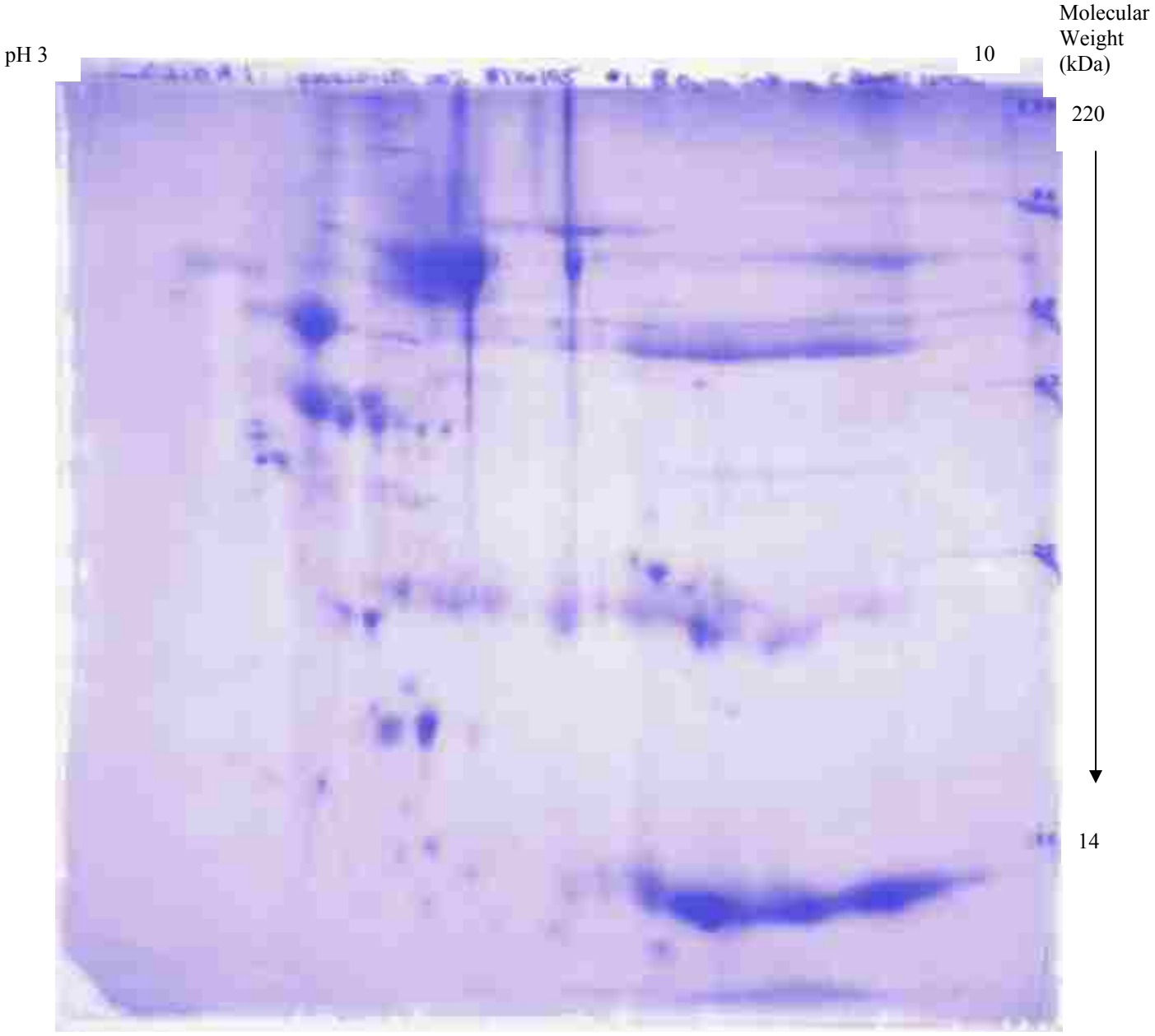

Figure 3.2. LF210-01 Intimal extract from a thoracic aorta of 80 years old. Lysis buffer (IPG) containing 7M urea, 2M thiourea, 30mM TRIS pH 7.3, 4% CHAPS, 1% SB 3-10. IEF performed with 3mm (id) tubes using 2% pH 3.5-10 Ampholines for 20,000 volt-hours. Staining performed with Commassie blue.

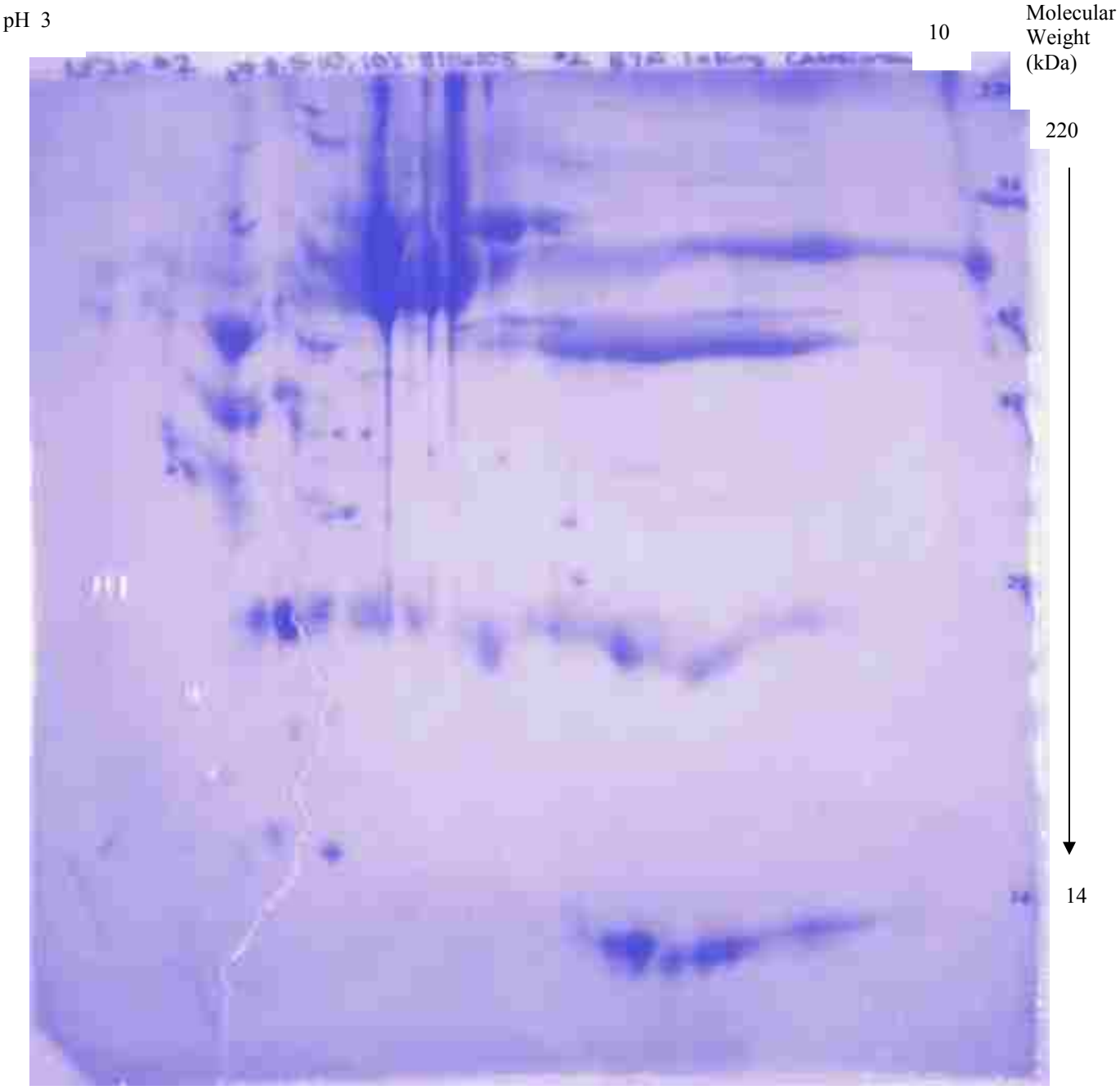

Figure 3.3. LF210-02 Media extract from thoracic aorta from 57 year old. Lysis buffer (IPG) containing 7M urea, 2M thiourea, 30 mM TRIS pH 7.3, 4% CHAPS, 1% SB 3-10. IEF performed with 3mm (id) glass tubes using 2% pH 3.5-10 ampholines for 20,000 volt-hours. Staining performed with Commassie blue.

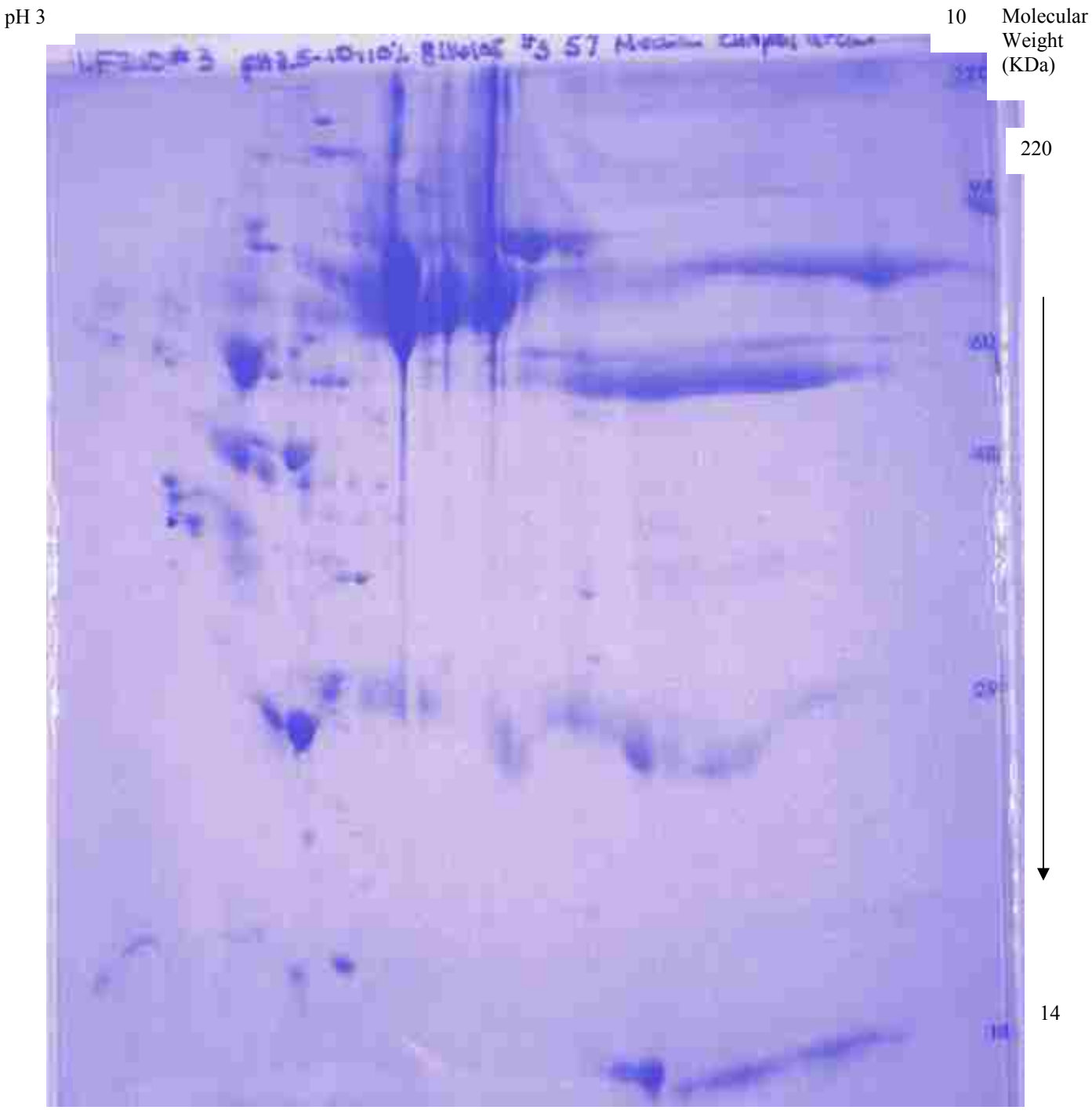

Figure 3.4. LF210-03 Media extract from thoracic aorta from 57 year old. Lysis buffer (IPG) containing 7M urea, 2M thiourea, 30mM TRIS pH 7.3, 4% CHAPS, 1% SB 3-10. IEF performed with 3mm (id) tubes using 2% pH 3.5-10 ampholines for 20,000 volt-hours. Staining performed with Commassie blue.

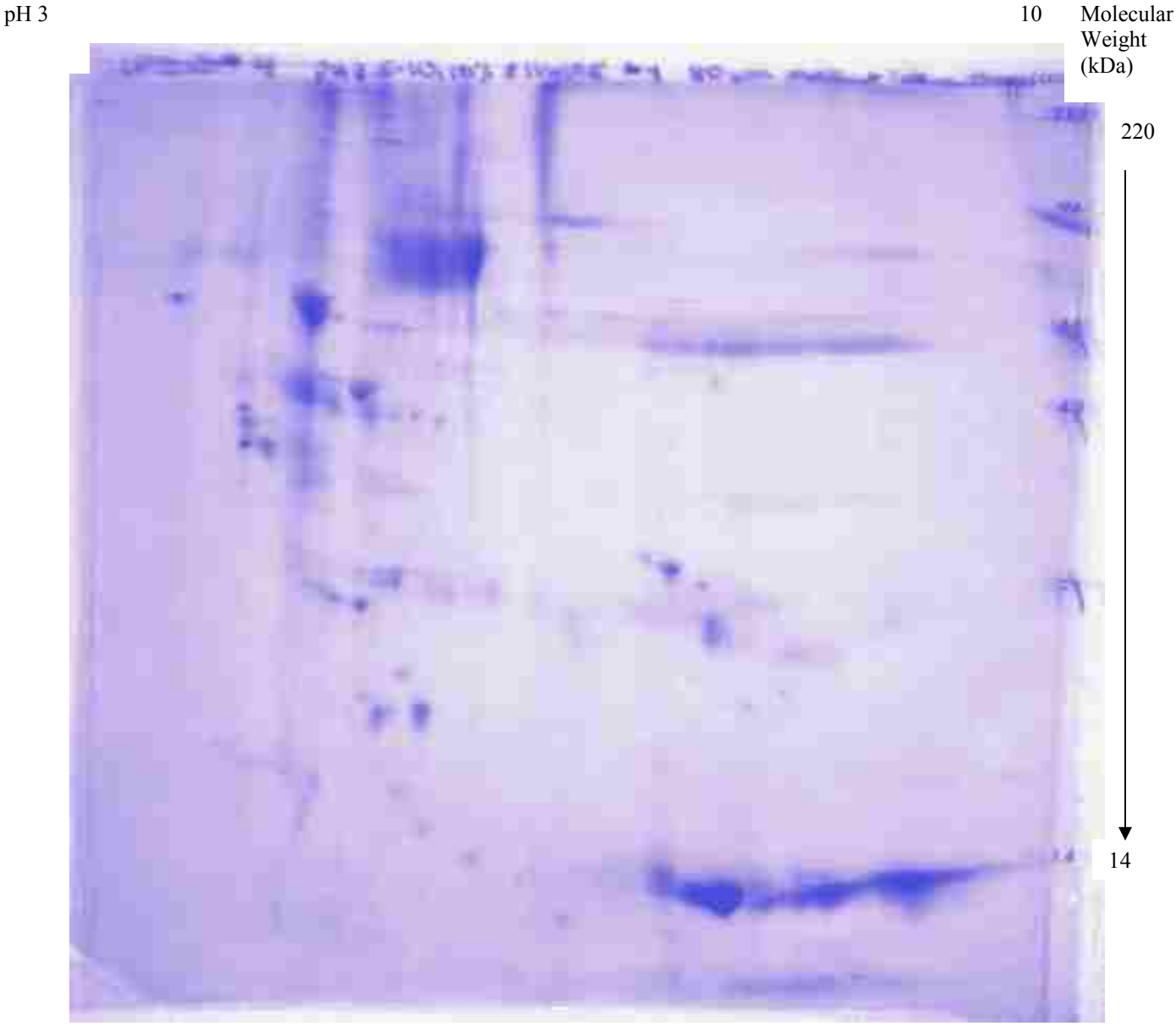

Figure 3.5. LF210-04 Intima/media extract from a thoracic aorta of 80 year old. Lysis buffer (IPG) containing 7M urea, 2M thiourea, 30mM TRIS pH 7.3, 4% CHAPS, 1% SB 3-10 IEF performed with 3mm (id) tubes using 2% pH 3.5-10 ampholines for 20,000 volt-hours. Staining performed with Commassie blue.

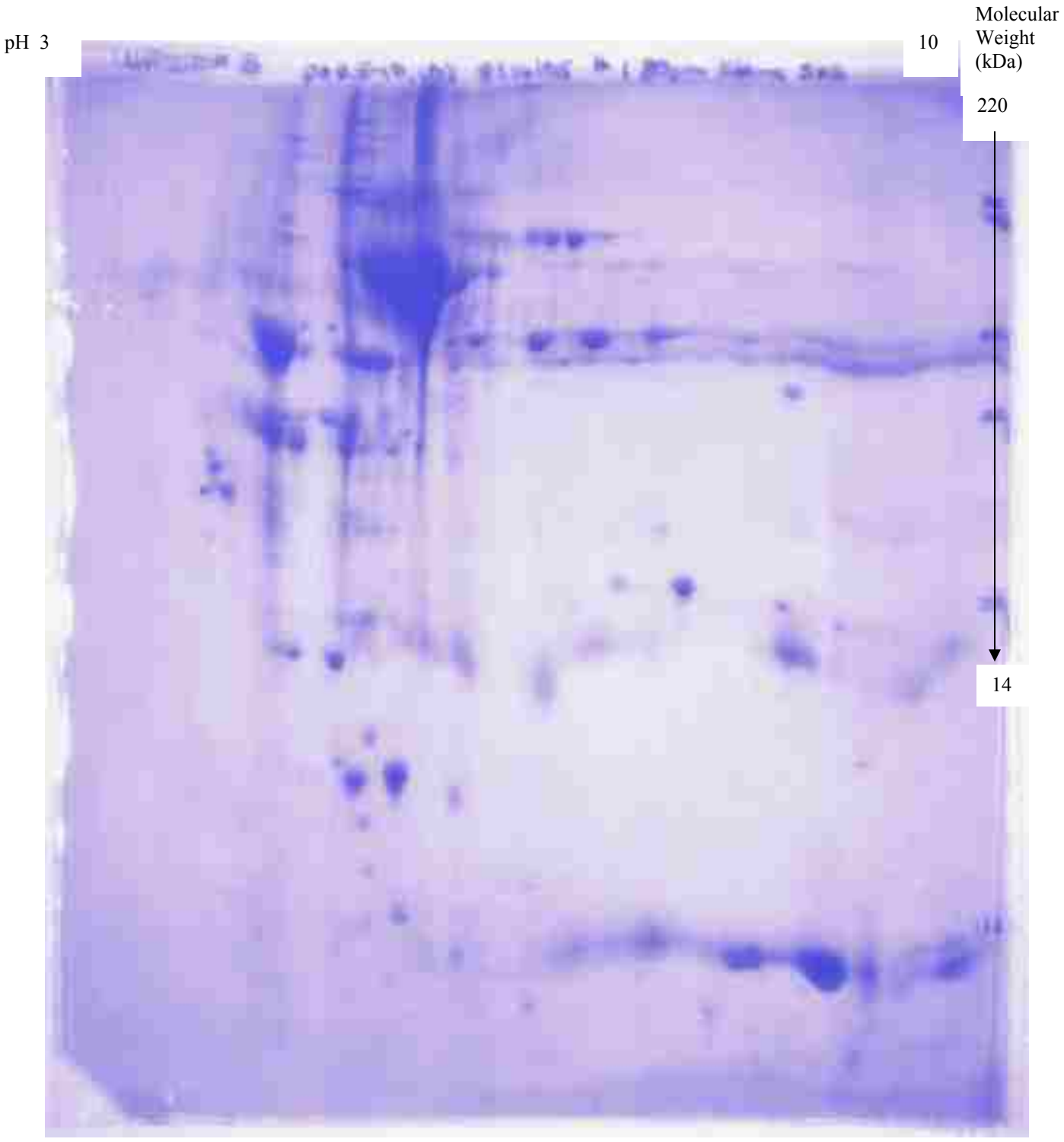

Figure 3.6. LF210-05 Intima extract from a thoracic aorta of 80 year old. Lysis buffer (IPG) containing sodium dodecylsulfate (1%). IEF performed with 3mm (id) glass tubes using 2% pH 3.5-10 ampholines for 20,000 volt-hours. Staining gel was performed with Commassie blue

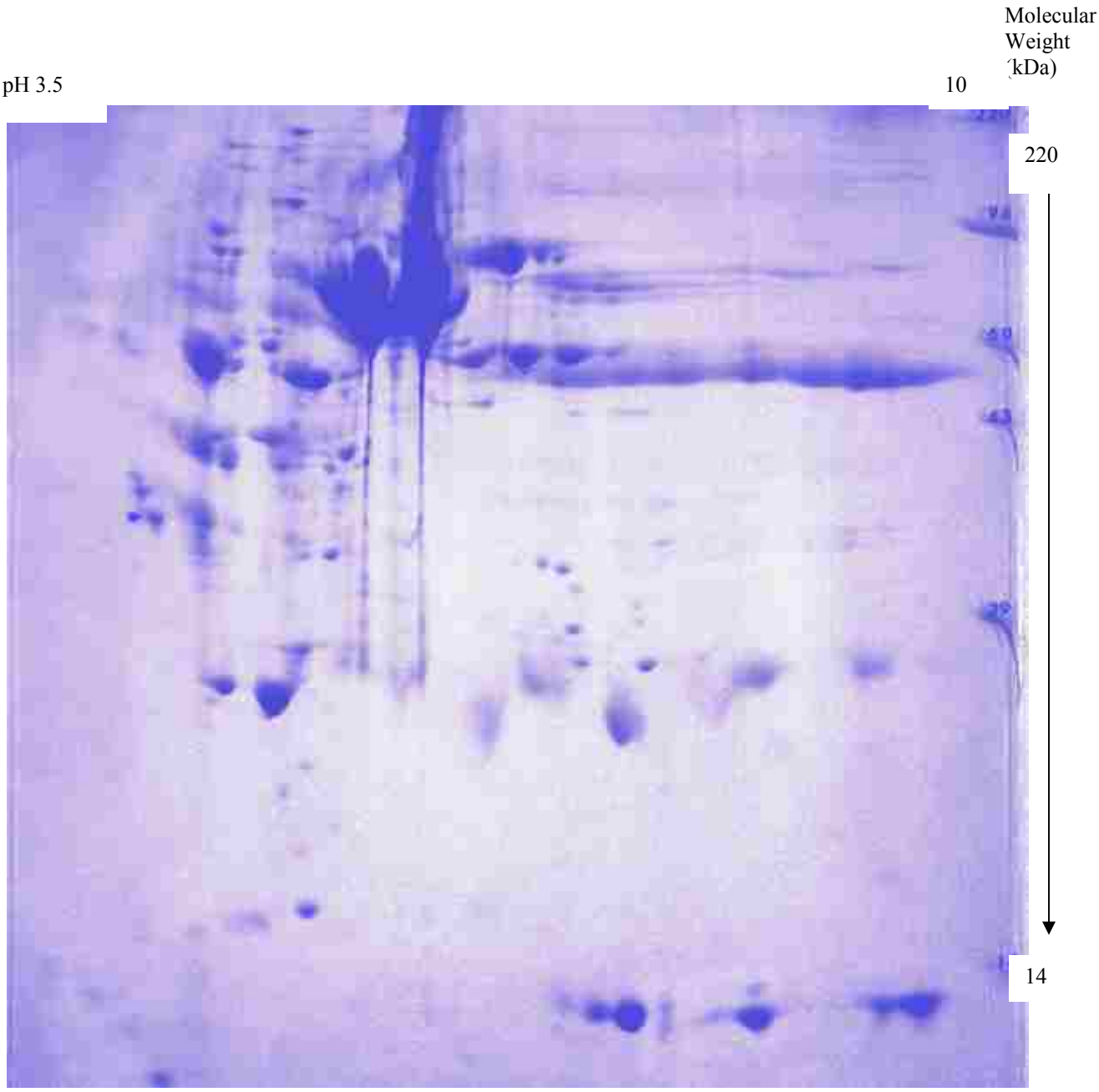

Figure 3.7. LF210-06 Media extract of thoracic aorta 57 year old. Lysis buffer containing sodium dodecyl sulfate (1%) IEF performed with 3mm (id) tubes using 2% pH 3.5-10 ampholines for 20,000 volt-hours. Staining performed with Commassie blue.

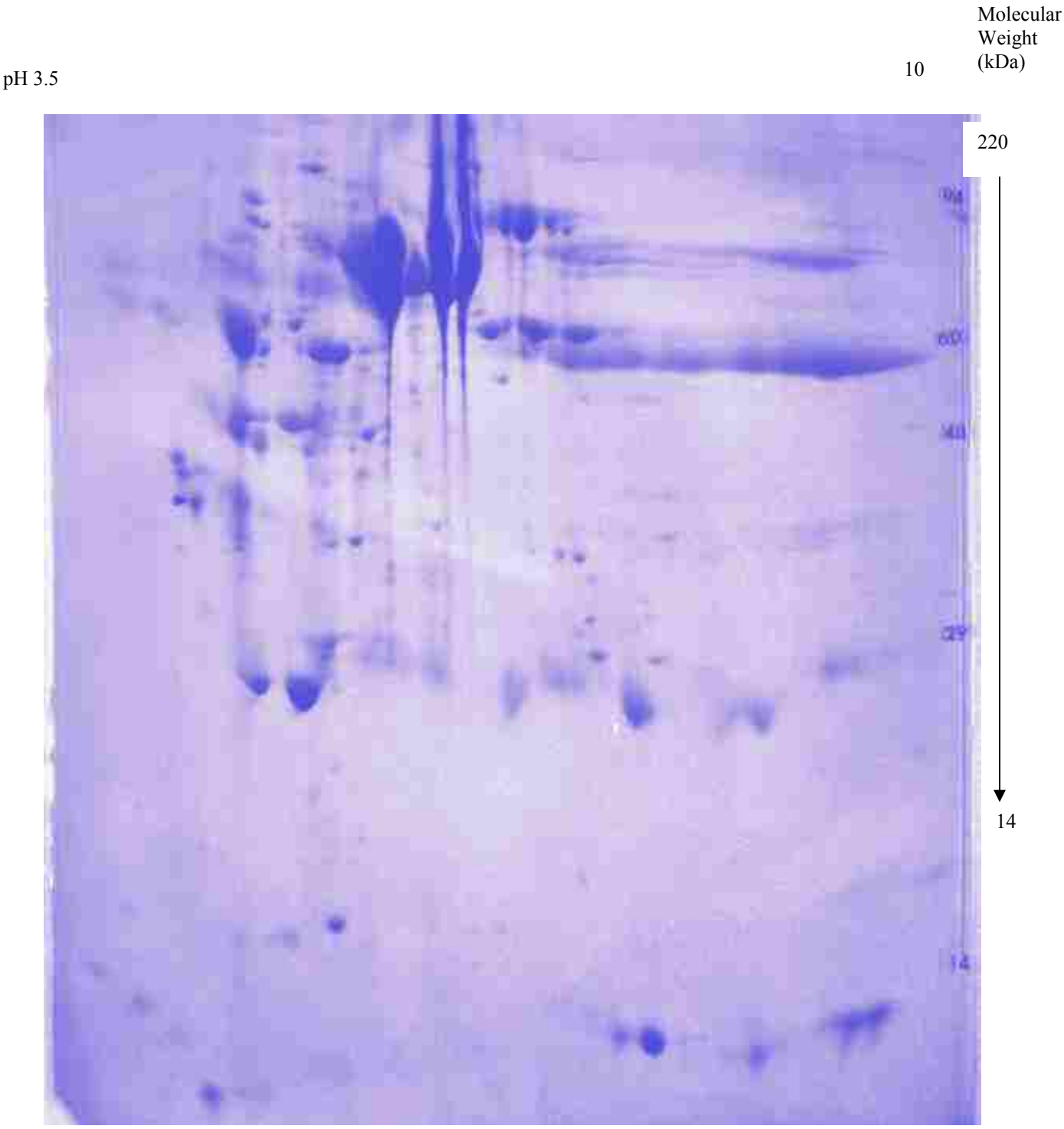

Figure 3.8. LF210- 07 Intimal extract from a thoracic aorta of 80 year old. Lysis buffer containing sodium dodecylsulfate (1%). IEF performed with 3mm (id) tubes using 2% pH 3.5-10 ampholines for 20,000 volt-hours. Staining performed with Commassie blue.

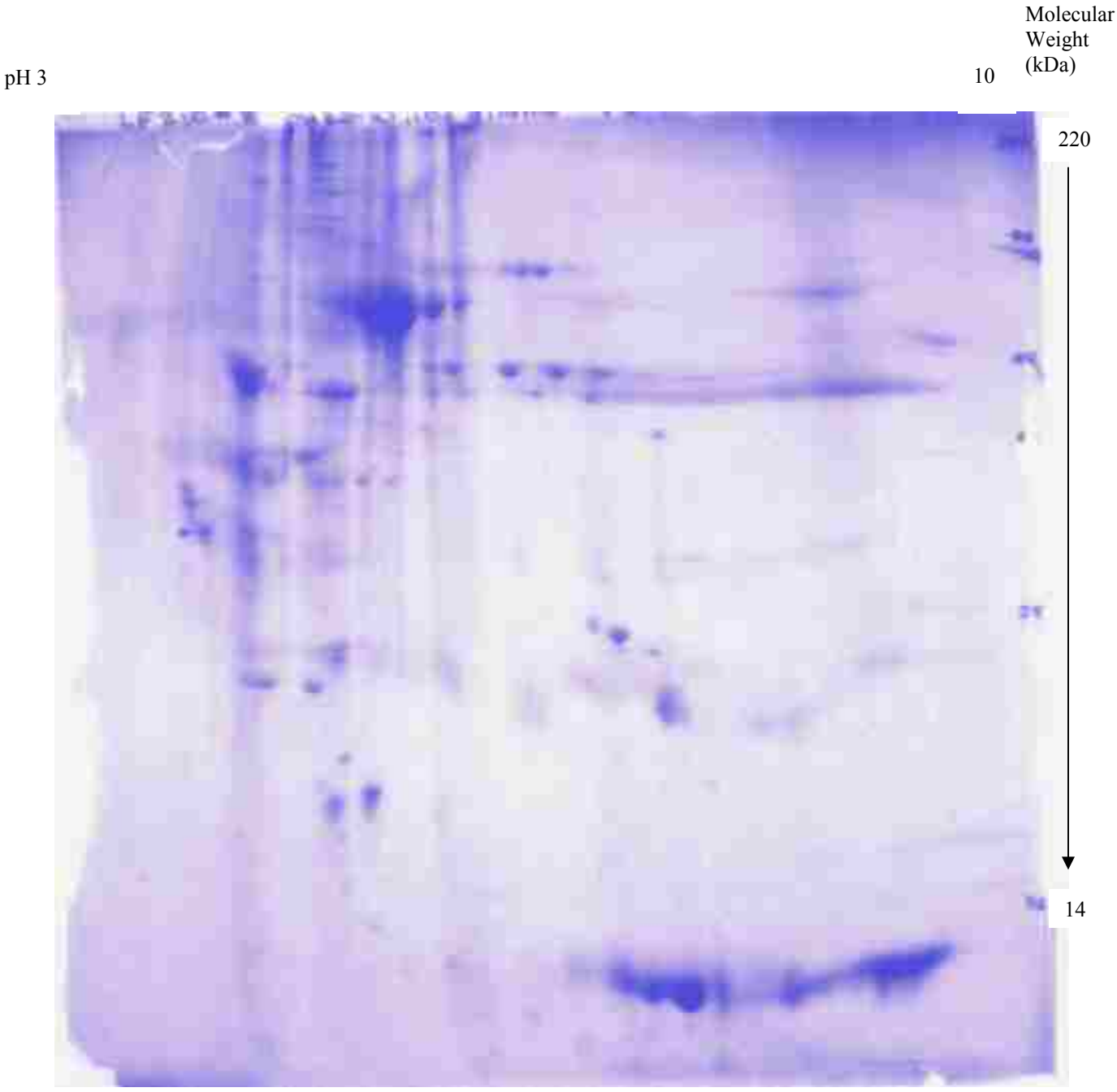

Figure 3.9. LF210-08 Intima / media extract of thoracic aorta of 80 year old. Lysis buffer containing sodium dodecylsulfate. IEF performed with 3mm (id) tubes using 2% pH 3.5-10 ampholines for 20,000 volt-hours. Staining performed with Commassie blue.

The spot counts from the various samples vary based on the different tissue areas dissected. Variability in the number of spots was observed from different tissue areas and from the components used in the lysis buffer. The protocols for the IPG approach was more desirable since current 2D analysis is performed using the IPG drystrips that were not amenable to high concentrations of SDS. A comparison of the two approaches is listed in Table 3.2. In instances where sample are boiled in SDS and diluted with reduced SDS concentrations, higher protein spot results when compared to dilutions with IPG buffer components.

Solubilization and separation of membranes are more complex due to their chemical character and compartmentalizaton where IPG strips are used for IEF [34]. SDS is a powerful ionic surfactant with high potential for hydrophilic and hydrophobic protein solubility. The property for protein solubility arises from the propensity to bind highly to proteins with one SDS molecule per every two protein molecule as well as the ability to couple with a strong polar head group. Its use is limited for IPG applications because it is a charge shifting reagent and is generally avoided. The limited use can be tolerated provided the final concentration is diluted below 0.25%. The uses of SDS in concentrations of 2% is compared to the same extraction method; however the final surfactant concentration is diluted with other surfactants using a nonionic or zwitterionic phase to solubilize the proteins prior to IEF on tube gel. The number of spots was compared to assess the number of proteins that may be resolved using the number of spots as the criteria in Table 3.2. By using this approach, the efficiency of using IPG strips with various chaotropes and other denaturants other than SDS can be monitored. Additionally, the number of proteins that can be identified can be compared particularly the more hydrophobic membrane proteins that are very alkaline. This use of urea and other chaotropes have been widely accepted to improve separation and solubility. From the table below, SDS produces a higher spot count than the solution diluted with IPG buffer.

Table 3.2 Comparison of lysis buffer type and protein spot count in various plaque tissue extracts from thoracic aortas. Spot count performed with Kodak 1D Gel Logic and manual.

Gel Identification	Sample No.	Tube Buffer	Protein Spot Count
LF210-01	80 year old intima	IPG	74
LF210-02	57 year old intima	IPG	56
LF210-03	57 year old media	IPG	40
LF210-04	80 year old media/intima	IPG	28
LF210-05	80 year old intima	SDS	63
LF210-06	57 year old intima	SDS	95
LF210-07	57 year old media	SDS	64
LF210-08	80 year old media/intima	SDS	38

Protein spots from sample LF210 - 06 were selected for further analysis by mass spectrometry. This particular sample was selected due to larger number of protein spots generated by 2D electrophoresis. The spot count is the best indication of the protein separation. These images were generated as regions of interest from molecular imaging software. The spots were excised and in-gel tryptic digestion with porcine sequence grade modified trypsin was performed. The peptides from the digested product were analyzed using the LTQ-FT mass spectrometer with capillary scale reverse phase high performance liquid chromatography. Figure 3.10 shows the gel image of LF210-06 with the initial spots that were analyzed. In this initial experiment, the spots were selected that were isolated and did not present contamination with adjoining spots during excision.

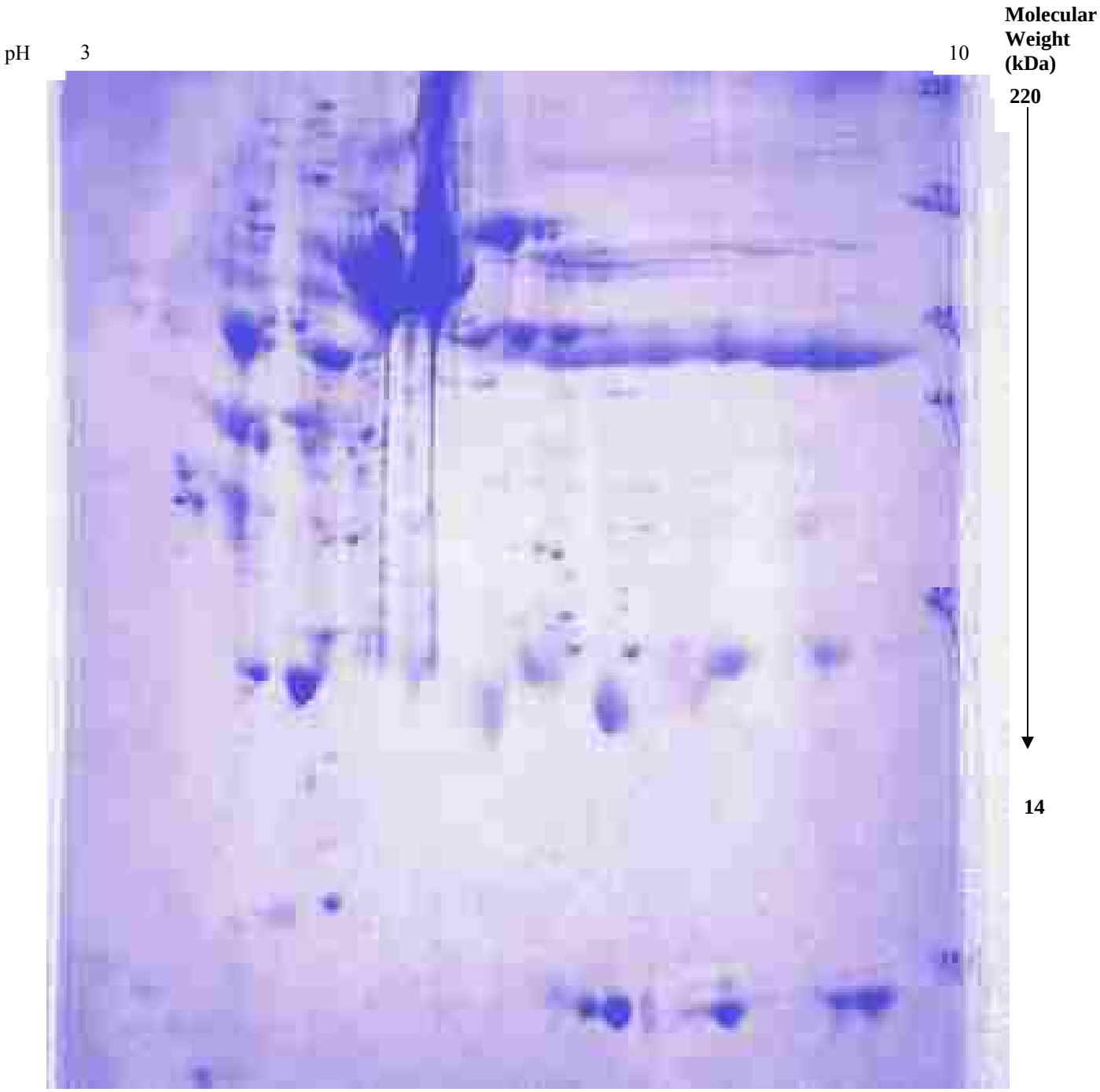

Figure 3.10. Illustration of a 2D gel LF210-06 for extracts of human thoracic aortas plaques Stained with Coomassie Blue. IEF performed with 3mm (id) glass tubes using 2% pH 3.5-10 ampholines for 20,000 volt-hours. Staining performed with Commassie blue. The spots were excised manually and enzymatic digestion performed with trypsin.

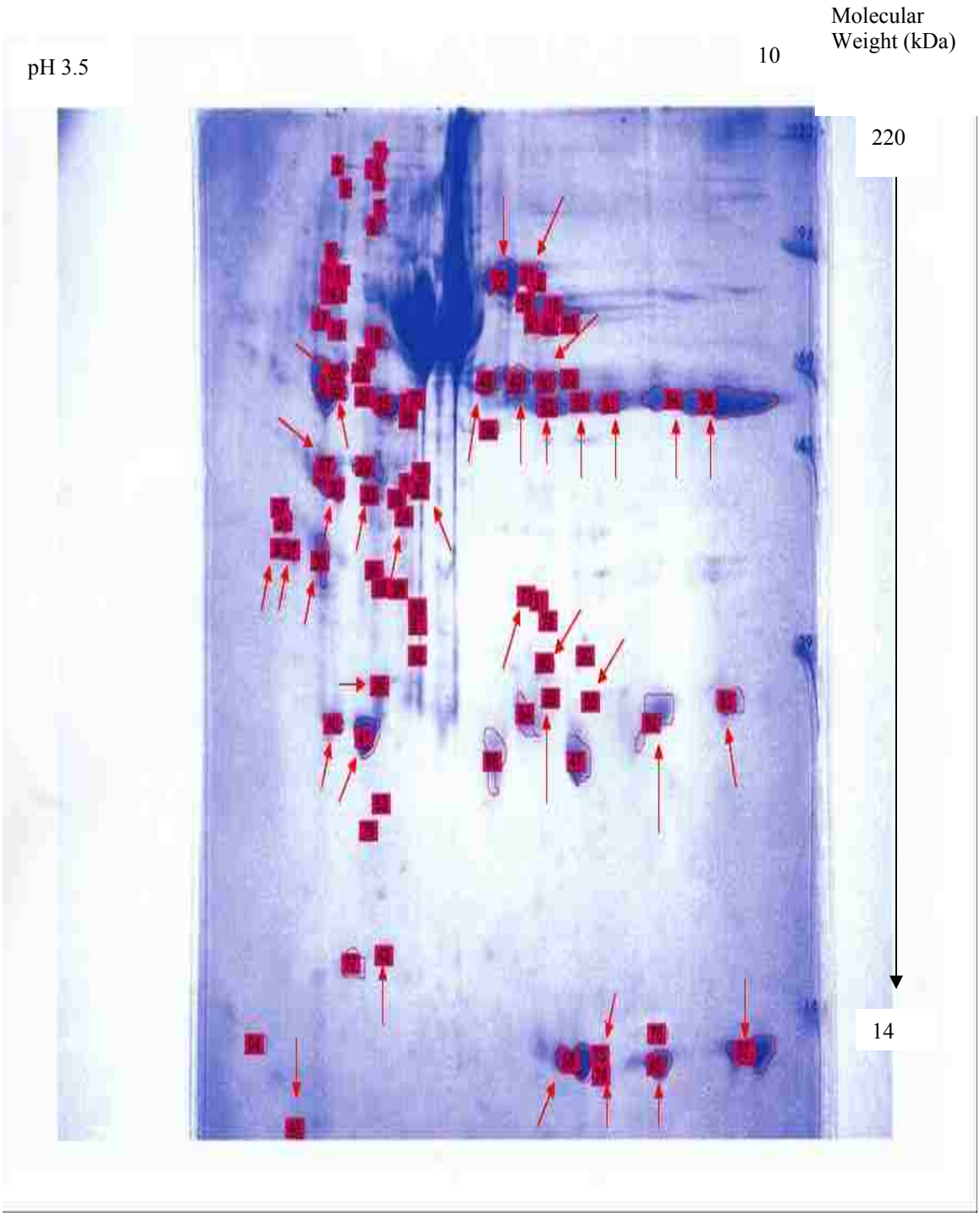

Figure 3.11 Illustration of a 2D gel LF210-06 from extracts of human thoracic aortas plaques stained with Coomassie Blue. Arrows indicate excised protein spots that were isolated and did not present contamination with adjoining ones. These spots were identified by mass spectrometry.

One of the challenges of the analysis lies in the determination of intact proteins that are potential disease markers embedded within the human plasma proteome. Proteins such as albumin and IgG comprise approximately 80% of the plasma proteome, leaving 20% as low abundant proteins that may have some significance in signal pathways that are critical in disease markers. We attempted to investigate proteins with molecular weights less than 60 kilodaltons as templates for later differential protein expressions. Mass analysis of 35 spots was conducted with the resulting peptide spectral data searched with the nonredundant database that was downloaded from the National Center for Biotechnology Information (NCBI) website (http:// www.ncbi.nlm.ih.gov/blast/db/fasta).

Data obtained from the analysis of spot 41 is shown in Figure 3.10. The linear quadrupole trap is used to provide MS and MS/MS analysis due its advantages over conventional traps that includes reduced space charge effects due to increased ion storage volume and increasing trapping efficiencies from externally injection ions. [Ritter Proteomics 2006 6 1735-1740]. The FTICR MS is used simultaneously and used for MS scan due to its high resolution (25,000 at m/z of 400) and its sensitivity (<2ppm). The FTMS is used isolate various charged ions depicted from the RPHPLC chromatogram analysis; then further MS/MS fragmentation is performed by the LTQ. Peptides selected from the full scan performed with the FTMS. Charge states (usually +3) are determined from the Xcalibur software. MS/MS scans were analyzed from the ITMS from the +2 charged that produced the best ion intensities measurements. The fragmentation of the doubly charged states produced b and y ion sequences. The use of Bioworks 3.2 and database analysis were used to correctly identify the peptide sequence.

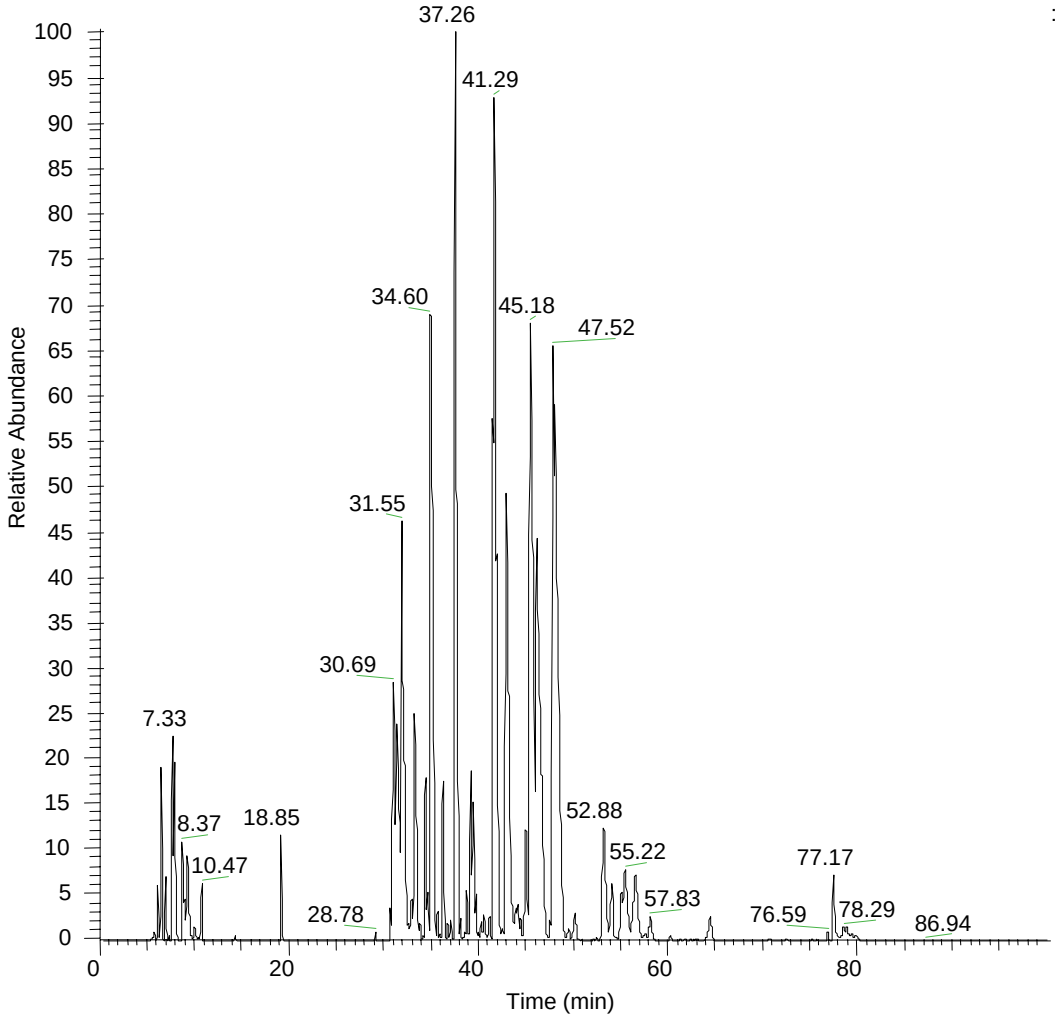

Figure 3.12. Base peak full scan analysis of nano RPHPLC chromatogram of tryptic peptides for spot 41 from 2D gel electrophoresis from tissue lysate of LF210-06.

linear trap and the ion cyclotron resonance cell for MS^2 assignments for the peptides. Various peptides have been selected and the sequences determined for the fragmentation of the b and y ions. Figure 3.11 illustrates the peptide at a retention time of 18.86 minutes. The expanded chromatogram of the tryptic digested peptides is shown in Figure 3.11A with peaks at retention times from 14.90 to 35.37. The peptide at 18.86 minutes was selected and the MS spectra is

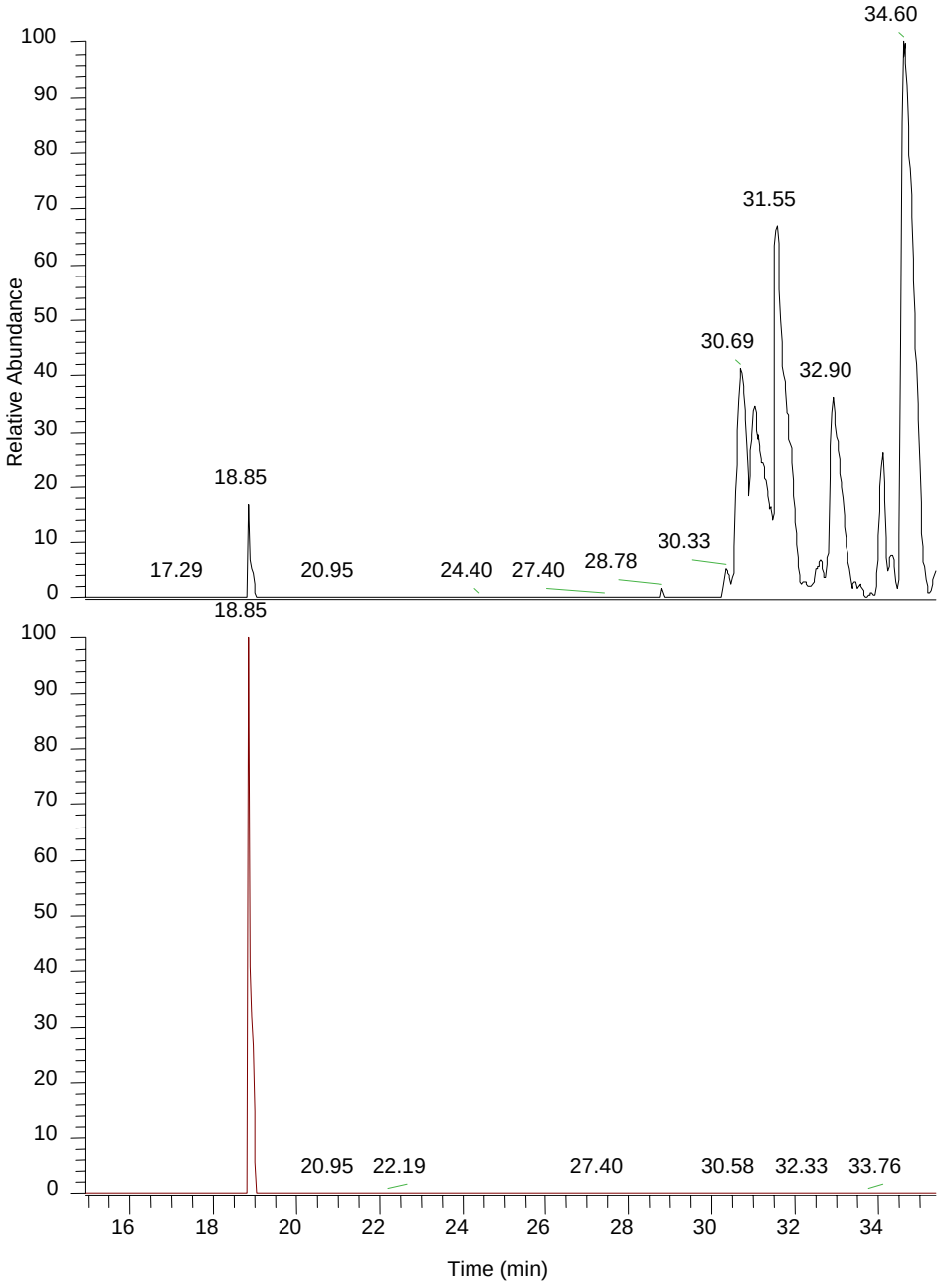

Figure 3.13. Nano C-18 reverse phase high performance liquid chromatograph scan from 14.90 to 35.37 minutes of base peak chromatogram of tryptic peptide for spot 41 resulting from 2D gel electrophoresis. The peak at 18.85 was selected for further analysis using MS/MS by ITMS

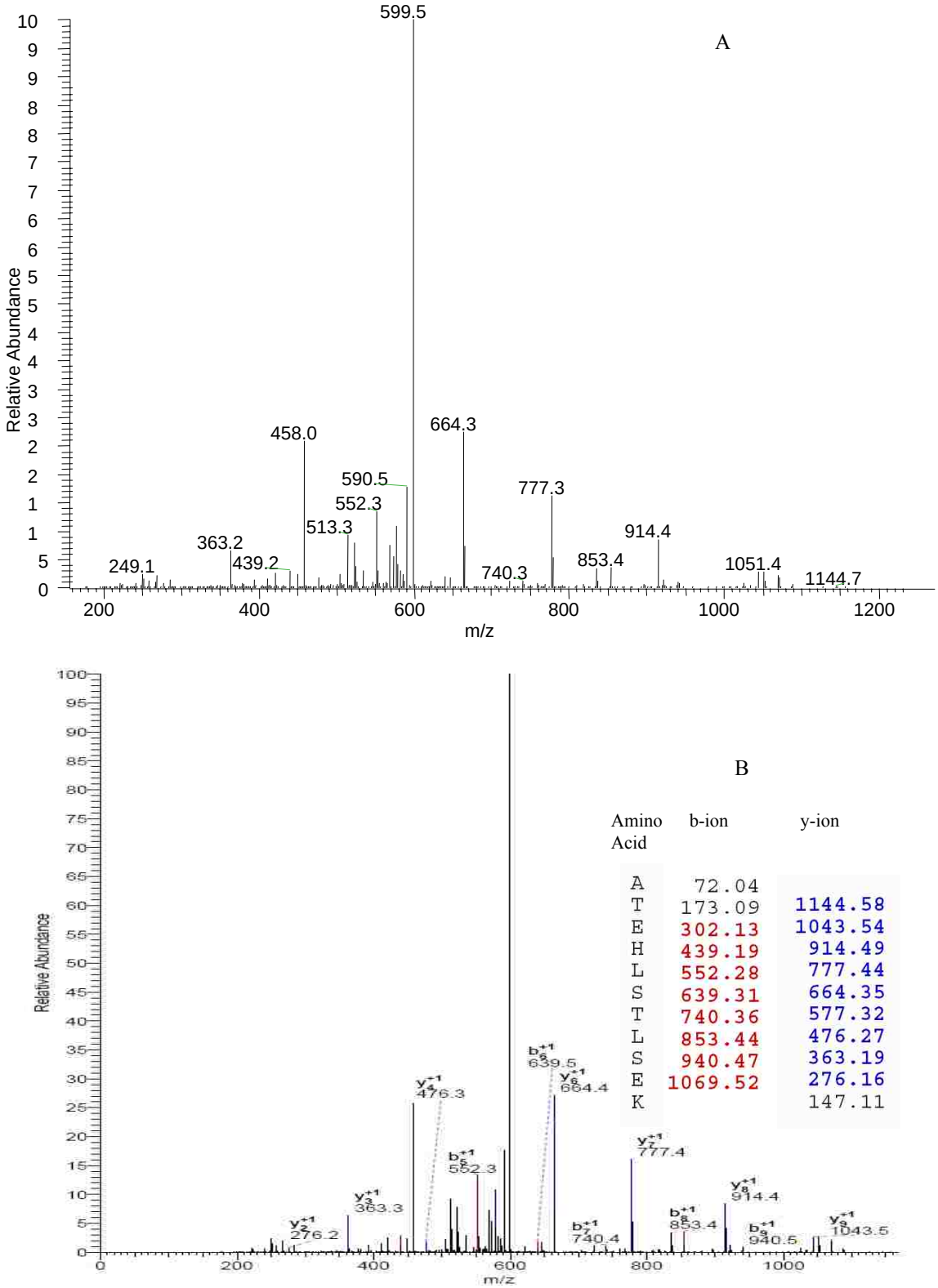

Figure 3.14. A) ITMS (MS) of doubly charged ion (m/z 608.32) at 18.86 minutes B)ITMS (MS/MS) fragmentation of doubly charge ion at m/z 608.32 producing singly charged b ions and y ions determined using Bioworks 3.2 and SEQUEST.

shown of the doubly charged precursor ion at a mass 654.32 from the linear ion trap is shown in Figure 3.13 A. The MS/MS fragmentation of the peptide from the ion trap produces y and b-ions whose sequence is shown in Figure 3.13B determined using Bioworks 3.2 with the database searches from Uniprot trembl fasta. The amino acid sequence of the peptide from the experimental data corresponds to ATEHLSTLSEK.

Additional RP-HPLC and mass spectral scans of five tryptic peptides sequenced by MS and MS/MS analysis are illustrated in Figures 3.14 to 3.25. The mass spectra of all scans first illustrate the base peak from the liquid chromatogram selected from the FTMS ICR cell. The doubly charged ions are shown from the ITMS followed by MS/MS fragmentation. MS/MS fragmentation occurs by collisional induced dissociation with helium gas. Table 3.3 summarizes the selected peptides and the sequences determined from database search and Bioworks 3.2 and SEQUEST software analysis.

Table 3.3 Summary of peptide sequences using MS and MS/MS analysis

Nano RP HP LC Retention Time (minutes)	Base Peak HPLC FTMS Scan Retention Time (minutes)	ITMS Scan +2 Charged Ion	ITMS MS/MS Sequence of +1 Charged ions
14.90-35.37	18.86	608.32	ATEHLSTLSEK
14.90-35.37	28.80	524.26	LSPLGEEM#R
14.90-35.37	31.77	714.34	KWQEEM#ELYR
28.01-49.55	33.52	690.86	VQPYLDDFQKK
28.01-49.55	35.79	637.00	LHELQEKLSPLGEEMR
28.01-49.55	37.60	651.33	THLAPYSDELR
28.01-49.55	44.95	734.71	LREQLGPVTQEFWDNLEK

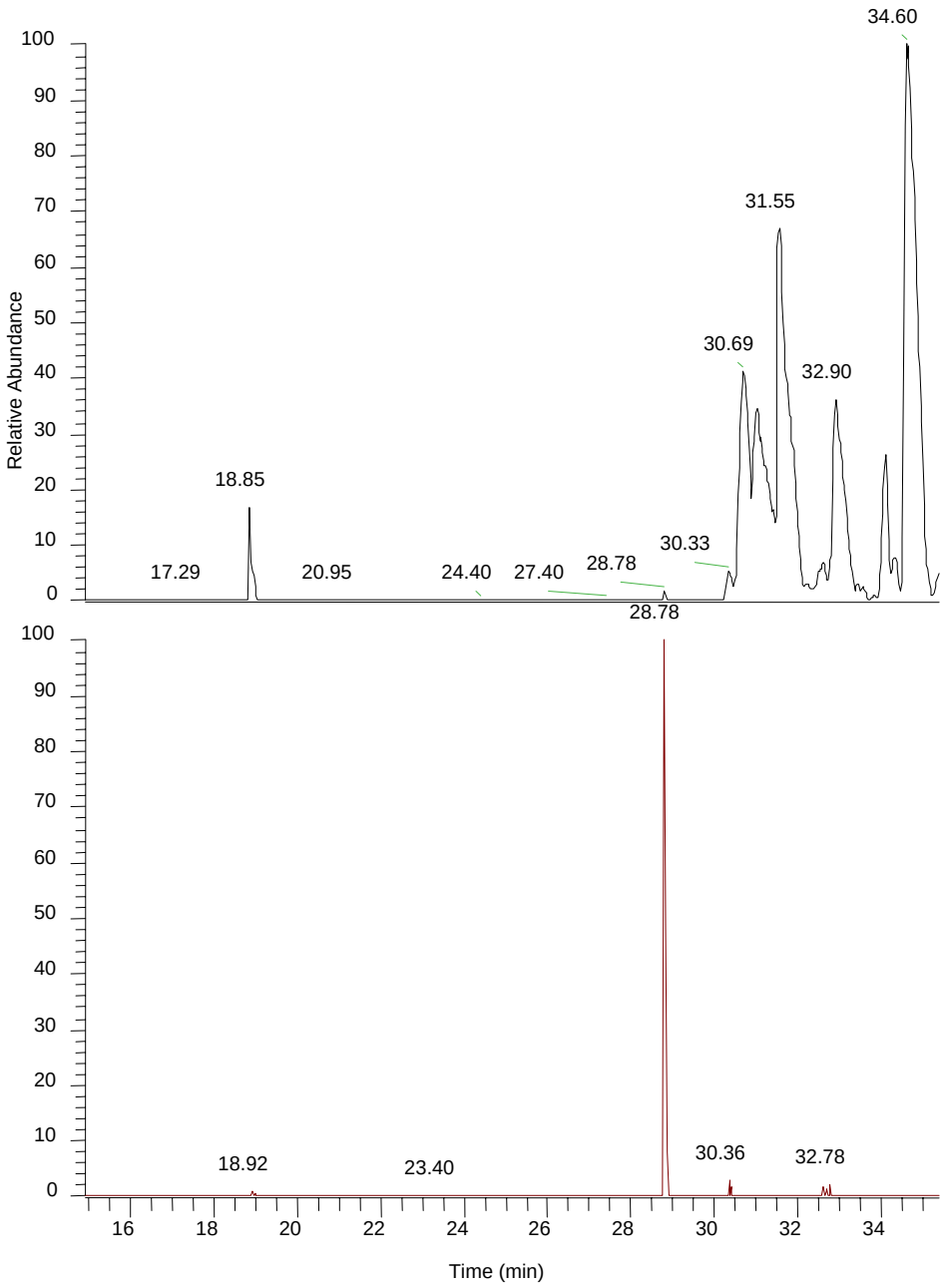

Figure 3.15. Nano C-18 reverse phase high performance liquid chromatograph scan from 14.90 to 35.37 minutes of base peak chromatogram of tryptic peptide for spot 41 resulting from 2D gel electrophoresis. The peak at 28.80 was selected for further analysis using MS/MS

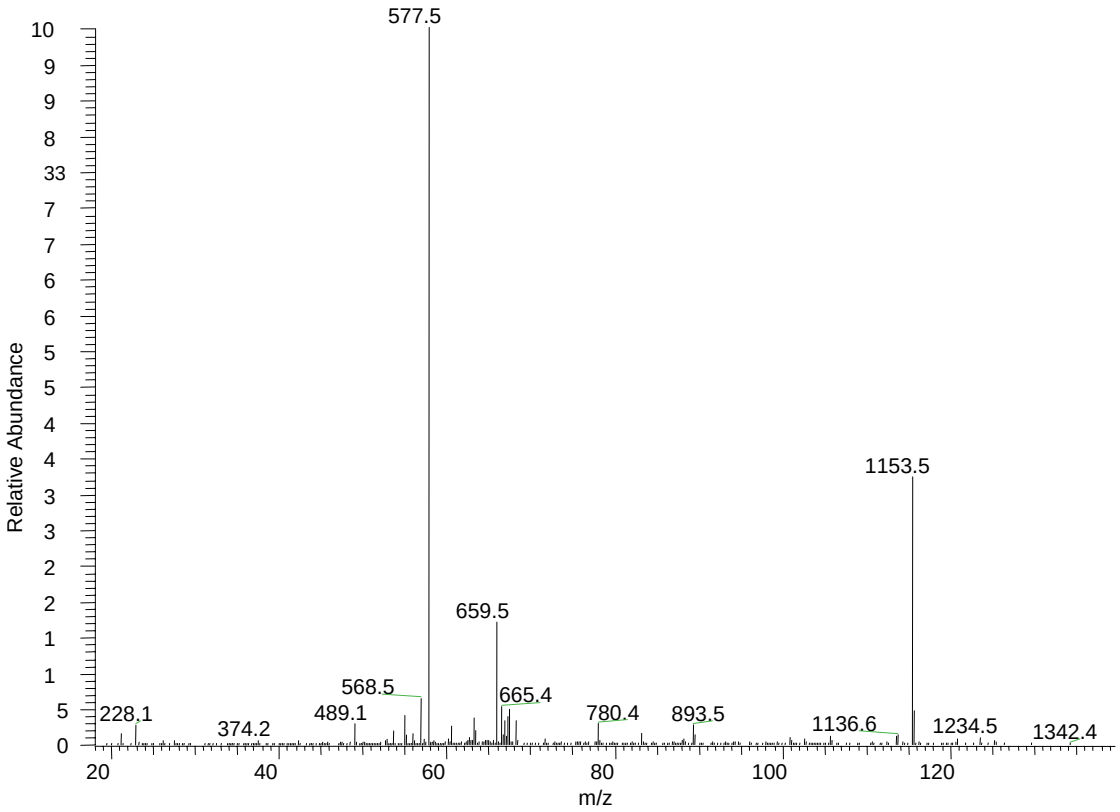

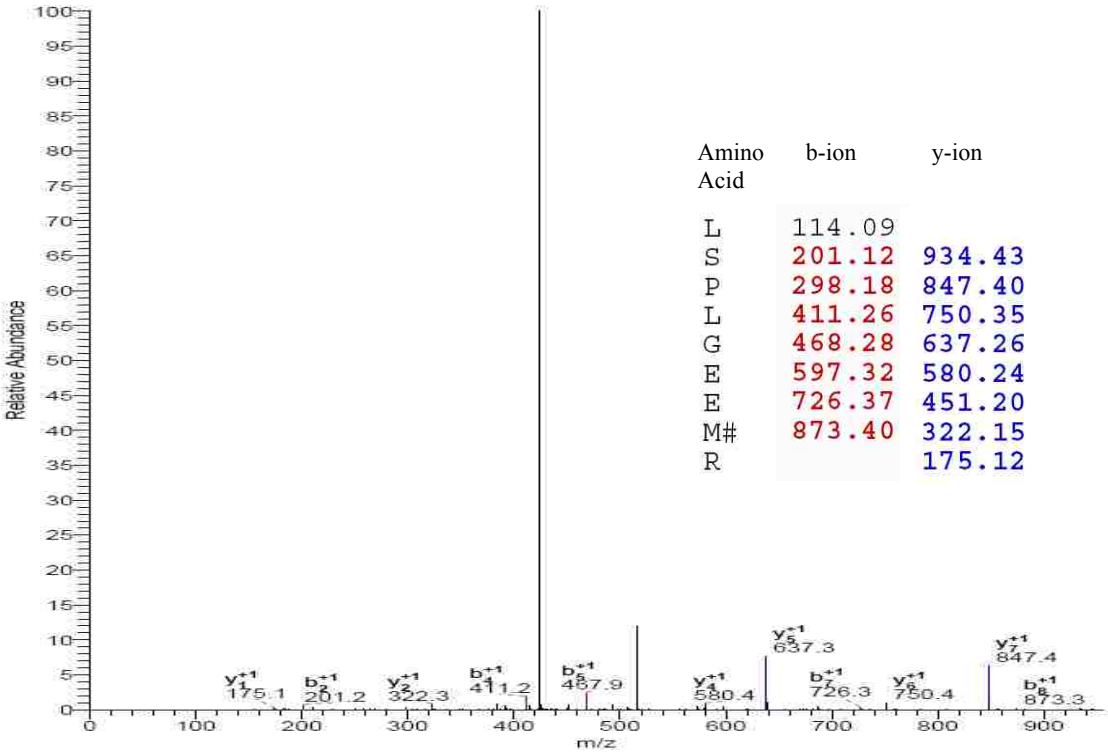

Amino Acid	b-ion	y-ion
L	114.09	
S	201.12	934.43
P	298.18	847.40
L	411.26	750.35
G	468.28	637.26
E	597.32	580.24
E	726.37	451.20
M#	873.40	322.15
R		175.12

Figure 3.16 A) ITMS (MS) of doubly charged ion (m/z 524.26) at 28.80 minutes B)ITMS (MS/MS) fragmentation of doubly charge ion at m/z 524.26 producing singly charged b ions and y ions determined using Bioworks 3.2 and SEQUEST.

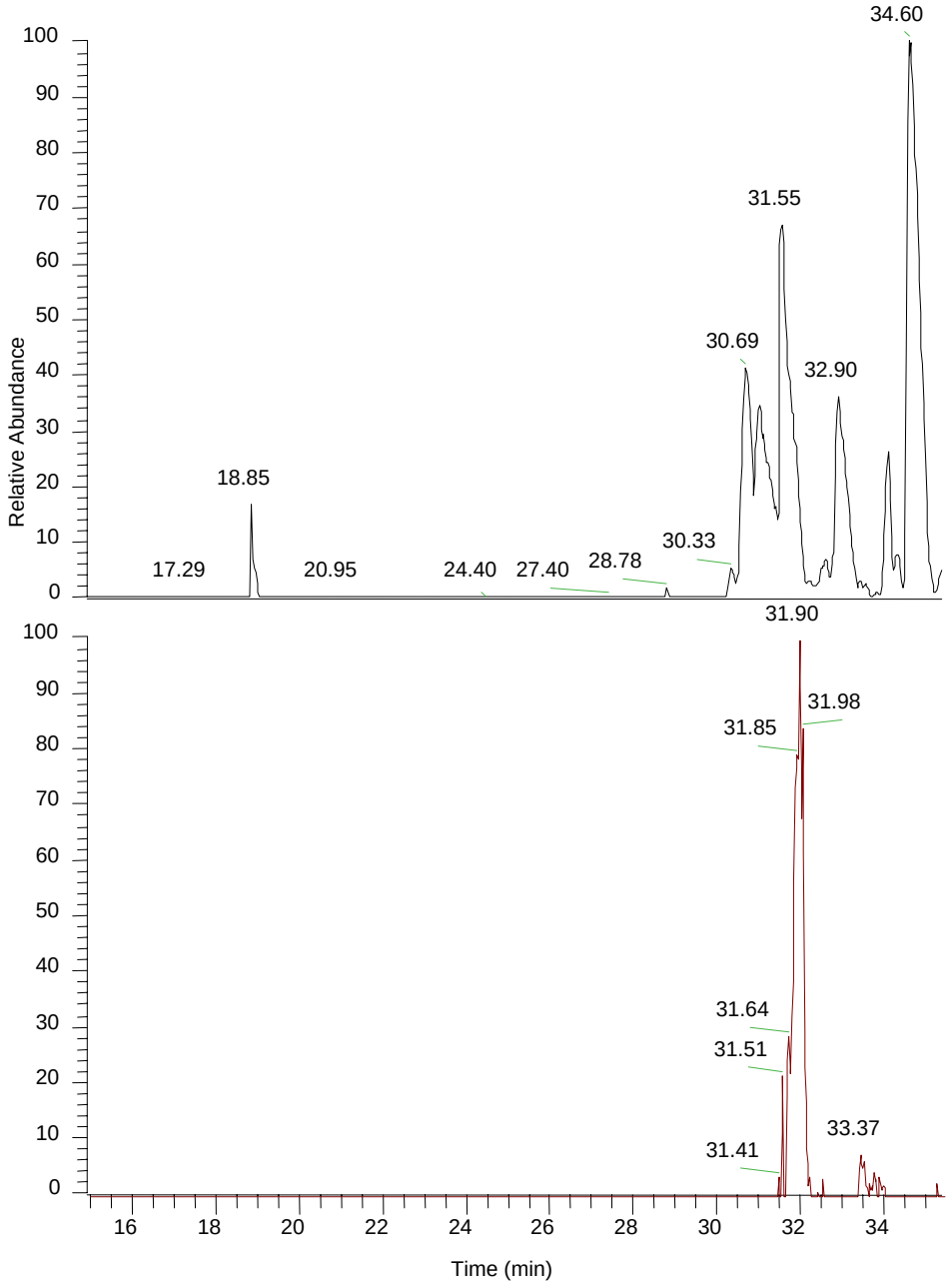

Figure 3.17. Nano C-18 reverse phase high performance liquid chromatograph scan from 14.90 to 35.37 minutes of base peak chromatogram of tryptic peptide from spot 41 resulting from 2D gel electrophoresis. The peak at 31.77 was selected for further analysis by MS and MS/MS by ITMS.

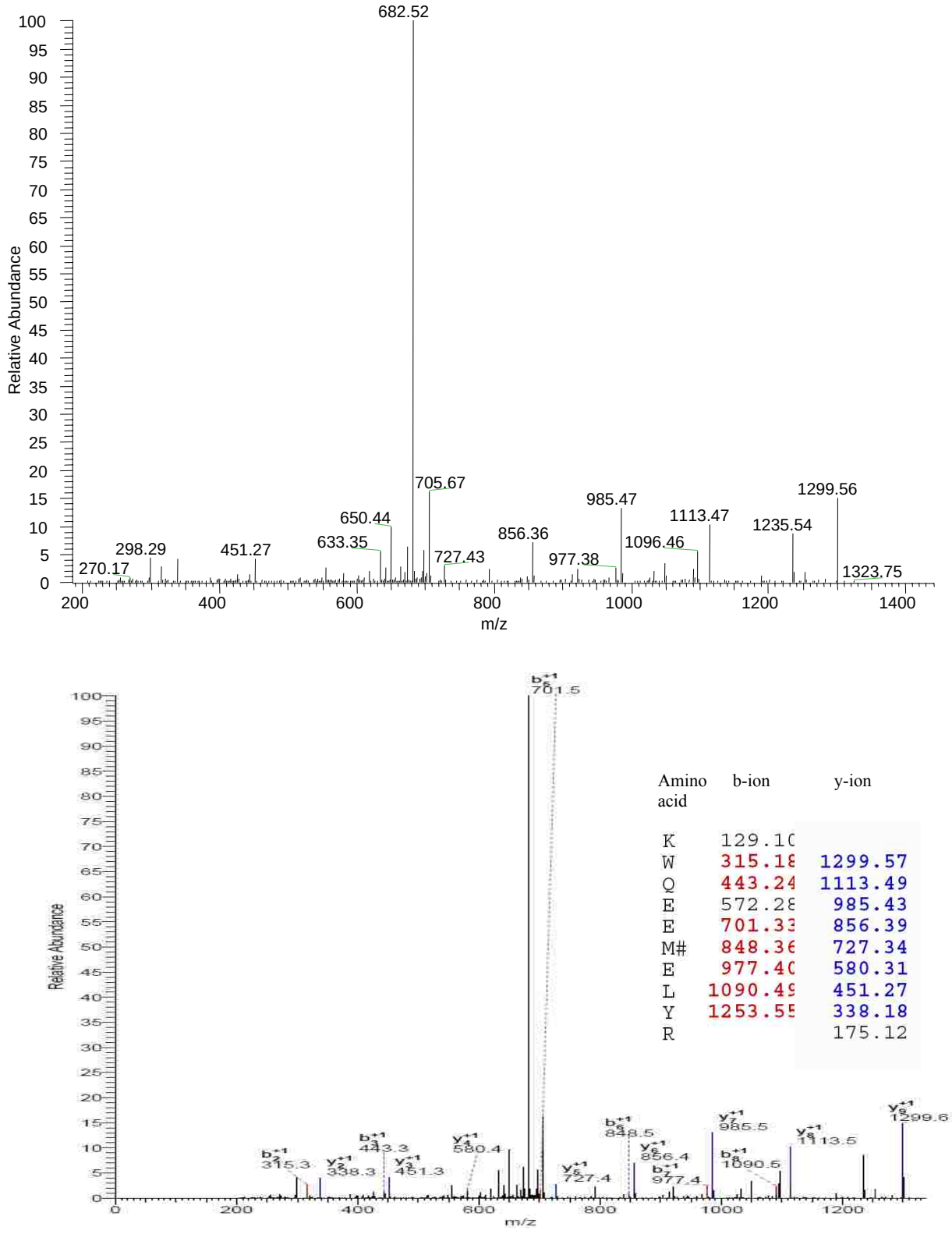

Figure 3.18. A) ITMS (MS) of doubly charged ion (m/z 714.34) at 31.77 minutes B)ITMS (MS/MS) fragmentation of doubly charge ion at m/z 714.34 producing singly charged b and y ions determined using Bioworks 3.2 and SEQUEST.

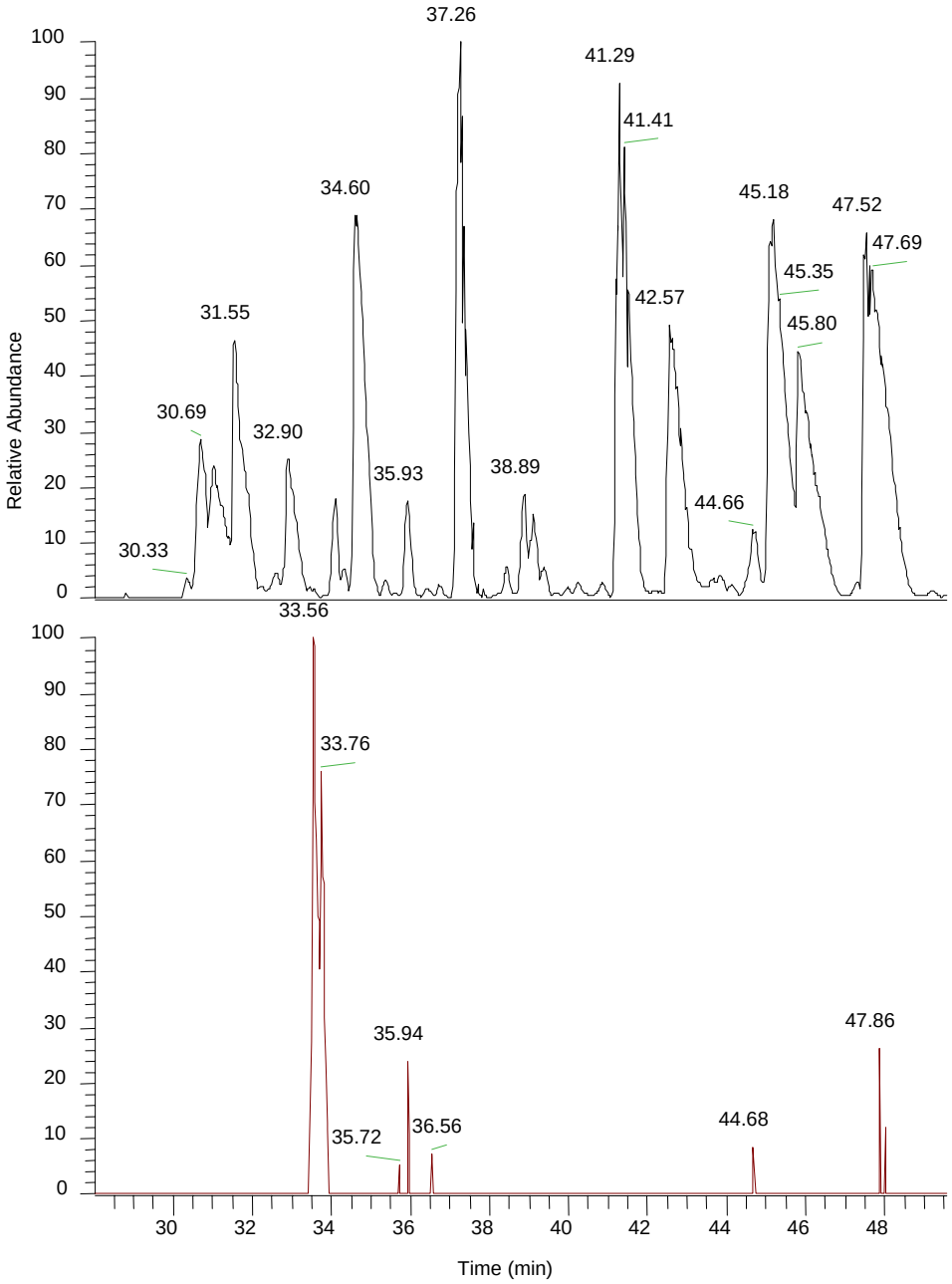

Figure 3.19. Nano C-18 reverse phase high performance liquid chromatograph scan from 28.01 to 49.55 minutes of base peak chromatogram of tryptic peptide from spot 41 resulting from 2D gel electrophoresis. The peak at 33.52 minutes was selected for further analysis by MS and MS/MS by ITMS.

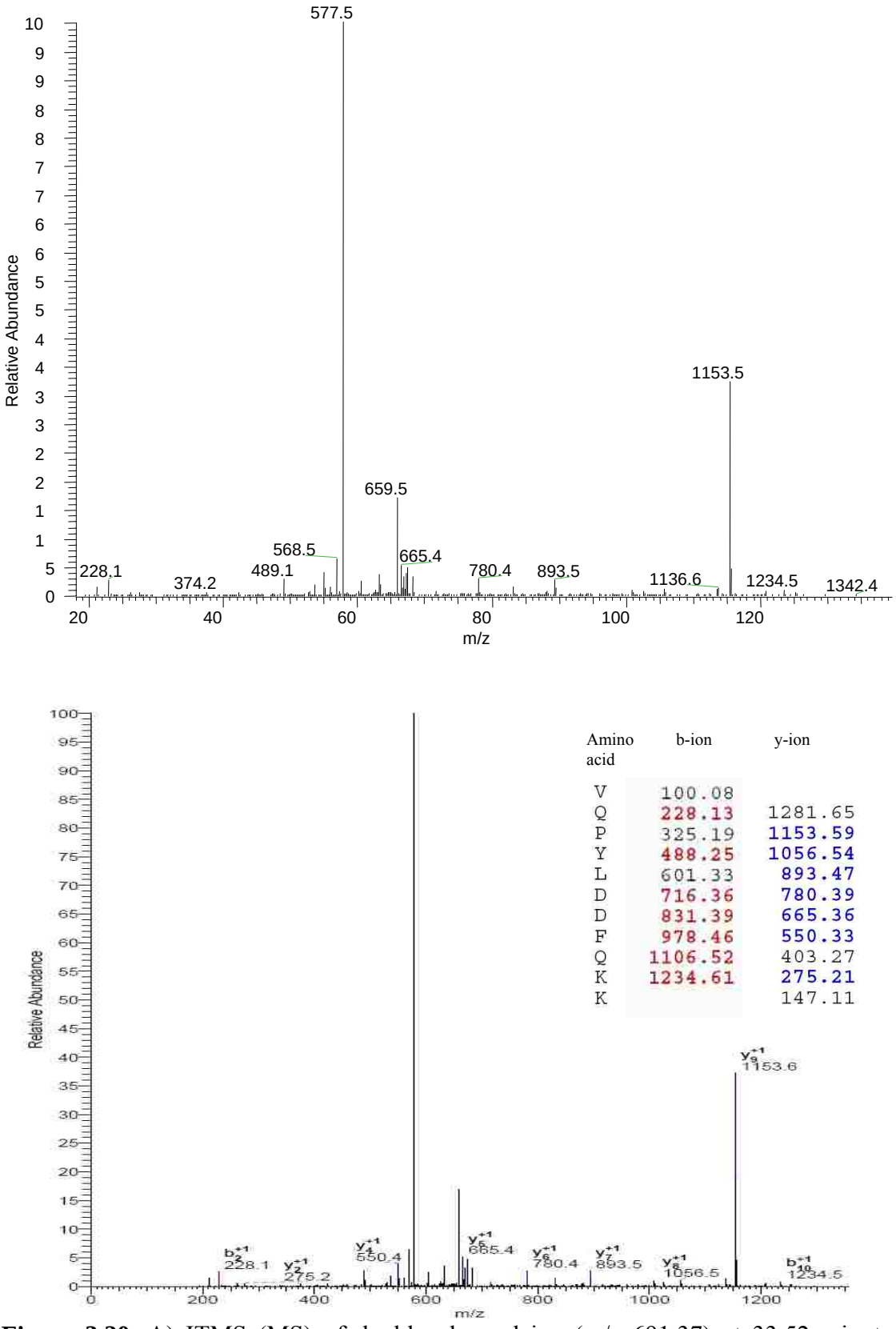

Figure 3.20. A) ITMS (MS) of doubly charged ion (m/z 691.37) at 33.52 minutes B)ITMS (MS/MS) fragmentation of doubly charge ion at m/z 691.37 producing singly charged b and y ions determined using Bioworks 3.2 and SEQUEST.

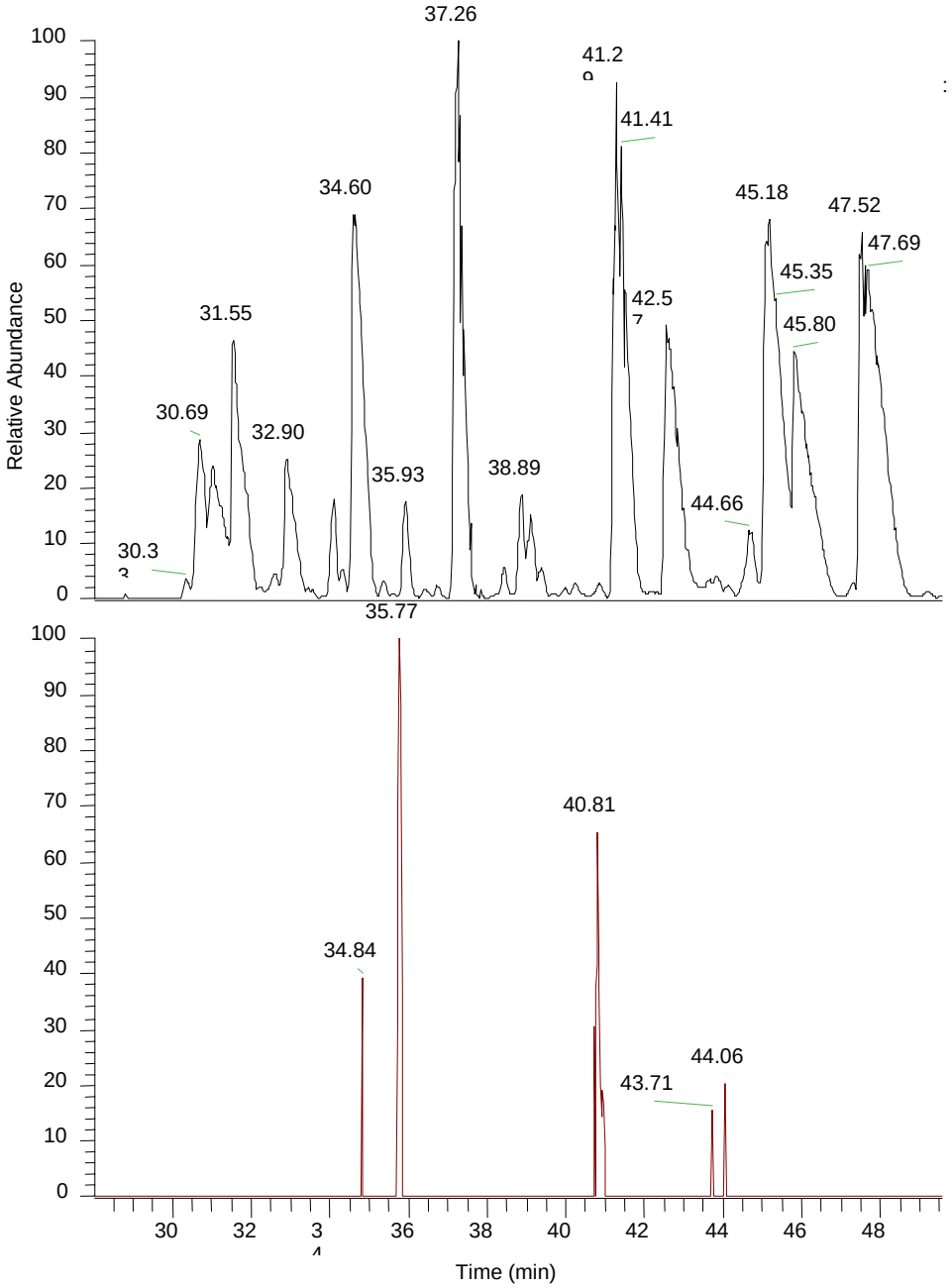

Figure 3.21. Nano C-18 reverse phase high performance liquid chromatograph scan from 28.01 to 49.55 minutes of base peak chromatogram of tryptic peptide for spot 41 resulting from 2D gel electrophoresis. The peak at 35.79 minutes was selected for further analysis by MS and MS/MS by ITMS.

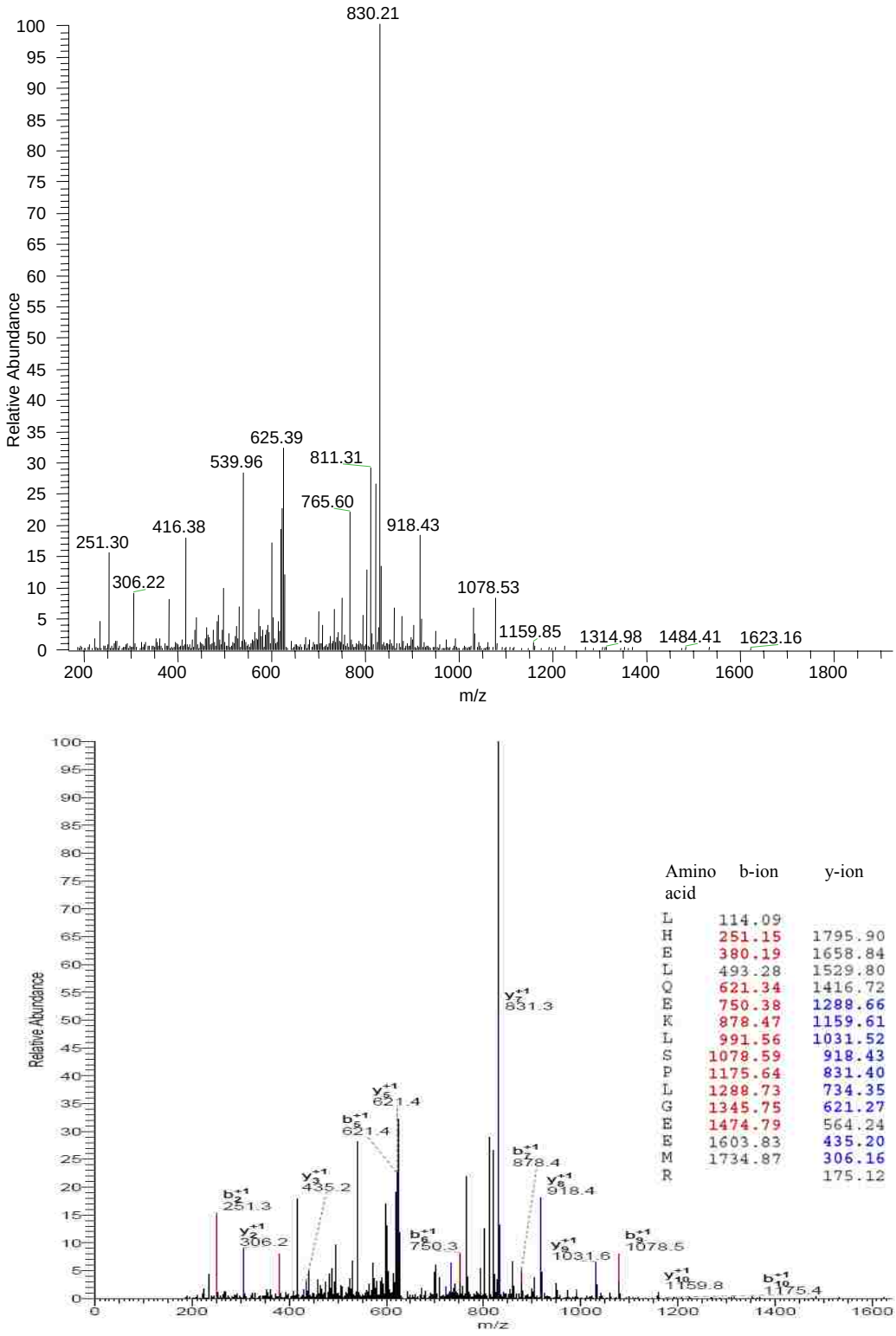

Figure 3.22. A) ITMS (MS) of doubly charged ion (m/z 637.34) at 35.79 minutes B)ITMS (MS/MS) fragmentation of doubly charge ion at m/z 637.34 producing singly charged b and y ions determined using Bioworks 3.2 and SEQUEST.

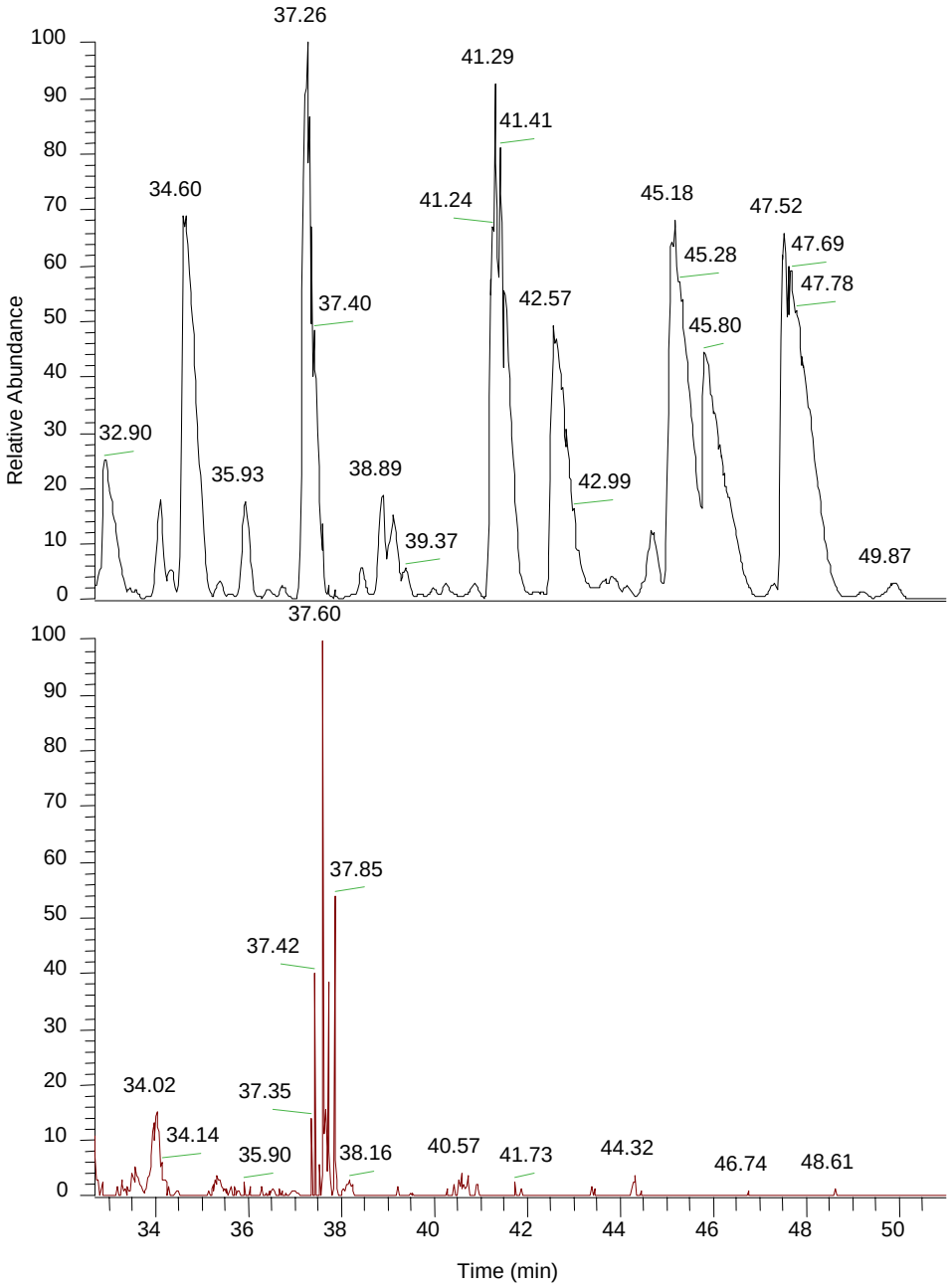

Figure 3.23 Nano C-18 reverse phase high performance liquid chromatograph scan from 32.67 to 50.98 minutes of base peak chromatogram of tryptic peptide for spot 41 resulting from 2D gel electrophoresis. The peak at 37.60 minutes was selected for further analysis by MS and MS/MS by ITMS.

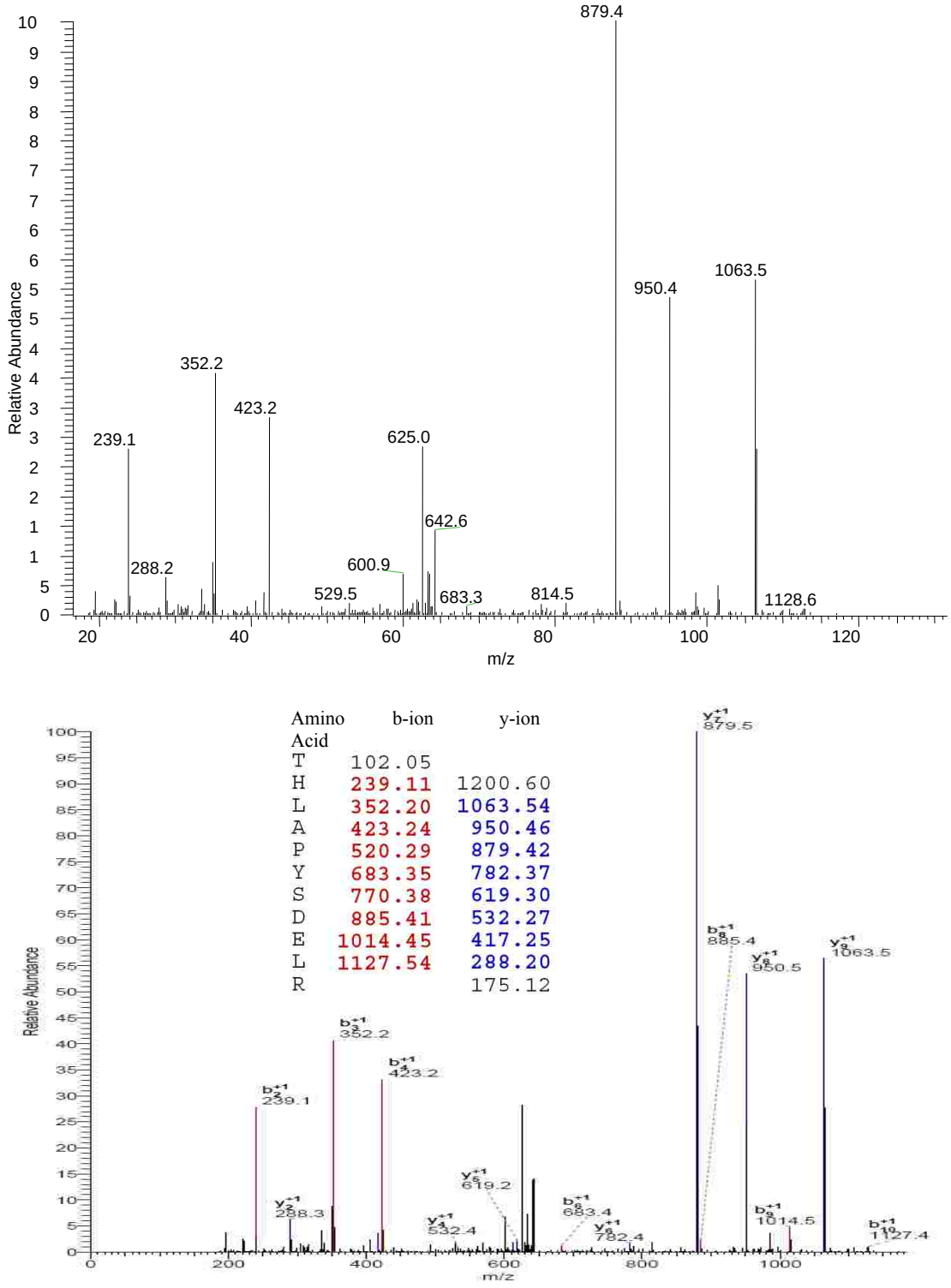

Figure 3.24 A) ITMS (MS) of doubly charged ion (m/z 651.33) at 37.60 minutes B)ITMS (MS/MS) fragmentation of doubly charge ion at m/z 651.33 producing singly charged b and y ions determined using Bioworks 3.2 and SEQUEST.

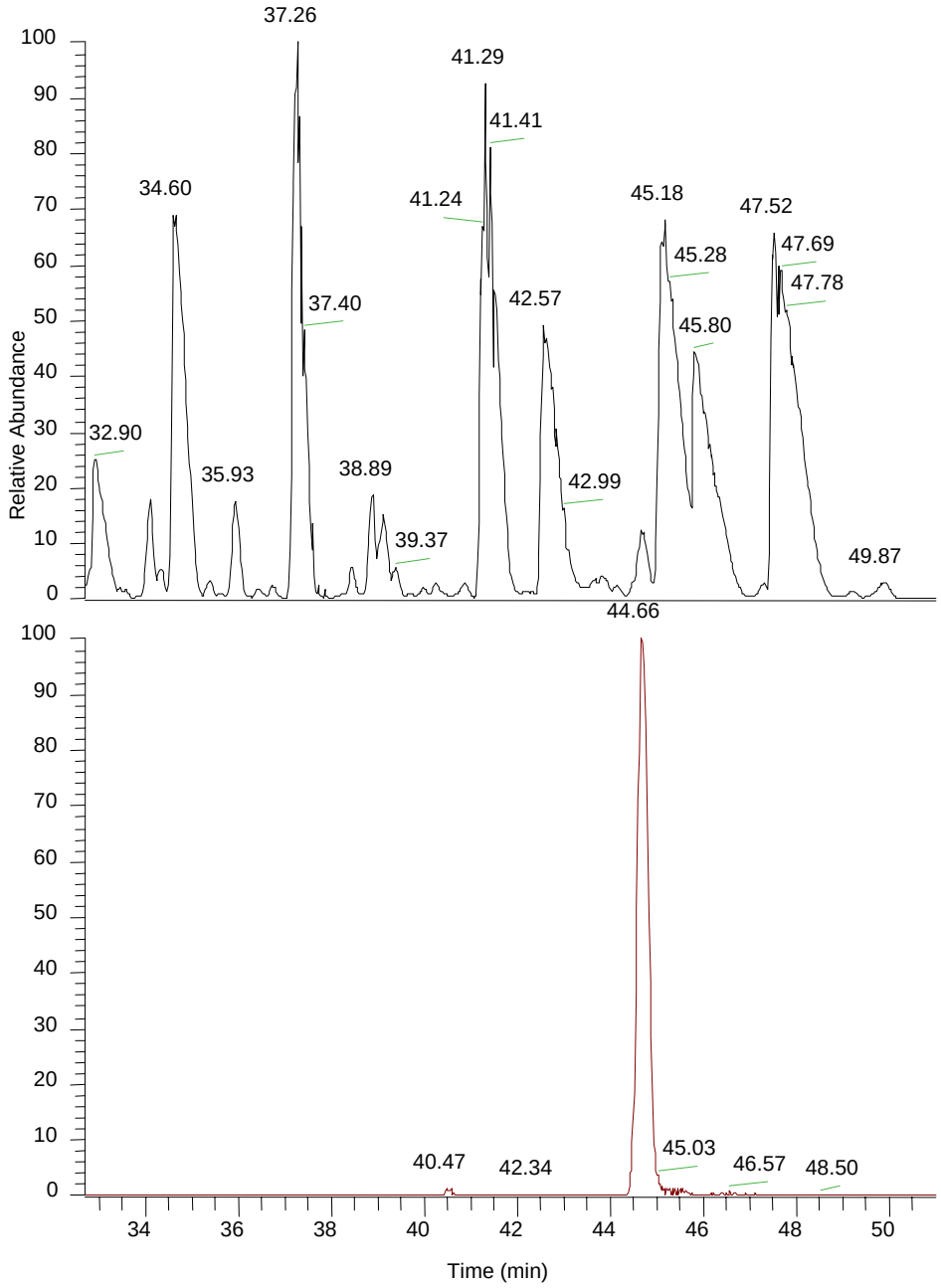

Figure 3.25 Nano C-18 reverse phase high performance liquid chromatograph scan from 32.67 to 50.98 minutes of base peak chromatogram of tryptic peptide for spot 41 resulting from 2D gel electrophoresis. The peak at 44.95 minutes was selected for further analysis by MS and MS/MS by ITMS.

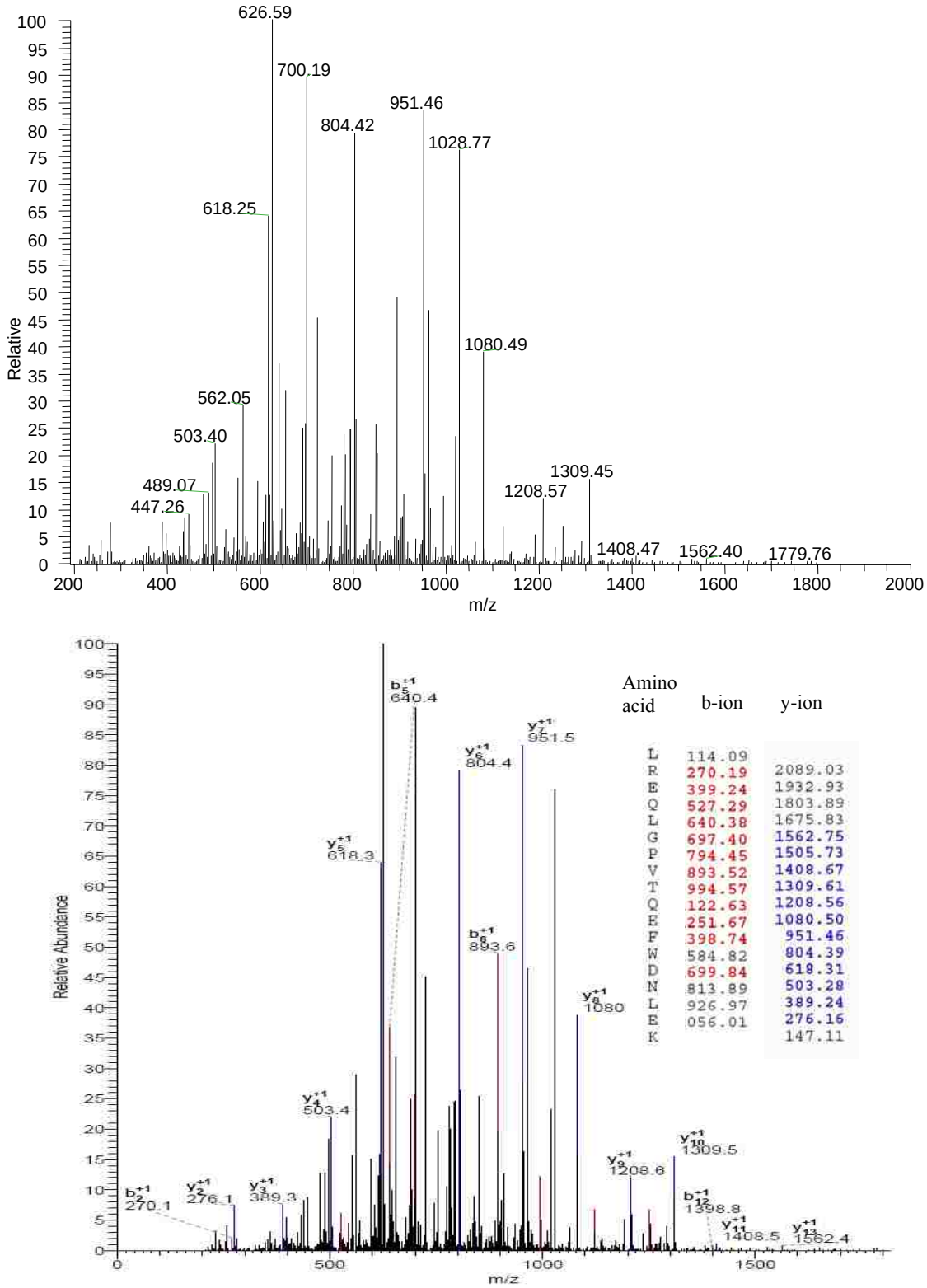

Figure 3.26 A) ITMS (MS) of doubly charged ion (m/z 735.05) at 44.95 minutes B)ITMS (MS/MS) fragmentation of doubly charge ion at m/z 735.05 producing singly charged b and y ions determined using Bioworks 3.2 and SEQUEST.

The protein identified at spot 41 was determined to be Apolipoprotein A-1 based on the database search parameters. The protein identification criterion from the database has a probability score of 3.16E-11 and a score of 402.29. The scoring function is produced form the peptide filtering software from SEQUEST. It is a measure of the fit of theoretical spectra that is created for the sequences b and y ions along with water and amine lossied compared to the actual MS/MS spectra that are acquired by the instrument. The spectra resemble a bar code that measures the mass and intensity. The P score or probability score is based on the statisitical expectation of misidentification. This value is the correlation of the fragment ion m/z values between the observed spectra and the theoretical spectra. Therefore, a peptide that has a low P value (<0.00001) is statistically a much better match than a higher P value (>.01). The protein is a major constituent of human plasma with a molecular weight of 28,300. It is a major constituent of high density lipoprotein and activates lecithin cholesterol acyltransferase. Apoliprotein B to A-1 ratio represents the balance of protherogenic and antitherogenic variable for coronary risk [35].

The ratio of low to high density lipoprotein cholesterol also represents similar coronary risk. However, evidence supports the idea that the ration of apolipoprotein (Apo B/Apo A-1) is a better index of risk of the disease [36]. Clearly from this evidence the presence of Apolipoprotein A-1 alone can be utilized as a marker of proteins that promote atherosclerosis.

Additional full scan spectra of two proteins identified for enzymatic digestion of spot 65 and 67 for the 2D gels are illustrated in Figures 3.26 and Figures 3.27. Amino acid sequence for Fibrinogen for singly charged b and y ion fragmentation is given as LTIGEGQQHHLGGAK. Similarly the protein characterized for spot 67 has been identified as Apolipoprotein A4 with a sequence of the one the digested peptides determined by MS/MS to be TQVNTQABQLR.

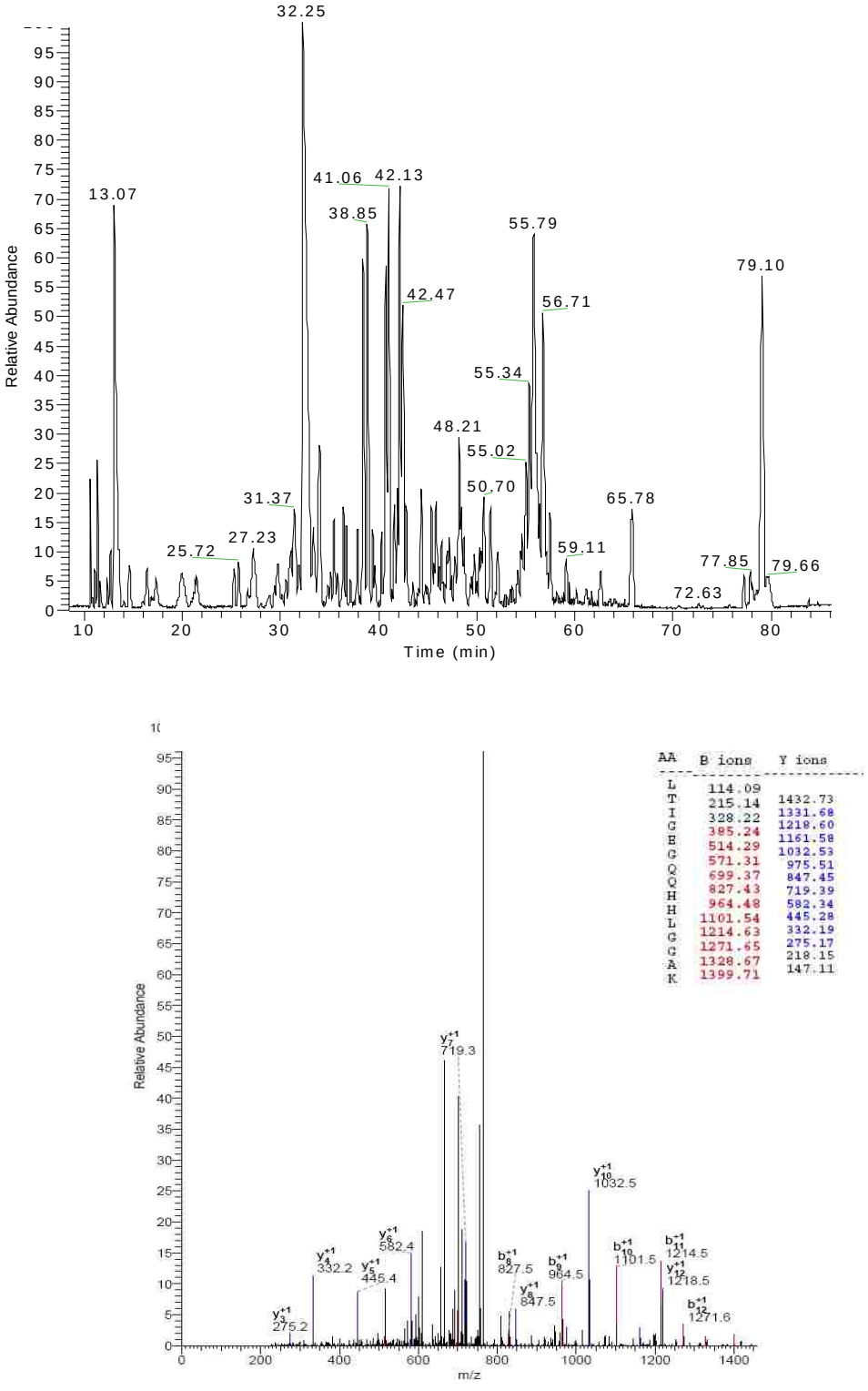

Figure 3.27 Full scan and LCMS/MS scan of peptide fragmentation of b and y singly charged ions for sequence LTIGEGQQHHLGGAK for Fibrinogen (Spot 65)

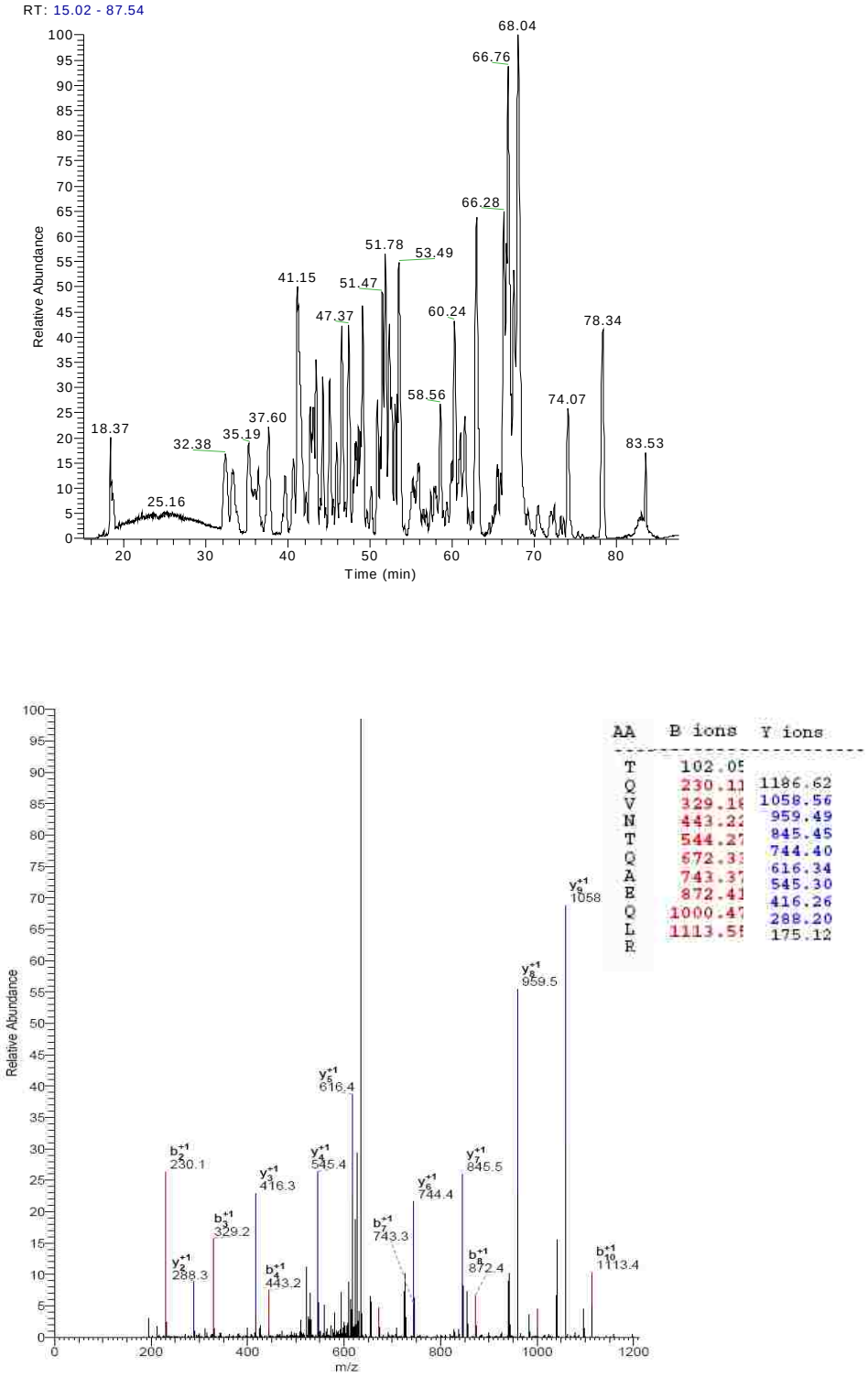

Figure 3.28 LC MS/MS full scan of spot 67 b and y ion fragmentation for peptide sequence TQVNTQABQLR for Apolipoprotein A4

A summary of proteins that were identified using LC/MS/MS fragmentation of the peptides for tryptic digest of the proteins is listed in Table 3.4. The sequences of the peptides were searched using the Bioworks 3.1 and the database the National Center for Biotechnology Information website. SEQUEST was used to calculate theoretical masses involved in the actual search was used to correlate b and y ion peaks with sequences in the database search. Parameters for the database search included proteolysis were using trypsin with one internal cleavage residue possible. A mass tolerance of 1 dalton was used in the DTA files against the predicted fragments. Peptide filter values were set at $10E^{-3}$. The X correlation values or scores that were used to increase confidence limits and determine acceptable peptide matches were 1.5 for digested peptides with a charge of one, 2.0 for +2 charge states and 2.5 for +3 charge states. These cross correlations measure the best fit parameters of the theoretical amino acids that are created from the b and y ions. The molecular weight and isoelectric points were calculated values from the accession numbers. Peptide coverages are in percentages derived from the database as well as the peptide hits are derived from the same search.

The P-score or probability is the statistical expectation of a misidentification. The magnitude of the probability empirically compares results from control mixtures of known proteins with similar search parameter to those used for the test. A low P value is a much better fit than a higher P value.

The protein spots were selected initially from the 2D images that were isolated and to reduce cross contamination from another spot in close proximity. The major problem in manual excision is the presence of plasma proteins that mask proteins of a proatherogenic nature. This is one major draw back in identifying proteins in a large pool from tissues interaction with plasma. Techniques to remove plasma proteins also reduce some proteins of interest.

Table 3.4 Summary of proteins identified by peptide sequencing with NCBI database

Spot No	Protein	Accession No	P (Pro)	Score	MW	PI	Coverage	Peptide Hits
41	Apolipoprotein A1	Q6Q785	3.16E-11	420.29	30777.83	5.56	82.40	218
42	Pre albumin		1.01E-13	90.35	15891.0		60.50	9
43	Alpha glob gene	P78461	2.55e-30	110.30	15229.9	8.16	38.00	11
44	Desmoplakin		1.06E-08	50.21	331,552.7		1.70	5
45	Alpha glop gene	P78461	1.00E-30	50.39	9054.8	8.16	49.40	5
46	Keratin 2a	Q4VAQ2	1.52E-13	268.30	65432.9	8.07	49.40	10
47	IGKC protein	Q502W4	1.00E-30	70.35	25936.23	8.69	36.40	104
48	Human hyp protein	Q3KPF2	6.45E-15	570.40	55928.15	8.54	71.10	224
49	Serum albumin	Q56G89	2.16E-10	242.29	69084.36	5.85	36.60	66
50	Hypo protein	Q3KPF2	1.11E-15	130.32	55928.15	8.54	31.00	15
51	Hepatitis B Virus	Q6PYX1	1.42E-13	88.26	38162.17	8.27	31.00	31
52	Hypo Prot DKFZ	Q6N093	7.82E-13	186.21	46060.96	7.63	35.00	57
53	Keratin 2a	Q4VAQ2	4.34E-16	272.31	65432.90	8.07	57.00	38
54	Keratin 10	Q14664	2.89E-14	106.28	59518.66	8.16	21.20	13
55	Keratin 2a	Q4VAQ2	7.30E-15	442.32	65432.90	8.07	71.80	55
56	HBV receptor	Q6PYX1	5.64E-13	70.26	1873.9		31.30	29
57	Alpha Glob gene	P78461	1.00E-30	80.37	9078.5	8.16	90.59	8
58	Beta globin gene	Q14473	3.11E-14	80.33	18930.80		60.57	8
59	Serum Alb	Q56G89	8.29E-11	130.25	69084.36	5.85	31.77	18
60	Serum Alb	Q56G89	7.61E-13	130.24	69084.36	5.85	20.20	13
61	C4A Var Protein	Q4LE82	1.00E-30	142.30	193446.30	6.61	9.59	15
63	IGKC Protein	Q502W4	1.00E-30	40.29	25936.23	8.69	21.00	4
64	Serum Alb	Q56G89	7.42E-09	230.26	69084.36	5.85	33.00	23
65	Fibrinogen	Q53Y18	8.82E-12	170.37	49496.54	5.70	41.00	17
66	Vimentin Variant	Q53H08	3.09E-12	250.31	77161.89	6.21	46.78	25
67	Apo A4 Protein	Q13784	2.79E-13	190.29	28157.52		68.00	19
68	Hyp Prot	Q3KPF2	1.44E-10	220.30	46090.96	8.54	25.80	22
69	Vitamin D Variant	Q53F31	7.77E-09	4.60	52950.61	5.34	4.60	1
70	Keratin 10	Q8N175	2.88E-08	10.22	59518.66	8.16	3.10	1
71	OTTHUMP	Q5VSY5	1.28E-10	70.27	93313.95		15.55	7
72	Transferrin var	Q53H26	4.44E-15	108.37	77079.85	6.68	14.90	11
74	Alpha Glob	P78461	8.93E-09	20.20	9078.50	8.16	35.30	2

Several proteins identified from the database may be implicated in the atherosclerotic process. Apolipoprotein A1, spot number 41, is a lipid containing complex found in plasma and

the cell that allows movement of apolar liquids through aqueous environments [37]. Its primary role is a passive carrier of lipids from one tissue to another. It is a major component of high density lipoprotein and activates lecithin cholesterol acyltransferase. It inversely affects atherosclerosis and vascular disease by removing cholesterol from tissues to the liver, antiflammatory, produces antioxidative activities and modulates vascular function [37].

Desmophlakin (spot 44) is produced in epithelial keratinocytes. Mutations in gene encoding desmosomal proteins have been identified as the mauor dysplasia / cardiomyopathy in which the right ventricular is replaced by fibro fatty tissue resulting in lethal arrhythmias [38].

Fibrinogen, spot 53 is a key factor in the coagulation cascade that exhibits proinflammatory properties, and plays a pivotal role in atherogenesis [39]. Fibrinogen triggers the formation of progressive atherosclerotic plaques. Mauriallo et al. determined that the plaque composition in patients with elevated fibrinogen was characterized by the presence of thick fibrous atheroma resulting in an increase in plaque rupture and thrombosis. A high number of inflammatory cells were localized in the shoulder and cap of the plaques [40].

Shah and colleagues have reported vimentin, spot 66, as a major component of cytoskeletal constituents of cells of mesenchymal origin that, based on in vitro studies, interacts with F-actin and polyphosphoinositide lipids. Functionally, relative to coronary heart disease, it was implicated in steroid synthesis via its role as a storage network for steroidogenic cholesterol containing lipid droplets [41].

C4a variant protein, spot 61, was studied by Fritzinger et al. [42]. This variant was a fragment of a large glycoprotein that has an important function in immune responses and host defense. The 4a component is referred to as anaphylatoxin which causes smooth muscle contraction, histamine release from mast cells, and enhancement of vascular permeability.

Additionally, these proteins mediate chemotoxins, inflammation, and generate cytotoxic oxygen radicals [43].

Apolipoprotein A4, spot 67, inhibits lipid peroxidation demonstrating antiatherogenic properties [44]. Vitamin D variant, spot 69, influences lipolysis and insulin secretion. The protein can be altered genetically to produce a polymorphism of the vitamin D receptor which has been associated with bone density mineral as well as with insulin dependent diabetes mellitus. There is evidence that the vitamin D receptor is also associated with calcific aortic valve stenosis [45].

Transferrin variant, spot 72, is normally a plasma protein that combines with iron. It is the vehicle the bound iron is carried around the body; however, free ferric ions are toxic. The presence of transition metals such as iron and copper catalyze hemolytic cleavage of LOOH to lipid peroxidation and other oxidation reactions [46].

Two proteins were identified in multiple spots 43, 45, 46, 57 and 74 matched the alpha globular gene or alpha thalassemia [47]. It is unclear of the multiple locations of the sample spots with different masses as well as pI. The protein is reported as deleted genes removed from thalassemia in which 30 different point mutations and small deletions are possible. Serum albumin, spots 42, 49, 59, 60, 64, 73, is a major component of plasma. Since the protein composes 80% of most proteomic analysis of tissues, it is a common problem in comparative proteomics of diseased and non diseased tissue extracts. A large number of proteins are normally represented by multiple spots that may be the result of post translational modifications such as phosphorylations, gylcosylations, etc. The exact biological significance for observed heterogenicities is uncertain.

Human hypothetical protein has been identified in spots 48, 50, and 52. To extent to that

these proteins occurs frequently in the database searches may be due to isoforms or various modifications that may exist in the protein.

3.5 Conclusions

The use of 2D gel electrophoresis combined with mass spectrometry using a linear quadrupole trap Fourier transform ion cyclotron trap mass spectrometer for analysis of 34 of 95 proteins spots from diseased areas of human thoracic aortas revealed nine proteins with proatherogenic properties. Nine proteins have been identified with some proatherogenic propensities. However, a more precise identification method using peptide sequencing is affected due to keratins contamination. The global method used to identify differences between normal and diseased tissues is time and labor intensive. This approach does not fully provide a comprehensive of analysis of the disease. To minimize the number of proteins for analysis, a method of differential imaging analysis of gels will be used to identify only those proteins that exhibit differences from normal tissue.

3.6 References

(1) Ross, R. *Nature* **1986**,362, 801-809.

(2) Ross, R. *New England Journal of Medicine* **1986,** 314, 488-500.

(3) Ross, R. New *England Journal of Medicine* **1999,** 340, 115-126.

(4) Doherty, T.M.; Fitzpatrick, L.A.; Inoue, D.; Qiao, J.; Fishbein, M.C.; Detrano, R.C.; Shah, P.K.; Rajavashisth, T. B. *Endocrine Reviews* **2004,** 25, 629-672.

(5) Ross, R. *New England Journal of Medicine* **1999**, 340(2) 115-126.

(6) Lusis, A. *Nature* **2000**, 407,233-241.

(7) Duran, M.C.; Mas, S.; Martin-Ventura, J.L.; Meilhac, O.; Michel, J.B.; Gallego-Delgado, J.; Lazaro, A.; Tunon, J.; Eqido, J.; Vivanco, F. *Proteomics* **2003**, 3, 973-978.

(8) Inzirati, D.; Eliasziw, M.; Gates, P. *N. Engl J Med.* **1999,** 340,115-126.

(9) Chabers, G.; Lawrie, L.; Cash, P.; Murray, G.I. *J Pathol,* **2000,** 192,280-288.

(10) Parekh, R. *Nat. Biotechnol*. **1999**, 17, 19 – 20.

(11) Donners, M.M.P.C.; Verluyten, M.J.; Bouwman, F. G.; Mariman, E.C.M.; Devreese, B.; Vanrobaeys, F.; van Beeumen van den Akker, L.; Daemen, M.J.A.P; Heeneman, S.; *J. Pat.,* **2005,** 206, 39-45.

(12) Mayr, M.; Chung, Y.L.; Mayr, U.; Yin, X.; Ly,L.; Troy, H.; Fredericks, S.; Hu, Y.; Griffiths, J.R.; Xu,Q. *Arteriosler. Thromb. Vasc. Biol.* **2005**, 25 1-9.

(13) Yan-Ling, Y.U.; Peng,-Yuan, Y.; Hui-Zhi, F.; Zhen-Yu, H.; Yao-Cheng, R.; Peng-Yuan, Y. *Acta Pharmocol Sin* **2003**, 9, 873-877.

(14) Ghazalpour, A.; Doss, S.; Yang, X.; Aten, J., Toomey, E.M.; Van Nas, A.; Wang, S.; Drake Lusis, A.J., *J. Lipid Res.* **2004**, 45, 1793-1805.

(15) Henkin, J.; Jennings, M.E.; Matthews, D.E.; Vigoreaux, J.O. *J. Biomole. Tech.* **2004,** 15, 230-237.

(16) Volker, E.; Gobom, J.; Seitz, H.; Giavalisco, P.; Lehrach, H.; Nordhoff, E. *Anal. Chem.* **2002**, 74, 1760-1771.

(17) http://www.matrixscience.com/home.html

(18) http://www.seqnet.dl.ac.uk/Bioinformatics/Webapp/mowse

(19) http://www.mann.embl-heidelberg.de/Services/PeptideSearch/

(20) http://www.prospector.ucsf.edu/ucsfhtml4.0/msfit.html

(21) http://prowl.rockefeller.edu/

(22) http://thompson.mbt.washington.edu/sequest

(23) Zaifman, D.; Rudich, Y.; Sagi, I.; Strasser, D.; Savin, D.W.; Goldberg, S.; Rappaport, M.; Heber, O.; *Int. J. Mass Spec.,* **2003**, 229, 55-60.

(24) Dass, C. In *Principles and Practice of Biological Spectrometry;* Desiderio, D.M., Nibbering, N.M.M. Eds. Wiley-Interscience Series on Mass Spectrometry; A John Wiley & Sons Inc. New York, **2001**; Chapters 1-5.

(25) Yamashita, M.; Fenn, J.B. *J. Phys. Chem.* **1984**, 4671-4675.

(26) Fenn, J.B.; Mann, M.; Meng, C.K.; Wong, S.F.; Whitehouse, C.M.; *Science*, **1989**,246, 64-71.

(27) Fenn, J.B.; Mann, M.; Meng, C.K.;Wong, S.F.; Whitehouse, C.M.; *Mass Spectrom Rev*, **1990**, 9, 37-70

(28) Bruins, A.; Covey, T.R.; Henion, J.D. *Anal. Chem.* **1987** 59, 2642-2646

(29) Smith, R.D.; Loo,J.A.; Loo Ogorzalek, R.R.; Busman, M.; Udseth, H.R.; *Mass Spectrom Rev* **1991,** 10, 359-451.

(31) Wilm,M.S.; Mann, M.; *Int. J Mass Spectrom Ion Proc* **1994**, 136, 167-180.

(32) Peterman, S.M. Dufresne, C.P., Horning, S.J., *J Biomole Tech* **2005**, 16,112-124.

(33) O'Farrell, P.H. *J Biol Chem*. **1975**, 250, 4007-4021.

(34) Molloy, M. *Anal Biochem*, **2000** 280, 1-10.

(35) Wallidus, G.; Jungner, I.; Aostviet, A.H.; Holme, I.; Furberg, C.D.; Sniderman, A.D. *Clin. Chem. Lab. Med.* **2004**, 42, 12, 1355-63.

(36) Rasouli, M.; Kiasari, A.M.; Mokhberi, V. *Clin. Chem. Lab. Med.* **2006,** 44 (8) 1015-21.

(37) Garber, D.W.; Handattu, S.P.; Satta, G.; Mishra, V.K.; Gupta, H.; White, C.R.; Anatharamaiah, G.M. *Curr. Pharm. Biotechnol*. **2006**, 7,4, 235-240.

(38) Garcia-Gras, E.; Lombardi, R.; Giocondo, M.J.; Wilerson, J.T.; Schneider, M.D.; Khoury, D.S.; Marian, A.J. *J. Clin Invest*. **2006**, 116, 1825-1828.

(39) Sabeti, S.; Exner, M.; Mlekusch, W.; Amighi, J.; Quehenberger, P.; Rumpold, H.; Maurer, G.; Minar, E.; Wagner, O.; Schillinger, M. *Stroke* **2005**, 36, 1400-1404.

(40) Mauriello, A.; Sangiorgi, G.; Palmieri, G.; Virmani, R.; Holmes Jr.; D.R., Schwartz, R. S.; Pistolese, R.; Ippoliti, A.; Spagnoli, L.G. *Circulation* **2000**, 101, 744-750.

(41) Shah, J.V.; Wang, L.Z.; Traub, P.; Janmey, P.A. *Biol Bull.* **1998**, 194, 402-405.

(42) Fritzinger, D.C.; Petrella, E.C.; Connelly, M.B.; Bredehorst, R.; Vogel, C.W. *J. Immunol.* **1992**, 149, 3554-3562.

(43) Ogala, R.T.; Rosa, P.A.; Zeptf, N.E. *J. Biol. Chem*. **1989**, 264, 16565-16572.

(44) Wang, W.M.; Gerry, A.B.; Putt, W.; Roberts, J.L.; Weinberg, R.B.; Humphries, S.E.; Leake, D.S.; Talmut, P.J. *Atherosclerosis* **2006,** 21,65-71.

(45) Ortlepp, J.R.; Laucsher, J.; Hoffman, R.; Hanrath, P.; Joost, H.G. *Diabet Med*. **2001,** 18, 10, 842-845.

(46) Stocker, R.; Keaney, Jr. J.F. *Physiol Rev* **2004**, 84, 1381-1478.

(47) Waye, J.S.; Eng, B.; Patterson, M.; Carco, D.H.K Hemoglobin **2001**, 25, 4,391-394.

CHAPTER 4

ISOLATION AND COMPARISONS OF PROTEINS IN ATHEROSCLEROTIC PLAQUES USING DIFFERENTIAL GEL ELECTROPHORESIS AND MASS SPECTROMETRY

4.1 Introduction

Atherosclerosis is a progressive disease that affects large and small blood vessels. The progressive process originates from the interaction between endothelial cells, the walls of the arteries, lipoproteins, and inflammatory cells that lead to the development of complex lesions or plaques that causes collapse of the arterial walls that leads to strokes or myocardial infarction and eventually death [1]. Lesions characterize the earliest form of the disease consist of sub endothelial accumulation of cholesterol filled macrophages referred to as foam cells. In human, the fatty streaks are found in the aorta in the first decade of life and in the coronary in the third to fourth decade [2]. The disease is very complex and has been shown to progress in seven stages based on studies by the American Heart Association [3]. These stages create a complex heterogeneous cellular composition of proteins that are up-regulated or down-regulated, depending on the stage on the disease. In Chapter 3, I identified proteins from whole lesions and tissue membranes from various parts of the aorta. Although my initial studies were successful in some respects, comparisons of diseased and non diseased areas needs to be further addressed.

In related prior studies human vessels for proteomic analysis of proteins secreted by human carotid atherosclerotic plaques were obtained by endarterfectomy [1]. Segments of normal arteries and different regions of the surgical pieces of arteries containing noncomplicated and complicated plaque with thrombus were cultured in protein-free medium and the secreted proteins in the supernatant were analyzed by two-dimensional gel electrophoresis and matrix assisted laser ionization mass spectrometry (MALDI-MS). Human saphenous vein medial smooth muscle proteins have been analyzed using actual tissue harvested from vein bypass grafts by McGregor et

al. [4]. Differential protein expression was assessed in atherosclerotic plaque progression by 2D gel electrophoresis (2DE) and validated by individual patients using western blotting and immunohistochemistry by Donners et al. [5]. Mass spectrometry analysis identified venexin –β and α_1- antitrypsin that was differentially expressed in plaques containing a thrombus [5]. Ghazalpour et al. have presented the integration of genetics, transcriptomics and proteomics combined with mathematical models to lead to an understanding of atherosclerosis and the networks associated with the disease [6]. Yan-Ling et al used 2DE to study the overall protein expression changes that were induced by oxidized low-density lipoprotein in U937 foam cells [7]. The study of the change in the profiles induced by oxidized low-density lipoprotein in U937 were used to support fundamental studies on the macrophage-derived foam cells in atherosclerotic pathologic states [7]. In the vast majority of the investigations of diseased and nondiseased states of vessels, comparisons of the changes in protein expression were observed through gel to gel changes. Although 2DE, mass spectrometry and bioinformatics are well established methods for proteome analysis, some disadvantages may limit the use of the classical approach to the assessment of biological variations of tissues or cells. The traditional approach involves the separation of samples on different gels and in the crudest fashion the researcher must visually pick the spots from the gel that is differentially expressed. This approach exposes the data to a high level of system variation [8]. Such variation may consist of protein uptake in the first dimension strip and second dimension gel protocols. The variation in the system can also be observed in positional variation and volume. One example of variability is produced when the same amount of protein is analyzed on different gels. The same protein can migrate to slightly different positions with different spot intensities causing problems in accuracy of spot volume quantitation and normalization across multiple gels for comparison and spot matching [8]. The classical approach can mask subtle induced biological changes that the experiment was designed

to detect. To overcome this problem, often numerous replications are necessary which is time consuming, expensive, and slow.

One of the methods to reliably compare differences between the tissues samples in by the use of fluorescent dyes to label the proteins of interest. Numerous studies have used this technique for changes in protein expression or the identification of biomarkers. Yan et al. [9] studied the protein expression induced by treating Escherichia coli with benzoic acid. Skynner et al. [10] identified the protein expression changes by different genetic alterations in mice. Protein biomarkers were determined using DIGE in oesophageal cancer [10]. Gharbi et al. [11] have characterized differential protein expression in the growth factor ErbB-2 in epithelial cells.

Alban et al. have described a novel experimental method for comparative 2DE that incorporates a pooled internal standard [12]. Two-dimensional difference gel electrophoresis is an emerging technique for comparative proteomics. The use of this technique was applied to Escherichia coli lysates with varying amounts of four different proteins [12]. Samples are labeled with spectrally resolvable dyes that are separated in the same gels which improves the reproducibility and reliability for differential protein expression analysis between samples. The difference gel electrophoresis method involves the labeling of sample prior to electrophoresis with spectrally resolvable fluorescent dyes, Cydye 2, Cydye 3, and Cydye 5 (Figures 4.1 and 4.2). The labeling dyes are structurally similar and undergo nucleophilic substitution with the ε- amino dye group of lysine thus forming an amide. The reaction is detailed in Figure 4.3 where the protein is labeled with the fluorophore for detection by a fluorescent imaging system. The use of the DIGE technique can be used to obtain statistical confidence in the observed changes that are essential for biological studies to be scientifically relevant.

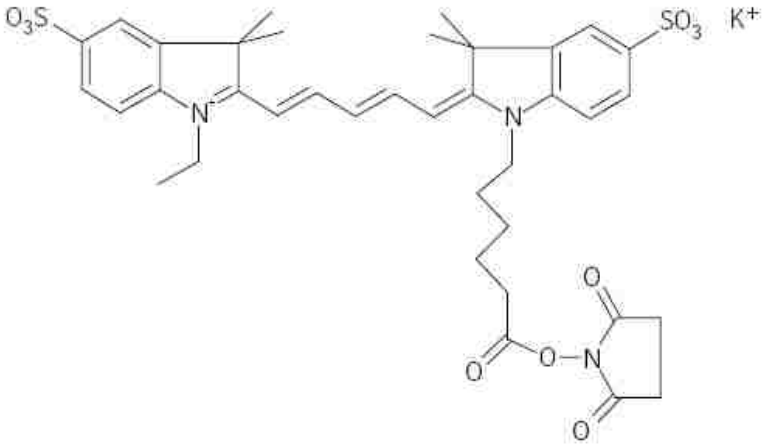

Figure 4.1 Cydye 5 NHS ester for labeling of protein at ε position on lysine

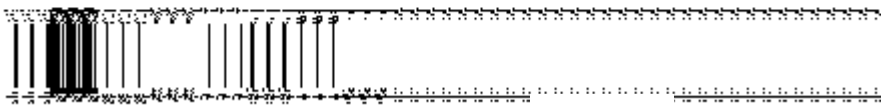

Figure 4. 2 CyDye 3 NHS ester for protein labeling at ε position on lysine

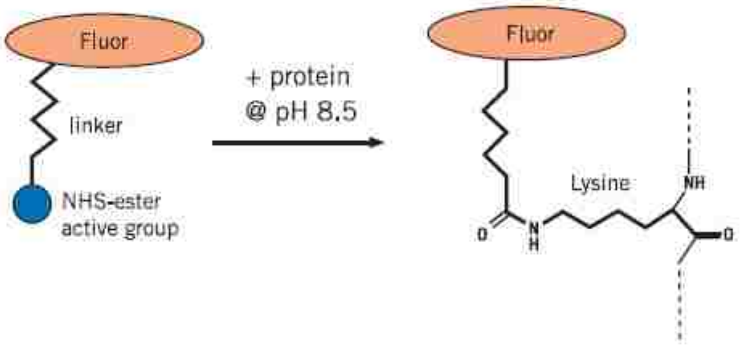

Figure 4.3 Reaction of fluorescent dye with the ε-amino acid group of lysine for differential gel electrophoresis analysis. Gel images detect attached proteins at the wavelength of the Cydye.

An illustration of the emission spectra of the various dyes including those used in this study of fluorescent imaging studies is shown in Figure 4. The dyes used for the proteins in the plaque extracts have similar molecular weights and remained positively charged, matching the charge that is replaced on the protein lysine residue [12]. This mass and charge are important so that the proteins of interest comigrate to the same point during electrophoresis [13]. More importantly, the added mass from the reaction

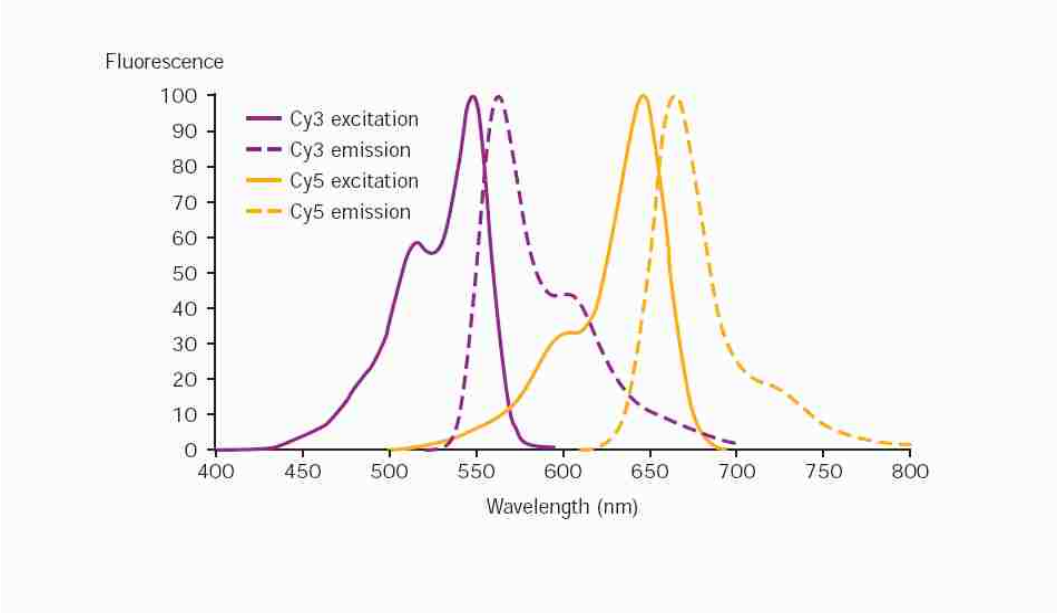

Figure 4.4 Fluorescence excitation and emission spectra of Cydye fluorescent dyes. The Cydye is detected in the gel by the Typhoon 9400 imager at the wavelengths indicated.

does not interfere with the identification during the analysis using peptide mass fingerprinting or tandem mass spectrometry interpretation. The fluorescent tag Cydye 3 produces an excitation at a wavelength 532 nm and an emission at 580 nm with a 30 band pass filter. Cydye 5 fluorophore has an excitation wavelength at 633 nm and an emission wavelength at 670 nm.

4.2 Research Goals and Objectives

The primary aim of this study was to develop a technique that distinguishes the protein expression differences between diseased and nondiseased tissues from human thoracic aortas incorporating fluorescent dyes as diagnostic tools to reduce gel changes not associated with changes in the biological variation. In addition our study investigates the differences in protein expression in native and bypass arteries using differential gel electrophoresis with 2DE and mass spectrometry analysis of the proteins.

4.3 Experimental

4.3.1 Methods and Materials

Tissue of thoracic aortas were obtained from Louisiana State University Health Science Center in New Orleans, Louisiana. Native and bypass arteries were also obtained from the same source. The samples were received and immediately frozen at -70ºC until the extraction procedure.

Urea, glycerol, glycine, thiourea, ASB -14, iodoacetamide, and Sigma Markers (for molecular standards) and guanidium hydrochloride were purchased from Sigma Aldrich Corp (St Louis, MO USA). All of the reagents were of the highest purity and when available specified electrophoresis grade. Sodium dodecyl sulfate (SDS) was obtained from BioRad (San Diego, CA USA) for electrophoresis. Tris (hydroxymethyl) aminomethane (TRIS) was obtained form Invitrogen (Carlsbad, CA USA). 3-[(3-Cholamidopropyl)dimethyl-ammonio]-1-propanesulfonate (CHAPS was purchased from Calbiochem (San Diego, CA USA). Dithiothreitol was obtained

from Fluka Biochemika (St Louis, MO.USA). Trichloroacetic acid was purchased from Fisher Scientific (Waltham, MA USA).

The immobiline pH gradient dry strips, immobiline pH gradient buffer pH 3-10 NL and mineral oil were obtained from GE Healthcare Inc. (Piscataway, New Jersey USA). The dry streak used was purchased from GE Healthcare, Inc. (Piscataway, New Jersey USA). The colloidal coomassie blue stain was obtained from Invitrogen (Carlsbad, CA USA). Methanol (HPLC grade) was obtained from EMD Chemical (Gibbstown, NJ USA).

4.3.2 Methods

Thoracic aortas and arteries from human hearts were obtained from Louisiana State University Health Science Center in New Orleans, Louisiana. The samples were frozen immediately with dry ice and then stored at -70º C until dissection. During the extraction procedure, the tissue was allowed to thaw to room temperature. Intima membrane from normal and diseased tissue was carefully removed from the media and adventitia. Approximately 250 to 350 milligrams of tissue was isolated and then placed in liquid nitrogen and ground with a mortar and pestle into a powder. The powder was place in lysis buffer composed of 7M urea, 2M thiourea, 4% CHAPS, 2% ASB -14 and 10 µl of protease inhibitor cocktail per ml of buffer. This was followed by the addition of 2.5 mg phenylmethylsulfonyl fluoride per ml for protease inhibition. The temperature of the lysis buffer was maintained at 4ºC and caution was taken to prevent the urea containing solution not to exceed 30ºC. Tissue extract was homogenized with a Tarazen Homogeniser for 1 minute followed by sonication at 4ºC for 4 minutes. The mixture was centrifuged at 12,000 x g for 20 minutes at 20ºC in an Eppendorf 540 Microcentrifuge. The supernatant was maintained at < 20ºC until the precipitation steps or for longer periods of storage at -70ºC.

4.3.3 Protein Quantification

Protein concentrations were determined by Bradford protein assay using a 6 point BSA standard concentration curve. For CyDye labeling, samples were aliquotted into 50µg fractions.

4.3.4 Cy-dye Labeling

The mixed internal standard methodology of Alban *et al*. [12] was used in these studies. Equal protein loading of Cydyes, treated, and the standard-sample mixture was based on the above Bradford protein assay results resolving between pH 3-10 per gel. Aliquots of 50 µg protein from each of the Cydyes and treated extracts from all samples were individually precipitated at room temperature with 10% TCA. The precipitates were solubilized in lysis buffer (7 M urea, 2 M ThioUrea, 4% CHAPS, 30 mM Tris, pH8.5) prior to labeling with 400 pmol of either Cy3 or Cy5 (vehicle and treated randomized). In a similar fashion, 50 µg of each of the samples (vehicle and treated) was pooled, precipitated and resuspended in lysis buffer, and labeled with 400 pmol Cy2 per 50µg standard. Labeling was performed for 30 min on ice in the dark, after which the reactions were quenched with the addition of 10 mM lysine for 10 min on ice in the dark. The quenched 50 µg Cy3 and Cy5 labeled samples for each subject were then combined and mixed with 50 µg of the quenched Cy2-labeled standard sample, after which an equal volume of rehydration buffer (7 M Urea, 2 M Thiourea, 4% CHAPS, 4 mg/ml DTT) supplemented with 2% BioLyte 3/10 Ampholytes (Bio-Rad) was added. The stoichiometry of Cydye labeling is specifically intended to achieve a minimal labeling (~1% of all proteins) and results in sensitivities on the order of SYPRO Ruby (~1 ng in our hands).

4.3.5 2-D gel electrophoresis and imaging

CyDye labeled samples for each subject (410 µL final volume) were actively rehydrated into 24 cm 3-10NL immobilized pH gradient (IPG) strips (Amersham) for 15 hours, followed by isoelectric focusing using a Protean IEF (Bio-Rad) for a total of 80,000 Vhrs (linear 20 min at

250V; linear 3.5 hours at 10,000V; rapid 70,000Vhrs at 10,000V; rapid 75 hours at 250V (a final hold step). The cysteines were reduced and carbamidomethylated while the proteins were equilibrated into the second-dimensional loading buffer by incubating the focused strips in equilibration buffer (6M Urea, 20% glycerol, 2% SDS, 375mM Tris, pH8.8) supplemented with 20 mg/ml DTT for 15 min at room temperature with shaking, followed by 25 mg/ml iodoacetamide in equilibration buffer for an additional 15 minutes incubation at room temperature. IPG strips were then cemented onto 2^{nd} dimension gels using an overlay consisting of 0.5% agarose in SDS running buffer (25mM Tris, 192mM glycine, 0.1% SDS, trace of Bromophenol Blue). 12% homogeneous polyacrylamide gels were cast with low-fluorescence glass plates using an Ettan-DALT caster. One glass plate from each gel was bind-silanized (Amersham Biosciences). This allows the gel to adhere to one glass plate preventing shrinkage, swelling and/or tearing of gels during manipulations and scanning. The second-dimensional SDS-PAGE was then performed on all gels simultaneously using a DALT6 (Amersham) at 5 W/gel for 30 min followed by 17 W/gel for 4 hours. The Cy2 (standard), Cy3 and Cy5 (vehicle or treated) for each gel were individually imaged using mutually exclusive excitation/emission wavelengths of 488nm (ex) and 520nm (em) BP40 (bandpass) for Cy2, 532nm (ex) and 580nm (em) BP 30 for Cy3, and 633nm (ex) and 670nm (em) BP30 for Cy5 using a Typhoon 9400 (Amersham). After imaging for Cy-dye components, the non-silanized glass plate was removed, and the gels were fixed in 10% methanol, 7% acetic acid for 1 hour, rinsed in water three times and then incubated in SYPRO Ruby in the dark overnight. The SYPRO Ruby post-stain allows for the correction of unlabeled protein's migration in relation to the 1% CyDye labeled migration, and ensures accurate protein excision. Sypro Ruby images were acquired on the same imager using 450nm (ex) and 610nm BP40 filter, as well as re-imaged post-excision to ensure accurate protein excision.

4.3.6 DIGE analysis

DeCyder software (Amersham) was used for simultaneous comparison of abundance changes across all samples, and for comparisons of individual Cy3 and Cy5 samples for each sample. The DeCyder differential in-gel analysis (DIA) module was used for pair-wise comparisons of each vehicle and treated sample to the Cy2 labeled standard present on each gel. For each pair-wise DIA comparison, the entire signals from each CyDye channel are normalized prior to the co-detection of protein spot boundaries and the calculation of the volume ratio for each protein spot. The DeCyder biological variation analysis (BVA) module was then used to simultaneously match all protein spot maps from all gels, and using the Cy3/Cy5:Cy2 DIA ratios, calculate abundance changes and paired Student's *t*-test *p*-values for the variance of these ratios for each protein pair across the samples were calculated. In addition, fold abundance changes were reported, whereby a fold increase is calculated directly from the volume ratio and a fold decrease by the inverse of volume ratio. The DIA module was also used to calculate the direct Cy5:Cy3 volume ratio for each paired sample individually (without the Cy2 mixed standard) to assess the contribution from each subject and reveal changes that were present in a group. The Cy3/Cy5 gel images were manually normalized and stacked. Because the images for each sample were separated on the same 2-D gel, alternating between the vehicle and treated images for all of the subjects simultaneously allowed for simple monitoring of protein changes that were specific to the samples studied, as well as targeting of proteins that were increasing in some tissues, but decreasing in others.

4.3.7 In-gel digestion

Proteins of interest were excised using the Ettan Spot Handling Workstation (Amersham) based on a hit list generated in DeCyder. Spots were automatically destained by successive changes of 20 mM ammonium bicarbonate and 50% acetonitrile, followed by dehydration with 20

minute incubation with 75% acetonitrile. Dehydrated gel plugs were digested in-gel with 10 µL 20 µg/ml porcine modified trypsin protease (Promega) in 20 mM ammonium bicarbonate for 6 hours at 37°C. Tryptic peptides were then extracted from the gel plugs in two cycles of 50% acetonitrile, 0.1% trifluoroacetic acid and dried by evaporation. Peptides were reconstituted in 3 µL 50% acetonitrile and 0.1% trifluoroacetic acid and 0.6 µL was mixed with an equal volume of 10 mg/ml α-cyano-4-hydroxy-cinnamic acid for spotting onto a MALDI plate.

4.3.8 Mass spectrometry and database interrogation

Matrix assisted laser desorption/ ionization time-of-flight mass spectrometry and tandem TOF/TOF mass spectrometry was performed on a Voyager 4700 (Applied Biosystems). Peptide mass maps were acquired in reflectron mode (20 kV accelerating voltage) with 155 ns delayed extraction, averaging 1000 laser shots per spectrum. Individual ions from each spectrum were inspected for resolution and isotopic distribution to identify potentially different peptides of similar mass (with overlapping isotopic distributions) and eliminate low-resolution ions that may result from metastable decomposition. Ions specific for each sample (discrete from background and trypsin-derived ions) were then used to interrogate human sequences entered in the SWISS-PROT and NCBInr databases using MASCOT [13].

Protein identifications from MALDI-TOF peptide mass maps were based on the masses of the tryptic peptides. Tandem mass spectrometry (MS-MS) was used to generate limited amino acid sequence information on selected ions if additional confirmation was required. Searches were performed without constraining protein molecular weight or isoelectric point, and allowed for carbamidomethylation of cysteine, partial oxidation of methionine residues, and one missed trypsin cleavage. Highest confidence identifications have statistically significant search score(s), are consistent with the gel region from which the protein was excised (MW and p*I*), and accounted for the majority of the ions present in the mass spectrum.

4.4 Results and Discussion

4.4.1 Differential In Gel Electrophoresis with Fluorescent Dyes

Two dimensional gel electrophoresis is a widely used technique for the separation of proteins based on their isoelectric point and molecular weights [14]. Thousands of proteins can be separated on one gel depending on various parameters such as the source of the sample, solubility, conformation, size and charge. For biological samples, the disease state of the sample to be analyzed becomes the focus of studies investigating whether the proteins are positively or negatively expressed. Because of this, spot pattern recognition based on location within the gel such as molecular weight, pI, or intensity is very important in the identification of the proteins. Patterns of spots can be used to monitor and compare whether the tissue or cells are normal or diseased. Protein quantitation from these studies can be determined from spot intensities. The use of 2DE to accurately determine the identification of the proteins is complimented by mass spectrometry analysis.

The traditional approach uses one sample per gel. This approach exposes the data to a high level of system variation due to initial sampling techniques, protein uptake onto the IPG drystrips, second dimension running conditions, and staining protocols [8]. The proteins that are imaged migrate to certain positions on the gel with volume variations. The accuracy of spot volume quantitation and normalization for a multiple of gels can be problematic for gel to gel and different samples that must be compared [15][16].

The uses of bypasses with veinous grafts have been studied; however the bypass artery tends to be sites of enhancement calcification or proliferation of atherosclerosis faster than the normal process. One of the methods to compare proteins that may contain biomarkers for atherosclerosis is the use of difference imaging gel electrophoresis. From this approach,

biological variations in the tissue may provide valuable information and better understanding of the process of calcification and the formation of protein formed in the plaques.

Proteins from human thoracic aortas extracts of intima and media membrane lining the walls of the vessels were separated by isoelectric focusing with an Ettan IPGhor unit with immobline drystrips at a 3-10 nonlinear pH range. Extracts from diseased and non diseased aortas were performed. In addition, protein extracts from intima of native and bypass coronary arteries were examined. The use of bypasses with veinous grafts has been studied; however the bypass artery tends to be sites of enhancement calcification or proliferation of atherosclerosis faster than the normal process.

Two sets of native and bypass arteries from different hearts and one set of thoracic aortas were used in the labeling experiments. The tissues were extracted in lysis buffer containing 7M urea, 4% CHAPS, 2M thiourea, 2% ASB-14 and protease inhibitors. Cydye 2, Cydye 3, and Cydye 5 fluorescent were mixed into each individual sample and reacted. The sulfhydryl esters of the dyes at pH 8.0 react with the ε-lysine of each protein forming an amide with charge retention. The mass of the protein changes slightly due to the added group but since the amount of dye is comparatively small (400 pgrams of Cydye to 50 μg of protein) spot migration and molecule weight modifications are minimized. Each plaque sample from the same heart is pooled and isoelectric focusing was performed. Gels from the pooled samples (S1) contain labeled proteins from the native and bypass from an 80 year subject. Sample S2 gel image contains fluorescent labeled proteins from a 72 year old heart of a native and bypass artery. The last sample S3 contains diseased and nondiseased tissue extracts from the thoracic aortas from the same heart of a 60 year old with the fluorophores. Images from the Typhoon 9400 laser imager are depicted in Figures 4.4-4.8.

pH 3 10

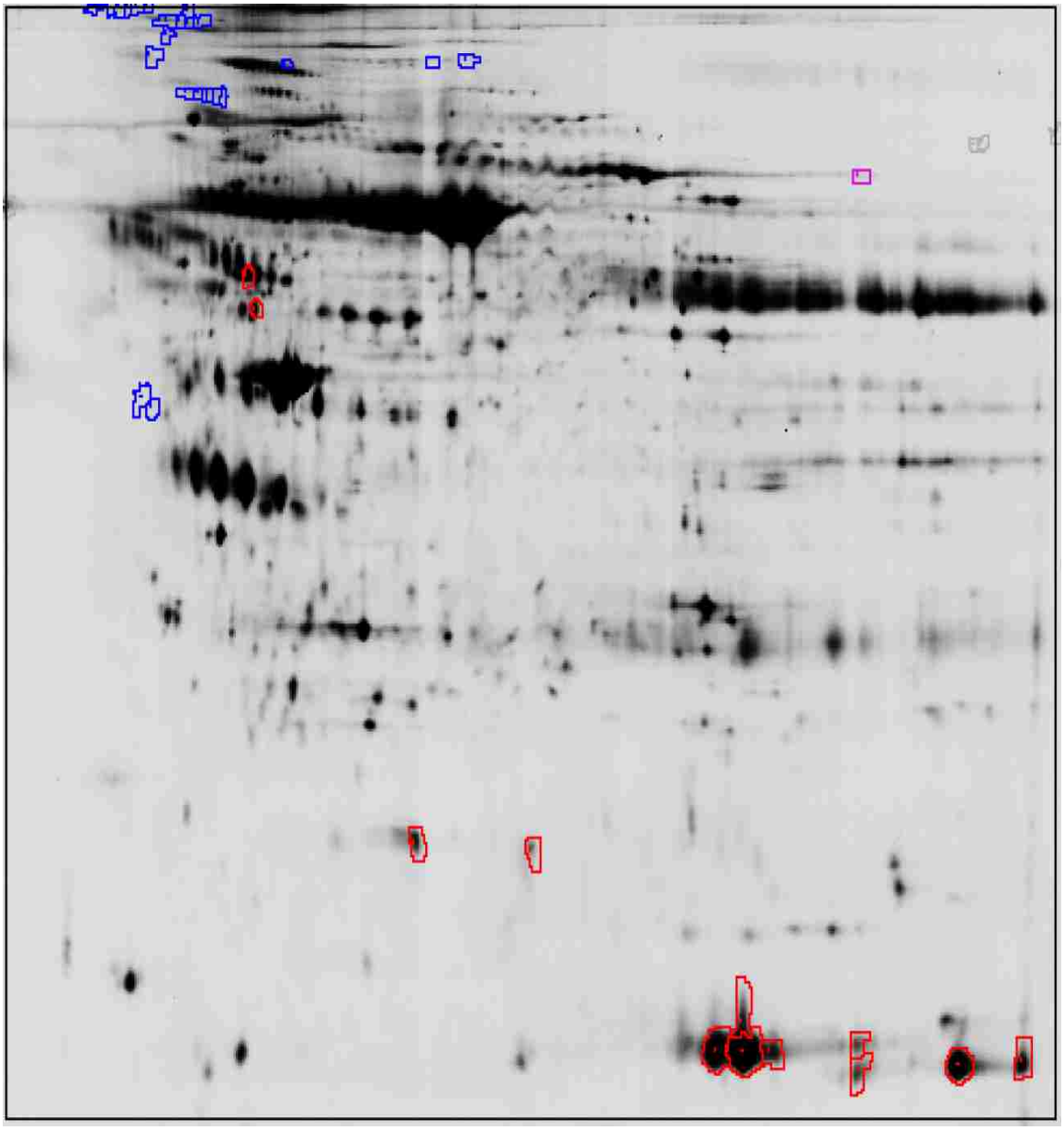

Figure 4.5. Gel image Cydye 3 of normal tissue of 60 year old thoracic aorta extract on sodium dodecyl sulfate polyacrylamide gel 12 % polyacrylamide concentration with isoelectric focusing on 3-10 pHdrystrip. Blue and red circles denote up-regulation and down-regulation in protein expression, respectively. Protein concentration is increased areas with blue circles.

pH 3 10

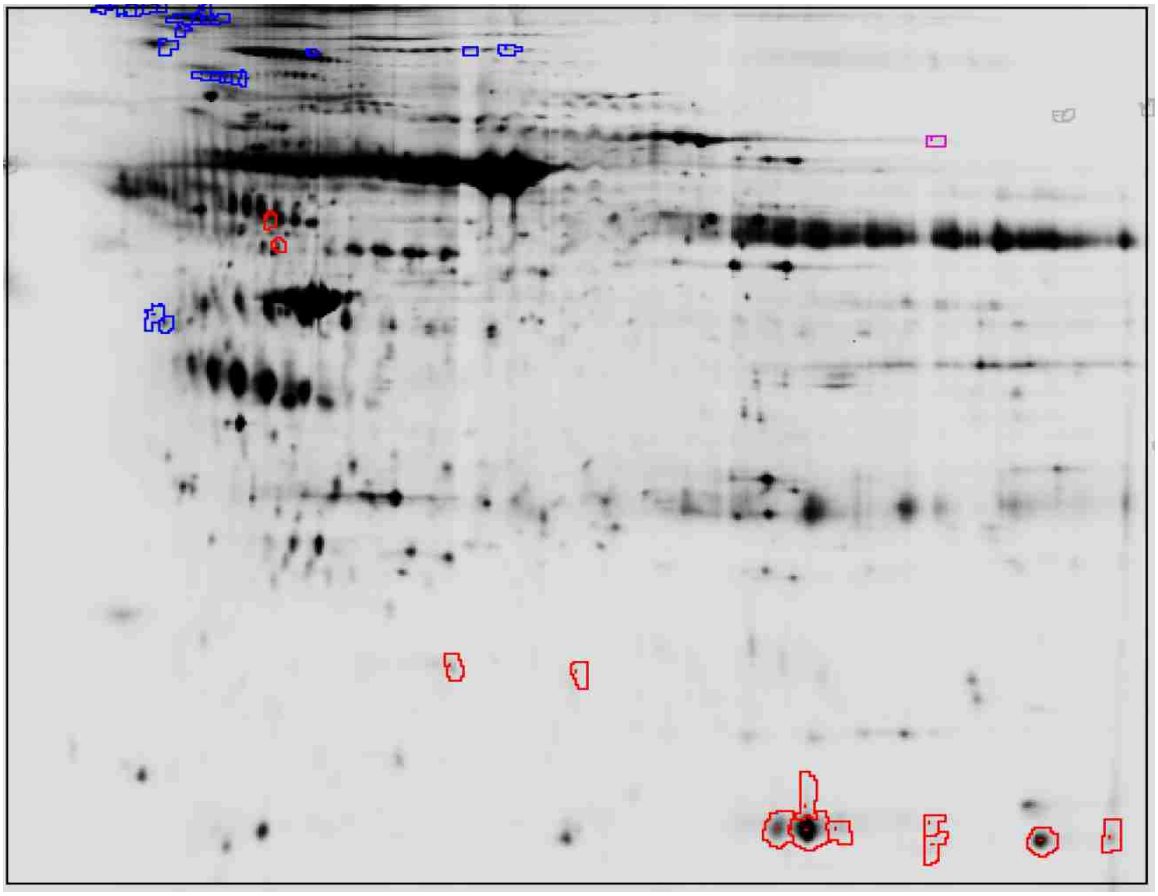

Figure 4.6. Gel image (Cydye 5) of a diseased tissue of 60 year old thoracic aorta extract on sodium dodecyl sulfate polyacrylamide gel 12% polyacrylamide concectration with isoelectric focusing on 3-10 nonlinear IPG drystrip. Blue and red circles denote up-regulation and down-regulation in protein expression, respectively. Protein concentration is increased areas with blue circles.

The images shown are the results of Cydye 3 and Cydye 5 labeling of proteins. The fluorescent tag Cydye 3 produces an excitation at a wavelength 532 nm and a emission at 580 nm with a 30 Bp. Cydye 5 fluorophore has an excitation wavelength at 633 nm and an emission wavelength at 670 nm. This process isolated a total 35 spots in the normal tissue and 37 spots in the diseased comparison that are identified as different expressed as up regulated or down regulated. Protein expressions that are increased are depicted in blue and decreased in expression

in red when the gels are read from Figure 4.5 to Figure4.6. The total number of spots exceeded 1100.

The second samples that were labeled consist of native and bypass coronary arteries from the same heart ran under similar conditions and imaged with a Typhoon 9400 (Amersham Bioscience) with the composite image comparison. Images of the native and bypass samples are shown in Figure 4.7 and Figure 4.8, respectively.

pH 3 10

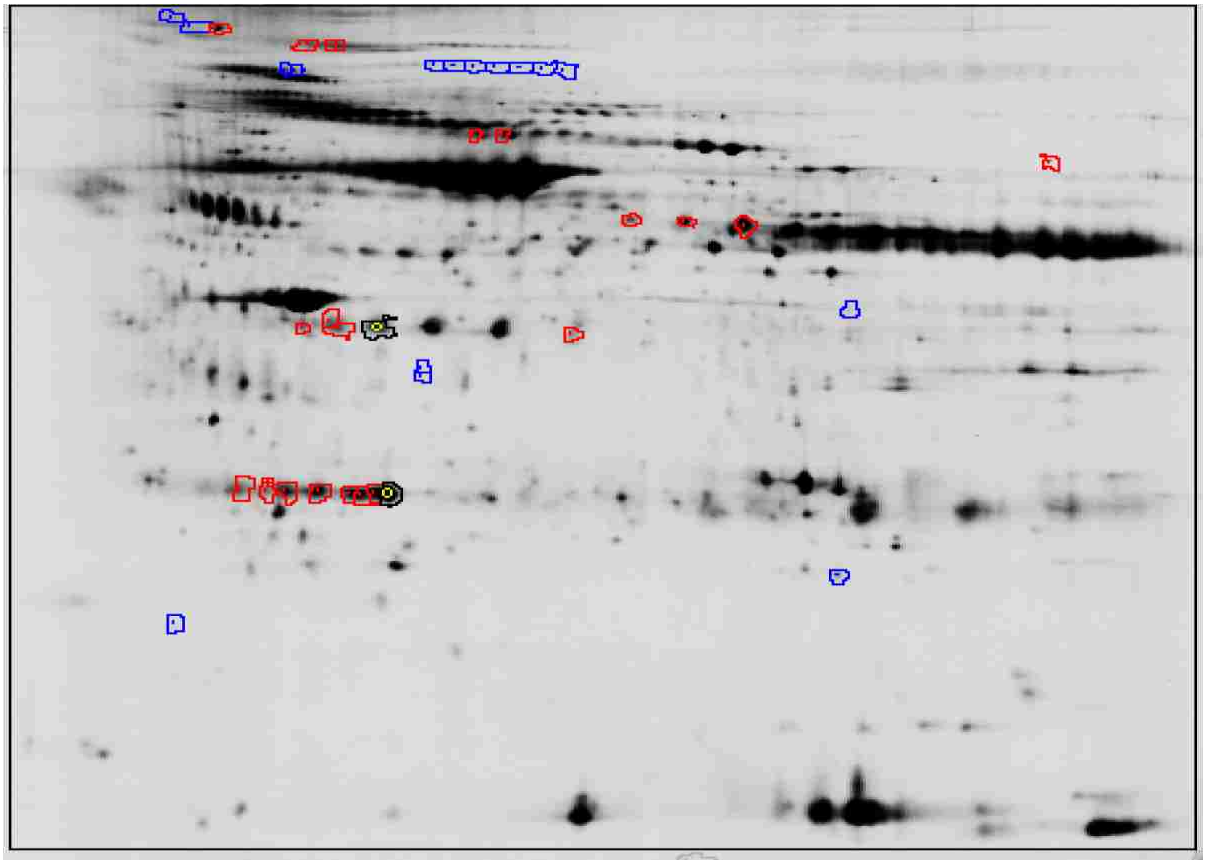

Figure 4.7 Gel image (Cydye 3) of native coronary artery extract of 70 year old on sodium dodecyl sulfate polyacrylamide gels at a 12% polyacrylamide concentration with isoelectric focusing on a 3-10 pH nonlinear drystrip. Blue and red circles denote up-regulation and down-regulation in protein expression, respectively. Protein concentration is increased areas with blue circles.

pH 3 10

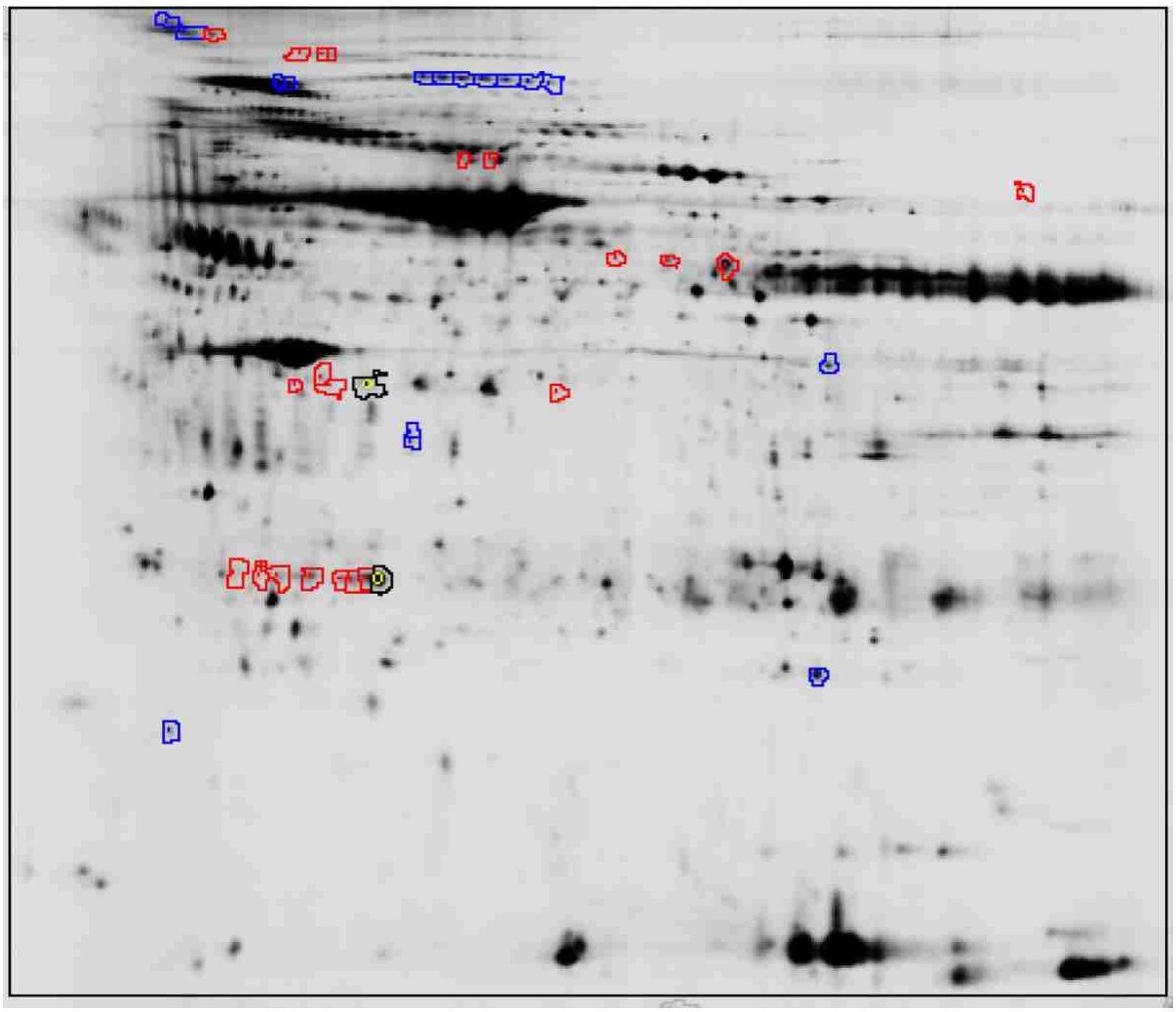

Figure 4.8 Gel image (Cydye 5) of bypass coronary artery extract of 70 year old with sodium dodecyl sulfate polyacrylamide gels at a 12% polyacrylamide concentration with isoelectric focusing on a 3-10 pH nonlinear drystrip. Blue and red circles denote up-regulation and down-regulation in protein expression, respectively. Protein concentration is increased areas with blue circles.

A comparison of the proteins labeled with the fluorescent tags of the native and bypass artery extracts produced 25 spots from the cydye label tissues that decreased (red) in expression and 15 spots that increased in expression (blue). The analysis of each spot can be visualized from the normal tissue to the diseased tissue in each case.

A third tissue extract of a coronary artery (native and bypass) for an 80 year old aorta in which isoelectric focusing was performed on immobiline pH gradient drystrips (pH 3-10 nonlinear). The SDS- PAGE image is depicted in Figures 4.9 and 4.10.

pH 3 10

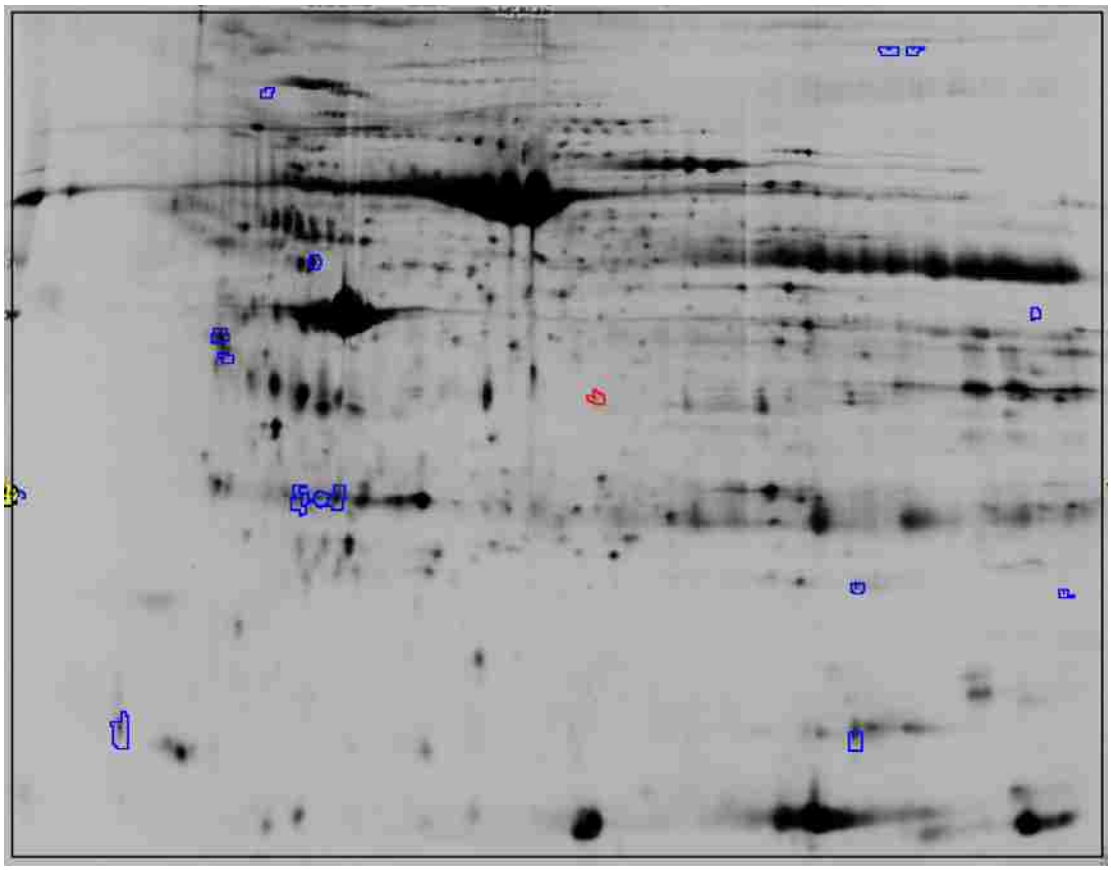

Figure 4.9 Gel image (Cydye 3) of native coronary artery extract of 80 year old at sodium dodecyl sulfate polyacrylamide gels at a 12% polyacrylamide concentration with isoelectric focusing on a 3-10 pH nonlinear drystrip. Blue and red circles denote up-regulation and down-regulation in protein expression, respectively.

pH 3 10

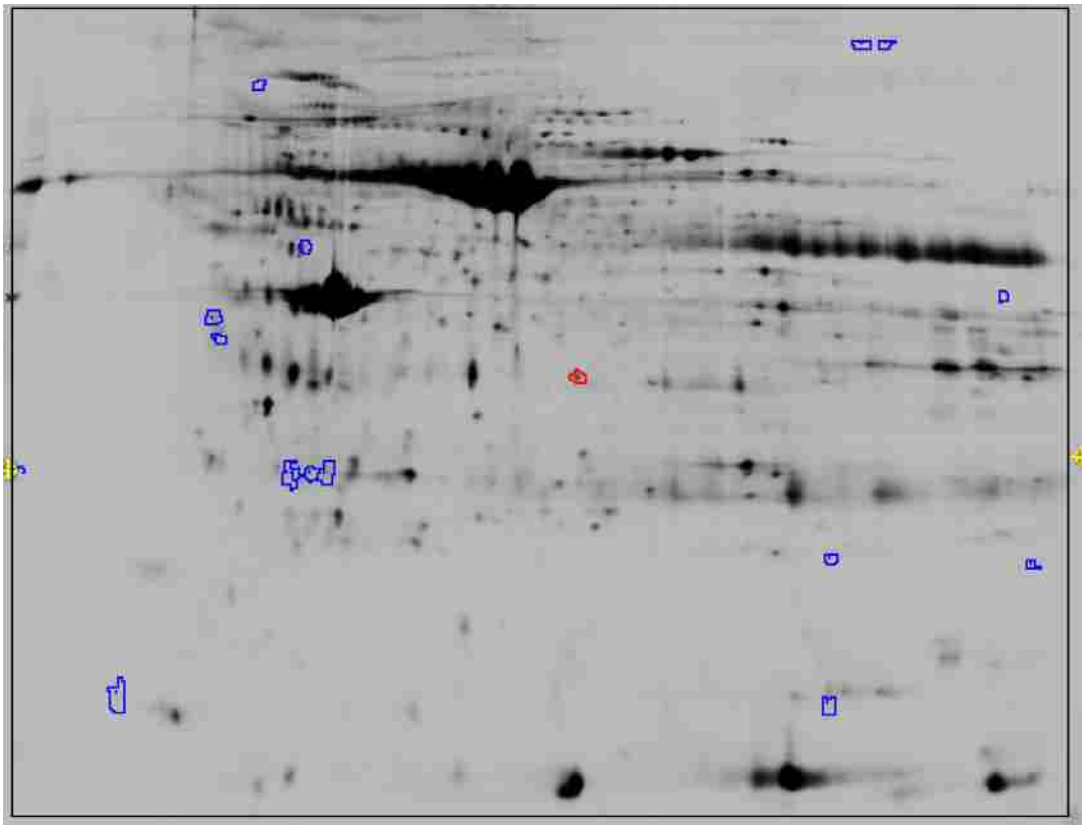

Figure 4.10 Gel image (Cydye 5) of bypass coronary artery extract of 70 year old at sodium dodecyl sulfate polyacrylamide gel at a 12% polyacrylamide concentration with isoelectric focusing on a 3-10 pH nonlinear drystrips. Blue and red circles denote up-regulation and down-regulation in protein expression, respectively. Protein concentration is increased areas with blue circles.

Examination of the images resulted in 14 spots with an increase in protein expression when comparing the images of native artery to bypass artery. Only one spot indicated a decrease in the protein expressed.

4.4.2 SyproRuby Staining of SDS PAGE Unlabeling of Fluorescent dyes

To ensure that the spots were differentiated proteins and no artifacts in the gels such as dust or gel imperfections, the gels were further stained with Sypro Ruby. This stain has a limit of detection ranging from 0.25 to 1.0 ng protein / mm^2 gel. Sypro stains are manually compared to

the previous fluorescent scans of the labeled protein to assess if the expression levels of protein are valid. If similar spots are retained by the Sypro Ruby fluorescent stain, excision and protein identification occurs. Sypro Ruby stains for the tissue extracts are shown in Figures 4.11 -4.13 with spot histograms of the spots of interest.

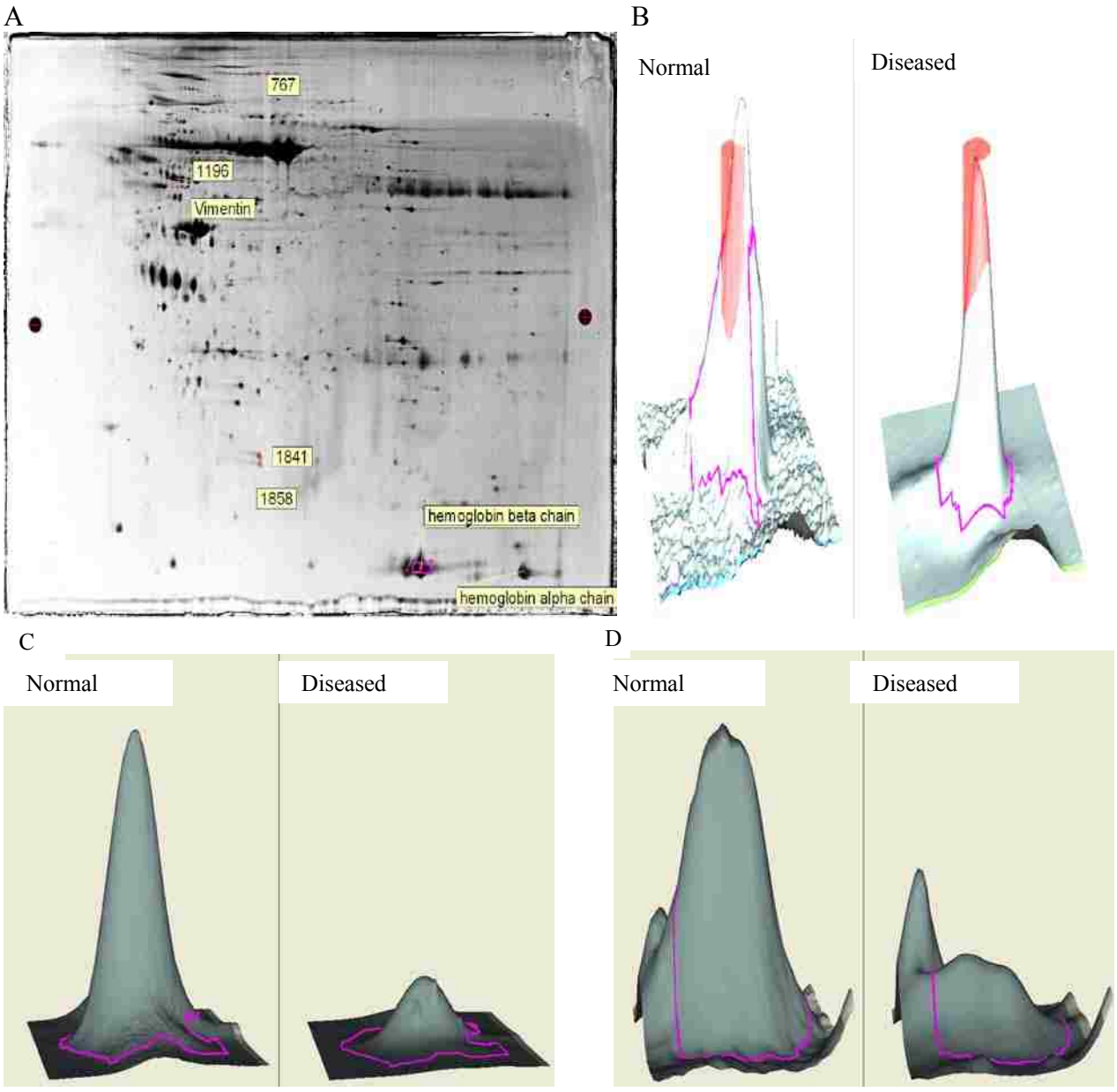

Figure 4.11 (A) Sypro Ruby stain gel image thoracic aorta extract. (B) 3D histogram of protein expression of hemoglobin alpha chain from the same gel. (C) 3D histogram of protein expression of hemoglobin beta chain. (D) 3D histogram of protein expression of vimentin.

To determine the global changes in protein expression patterns that may be caused by Cydye 3 or Cydye 5 labeling, the same gel was stained with Sypro Ruby. From this data, the two images are superimposed without gel variation and the spots the stained gel manually compared to the ones for the labeled dyes. If the protein patterns are similar, the spots that either increased in protein expression or decreased should also be present and further analyzed. Problems that fluorescent labeling produces could cause subtle differences between the two gel images may be due to two factors (1) the increase in molecular mass of the label protein that increases the masses by approximately 500 daltons, and (2) the abundance of the proteins may be increased or decreased depending on the number of lysine that are actually in the proteins. The Sypro Ruby stained image gave 7 spots that were expressed different between the normal and diseased samples. Three dimensional simulations of the proteins that were up-regulated or down-regulated are illustrated in Figures 4.11B -4.11D representing the normal and diseased state of the tissue extracts. This analysis of protein expression was calculated using Decyder –DIA software. The peak of the protein spot was obtained based on pixel versus area data generated from the 2D Master Imager. In quantification experiments, the protein area indicates the distribution of the spot and the volume is correlated with the amount [10]. The identification of the proteins of interest is listed on the gel and will be discussed in the protein identification section.

Similar 2D gel images of the Sypro Ruby were obtained from the extraction of tissues from native and bypass arteries from a 72 year old and an 80 year old specimen. The two previous fluorescent images of the Cydye 3 and Cydye 5 gels were unlabeled and stained with SyproRuby. The Sypro Ruby stain of the 72 year old is shown in Figure 12A while the 3D version of each spot expression is illustrated in Figures 12B-E.

A

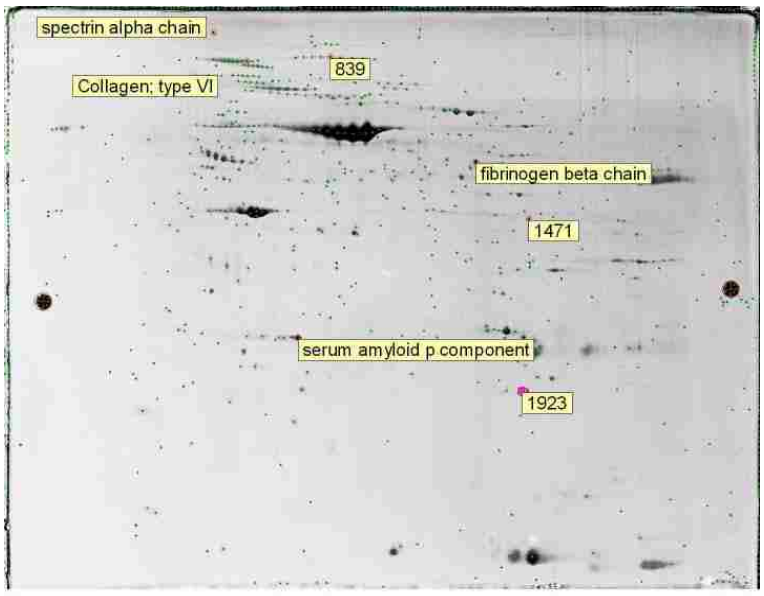

B

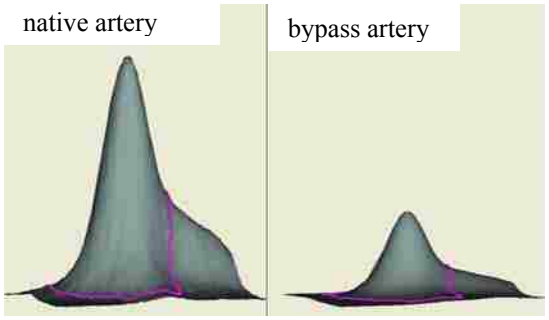

C

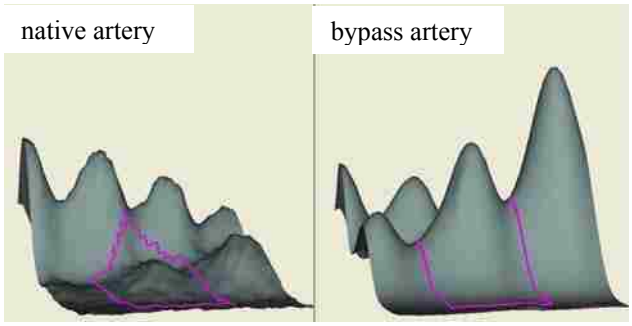

D

E

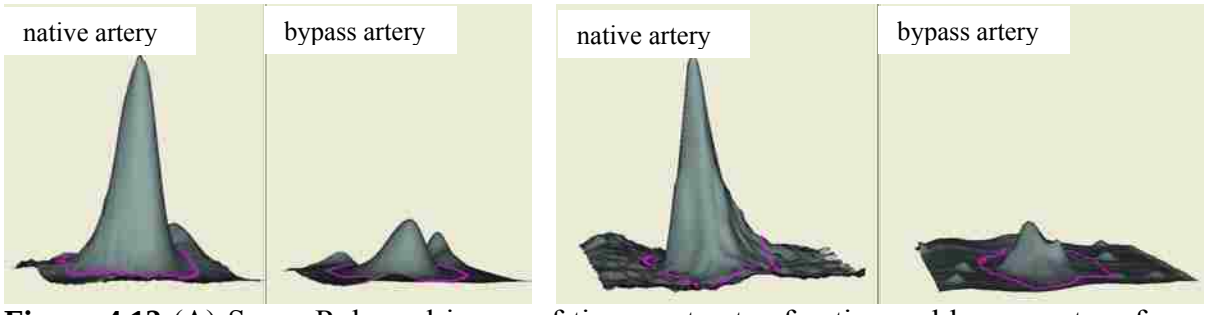

Figure 4.12 (A) Sypro Ruby gel image of tissue extracts of native and bypass artery from a 72 year old. (B) 3D image of amyloid protein from tissue extract. (C) 3D image of collagen Type VI protein from tissue extract. (D) 3D image of fibrinogen protein from tissue extract. (E) 3D image spectrin protein tissue extract.

2D gel images of the Sypro Ruby resulted in 7 spots that were visualized as differentially expressed when the native and bypass gels were compared. The gel patterns were consistent with the labeled proteins in Figure 4.8. Protein spot identification by mass spectrometric analysis of the tryptic digested peptides followed by database search will be covered in a later section. The 3D patterns of each protein are shown in Figures 4.12 B-12E. Serum amyloid p component of native and bypass (Figure 4.12B) in spot comparisons in 3D image analysis shows upregulated protein expression in the native artery compared with bypass. This phenomenon may suggest that the protein may participate in the pathogenesis of the disease, since the bypass is normally disease free. Conversely, the collagen VI protein spot shows that its presence is down regulated in the native vessel.

Fibrinogen is a protein whose concentration may increase in the plasma as a response to inflammatory stimuli such as arteriosclerosis [17]. Based on 3D volume and pixel comparison, it is upregulated or increased in the native in comparison to the bypass artery sample.

Spectrin, from the 3D simulation, (Figure 4.12E) is surrounded by complimentary proteins that may be polypeptides. Results indicate that its presence in the vessels is upregulated in the native sample.

A second sample of tissue extracts of an 80 year old was performed and the labeling results previously discussed. Removal of the labeled proteins and staining with Syproruby reveals if some of the spots imaged contain artifacts (Figure 4.13 A-C).

A SyproRuby stained gel of native and bypass coronary artery extracts of an 80 year old gel image is illustrated in Figures 4.13. The use of additional staining provided a means to evaluate global differences between the gels eliminating false positives that may from artifacts in the gel or contaminates. 14 spots were found from the analysis of the labeling experiments:

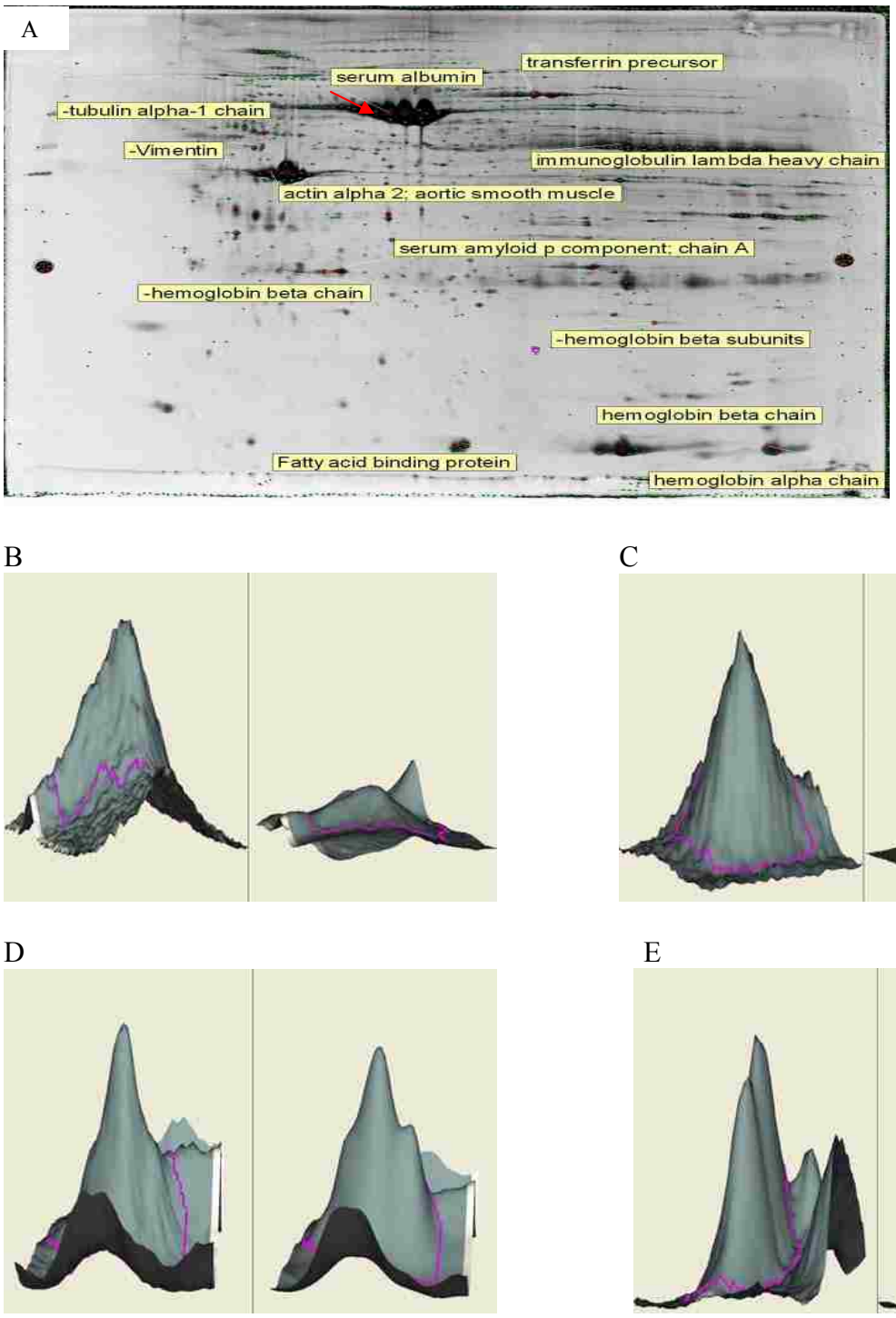

Figure 4.13 (A) Sypro Ruby gel image of tissue extracts of native and bypass artery from a 80 year old. (B) 3D image hemoglobin beta chain protein from tissue extract. (C) 3D image of hemoglobin beta unit protein from tissue extract. (D) 3D image of tubulin protein form tissue extract. (E) 3D image vimentin protein from tissue extract. The volume of each spot was calculated from Decyder –DIA software.

however only 4 exhibited protein that indicated changes in expression. These spots are annotated in the imaged gel and the 3D volume simulations depicted (Figure 4.13 B-D). In each case, the proteins were more abundant in the native artery as compared to the bypass artery

4.4.3 Protein Identification by Matrix Assisted Laser Desorption Ionization Mass Spectrometry

Following the staining procedure, the spots of interest were excised manually and subjected to in-gel digestion. The resulting peptides were analyzed using Voyager 4700 (Applied Biosystems) MALDI TOF-TOF mass spectrometer. Peptide masses were acquired in reflectron mode (20 kV accelerating voltage) with 155 ns delayed extraction, averaging 1000 laser shots per spectrum. The individual ions from each spectrum were inspected for resolution and monoisotopic distribution to identify potentially different peptides of similar masses. The peptides were used with search parameters for human subjects and entered in the SWISS-PROT and NCBInr databases using MASCOT [14]. Database searches were performed without constraining protein molecular weight or isoelectric point, and allowed for caramidomethylation of cysteine, partial oxidation of methionine residues, and one missed cleavage. Highest confidence identifications have statistically significant search score(s), are consistent with the gel region from the protein was excised (MW and pI) and accounts for the majority of the peptides the spectra. The mass spectra of the spots that were picked from the gel stained with SyproRuby with differences in protein expression between the diseased and nondiseased tissue. The peptide mass spectra are in-gel tryptic digest of thoracic aorta extracts and illustrated in Figures 4.14 to 4.21.

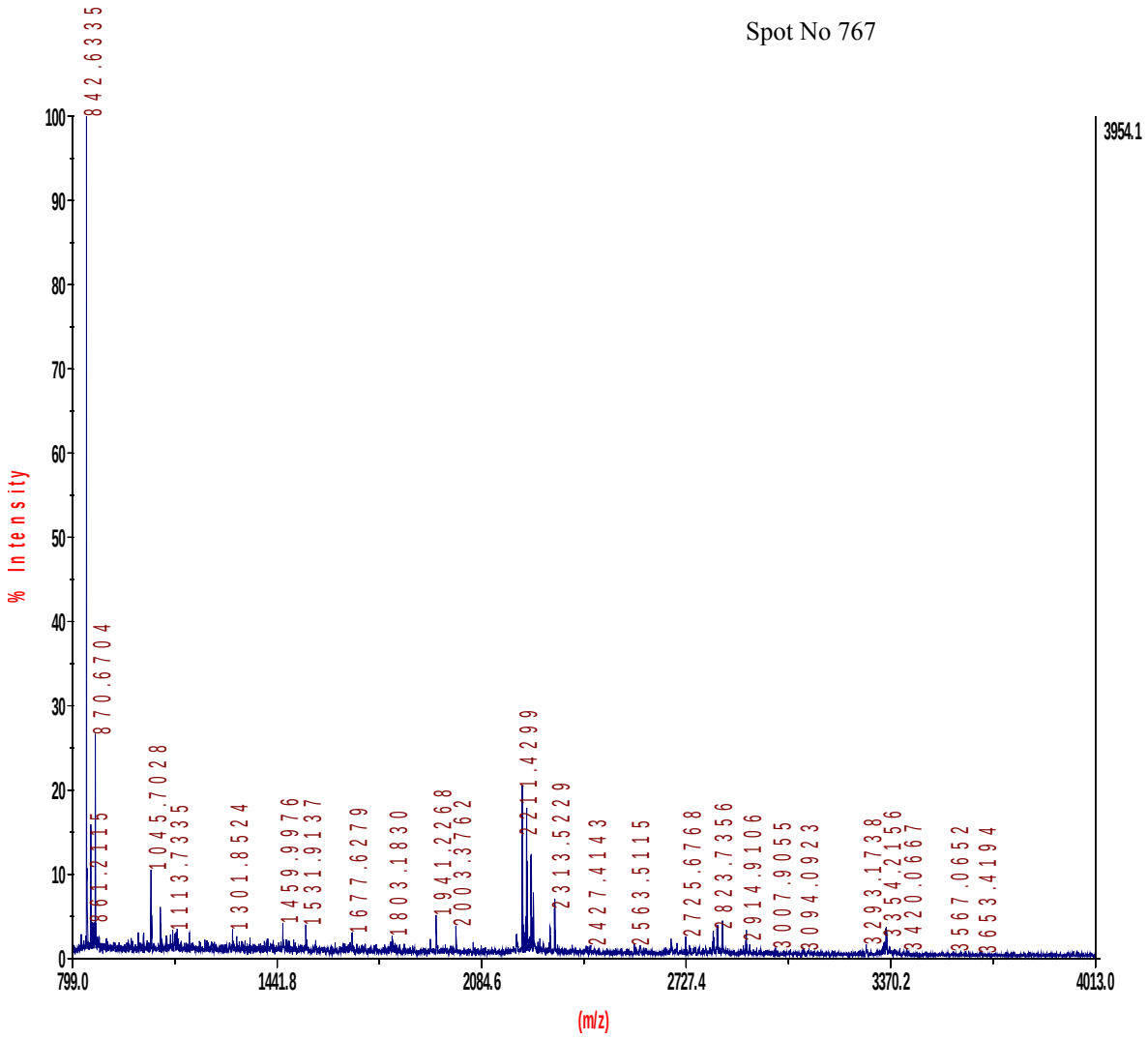

Figure 4.14. Peptide mass spectra of in-gel tryptic digest of intimal extract from human thoracic aorta (S1) of a 60 year old. The spot numbers are the designed numbers from the gel that showed protein expression. The peptide masses from MASCOT database search gave low scores for hypothetical protein.

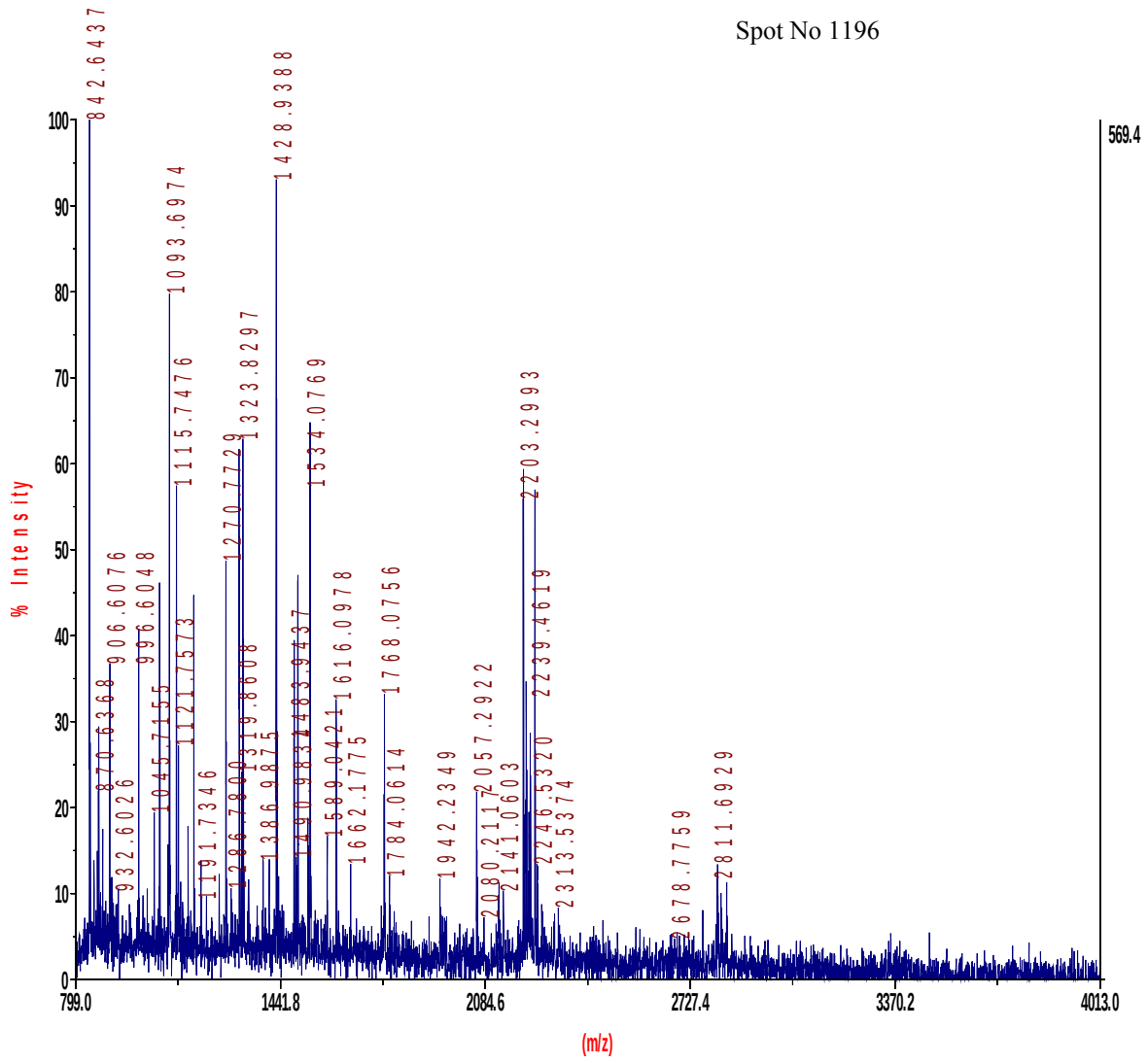

Figure 4.15 Peptide mass spectra of in-gel tryptic digest of intimal extract from human thoracic aorta (S1) of a 60 year old. The spot numbers are the designed numbers from the gel that showed protein expression. The peptide masses from MASCOT database search gave low scores for NID Mus musculus.

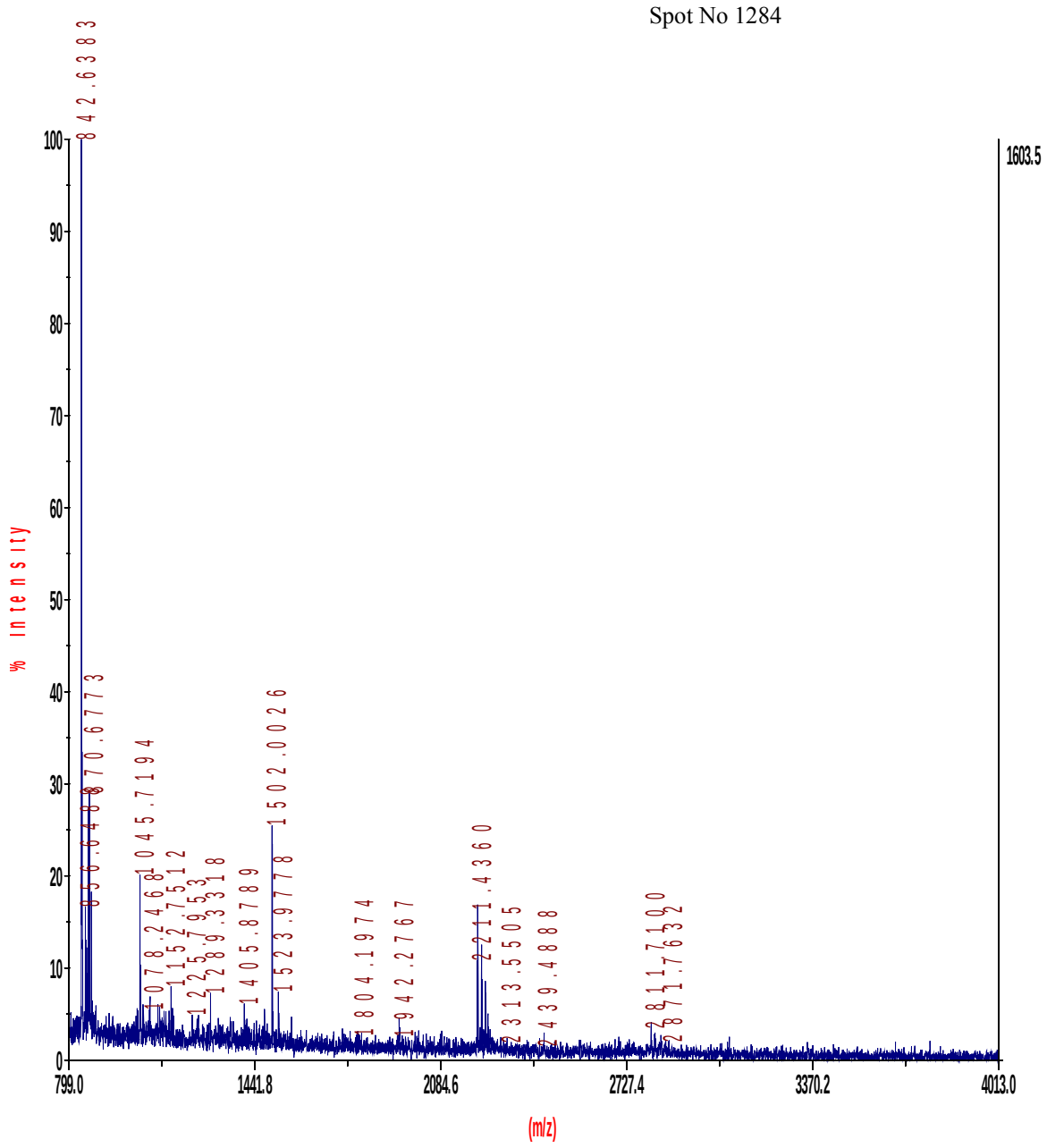

Figure 4.16. Peptide mass spectra of in-gel tryptic digest of intimal extract from human thoracic aorta (S1) of a 60 year old. The spot numbers are the designed numbers from the gel that showed protein expression. The peptide masses from MASCOT database search identified the protein as vimentin.

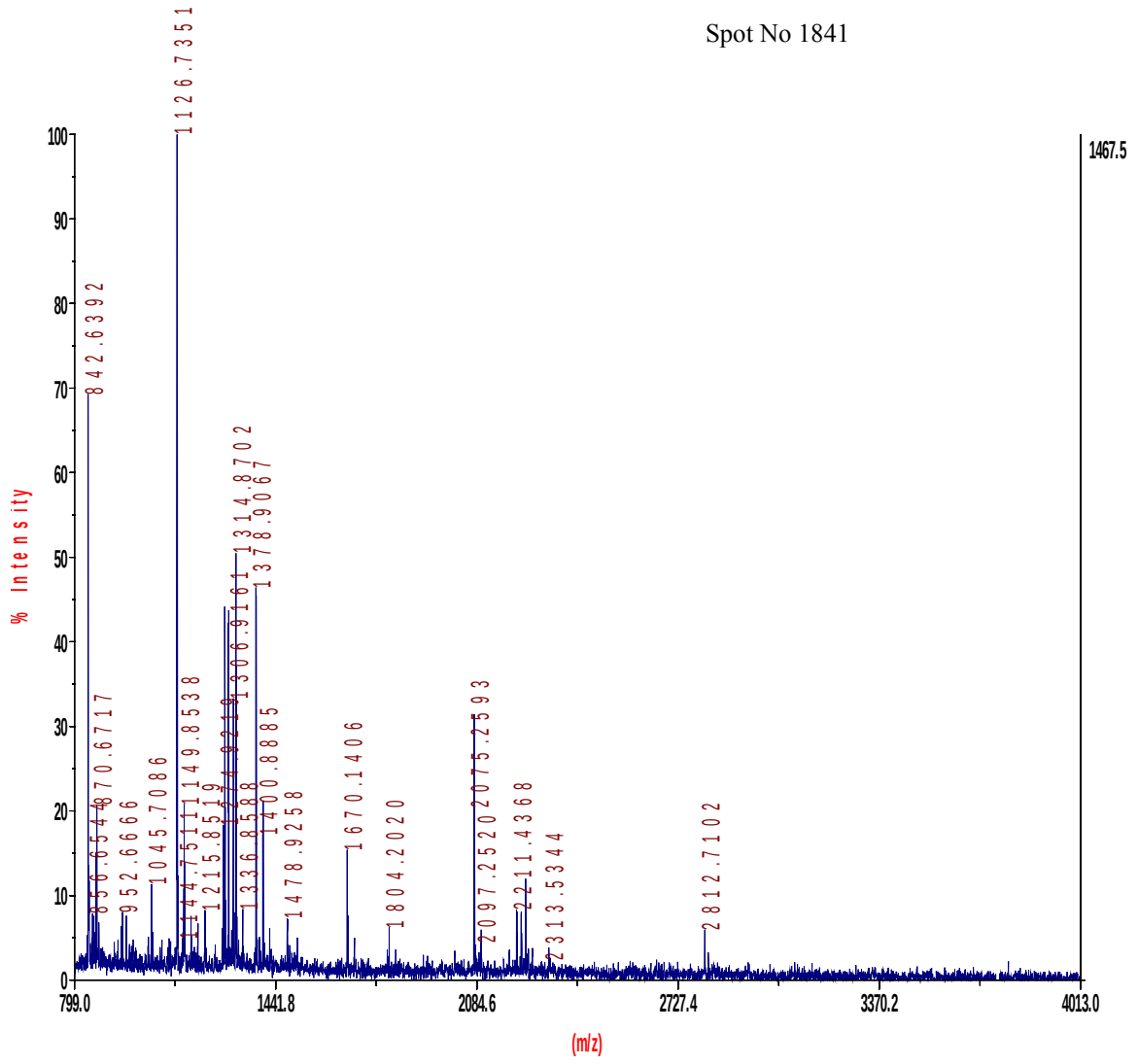

Figure 4.17 Peptide mass spectra of in-gel tryptic digest of intimal extract from human thoracic aorta (S1) of a 60 year old. The spot numbers are the designed numbers from the gel that showed alterations in protein expression. The peptide masses from MASCOT database search gave low scores for SSB3 protein-human.

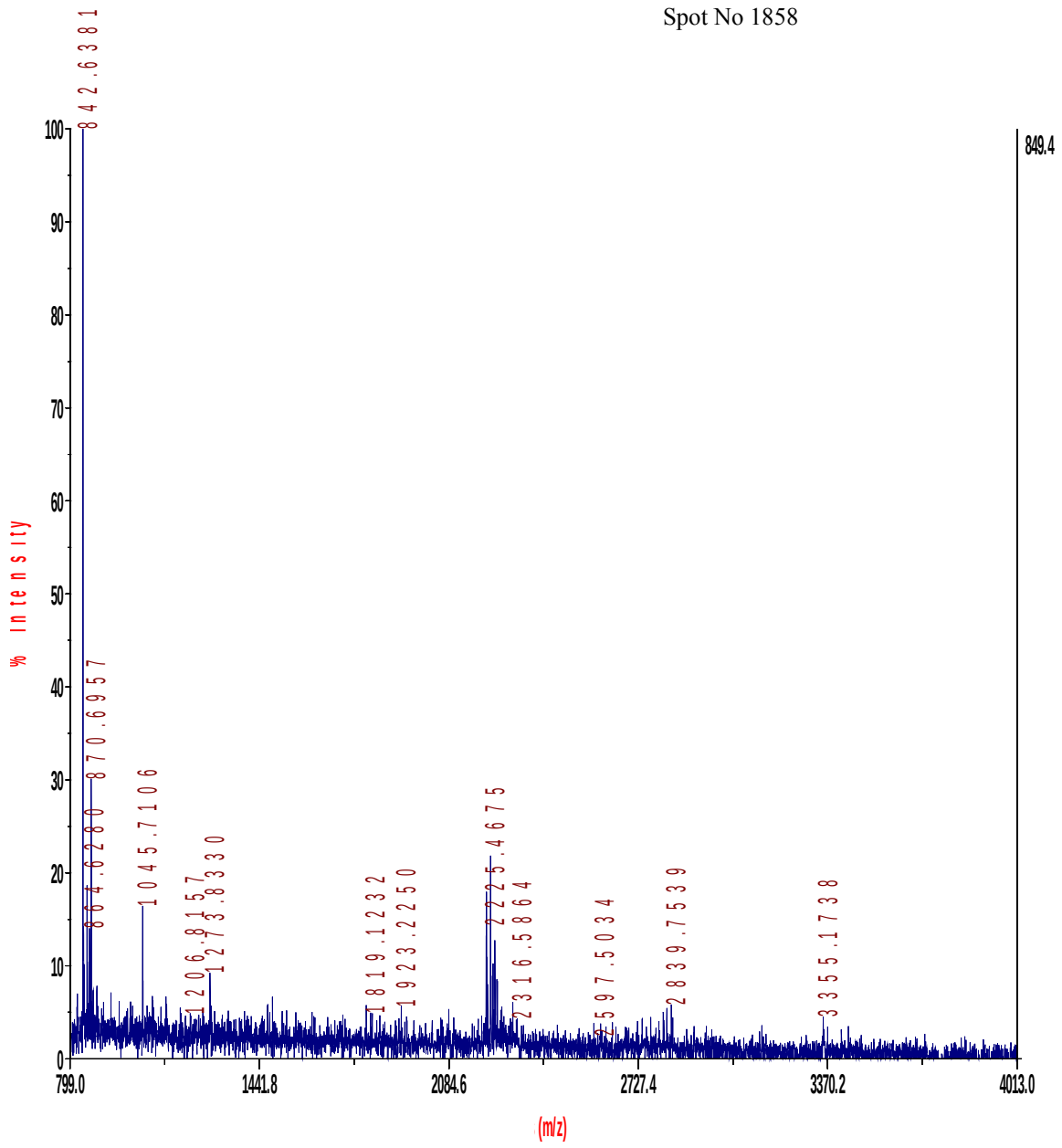

Figure 4.18 Peptide mass spectra of in-gel tryptic digest of intimal extract from human thoracic aorta (S1) of a 60 year old. The spot numbers are the designed numbers from the gel that showed protein expression. The peptide masses from MASCOT database search gave low scores for AX885349 NID Homo sapiens.

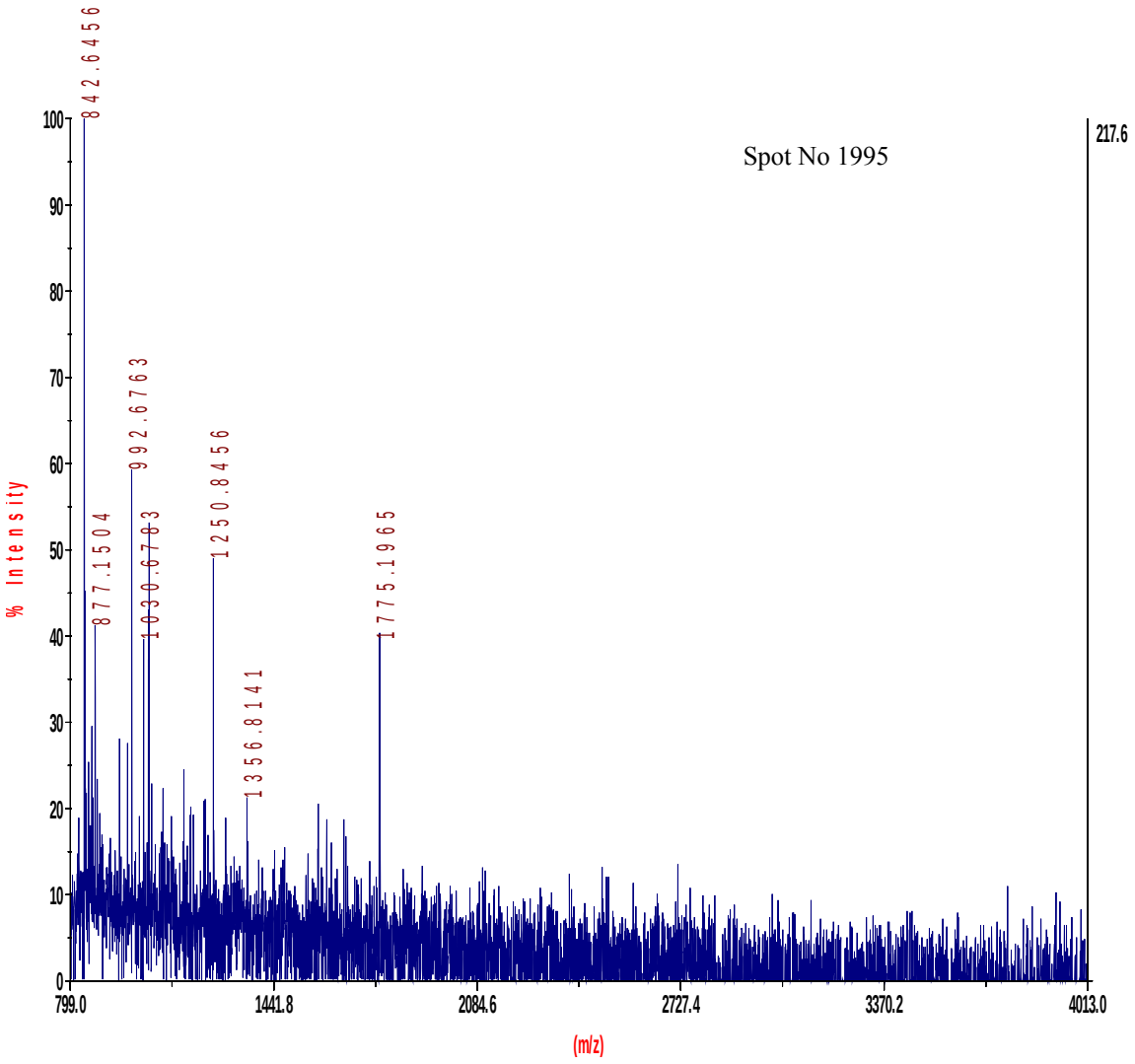

Figure 4.19 Peptide mass spectra of in-gel tryptic digest of intimal extract from human thoracic aorta (S1) of a 60 year old. The spot numbers are the designed numbers from the gel that showed protein expression. The peptide masses from MASCOT database search identified the protein as hemoglobin mutant chain.

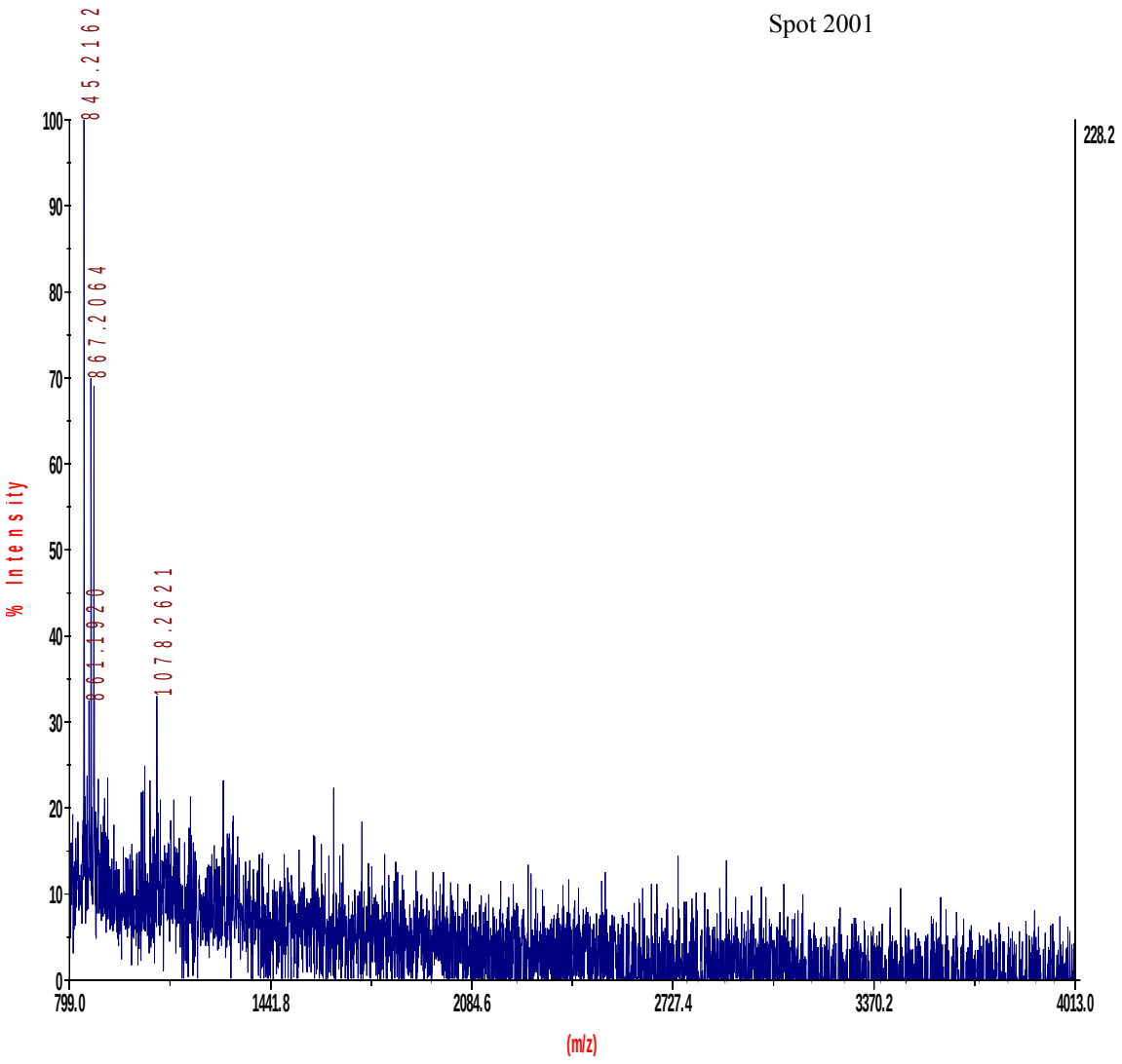

Figure 4.20 Peptide mass spectra of in-gel tryptic digest of intimal extract from human thoracic aorta (S1) of a 60 year old. The spot numbers are the designed numbers from the gel that showed protein expression. The peptide masses from MASCOT database search identified the protein as des his deoxyhemoglobin HIS 146 beta removed chain B human.

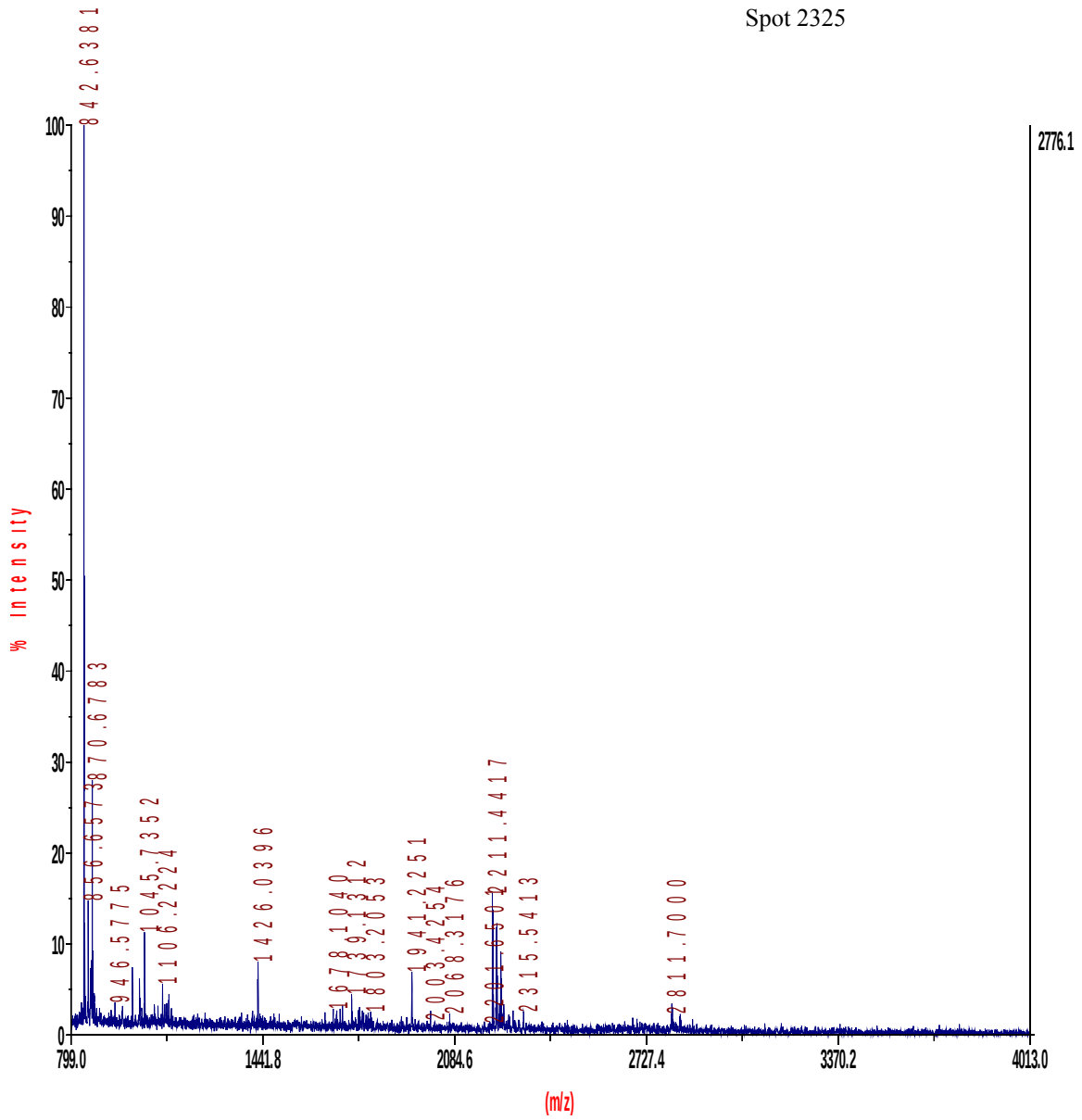

Figure 4.21 Peptide mass spectra of in-gel tryptic digest of intimal extract from human thoracic aorta (S1) of a 60 year old. The spot numbers are the designed numbers from the gel that showed protein expression. The peptide masses from MASCOT database search identified the protein as des hisdeoxyhemoglobin HIS 146 beta removed chain B_human.

Six external standards used for the calibration were from a mass standard kit for the 4700 proteomics analyzer calibration mixture. The calibration standard solution contains 50 pmol/µl des-Arg1-Bradykinin, angiotensin, Glu1-fibrinopeptide B, ACTH (1-17), ACTH (18-39), and ACTH (7-38). From the data shown, eight peptides from in-gel digest of protein from intimal extracts of normal and diseased tissue were expressed as either up-regulated or down-regulated from the gel analysis using DyCyder software with 3D images of the histogram of the proteins of interest. The proteins ranged in molecular weights from 13.5 to 80.3 kDa. The pI of the proteins ranged from 5.5 to 8.9. Four of the eight spots were identified by peptide mass fingerprinting using MASCOT.

Figures 4.22 – 4.28 are peptides produced from in-gel tryptic digest of intimal extracts of a native and bypass coronary artery from the same heart. The spots were automatically excised from the same gel stained with SyproRuby. The SyproRuby stain is also fluorescent with emission spectra at 610 nm. The spots were selected by comparing the gel images produced from the Cydye and the Sypro Ruby stain to determine if quantitatively enough protein is present for further treatment with trypsin. Artifacts such as dust particles may be observed in gels reacted with the Cydyes it is imperative validate the area of interest. Additionally, gel to gel variations could possibly cause spots or streaks in stains that may produce false positives.

MALDI-TOF TOF analysis was performed on a Voyager 4700 (Applied Biosystems). Peptide mass spectra were acquired in reflectron mode (20kV accelerating voltage) in positive ion mode with 155 ns delayed extraction averaging 1000 laser shots per spectrum.

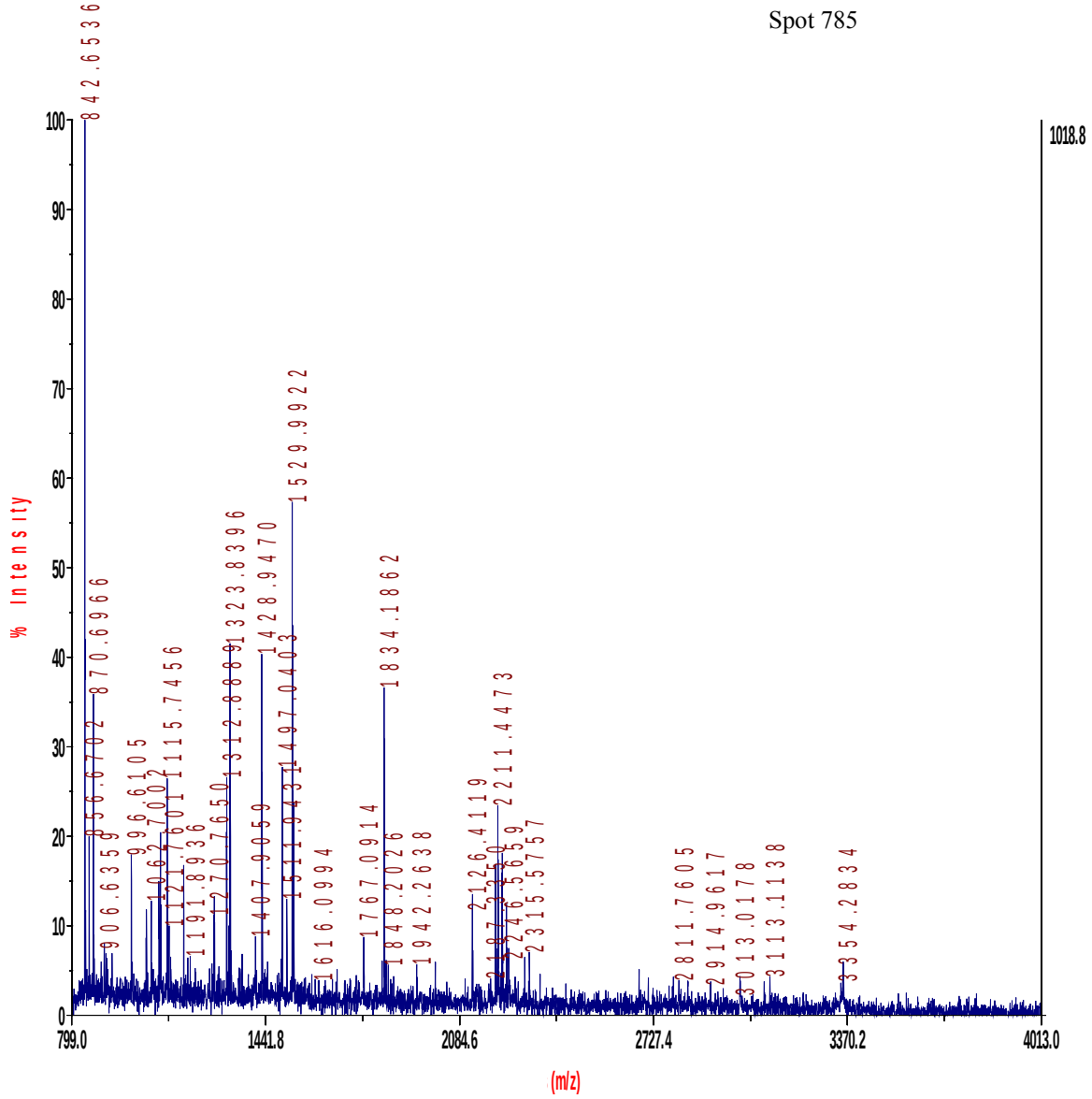

Figure 4.22 Peptide mass spectra of in-gel tryptic digest of intimal extract from native and bypass coronary artery (S2) of a 70 year old. The spot numbers are the designated numbers from the gel that showed protein expression. The peptide masses from MASCOT database search identified the protein as spectrin alpha.

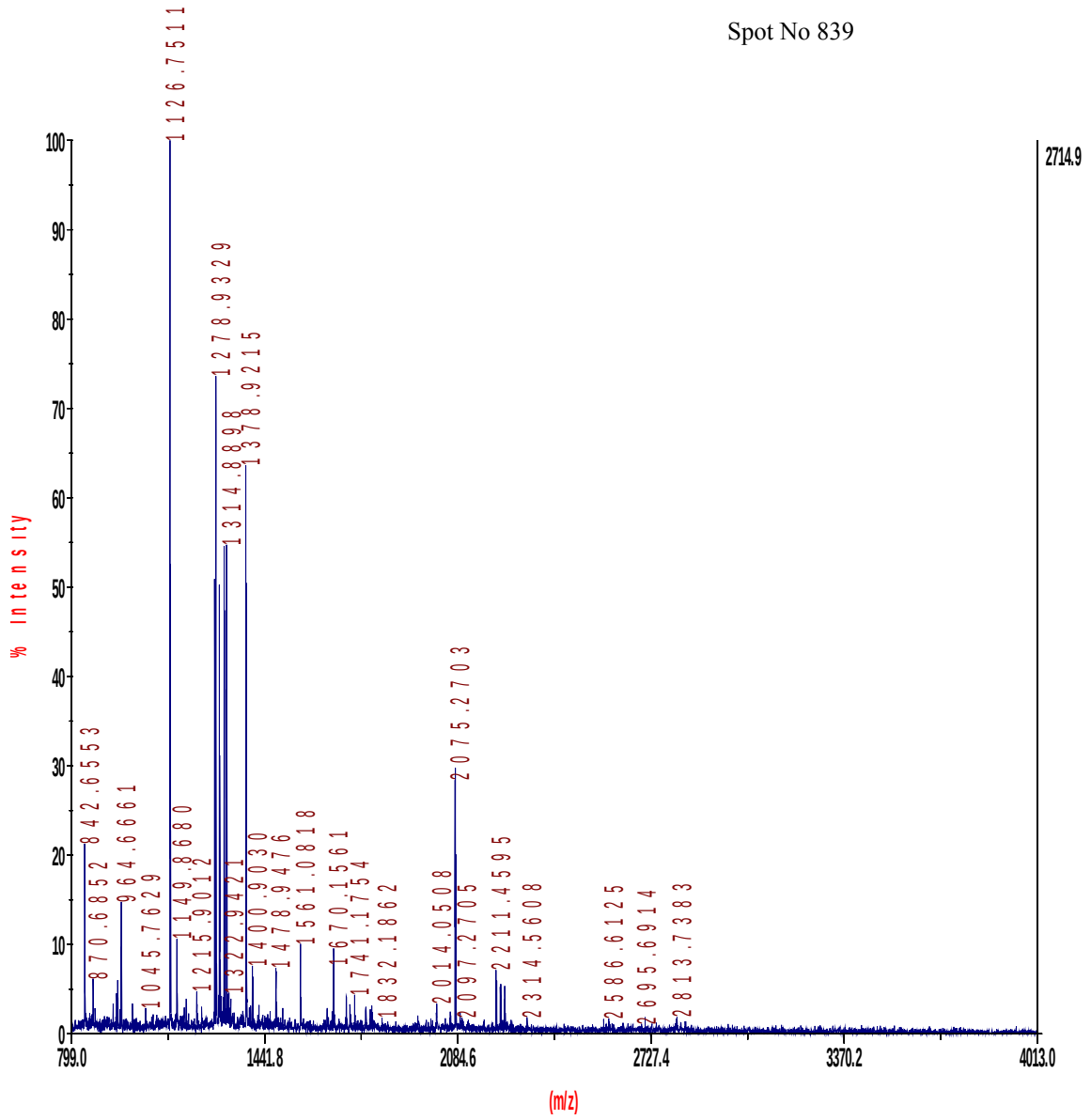

Figure 4.23 Peptide mass spectra of in-gel tryptic digest of intimal extract from native and bypass coronary artery (S2) of a 70 year old. The spot numbers are the designated numbers from the gel that showed protein expression. The peptide masses from MASCOT database search gave low scores for hypothetical protein. No positive identication was obtained.

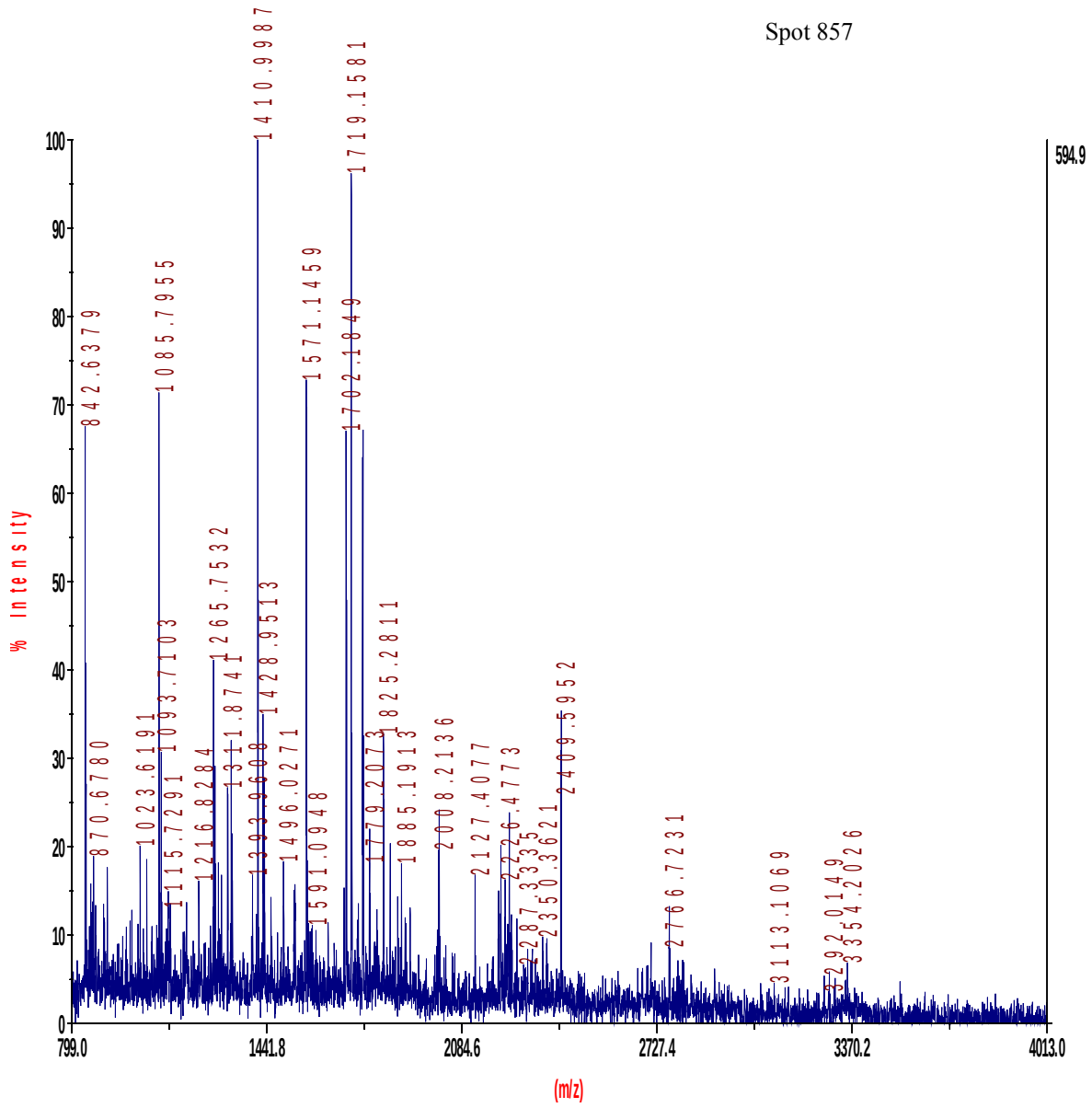

Figure 4.24 Peptide mass spectra of in-gel tryptic digest of intimal extract from a native and bypass coronary artery (S2) of a 70 year old. The spot numbers are the designated numbers from the gel that showed protein expression. The peptide masses from MASCOT database search identified the protein as collagen type VI.

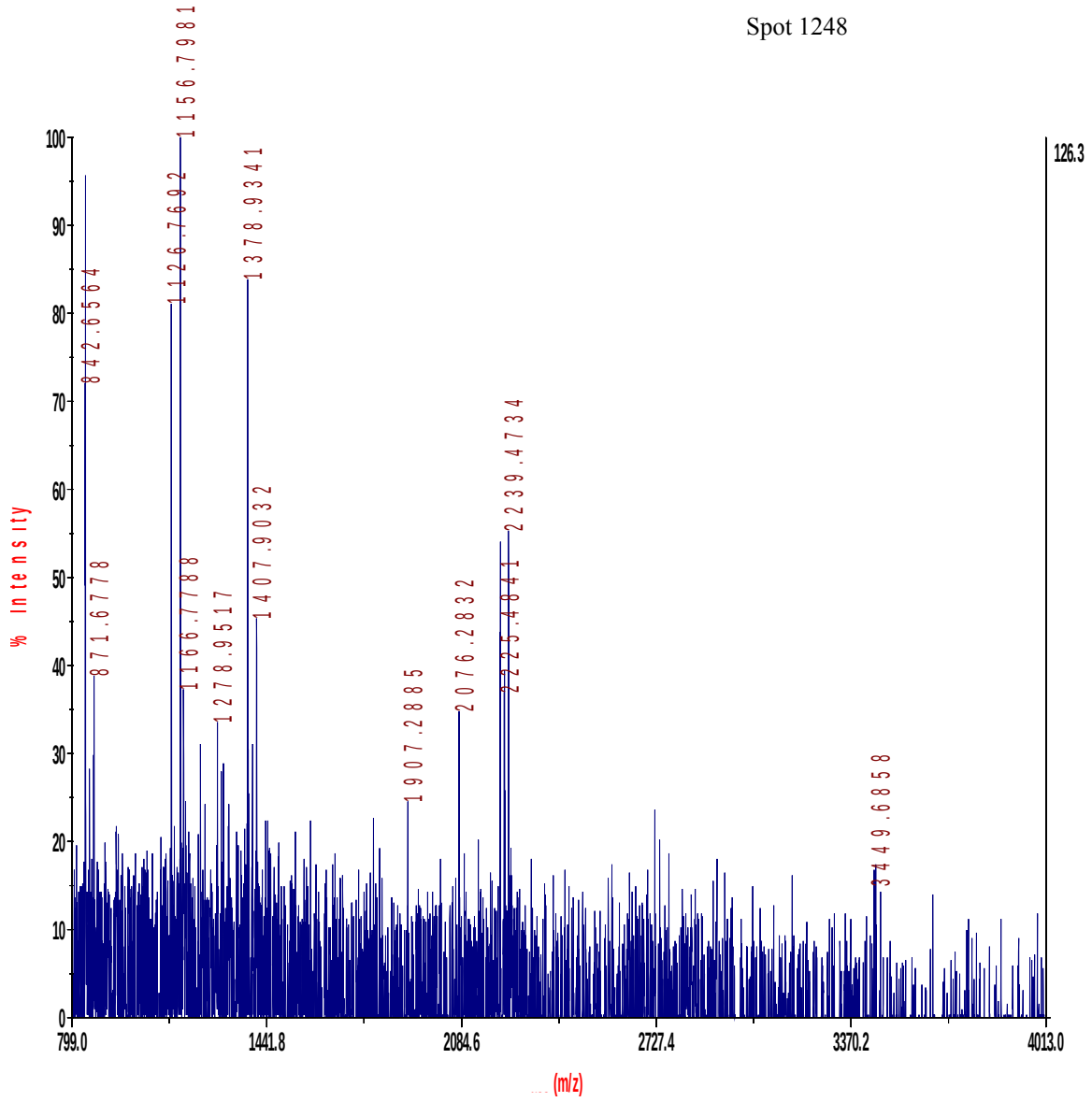

Figure 4.25 Peptide mass spectra of in-gel tryptic digest of intimal extract from a native and bypass coronary artery (S2) of a 70 year old. The spot numbers are the designated numbers from the gel that showed protein expression. The peptide masses from MASCOT database search identified the protein as fibrinogen beta chain precursor.

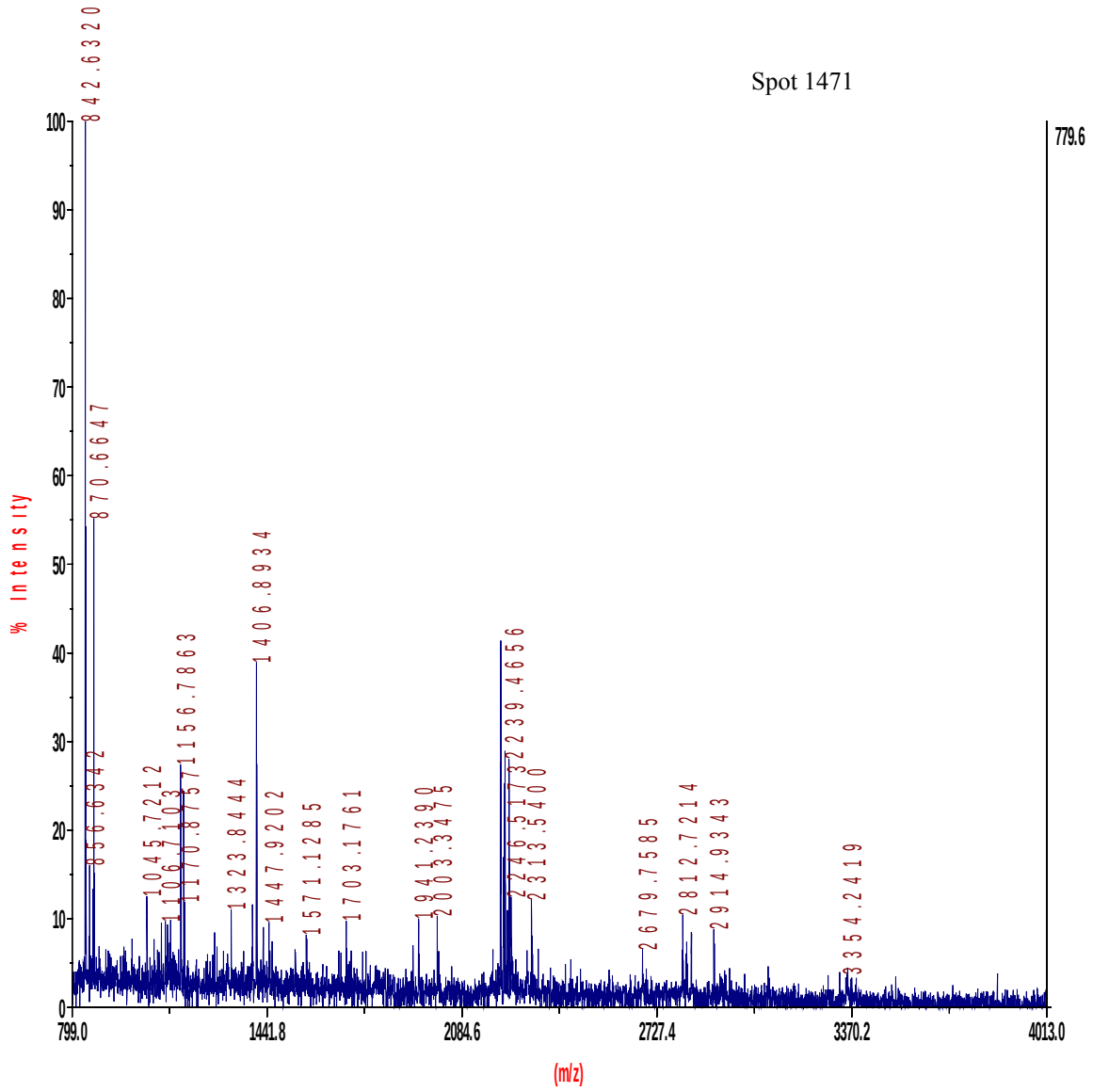

Figure 4.26 Peptide mass spectra of in-gel tryptic digest of intimal extract from a native and bypass coronary artery (S2) of a 70 year old. The spot numbers are the designated numbers from the gel that showed protein expression. The peptide masses from MASCOT database search gave low scores I -309 frgament. No protein identification was obtained.

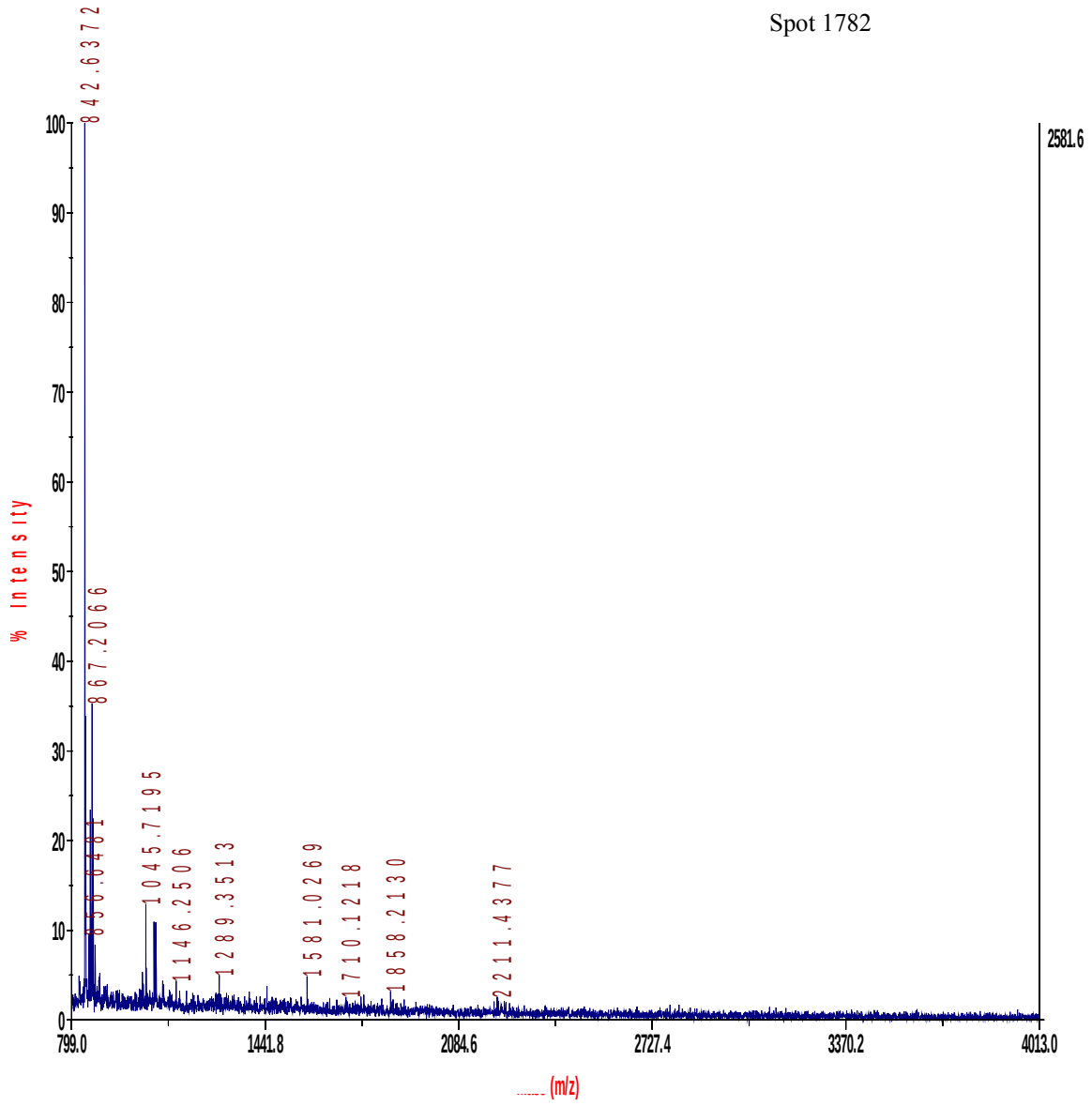

Figure 4.27 Peptide mass spectra of in-gel tryptic digest of intimal extract from native and bypass coronary artery (S2) of a 70 year old. The spot numbers are the designated numbers from the gel that showed protein expression. The peptide masses from MASCOT database search identified the protein as serum amyloid p-component chain A.

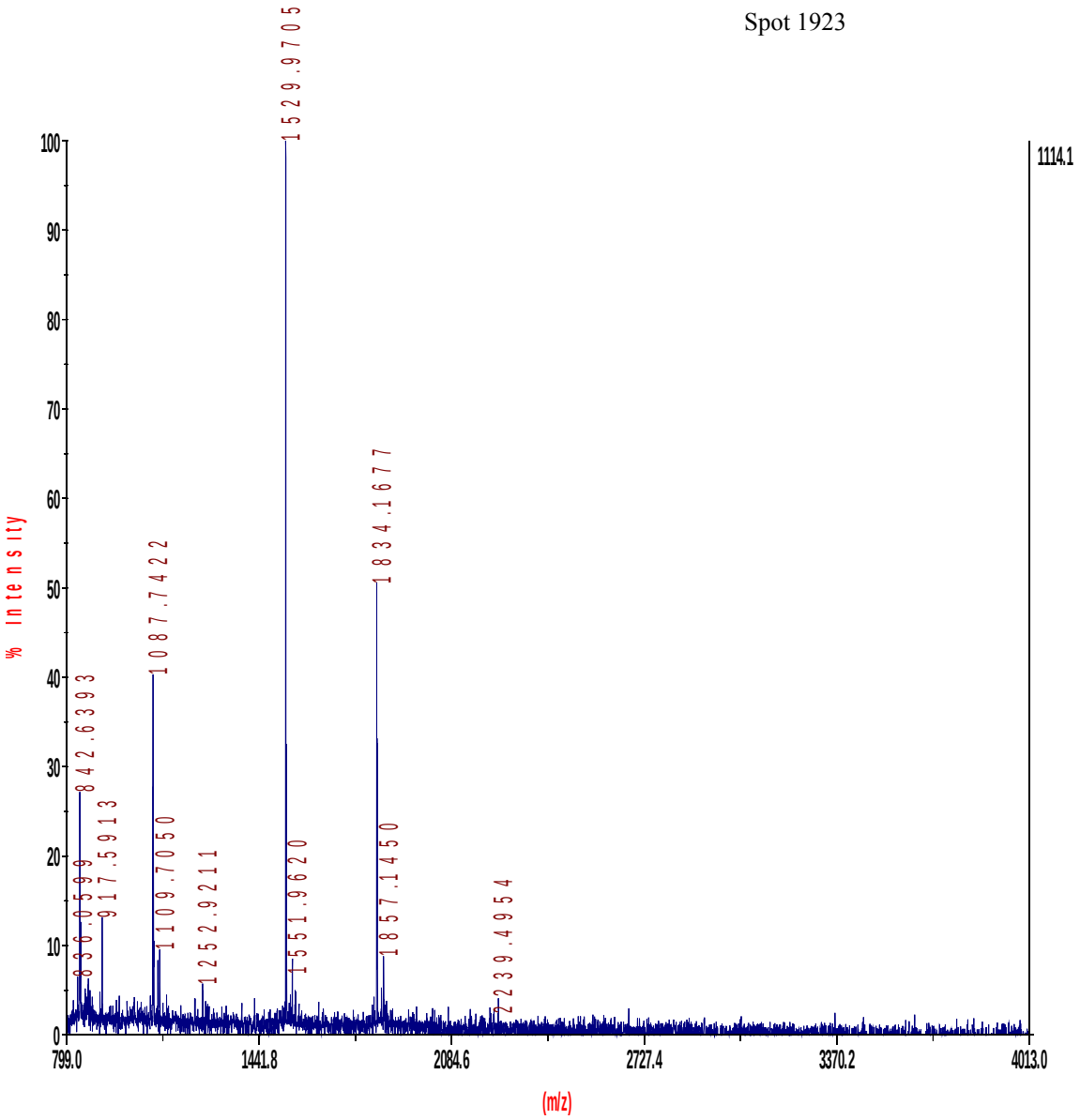

Figure 4.28 Peptide mass spectra of in-gel tryptic digest of intimal extract from native and bypass coronary artery (S2) of a 70 year old. The spot numbers are the designated numbers from the gel that showed protein expression. The peptide masses from MASCOT database search identified the protein as Mn superoxiddismutase.

Additional tissue extract of the intima from a native and bypass coronary artery from an 80 year old subject by lysis buffer was conducted. Following isoelectric focusing, SDS-PAGE in the second dimension and differential imaging, spots were excised. In-gel digest produced peptides from those spots that exhibited differences based on imaging comparisons (Figure 4.29

and 4.31). Four proteins were isolated and picked for analysis. The calculated masses based on datasearch from MASCOT and Swissprot ranged from 15.9 to 49.7 kDa and a pI range of 4.9 to 7.2 which is lower than expected for membrane proteins.

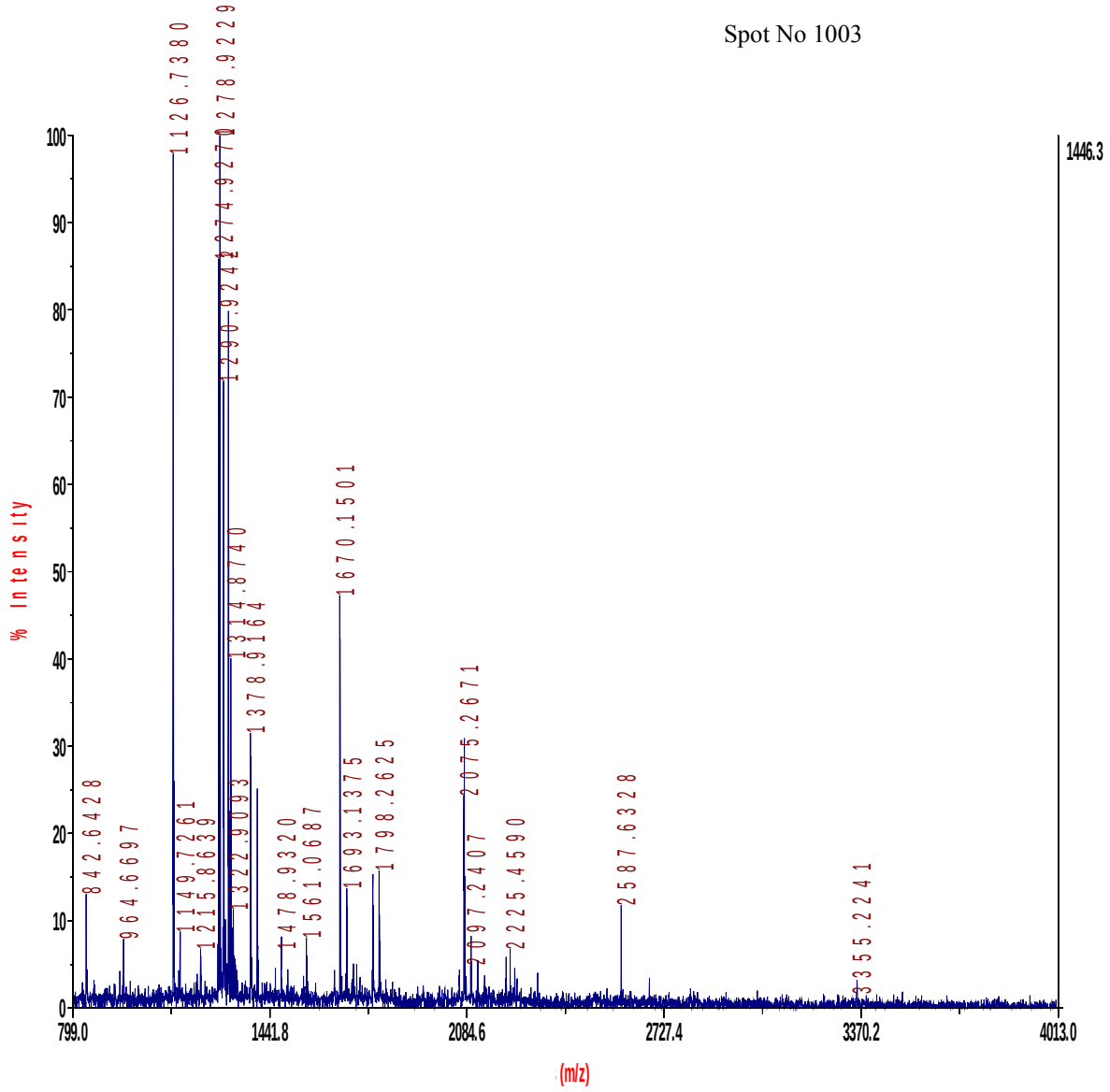

Figure 4.29 Peptide mass spectra of in-gel tryptic digest of intimal extract from native and bypass coronary artery (S3) of an 80 year old. The spot numbers are the designated numbers from the gel that showed protein expression. The peptide masses from MASCOT database search identified the protein as alpha tubulin fragment.

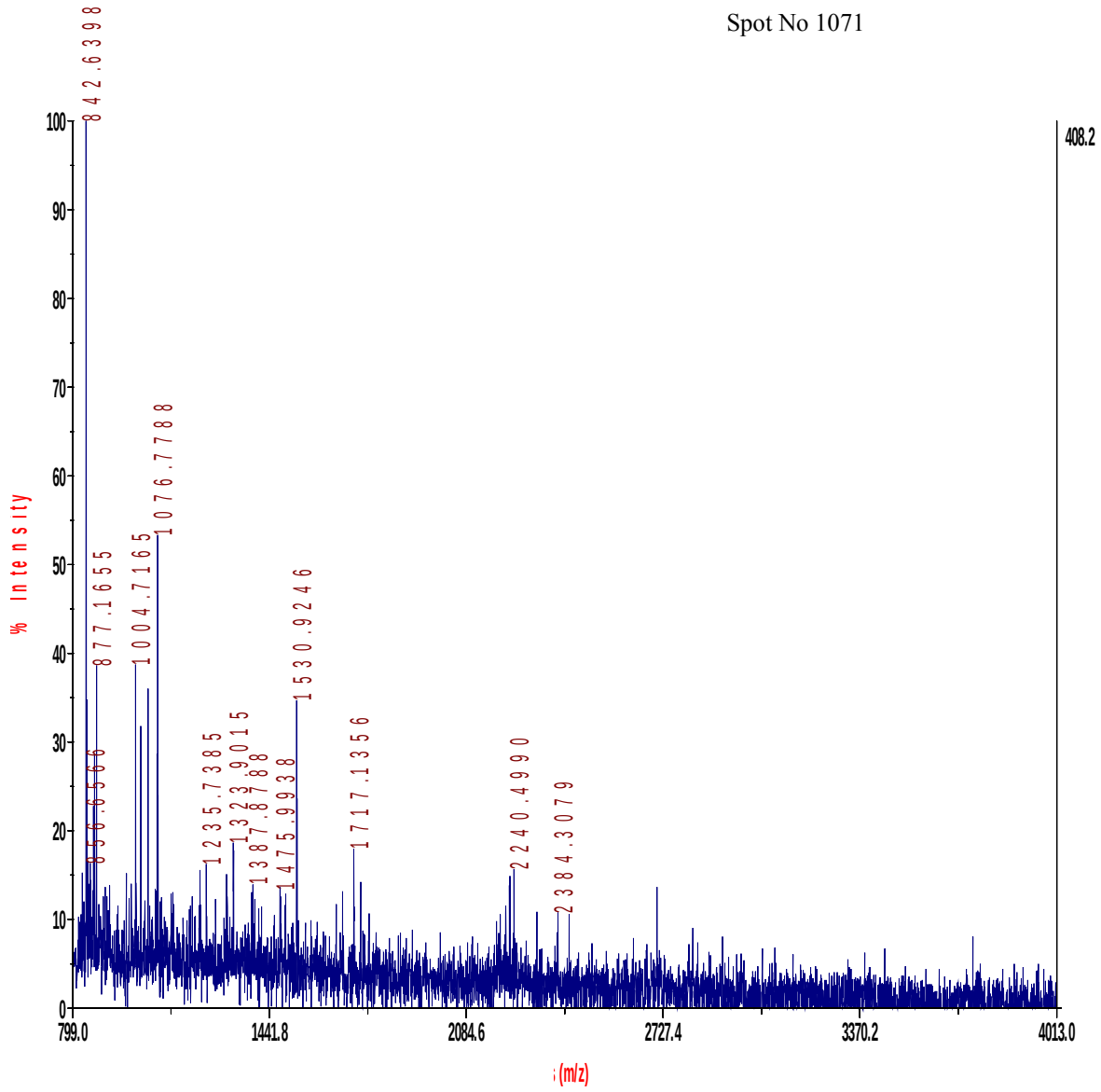

Figure 4.30 Peptide mass spectra of in-gel tryptic digest of intimal extract from native and bypass coronary artery (S3) of an 80 year old. The spot numbers are the designated numbers from the gel that showed protein expression. The peptide masses from MASCOT database search identified the protein as vimentin.

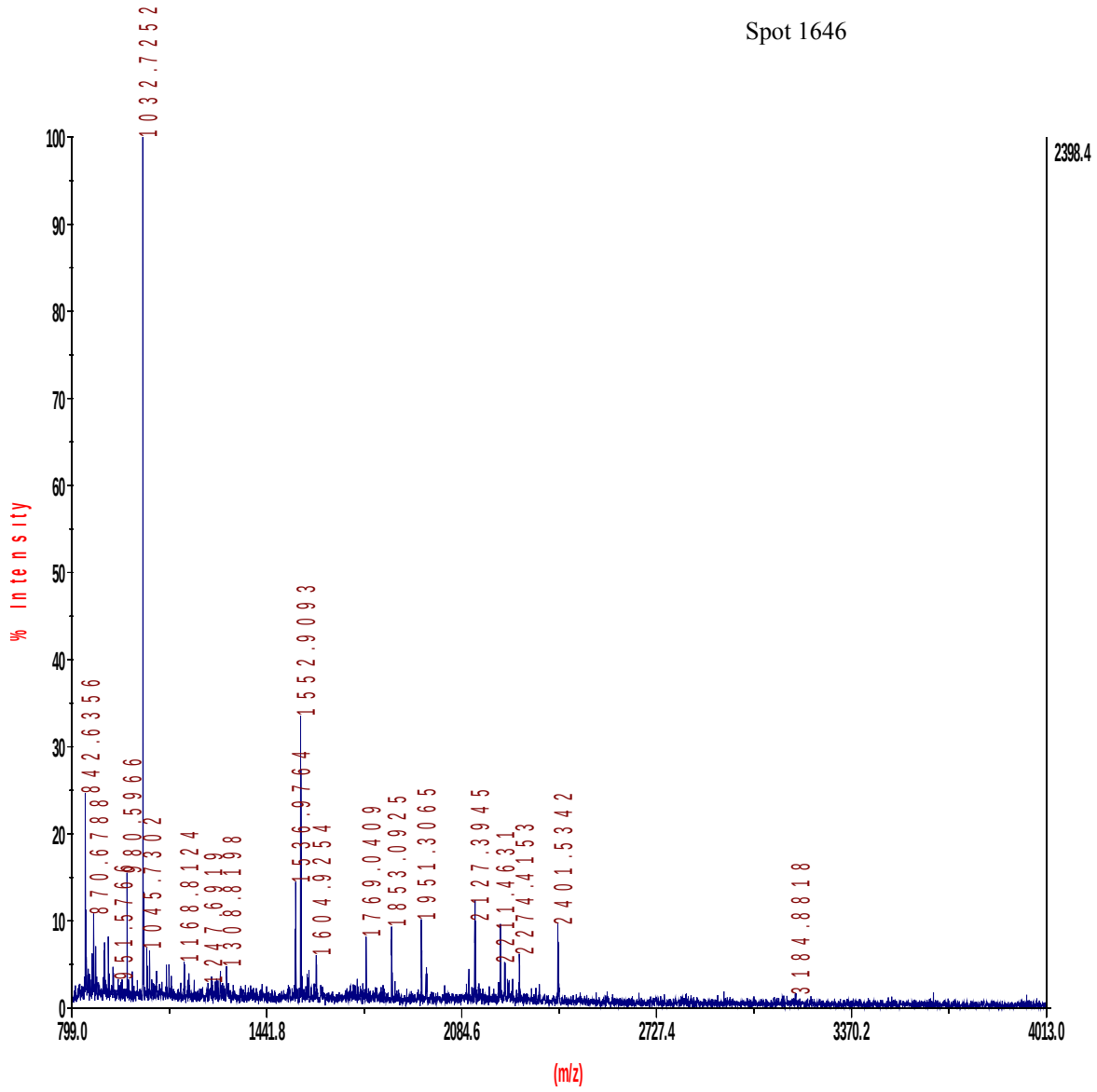

Figure 4.31 Peptide mass spectra of in-gel tryptic digest of intimal extract from native and bypass coronary artery (S3) of an 80 year old. The spot numbers are the designated numbers from the gel that showed protein expression. The peptide masses from MASCOT database identified the protein as hemoglobin beta chain

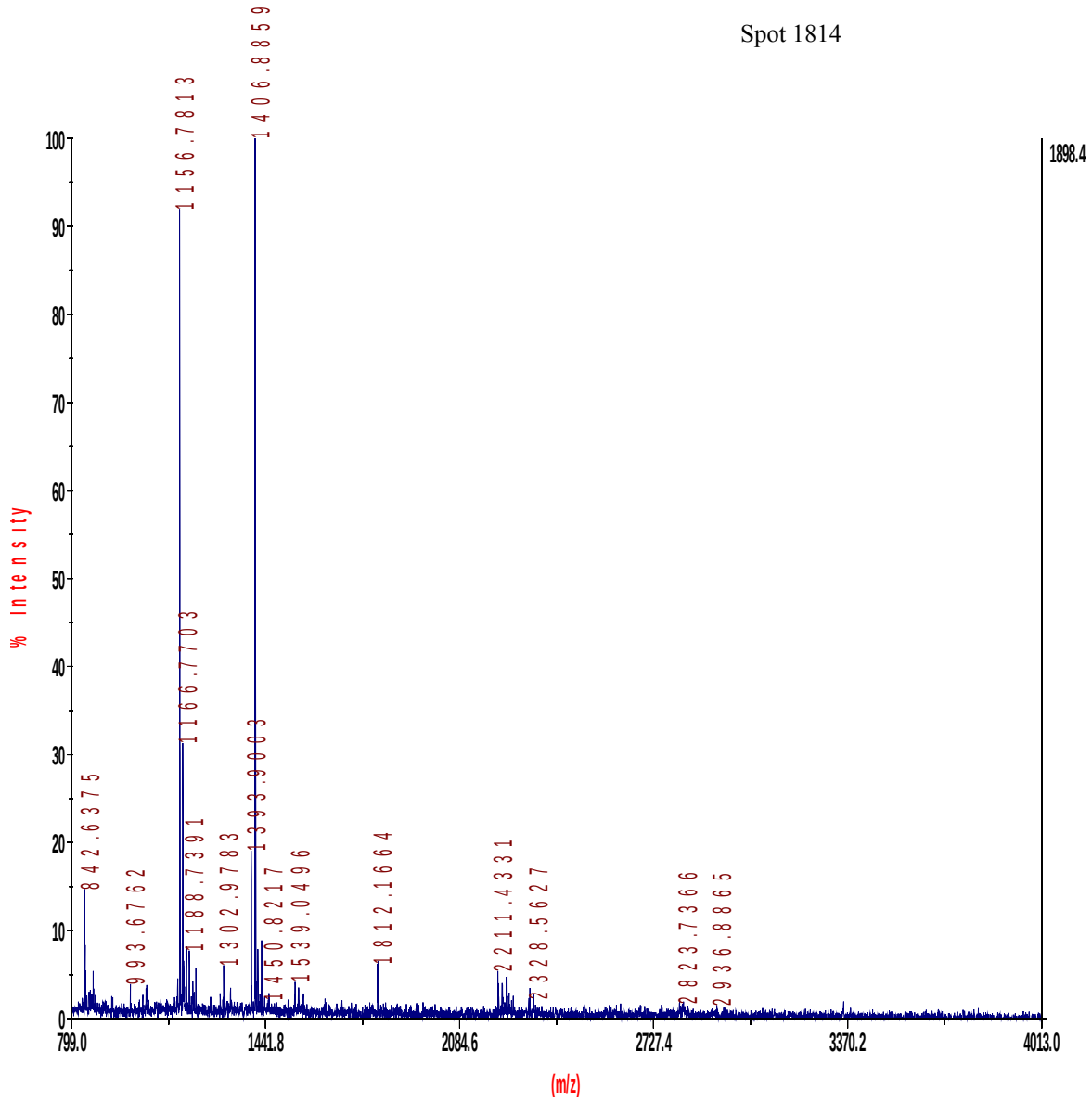

Figure 4.32 Peptide mass spectra of in-gel tryptic digest of intimal extract from native and bypass coronary artery (S3) of an 80 year old. The spot numbers are the designated numbers from the gel that showed protein expression. The peptide masses from MASCOT database search identified the protein as des his deoxyhemoglobin a mutant HIS 146.

The peptides were entered in a database search with the preset search criteria set mentioned in the Materials and Methods section. All peptide values were based on the algorithm specific in the search. The masses were search against human protein database. Table 4.1 lists the sample, spot number, rank, protein identification, accession number, molecular weight, pI, protein scoring algorithm (> 75% significant criteria) and the confidence interval which is equivalent to MASCOT expect values of $p<0.05$. These values are the selection criteria for positive identification of the proteins examined.

All proteins were identified in the NCBI and in the SwissProt database with species restriction. The criteria for protein scores and protein confidence interval are > 75 and 95%, respectively.

The 2D analysis of human thoracic aorta exhibiting proliferating atherosclerotic plaque features (foam cells, cholesterol formation, calcification, or thrombus) was differentially imaged. Proteins spots consisted of molecular weights ranging from 15 to 100 kDa and pI that separated within the range of the IPG drystrip (pH 3-10). The use of differential in-gel electrophoresis analysis of sample S1 resulted in eight proteins, four of which gave positive identifications based on the database search criteria. Spot assignments 767, 1196, 1841, and 1848 produced search parameters with protein scores of 44, 47, 42, 60 with confidence intervals not within the range stipulated (> 95%). Based on these results, there were no matches for those four spots.

Spot 1284 was identified as vimentin. Shah and colleagues have reported vimentin as a major component of cytoskeletal constituents of cells of mesenchymal origin that, based on in vitro studies, interacts with F-actin and polyphosphoinositide lipids [19].

Table 4.1 Summary of database search results of the proteins expressed in human atherosclerotic plaques extracts from thoracic aortas

Sample	Spot No.	Rank	Protein Name	Accession Number	Protein Molecular Weight	Protein PI	Protein Score	Protein Score CI%
60 Y-S1 aorta	767	1	Hypothetical protein DKFZp586F0420	Q9UG54_HUMAN	29023.3	6.92	44	0
	1196	1	AK045750 NID NID Mus musculus	BAC32480	80290.3	6.34	47	0
	1284	1	Vimentin - Human	Q5JVT0_HUMAN	49680	5.19	363	100
	1841	1	SSB3 protein Human	Q49A96_HUMAN	25827.8	9.62	42	0
	1858	1	AX885349 NID Homo Sapiens	CAE99479	13540.7	5.50	60	70.69
	1995	1	Hemoglobin mutant Chain A	1ABWA	30418.8	8.91	237	100
	2001	1	Des his deoxyhemoglobin HIS 146 Beta removed chain B - human	1AXFB	15834.2	6.76	291	100
	2325	1	Des his deoxyhemoglobin mutant HIS 146 BETA Removed,chain B_human	1AXFB	15834.2	6.76	433	100
70 Y-S2artery	785	1	Spectrin alpha chain	SPTA1_HUMAN	280884.4	4.96	73	98.462
	839	1	Hypothetical proein FLJ16140 Homo-Sapiens	Q6ZNG1_HUMAN	85840.9	9.41	46	0
	857	1	Collagen type VI alpha 1_Human	Q7Z645_HUMAN	109602.4	5.26	80	99.679
	1248	2	Fibrinogen beta chain precursor	FGHUB	56463.6	8.72	155	100
	1471	1	I -309 Fragment Human	Q76BR7_Human	3434.6	4.79	28	0
	1782	1	Serum amyloid p-component chain A	1LGNA	23358	6.12	255	100
	1923	2	Mn-Superoxiddismutase Human	CAA01016	19945.1	7.96	65	90.068
80 Y-S3artery	1003	1	Alpha tubulin Fragment	Q9GLW6_MACM	49662.3	4.9	295	100
	1071	1	Vimentin	Q5JVT0_HUMAN	49680.1	5.19	244	100
	1646	1	Hemoglobin beta chain	1HBAB	15941.3	7.26	104	99.20
	1814	1	Deshis deoxyhemoglobin a mutant HIS 146	1AXFB	15834.2	6.76	362	100

Spot 1995, human globin mutant chain A, is a dissociated dimer of hemoglobin that is cleared by renal filtration which can result in long term kidney damage. The fusion of the two α-globins units prevents dissociation into β units and eliminates renal toxicity [20]. This molecule is a hemoglobin recombitant designed as a blood substitute.

Spot 2001 was identified as des his deoxyhemoglobin HIS 146 Beta removed chain B and spot 2325 is a mutated site of hemoglobin Rothschild (37 beta Trp-Arg) critical for hemoglobin function the results in greatly reduced cooperactivity and oxygen affinity. In des HIS – 146 β, the COOH terminal histidine residue that promotes lower affinity for oxygen and change in quarternary structure has been removed [21].

Coronary artery extracts in sample S2 produced eight protein expressions when native and bypass arteries were compared. The expression of the individual protein spots has been previously discussed. Spectrin, spot 785, have implied to play a pivotal role in initiating integrin induced physiological and pathological events such as development, proliferation, cell survival, wound healing, metatasis, and atherosclerosis[22].

Spot 857 was identified as collagen VI. Steinhubl et al. studied the role of the platelet in the pathogenesis of atherthrombosis [23]. Platelet tethering and adhesion to the arterial walls under high shear forces was achieved by multiple interactions between platelet membrane receptors integrins and ligands within the exposed subendothelium most notably collagen and von Willebrand factor [23].

Spots 1248 and 1282 gave excellent scores and confidential intervals (Table 4.1). Three proteins that similarly respond are fibrinogen, C-reactive protein, and serum A amyloid (SAA) [24]. These molecules are produced by hepatocytes and are upregulated by cytokines interleukin

-6 (for CRP and fibrinogen) and interleukin–1 (for SAA). Serum p amyloid component protein may contribute to amyloid deposition by stabilizing the fibrils and decreasing their clearance [24]. Although the parameters for spot 1923 were slightly lower than those meeting the criteria, Mn superoxiddismutase has implications in the atherosclerotic process for reducing oxidative stress [25].

Four proteins were identified from an 80 year old (S2) of native and bypass coronary arteries. Three of the spots, 1071, 1646 and 1814, have already been discussed and their functions relative to the proliferation of atherosclerosis. Spot 1003 was identified as tubulin. Evidence has suggested that alpha tublin detyrosination is a required event in the proliferation of vascular smooth muscles that are a hallmark of atherosclerosis and related vascular complications [26].

4.5 Conclusions

Differential gel electrophoresis was used to identify differentially expressed proteins separated by two dimensional gel electrophoresis. Tissues were extracted from intimas of normal and diseased thoracic aorta and native and bypass coronary arteries. Eight proteins in the aorta extracts were detected using fluorescent dyes Cydye 3 and Cydye 5. In this tissue, four proteins were identified by MALDI- TOF MS and MALDI TOFTOF-MS. Peptide masses were searched using MASCOT and SwissProt database. The native and bypass coronary samples revealed seven proteins in the 70 year old extract and four proteins in the 80 year old extracts that underwent differential expression. The technique has the sensitivity and dynamic range useful in the analysis of normal and diseased tissues.

4.6 References

(1) Duran, M.C.; Mas,S.; Nartin-Ventura, J.L.; Melihac, O.; Michel, J.B.; Gallego-Delgado,J.; Lazaro, A.; Tunon, J.; Egido, J.; Fernando,V. *Proteomics,* **2003,** 3,973-978

(2) Lusis, A. *Nature* **2000**,407,233-241.

(3) Virmani, R.; Kolodgie, F.D.; Burke, A.P.; Farb, A.; Schwartz, S.M. *Arteriosler. Thromb Vasc. Biol.* **2000**, 20, 1262-1275.

(4) McGregor, E.; Kempster, L.; Wait, R.; Welson, S.Y.; Gosling, M.J.; Dunn, M.J.; Powell, J.T.; *Proteomics* **2001**,1405-1414.

(5) Donners, M.M.P.C.; Verluyten, M.J.; Bouman, F.G.; Mariman, E.C.M.; Devreese, B.; Vanrobaeys, F.; van Beeumen, J.; van der Akker, L.H.J.M.; Daemen, M.J.A.P.; Heeneman, S.; *J. Pathol.* **2005**, 206, 39-45.

(6) Ghazalpour, A.; Doss. S.; Yang, X.; Aten, J.; Toomey, E.M.; Van Nas, A.; Wang, S.; Drake, T.A.; Lusis, A.J. *J. Lipid Res.* **2004**, 45,1793-1805.

(7) Yu, Y.L.; Yang, P.Y.; Fan, H.Z.; Huang, Z.Y.; Rui, Y.C.; Yang, P.Y.; Peng-Yuan, Y.; *Acta Pharmacol Sin* **2003**,9,873-877.

(8) Prime, J.; Alban, A.; Hawkins, E.; Hughes, B. The Quantitative Advantages of an Internal Standard in Multiplexing 2D Electrophoresis. In *Methods in Proteome and Protein Analysis*; Kamp, R.M., Calvete,J. J., Choli-Papadopoulou, T.,Eds; Springer-Verlag Berlin Heidelberg: New York, **2004**; pp 233-250.

(9) Yan, J.X.; Devenish, A.T.; Wait, R.; Stone, T.; Laurie, S.; Fowler, S. *Proteomics* **2002,** 2, 1682-1698.

(10) Skynner, H.A.; Rosahl, T.W.; Knowles, M.R.; Salim, K.; Reid, L.; Cothliff, R.; McAllister, G.; Guest, P. *Proteomics* **2002**, 2, 1018-1025.

(11) Gharbi, S.; Gaffney, P.; Yang, A.; Zvelebil, M.J.; Cramer, R.; Waterfield, M.D.; Timms, J.F. *Proteomics* **2002**, 1, 91-98.

(12) Alban, A.; David, S.O.; Bjorkesten, L.; Andersson, C.; Sloge, E.; Lewis, S.; Currie, I. *Proteomics* **2003**, 3, 36-44.

(13) Zhou, G.; Li, H.; Decamp, D.; Chen, S.; Shu, H.; Gong, Y.; Flaig, M.; Gillespie, J.W.; Hu, N.; Taylor, P.R.; Emmert-Buck, M.R.; Liotta, L.A.; Petricon III, E.F.; Zhao, Y. *Mol.Cell Prot.,* **2002**, 1, 117-124.

(14) http//:www.matrixscience.com

(15) Gorg, A.; Obermaier, C.; Boguth, G.; Harder, A.; Scheiber, B.; Wildgruber, R.; Weiss, W. *Electrophoresis* **2000**, 21,1037-1053.

(16) Voss, T.; Haberl, P. *Electrophoresis* **2000**,21, 3345-3350.

(17) Alfonso, P.; Nunez, A.; Madoz-Gurpide, J.; Lombardia, L.; Sanchez, L.; Casal, J.I.; *Proteomics* **2005** 5, 2602-11.

(18) Kumar, V.; Abbas, A.K.; Fausto, N. Acute and Chronic Inflammation. In *Robbins and Cotran Pathologic Basis of Disease*; Elsiever-Saunders, Philadelphia, Pennsylvania, **2005** p.83.

(19) Shah, J.V.; Wang, L.Z.; Traub, P.; Janmey, P.A. *Biol Bull.* **1998**, 194,402-405.

(20) Looker, D.; Abbott-Brown, D.; Cozart, P.; Durfee, S.; Hoffman, S.; Matthews, A.J.; Miller-Roehrich, J.; Shoemaker, S.; Trimble, S.; Fermi, G. *Nature* **1992**, 356, 258-260.

(21) Bettati, S.; Kwiatkowski, L.D.; Kavanaugh, J.S.; Mozzarelli, A.; Arnone, A.; Rossi, G.L.; Noble, R.W.; *J. Bio.l Chem.* **1997**, 272, 52, 33077-33084.

(22) Bialkowski, K.; Saido, T. C.; Fox, J.E. *J. Cell Sc.,* **2005**, 118,381-395.

(23) Steinhubl, S. R.; Moliterno, D.J. *Am Cardiovasc Drugs*, **2005**, 5(6), 399-488.

(24) Pawlak, K.; Pawlak, D.; Mysiwiec, M. *Med. Sc.i Monit.* **2006**, 12, 181-185.

(25) Phung, A.D.; Soucek, K.; Kubala, L.; Harper, R.W.; Chloe-Bulinski, J., Eiserich, J.P; *Eur J. Cel.l Biol.* **2006**, 85, 12, 1241-1252.

CHAPTER 5

SEPARATION, IDENTIFICATION AND QUANTIFICATION OF CHOLESTEROL AND CHOLESTEROL ESTERS IN HUMAN ATHEROSCLEROTIC PLAQUE USING HIGH PERFORMANCE LIQUID CHROMATOGRAPHY ATMOSPHERIC CHEMICAL IONIZATION MASS SPECTROMETRY

5.1 Introduction

One of the primary risk factors for coronary heart disease is high levels of cholesterol in the blood. As the levels in the blood are consistently elevated, accumulation occurs and contributes to the formation of atherosclerotic plaques [1]. The development of cholesterol in plaque in mammals by the accumulation of lipid rich necrotic debris and smooth cells has been investigated [2]. Plasma lipoproteins contain neutral lipids in the interior and phospholipids, cholesterol and protein at the surface [1]. The cholesterol in the plasma exists as free sterol and as cholesterol esters. Esterification occurs at the cholesterol hydroxide position with a long chain fatty acid usually unsaturated. The synthesis of the esters in the plasma is from the reaction of cholesterol and an acyl chain on phosphotidylcholine that is acted on by lecithin: cholesterol acyltransferase, an enzyme secreted from the liver into the bloodstream. Since cholesterol esters are more hydrophobic than cholesterol itself, the other method for cholesterol uptake in the body is in food uptake. The foremost theory for the relationship for elevated cholesterol levels and atherogenesis was demonstrated by Brown and Goldstein [3]. Their work demonstrated that since cholesterol esters are too hydrophobic to transverse cell membranes, a receptor mediated process is necessary and the quantity of receptors themselves is regulated [3].

Key to the initial response of atherosclerosis lies in the oxidation of lipoprotein that has a major affect on the accumulation of cholesterol in the plaque [4]. Plaque formation involves an inflammatory response to modified plasma lipids that have entered the intima [5]. The low

density lipoprotein (LDL) is modified on the endothelial surface to a proinflammatory molecule [6].

The analysis of lipids using gas chromatography mass spectrometry has long been a challenge due to the high molecular weight and the nonvolatility of the compounds. Many approaches have addressed this problem including particle beam, thermospray, continuous flow fast atom bombardment, electrospray ionization (ESI), and atmospheric pressure chemical ionization (APCI) [7]. ESI is the soft ionization method for biological molecules; however APCI is a similar technique, but some degree of fragmentation is produced for structural characterization. Therefore APCI is the method of choice for the analysis for cholesterol and its esters in this study. The simple design of the APCI source includes the following components: a capillary containing a liquid from the high performance liquid chromatograph that is sprayed through a nozzle with a concentric nebulizer gas that surrounds the capillary, a heated vaporizer tube that desolvates the analyte molecules, and a corona needle [8]. The effluent is sprayed into a heated chamber in which the analyte undergoes minimal degradation. The concept of APCI involves gas phase ions produced by a source of electrons introduced on-axis with the heated spray. The electrons are usually supplied by a discharge source such as a Ni emitter. A coronary discharge is produced from a needle charged in the range from 5-10 kV. The ions from the discharge are from the source gases composed of nitrogen or water. A general reaction also involves ionization of N_2 and O_2 from the formation of hydronium ions and water clusters [9].

5.2 Research Goals and Objectives

The aim of this study is to use RPHPLC- APCI-MS technique to separate, identify and quantify cholesterol and its esters extracted for intimas of human thoracic aortas. Additionally, correlation analysis will be performed to determine the effect of ester concentration on the progression of atherosclerosis.

5.3 Experimental

5.3.1 Materials and Reagents

Tissue samples of human thoracic aortas were obtained from Louisiana State University Health Science Center, New Orleans, Louisiana. The sample were frozen and stored at -70ºC until lipid extraction. Urea, dithiothreotol (DTT), 3-[(3-cholamidopropyl0dimethyl-ammonio]-1propanesulfonate (CHAPS), sodium azide, sodium azide, phenyl methyl sulfonyl fluoride were obtained from Sigma (St. Louis, MO USA). Chloroform, methanol, isopropanol, acetonitrile were obtained from Aldrich (St. Louis, MO USA). External standards of cholesterol, cholesterol linolenate, cholesteryl linoleate, cholesteryl oleate, cholesterol palmitate, and cholesteryl stearate were purchased from Sigma (St. Louis, MO, USA).

5.3.2 Extraction of Cholesterol Esters from Heart Plaque

The intial protocol for the extraction of thoracic aorta plaques is summarized for samples 1-4. The intima from the tissue was excised and pulverized in liquid nitrogen with a mortar and pestle into a fine powder. The powdered sample was mixed with lysis buffer containing 9.5M urea, 2% CHAPS, 0.8% immobiline pH gradient buffer, and 1% DTT. This mixture was homogenized with a Tauzon (Fisher Scientific Inc) handheld homogenizer and then sonicated in ice for 5 minutes. The mixture was centrifuged at 13,000 x g at 20º C for one hour. A 10 g aliquot was mixed with 8 grams of deionized water followed by the addition of 1:2 (v/v) methanol / chloroform with homogenization. An additional mixture 1:1 (v/v) water/chloroform was again added with further homogenization. The resulting solution was filtered with a 2 micron nylon filter. The filtered solution was added to a separatory funnel and the organic and aqueous was allowed to form. The cholesterol esters or lipids were solubilized in the organic layer containing the chloroform. This layer was separated and dried under nitrogen to constant weight. This final

weight was recorded and dissolved in 3ml of a mixture of isopropanol / acetonitrile (50:50) solvent. This sample was used for analysis by RP-HPLC/ APCI-MS.

5.3.3 Extraction of Cholesterol Esters from Heart Plaques

A second extraction procedure was used in sample numbers 5 through 36 to investigate the presence of proteins in the aqueous phase of the separation. Denaturants and protease inhibitors such as sodium azide and vanadate were added to protect the proteins in the plaques during extraction. Intima tissue was dissected from thoracic aortas kept cold on ice. The tissue was further excised in small pieces and pulverized in liquid nitrogen into a fine powder using a mortar and pestle. The powder 200 mg was added to 15 ml of a mixture of acetone / tributyl phosphate (80:20 v/v) and the solution was kept at -20º C for 12 hours. The resulting mixture was centrifuged at 4º C for 20 minutes at 15,000 rpm and the supernatant removed and stored. The mixture was added to lysis buffer composed of 9.5M urea, 2 % (w/v) CHAPS, 0.8% IPG buffer (w/v), 1% (w/v), sodium vanadate (12.2mg), sodium azide (6.5 mg), PMSF (17.4 mg) in a 1:10 (w/v) ratio. The mixture was stirred overnight at 4ºC and a 10 g aliquot was mixed with 8 g of deionized water. 20 ml of a 50:50 (v/v) of chloroform / methanol was added and the mixture homogenized for 2 to 4 minutes. An additional mixture of chloroform / methanol was added with further homogenization. The solution was filtered combined with the acetone supernatant into a separatory funnel. After allowing the formation of the aqueous and organic layer, the two layers were separated, and the organic layer dried with nitrogen to a constant weight. The solid was dissolved in 3ml of a 50:50 (v/v) mixture of isopropanol: acetonitrile which was used for the analyte for RP-HPLC/ APCI/MS

5.3.4 Instrumentation

A Shimadzu high performance liquid chromatograph LC-10Avp (Kyoto, Japan) equipped with a Shimadzu SiL-10ADvp auto injection system was used for the analysis of cholesterol and

its esters. The analytes were separated on a ProtonSil 120-3 C-18 SH reversed phase high performance liquid chromatograph column, 100 x 4.6 mm i.d. purchased from MAC-MOD Analytical, Inc. (Chadds Ford, PA USA). Injection volumes for the analysis were either 10 or 20 µl; however, the optimum component analysis was achieved for the 20 µl volume. The analysis was conducted in gradient mode with a mobile phase consisting of isopropanol: acetonitrile: formic acid (71:29:0.10, v/v/v) at a constant flow rate of 0.30 ml/min. The mobile phase concentration prepared for HPLC pump A was 90% isopropanol/9.9% acetonitrile/0.10% formic while the concentration of pump B was 90% acetonitrile/10% isopropanol/0.10% formic acid. Each separation was programmed at 100% pump A initially and decreased to 0% for a period of one hour. The mobile phase was pumped through a UV-Visible detector equipped with a continuous flow cell with the analytes detected at 201 nm.

The mass spectrometer for the study was a Shimadzu LCMS 2010 system coupled to an atmosphere pressure chemical ionization (APCI) probe. The ionization occurs outside the mass spectrometer that outside high vacuum needed to conduct the mass analysis. The samples molecules ion probe directly from the liquid chromatograph and becomes ionized to produce an ion beam of pseudo molecular ions for the APCI probe by charging the ions with high voltage from a corona needle. Ions enter the mass spectrometer where a quadrupole analyzer separates the gas phase pseudo molecular ion by mass. The ion mode was conducted in positive mode where the initial step involves the creation of proton hydrates $H_30+[H_20]n$, by a cascade of other processes that produce primary ions such as N_2+, O_2+, H_2O+ and NO+. These particular ions are formed by electron impact from the corona needle. The APCI probe was operated in the positive mode at a nitrogen flow rate of 2.5 L/min. The curved desolvation line was adjusted to a temperature of 250ºC and a block temperature of 400ºC was maintained. Voltage parameters for the mass analyzer detector and the probe needle were 1.7kV and 4.5kV, respectively.

5.4 Results and Discussion

Cholesterol and cholesterol esters are key components in the formation of atherosclerosis. The structural elucidation of the sterols in this study is illustrated in Figure 5.1. Selection of these are based on previous studies by Smith et al[11,12] that predict the severity of the disease based on the relative ratios of these components. The analytes are the simplest of the lipids that are more complex when covalently bound to proteins such as lipoproteins. Naturally occurring fatty acids are usually unsaturated containing an even number of carbons and exist in the cis form. Unsaturated fatty acids bound to cholesterol in this study include the oleate, linoleate, and linolenate, while the saturated fatty acids consist of the palmitate and stearate esters.

Standard mixture of cholesterol, cholesteryl linolenate, cholesteryl linoleate, cholesteryl oleate, cholesteryl palmitate, and cholesteryl stearate was prepared in isopropanol: acetonitrile (50:50, v/v) with concentrations of 0.4 mg/ml; however the oleate concentration was 0.375 respectively. The UV-Visible chromatogram of the standards detected at 210 nm is shown in Figure 5.2. The mass spectral analysis using APCI interfaced with a mass analyzer operated in positive ion mode is illustrated in Figure 5.2. Initial analysis operated in the scan mode resulted in low resolution and low sensitivity of the extracted analytes. Since quantitation of standards was performed using RP-HPLC, the method of scanning the peaks of interest was altered to take advantage of fragmentation of certain ions to optimize sensitivity and reduce interfering analytes. The total ion chromatograph and the mass spectra were determined by operating the mass analyzer in the selective ion monitoring (SIM) mode. The extracted peak isolated produced mass of 369 is isolated for each peak for the cleaved cholesterol mass. This ion was fragmented in each of the esters when the mass analyzer is operated in positive ion mode with the loss of the mass of the ester. SIM of the ester masses alone were not as reproducible as the fragment ion attributed to cholesterol.

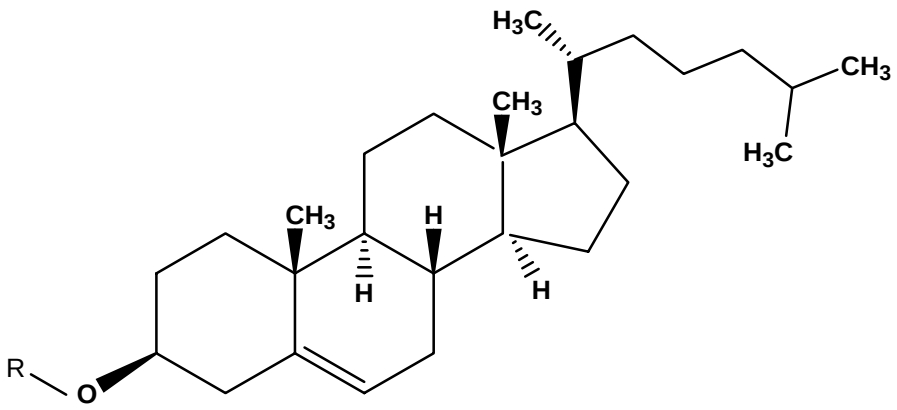

R = H **Cholesterol**

R = $C_{17}H_{31}$ **Cholesteryl linoleate**

R = $C_{15}H_{31}$ **Cholesteryl palmitate**

R = $C_{17}H_{35}$ **Cholesteryl stearate**

R = 17 33 **Cholesteryl oleate**

Figure 5.1 Structure of cholesterol and cholesterol esters analyzed in atherosclerotic plaques from thoracic aortas

Mass detection of cholesterol at mass 369 was performed to enhance the signal-to noise ratios by acquiring the mass chromatograms during the analysis by means of selected ion monitoring (SIM). In this mode of operation, the data is acquired in a particular mass window that is approximately 0.6 daltons in width. Although structural information is lost the signal-to-noise ratio is improved and useful when quantitative analysis is performed. One disadvantage may be encountered when baseline noise is interpreted as actual masses at the retention time specified for the cholesterol fragment.

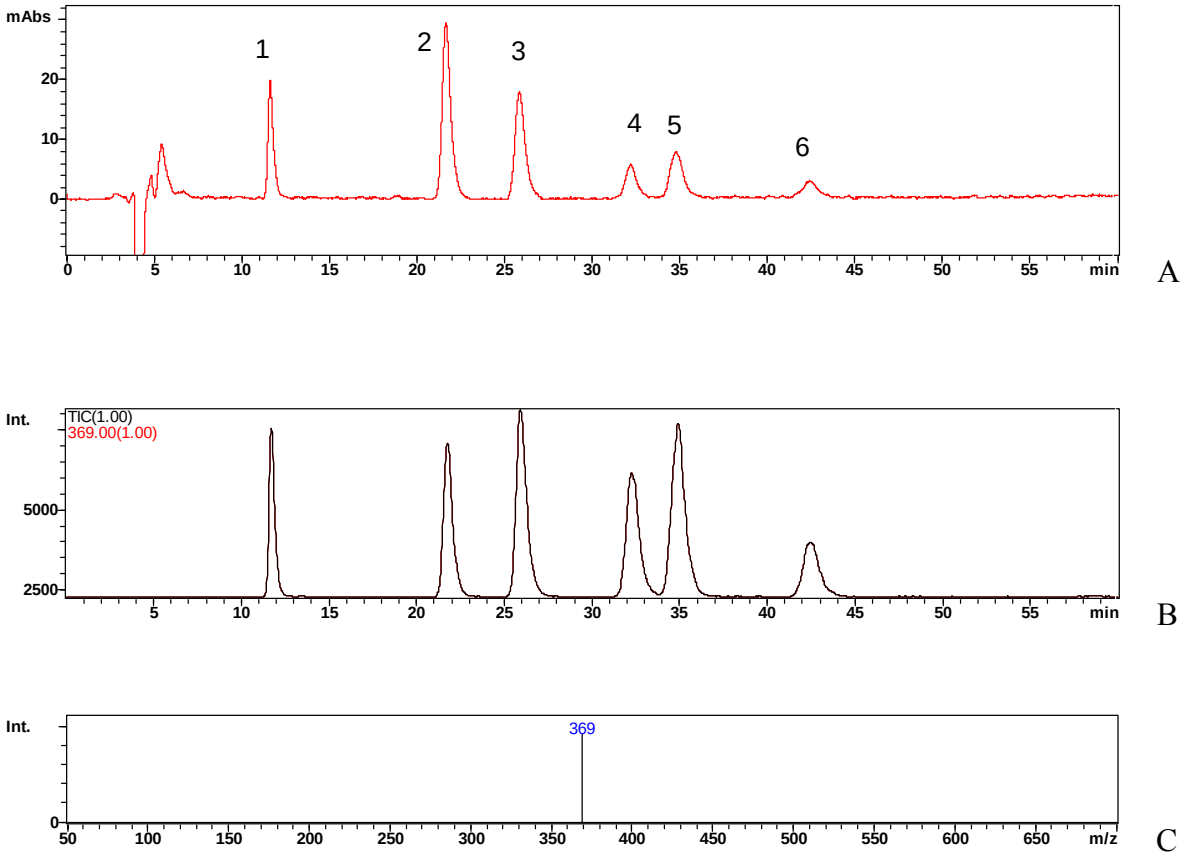

Figure 5.2 A) Standard UV- visible chromatogram of cholesterol and cholesteryl esters detected at 210 nm. Peaks in the chromatogram are identified as: 1. cholesterol 2. cholesteryl linolenate; 3. cholesteryl linoleate; 4. cholesteryl oleate; 5. cholesteryl palmitate; 6. cholesteryl stearate . B) Total ion chromatograph of each standard. C) Selective ion monitoring mode at m/z 369 corresponding to cholesterol.

External standard calibration curves constructed for each analyte are shown in Figure 5.3. A plot of peak area versus concentration gave excellent correlation coefficients (R^2 = 0.9965 to 1.0000).

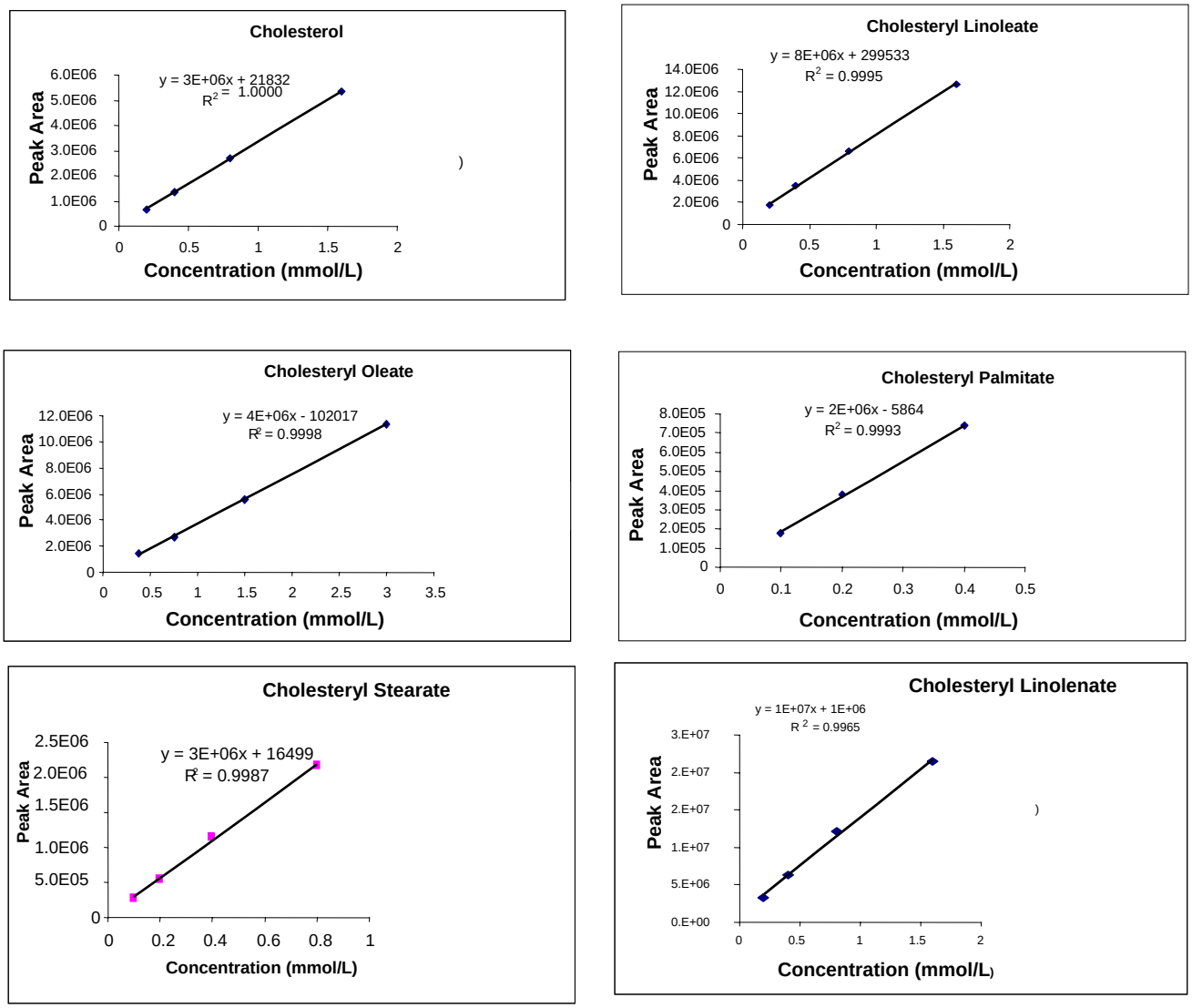

Figure 5.3 Calibration curves for quantitation of cholesterol and cholesteryl esters in extracts of thoracic aortas.

Thirty five thoracic aortas were examined from autopsied cadavers varying in age from 20 to 80 years old. Crystalline cholesterol (sample no. 1 Figure 5.4) was collected from a calcified

plaque without dissection in our laboratory. The composition of the plaque contained a higher concentration of cholesterol; however, the linoleate ester gave a higher concentration (0.156 %) than expected.

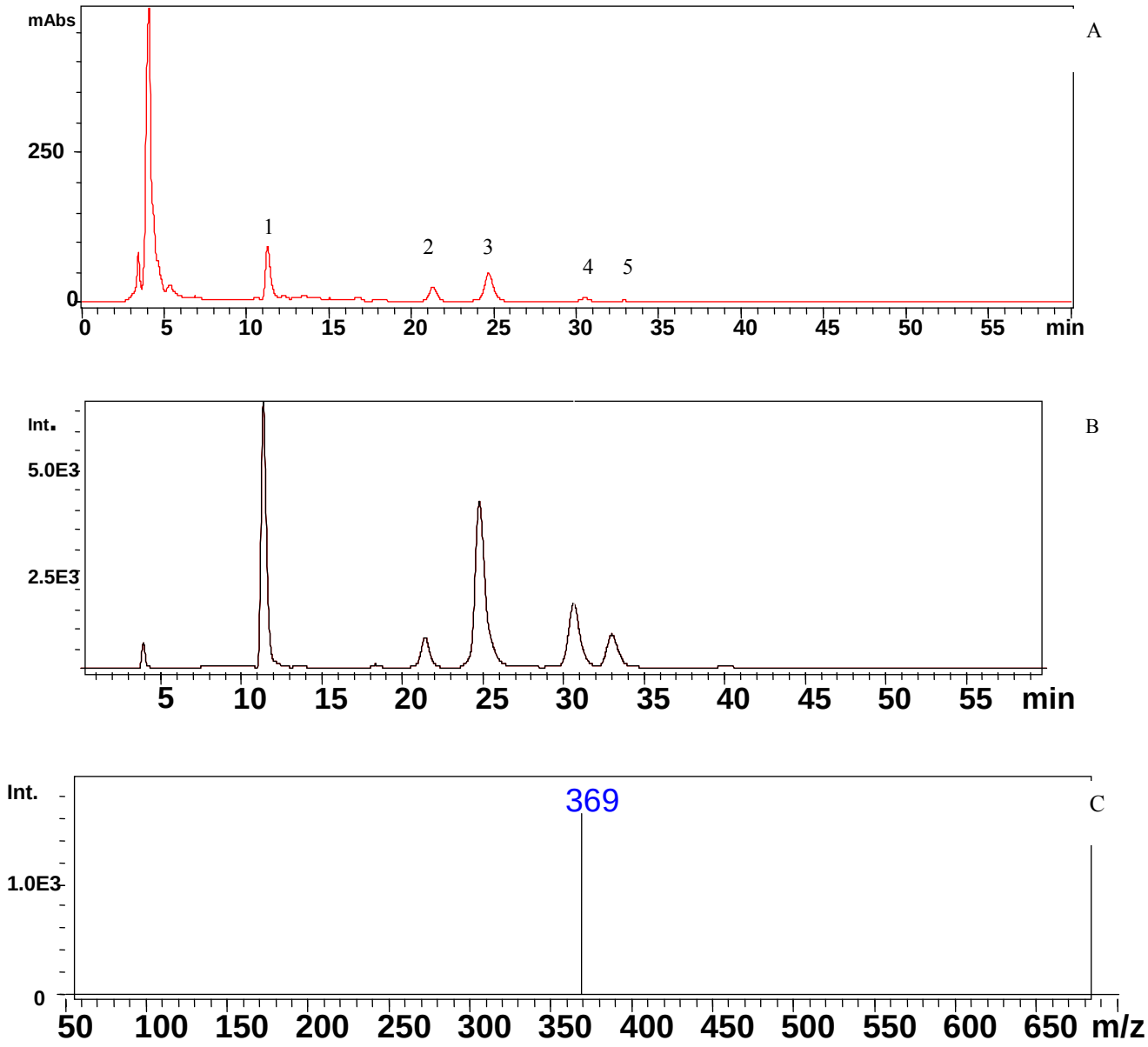

Figure 5.4 A) UV-visible chromatograph of crystalline cholesterol. 1. cholesterol, 2. cholesteryl linolenate, 3. cholesteryl linoleate, 4. cholesteryl oleate, 5. cholesteryl palmitate, 6. cholesteryl stearate. B) Total ion chromatograph of crystalline cholesterol; C) Selective ion monitoring of cholesterol m/z 369.

The analysis of atherosclerotic plaque gruel from sample two gave higher concentrations (w/w) of esters as well as cholesterol (Figure 5.5). These two samples illustrate the complexities and variability in the composition of plaques. UV visible chromatogram and MS analysis of all samples in this study is listed in Appendix A.

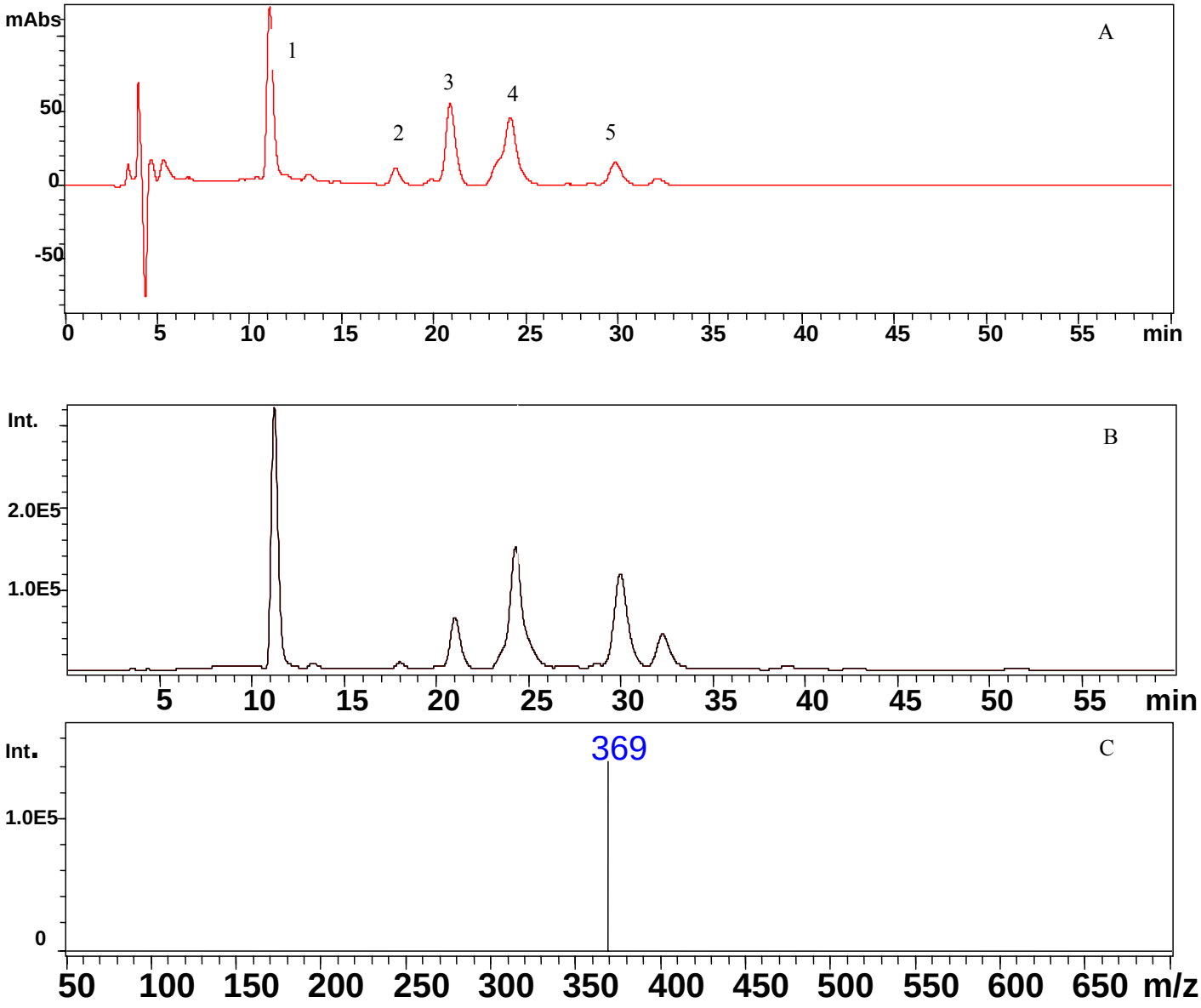

Figure 5.5 A) UV-visible chromatogram of atherosclerotic plaque gruel; 1. cholesterol, 2. cholesteryl linolenate, 3. cholesteryl linoleate, 4. cholesteryl oleate, 5. cholesteryl palmitate, 6. cholesteryl stearate. B) Total ion chromatogram; C) Selective ion monitoring mode at m/z 369.

Table 5.1 Summary of the Quantitative Analysis of Cholesterol and Cholesteryl Esters using HPLC APCI MS Analysis

NO.	Description of Sample Extract	Cholesterol (wt %)	Linolenate (wt %)	Linoleate (wt %)	Oleate (wt %)	Palmitate (wt %)	Stearate (wt %)	Total weight percent
1	Cholesterol Crystalline	0.298	0.00125	0.156	0.0810	0.0618		0.598
2	Atherosclerotic Plaque Gruel	2.66	1.81	1.83	1.48	1.45		9.23
3	33 year old male Aorta	5.19	4.32	10.0	5.60	4.19	0.599	29.9
4	80 year old male Aorta	1.31	0.860	2.12	1.15	0.870		6.31
5	74 year old female Aorta Extract	0.206	0.113	0.223	0.102	0.0467		0.690
6	62 year old male Aorta	1.49	0.427	0.815	0.367	0.131		3.23
7	70 year old male Aorta Media Extract	1.67	0.556	1.35	0.663	0.186		4.43
8	70 year old male Aorta Intima+Media	13.8	4.15	8.60	3.27	1.39		31.2
9	79 year old male sample	0.121	0.142	0.260	0.151	0.135		0.667
10	81 year old male Aorta	31.7	10.4	20.1	14.3	21.4		97.9
11	80 year old male Aorta	3.47	0.556	1.37	0.91	0.53		6.83
12	62 year old male Aorta	18.1	12.3	22.1	13.3	16.5	5.16	87.4
13	68 year old male Aorta	5.74	2.29	4.84	3.43	3.93		20.2
14	81 year old male Aorta plaque intima/media	17.7	7.95	17.1	11.9	10.0	4.43	69.1
15	56 year old male Aorta	6.10	2.45	3.64	3.12	3.55		18.9
16	64 year old male Aorta	7.08	3.71	7.41	5.70	5.72		29.6
17	81 year old male Aorta plaque	20.5	6.32	14.6	9.65	11.2		62.3
18	54 year old male Aorta	12.9	3.49	16.6	11.0	6.74		50.7
19	56 year old male Aorta	4.87	16.3	5.32	4.74	3.74		34.9
20	56 year old male Aorta	24.5	9.58	23.8	10.5	5.15		73.5

Table 5.1 (continued) Summary of the Quantitative Analysis of Cholesterol and Cholesteryl Esters using HPLC APCI MS Analysis

21	**57 year old male Aorta**	**63.7**	**1.24**	**14.6**	**8.67**	**7.28**		**95.6**
22	**61 year old male Aorta**	**29.7**	**8.97**	**16.3**	**9.58**	**5.40**		**69.9**
23	**69 year old male Aorta**	**4.76**	**3.56**	**6.18**	**3.76**	**1.28**		**19.5**
24	**36 year old male Aorta**	**14.1**	**2.05**	**3.94**	**2.51**	**1.30**		**23.9**
25	**53 year old female Aorta**	**26.1**	**10.9**	**19.6**	**11.2**	**8.66**		**76.3**
26	**59 year old male Aorta**	**8.89**	**4.10**	**8.04**	**5.19**	**4.45**		**30.7**
27	**60 year old male Aorta**	**22.3**	**13.9**	**25.6**	**14.7**	**14.1**		**90.6**
28	**66 year old female Aorta**	**20.1**	**7.80**	**14.1**	**10.5**	**12.9**		**65.5**
29	**86 year old male Aorta**	**15.1**	**6.28**	**13.9**	**10.1**	**9.11**		**54.6**
30	**47 year old female Aorta**	**15.5**	**8.87**	**19.7**	**15.9**	**18.8**		**78.9**
31	**52 year old male Aorta**	**11.2**	**6.79**	**14.6**	**10.7**	**7.40**		**50.6**
32	**53 year old female Aorta**	**28.1**	**22.2**	**40.3**	**24.9**	**31.7**		**147**
33	**54 year old male Aorta**	**27.4**	**14.1**	**26.6**	**17.7**	**18.3**		**104**
34	**34 year old male Aorta**	**43.7**	**12.0**	**17.6**	**3.82**	**1.95**		**79.0**
35	**20 year old male Aorta**	**3.81**	**0.400**	**2.81**	**2.97**	**3.90**		**13.9**

The results of the levels of the cholesterol and cholesterol esters in various samples are shown in Table 5.1. The data in Table 5.1 was analyzed for correlations between the age of an individual and the concentration of cholesterol and its esters. The implications of cholesterol and its esters that accumulate in the arterial walls are important contributions to atherosclerosis [13]. A graphical depiction of the correlation of age to cholesterol and its esters is shown in Figures 5.6 to 5.8. Using one dimensional analysis, no apparent correlation can be observed between the cholesterol and age. Additionally, same scattered data is seen in linolenate, linoleate, or oleates which are unsaturated fatty acids. This same holds true when examining patterns in the palmitate ester of cholesterol, a saturated fatty acid.

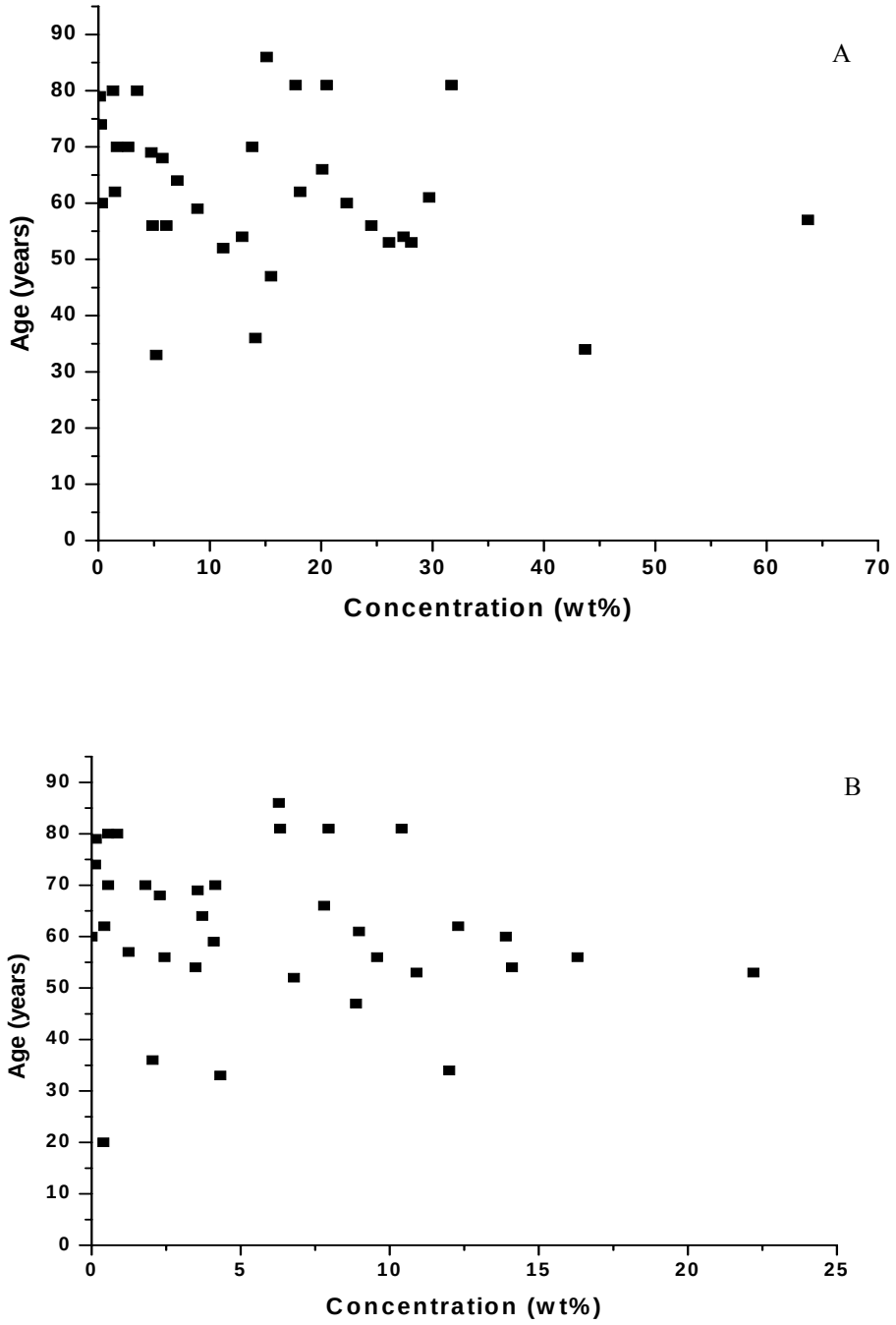

Figure 5.6 Plot of age versus the concentration of cholesterol and cholesteryl linolenate. Linolenate is a naturally occurring fatty acid formed as lipid droplets in arterial walls. No graphical correlation of ester concentration with age can be observed.

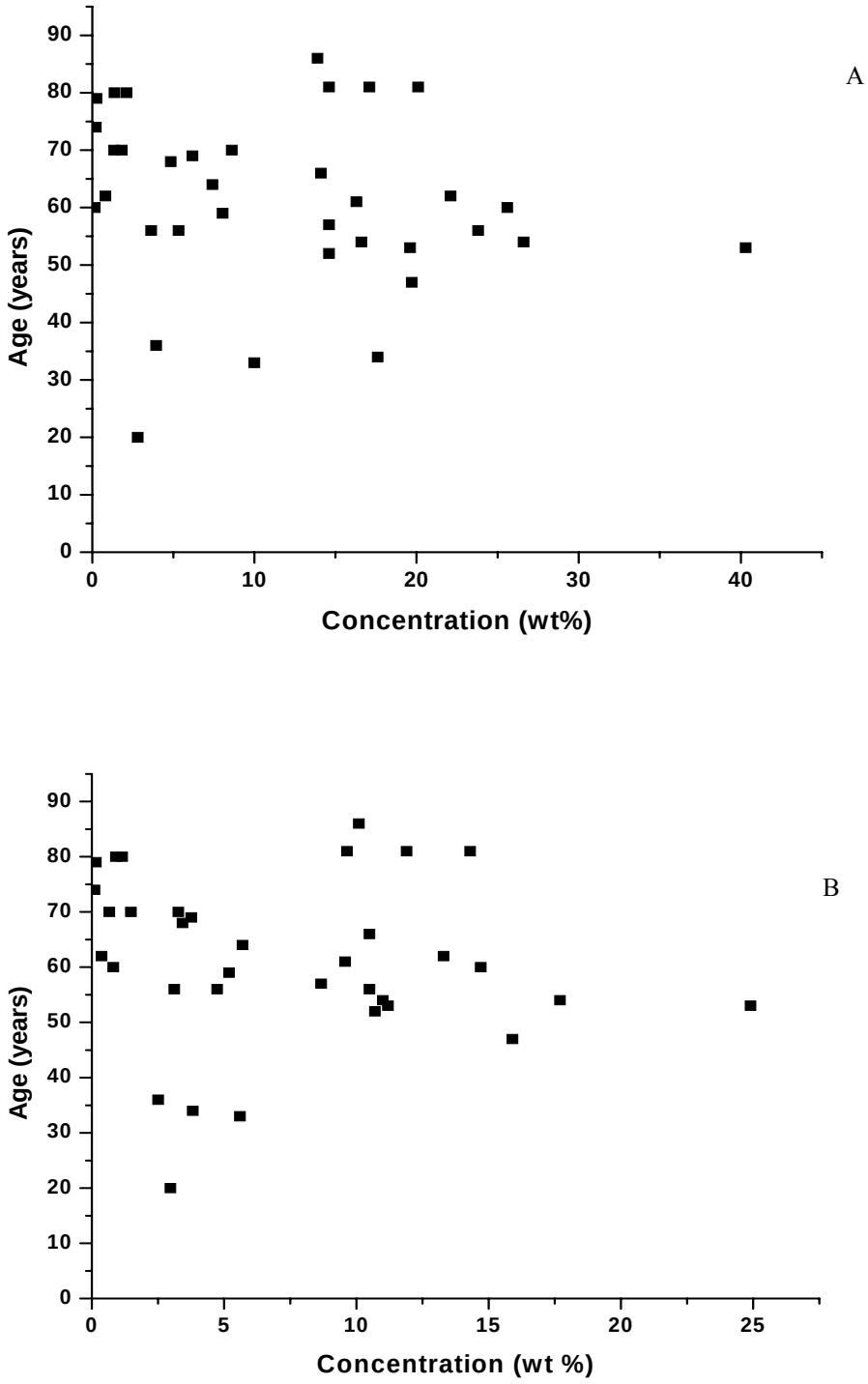

Figure 5.7 Plot of age versus the concentration of cholesteryl linoleate and cholesteryl oleate. Each ester is a naturally occurring fatty acid formed as lipid droplets in arterial walls. No graphical correlation of ester concentration with age can be observed.

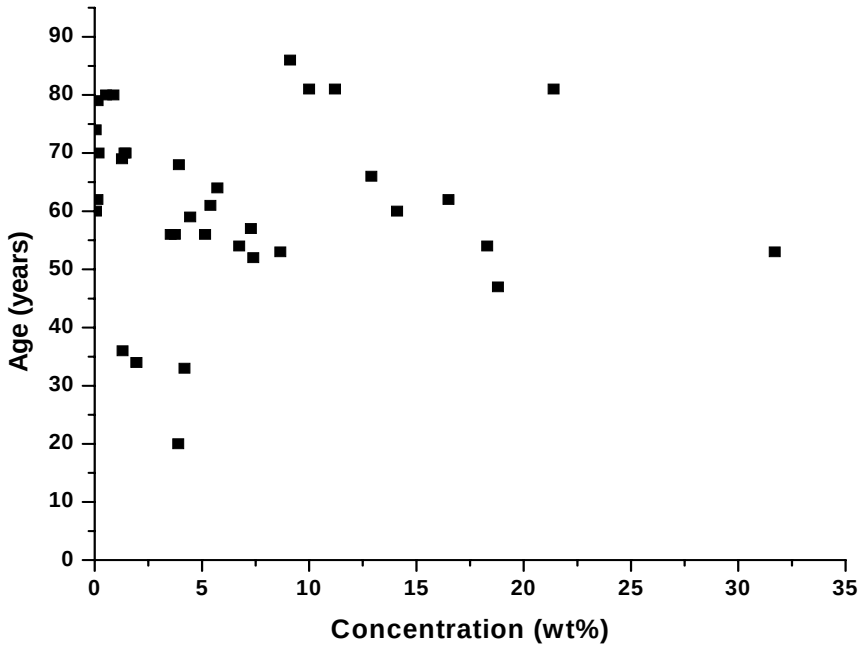

Figure 5.8 The plot of age versus cholesteryl palmitate in aorta extracts.

5.4.1 Principal Component Analysis

The graphical representation of age with the concentration of cholesterol and its esters shown in Figures 5.6 -5.8 provide no useful correlation or pattern for all the samples analyzed. Therefore, traditional approach of data analysis for pattern recognition between variables could not be used in this study. The modern method of pattern recognition in data for the determination of important similarities and differences involves the use of principle component analysis (PCA). PCA technique uses mathematical relationships of functions derived from matrices and eigenvalues to represent the data in a new orthogonal system known as principal component. Usually, the first initial principal components are enough to represent the data set since they contain the most useful information in the data. In addition, the plot of the data set in the new orthogonal system may reveal the hidden information not apparent in the raw data set. In most cases, the grouping of data is always observed in the principal component plot data with similar characteristic groups. The summary of the PCA using the results of concentration of cholesterol

and its esters in Table 5.1 is shown in Figure 5.9. The numbers in Figure 5.9 correspond to experiment numbers from Table 5.1.

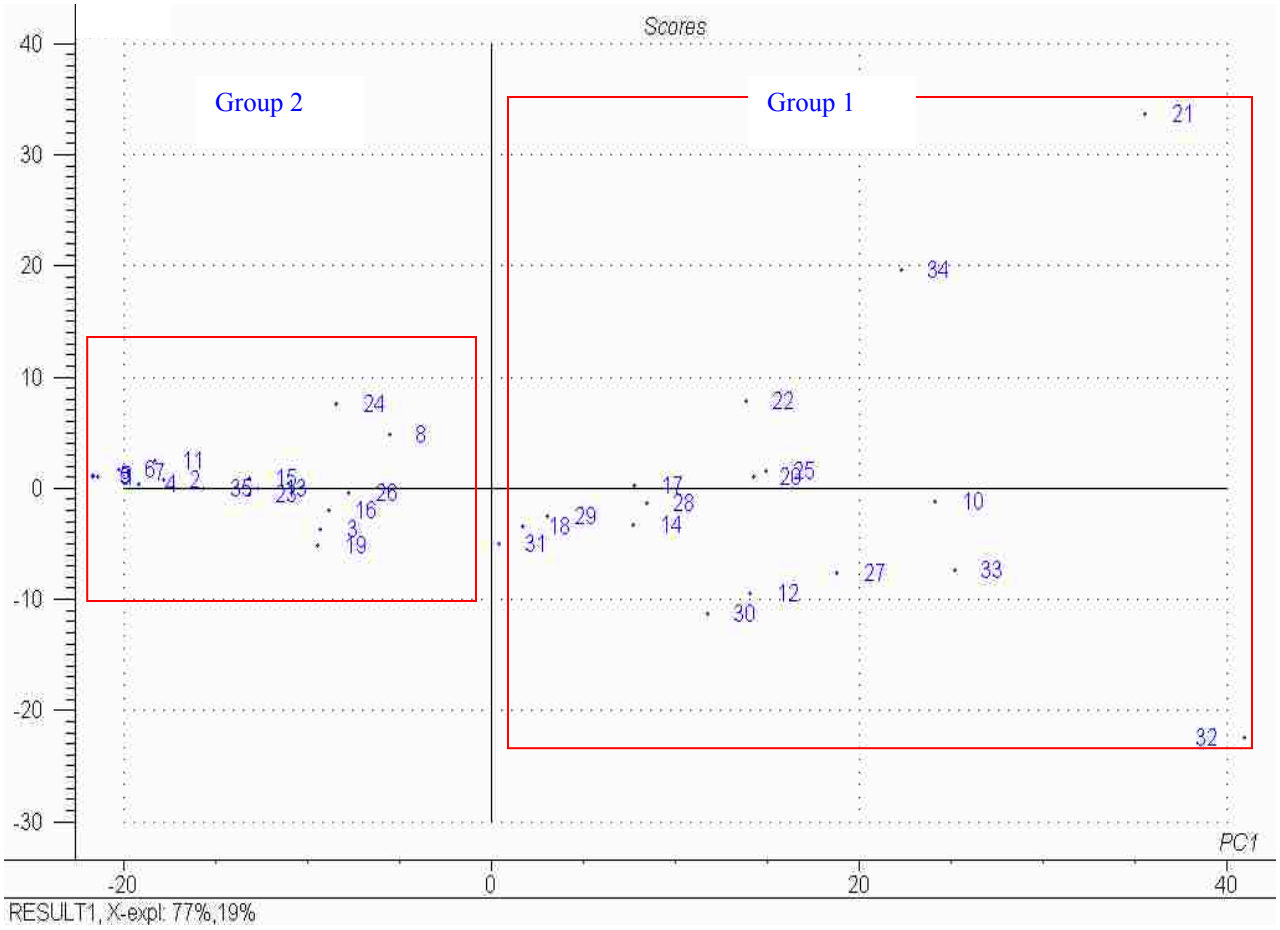

Figure 5.9 Principal component analysis of age of the individual and the concentration (wt %) of cholesterol and its esters. The data points separate the sample analysis into two groups or clusters.

From Figure 5.9, it is apparent that the data can be grouped be separated into two distinct groups. Lower concentrations of cholesterol and its esters were demonstrated in group 1; however higher concentration are illustrated in group 2. The data from group 1 and 2 were averaged and compared with overall averages (Figure 5.10). The average concentrations of cholesterol as well as concentrations of the esters in group 1 are comparatively higher than group 2. In addition, the results of the analysis indicated that lower concentrations of the analytes were

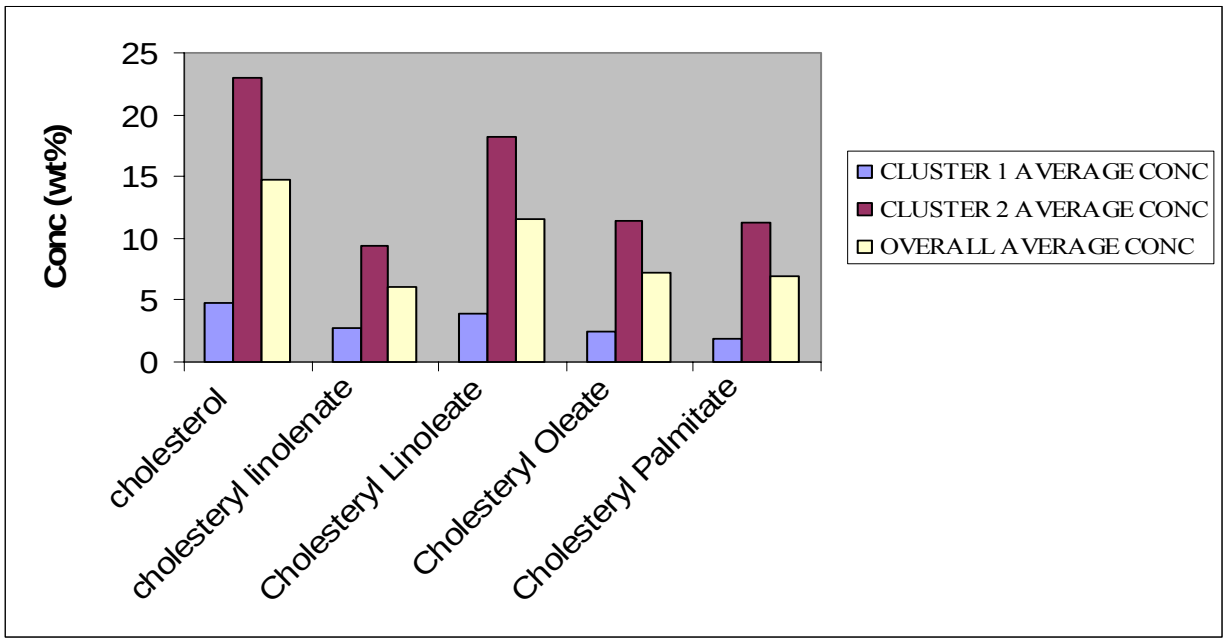

Figure 5.10 Comparison of PCA group 1 and group 2 age averages and the concentration of the cholesterol and its esters.

obtained in group 2 compared with the overall concentration of the analytes in the entire data set. In contrast, higher concentrations of analytes were obtained for group 1 data set compared to the overall concentration analytes. Furthermore, the average age of the individuals in group 2 is lower than group 1.

5.4.2 Disease Severity Index (DSI)

Studies by Kritchevsky et al. [14] have demonstrated the atherogenic effects of using saturated fatty acids such as palmate in comparison to unsaturated acids in the diet. Their findings also emphasized the beneficial effects of polyunsaturated fatty acids and further showed that the monounsaturated fats lowered total serum cholesterol without reducing the high density lipoprotein (HDL) cholesterol levels [14].

Cholesterol and its esters have been isolated in the arterial walls at various stages of disease development. These compounds have also been implicated as agents in atherosclerosis.

[14]. In our study, a further analysis of the data was performed to determine if any correlations exist between the cholesteyl esters and the extent of the disease by calculating the disease severity index (DSI). The disease severity index (DSI) is defined as the ratio of concentration of the ester to the free cholesterol in the plaques. The results of the calculated DSI of group 1 and group 2 are shown in Table 5.2. A low DSI is indicative of a decrease in atherosclerosis. In contrast, a high ratio shows an increase in disease state [14]. Comparisons of the average DSI for group 1 and group 2 shows that a lower index is observed in group 1 resulting in a decrease in atherogenicity. When this pattern is compared with age, the lower index is also observed in the lower age group indicating that DSI is related to the age. Older individuals tend to have higher DSI and have higher risk for atherosclerosis.

Table 5.2 Comparison of disease severity index of cholesterol esters in group 1 and group 2

Disease Severity Index	Cholesteryl Linolenate/Cholesterol	Cholesteryl Linoleate / Cholesterol	Cholesteryl Oleate/ Cholesterol
Group 1	0.57	0.91	0.62
Group 2	0.65	0.97	0.74

5.5 Conclusions

The Diseased Severity Index gave higher ratios in group 2, the older average age group. The higher index (average), which is the ratio of low free cholesterol to ester, indicates greater severity of atherosclerosis.

Our study has demonstrated the use of APCI-HPLC MS in the separation and analysis of cholesterol and various fatty acid esters extracted for thoracic aortas. Thirty-seven samples were separated using reverse phase high performance liquid chromatography from various age groups. Correlation coefficients of >0.999 were derived for cholesterol, cholesteryl linolenate, cholesteryl linoleate cholesteryl oleate, cholesteryl palmitate and cholesteryl sterate, respectively. The selective ion monitoring mode from the APCI-MS using m/z of 369, the mass of the free

cholesterol molecule, provided a qualitatively identification of the each component at the corresponding retention times from the UV detector.

The data was further analyzed for pattern recognition by principal component analysis. Two different groups resulted from the average of the cholesterol and its ester composition and age. The data in goup 1, the younger age group, produced lower average cholesterol /ester ratios. Conversely, group 2 with the higher average age similarly has higher average concentrations of cholesterol and its esters.

5.6 References

(1) Matthew, C.K.; van Holde, K.E.; Ahern, K.G.; Lipid Metabolism I: Fatty Acids, Triacylglycerols and Lipoproteins. Biochemistry, 3rd ed., Robin Hedyen: San Francisco, CA, **2000**, pp 626-666.

(2) Lusis, A. *Nature* **2000**, 407, 233-241.

(3) Brown, M.; Goldstein, J.L. *Science* **1986**, 34-47.

(4) Ross, R. *New Engl. J. Med.* **1999**, 340, 2, 115-126.

(5) Davies, M.J. *Am. J. Cardiol.* **2001**, 88 2f-9f.

(6) Steinberg, D.; Parthasarathy, S.; Carew, T.; Khoo, J., Witzum, J. *N. Engl. J Med*. **1989**, 320, 915-924.

(7) Niessen, W.M.A.; In Liquid Chromatography-Mass Spectrometry 2nd Ed. Niessen, W.M.A., Ed. Marcel Dekker Inc., New York, NY p 99.

(8) Byrdwell, W.C. *Lipids* **2001**, 35, 4, 327- 346.

(9) Willoughby, R.; Sheehan, E.; Mitrovich, S.; A Global View of LC/MS, 2nd ed.; Global View Publishing: Pittsburg, PA, 2002; pp. 470-471.

(10) Toru, S. *The Journal of Clinical Investigation* **2005**, 115(8), 2214-2222

(11) Katz, S.S.; Small, D.M.; Smith, F.R.; Dell, R.B.; Goodman, D.S. *J. Lipid Res*. **1982**, 23, 733-737.

(12) Kruth, H. *Current Mole. Med*. **2001**, 1, 633-653.

(13) Pentikainen, M.O.; Oorni, K.; Ala-Karpela, M.; Kovsnen, P.T. *J. Intern. Med.* **2000** 247, 359-370.

(14) Kritchevsky, D.; Tepper, S.A.; Wright, S.; Czarnecki, S.K.; Wilson, T.A.; Nicolosi, R.J. *J. Am. Coll. Nutrit*. **2003**, 22, 1, 52-55.

CHAPTER 6

CONCLUSIONS AND FUTURE STUDIES

The objectives of this dissertation were to utilize techniques in proteomics to isolate and characterize protein involve in atherosclerotic plaques. The study was used to note differences between plaques in (a) heart bypass (b) native heart arteries and (c) aortas. The aorta comparison was between diseased and nondiseased states as well. Several techniques analytical tools were used to study proteins in this disease. These techniques include two dimensional gel electrophoresis, SDS-PAGE, fluorescent dyes for protein expression in normal and diseased tissues, mass spectrometry, and high performance liquid chromatography.

In the introduction, the description of the pathogenesis of atherosclerosis and the present predominant theories responsible for the disease was discussed. Various analytical techniques and instrumentation were discussed in addition to the theories involved for each instrument.

Chapter 2 used a design study based on the Box Behnken design to optimize the number of spots (proteins) by two dimensional gel electrophoresis analysis. The components in the lysis buffer, usually to solubilize membrane proteins, were necessary to maximize separation during isoelectric focusing on to an immobiline pH gradient strip. The first separation of the proteins was conducted based on pI followed by separation by molecular weight using SDS-PAGE.

In the Chapter 3, proteins were separated using carrier ampholytes and tube gels in two two dimensional gel electrophoresis. The proteins were digested with trypsin and the resulting peptides were sequenced using a linear quadrupole ion trap Fourier transform ion cyclotron resonance mass spectrometer. Nine proteins were identified that were involved in atherosclerosis.

A differential gel electrophoresis technique was used in Chapter 4 to determine protein expression in normal and diseased tissues from thoracic aortas with fluorescent dyes. This method was also used to detect variations in native and bypass arteries. Proteins that were differentially expressed were analyzed using MALDI –MS and peptide mass fingerprinting from database searches.

Chapter 5 used RPHPLC-APCIMS to separate and quantify cholesterol and cholesteryl esters formed in the intima of various plaques in thoracic aortas. To elucidate patterns in the data principal component analysis was used. Our data analysis technique determined that two distinct groups were present for the correlation of concentration of the cholesterol and its ester to the age of the individual.

6.1 Future Studies

Additional studies to determine protein expressions in normal and diseases vessels involved in atherosclerosis should focus on the use of surfactants that enhance the solubility of hydrophobic membrane protein separated by gel electrophoresis. In addition, molecular micelles are used as denaturates in capillary electrophoresis; however, their use may enhance protein solubility and resolution in both two dimension gel electrophoresis and SDS-PAGE. Due to their nonionic nature, the molecular micelles are attractive for use in isoelectric focusing on a immobiline pH gradient strips. Ionic surfactants, such as SDS cannot be use because of cathode charge overload, preventing protein separation.

The use of differential gel electrophoresis was useful in demonstrating protein expression in various plaques samples. To assess biological variations in the protein expressions in various plaques, a larger sample pool is needed. From this data statistical analysis can be derived and a

database created for protein expression in normal and diseased samples. Further immunochemical studies may be used to assess the role that glycoproteins play in the disease.

The disease severity index was calculated in the analysis of cholesterol and its esters in chapter 5. Metals in the plaque may play a role in atherosclerosis. ICPMS analysis of various plaques could be correlated with the DSI, further providing evidence of the complexity of the disease.

APPENDIX

RPHPLC CHROMATOGRAMS AND MASS SPECTRA OF CHOLESTEROL AND CHOLESTERYL ESTERS IN HEART PLAQUES

Sample 5: 74 year old female Aorta Extract

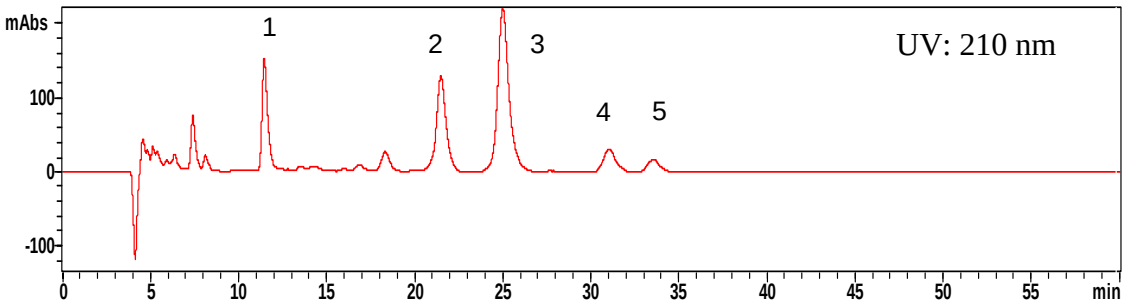

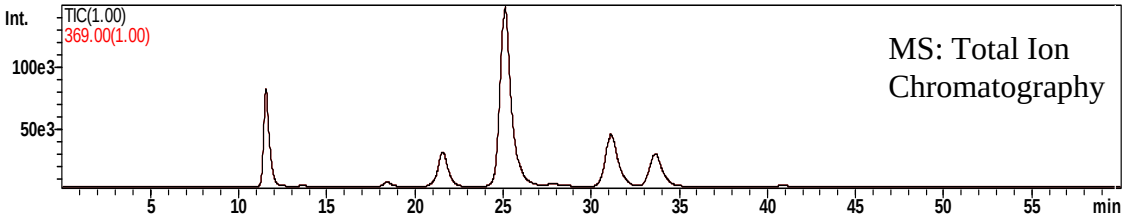

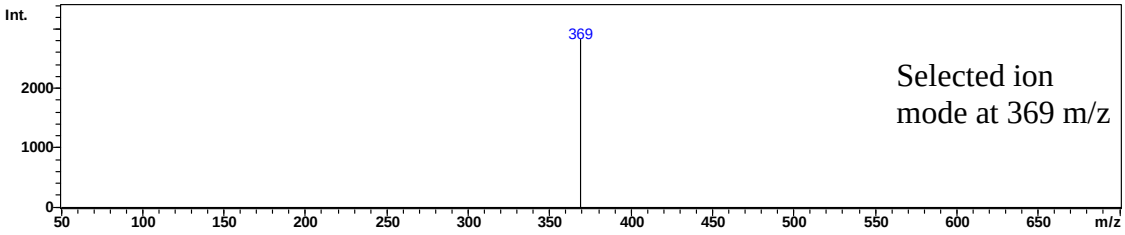

Injection: 10 µL
Peaks: 1. Cholesterol: 2. Linolenate: 3. Linoleate: 4. Oleate: 5. Palmitate

Sample 6: 62 year old male Aorta Extract

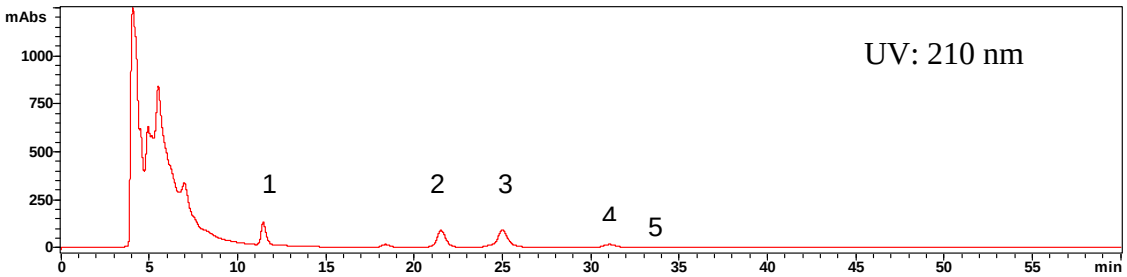

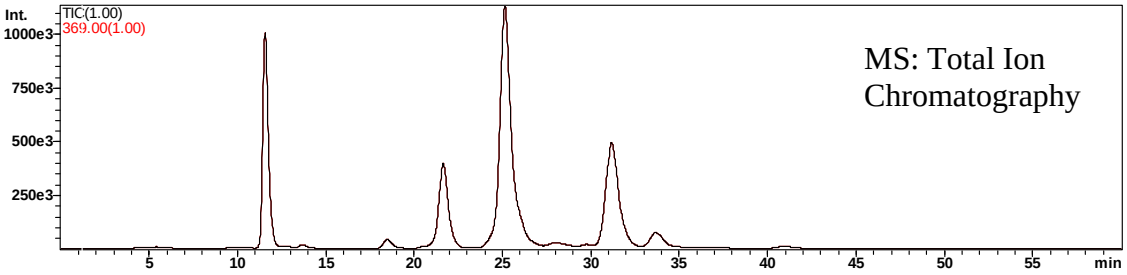

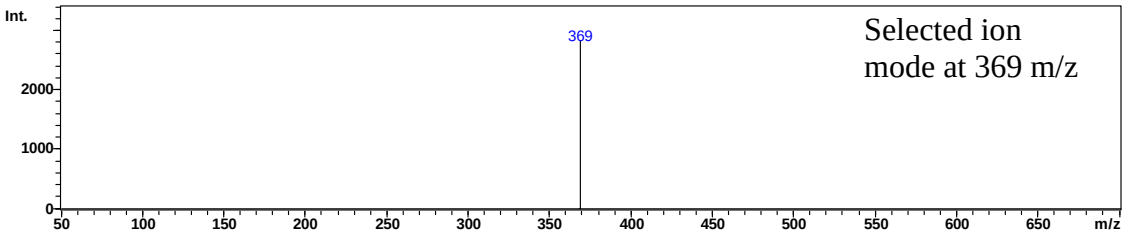

Injection: 10 µL
Peaks: 1. Cholesterol: 2. Linolenate: 3. Linoleate: 4. Oleate: 5. Palmitate

Sample 7: 70 year old male Aorta Media Extract

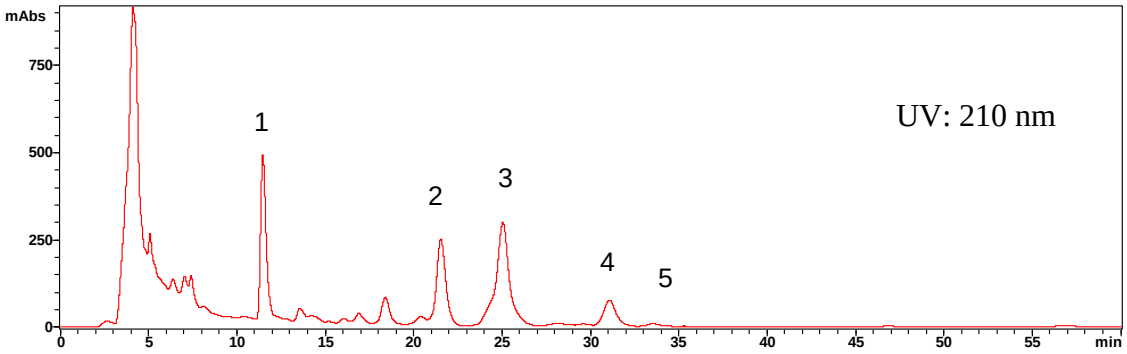

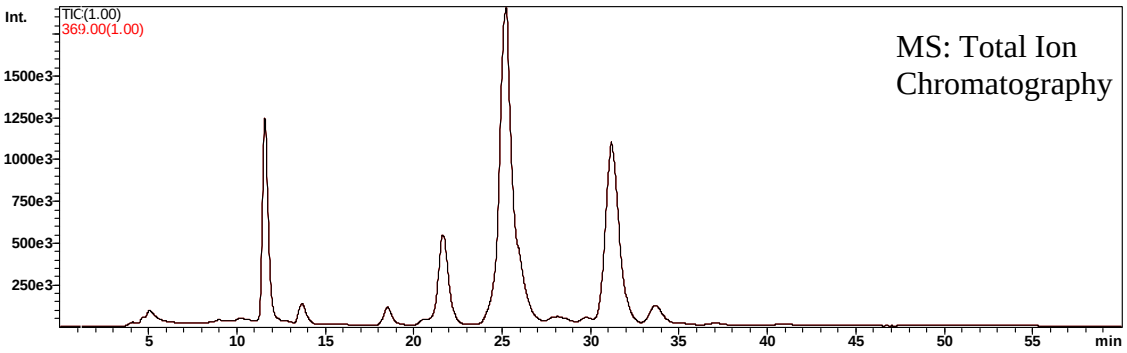

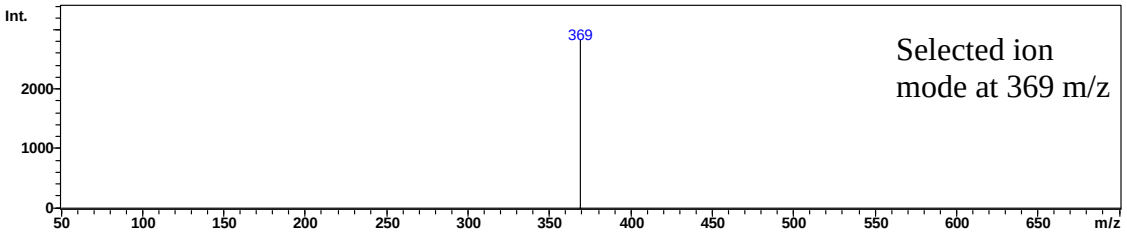

Injection: 10 µL
Peaks: 1. Cholesterol: 2. Linolenate: 3. Linoleate: 4. Oleate: 5. Palmitate

Sample 8: 70 year old male Aorta Intima+Media Extract

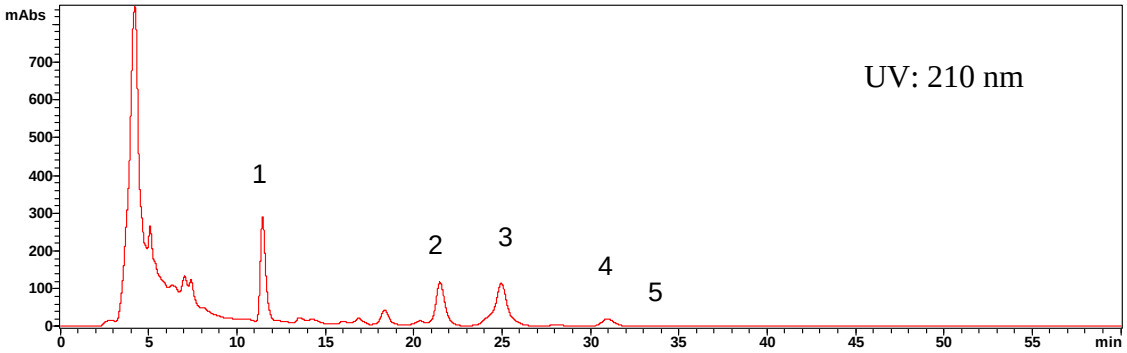

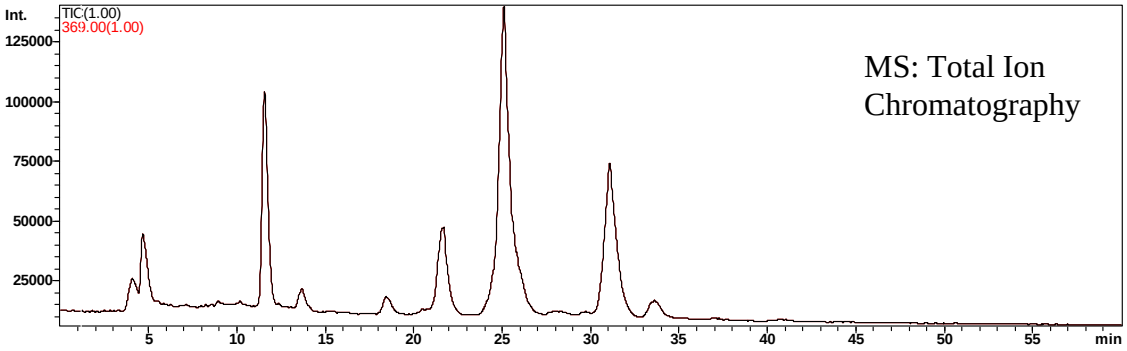

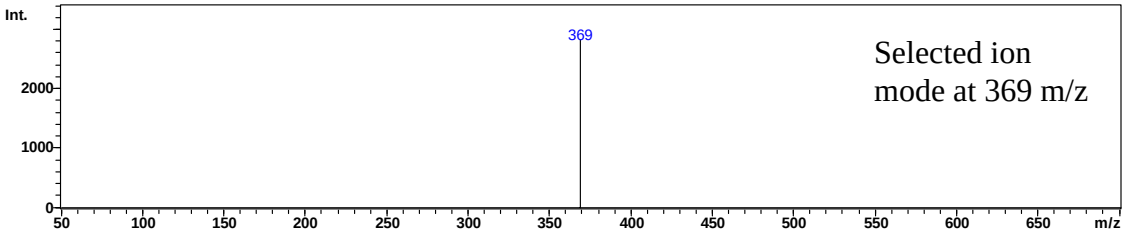

Injection: 10 µL
Peaks: 1. Cholesterol: 2. Linolenate: 3. Linoleate: 4. Oleate: 5. Palmitate

Sample 9: 79 year old male sample A Extract

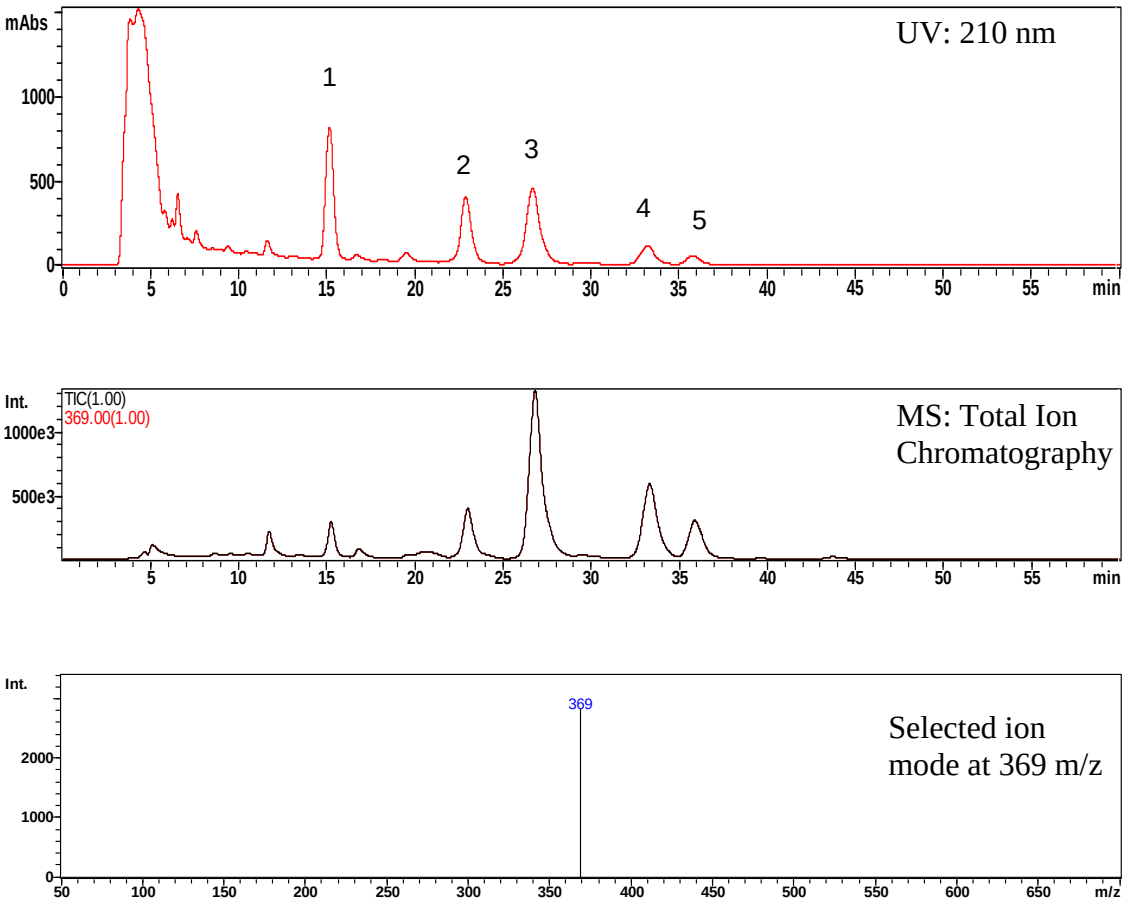

Injection: 10 µL
Peaks: 1. Cholesterol: 2. Linolenate: 3. Linoleate: 4. Oleate: 5. Palmitate

Sample 10: 81 year old male Aorta Plaque Gruel Extract

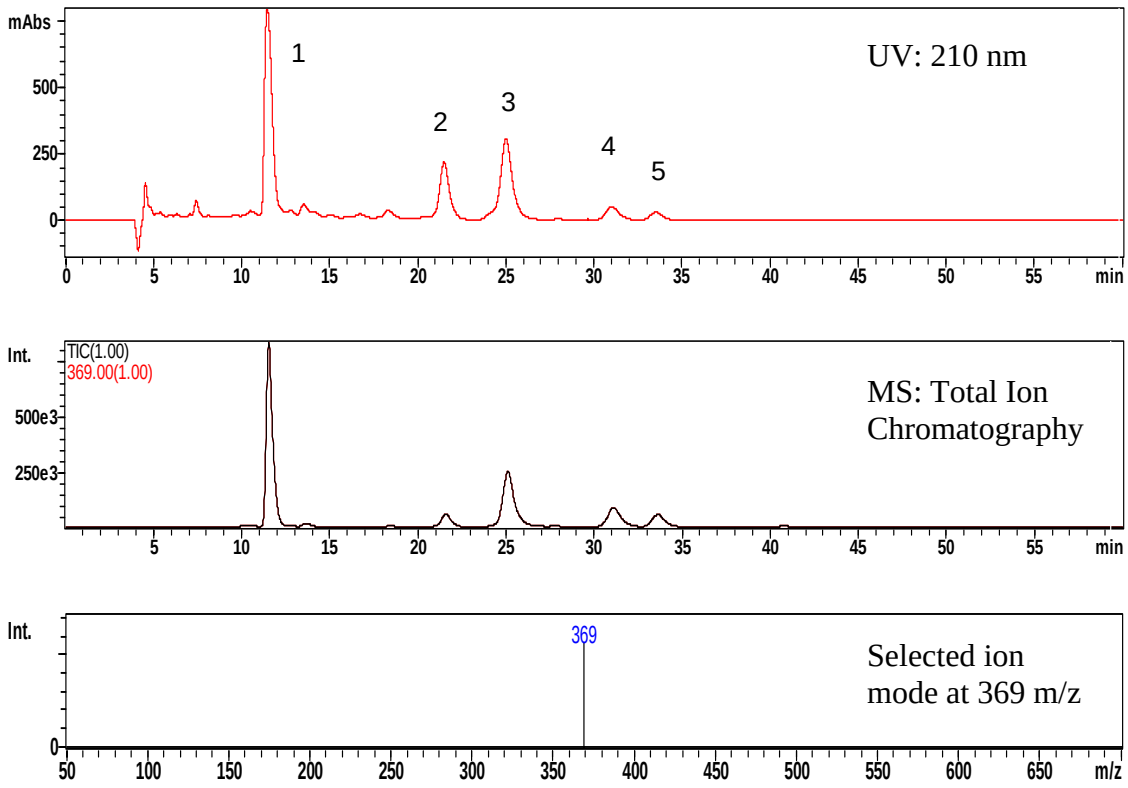

Injection: 10 µL
Peaks: 1. Cholesterol: 2. Linolenate: 3. Linoleate: 4. Oleate: 5. Palmitate

Sample 11 80 year old male Aorta Extract-highly calcified

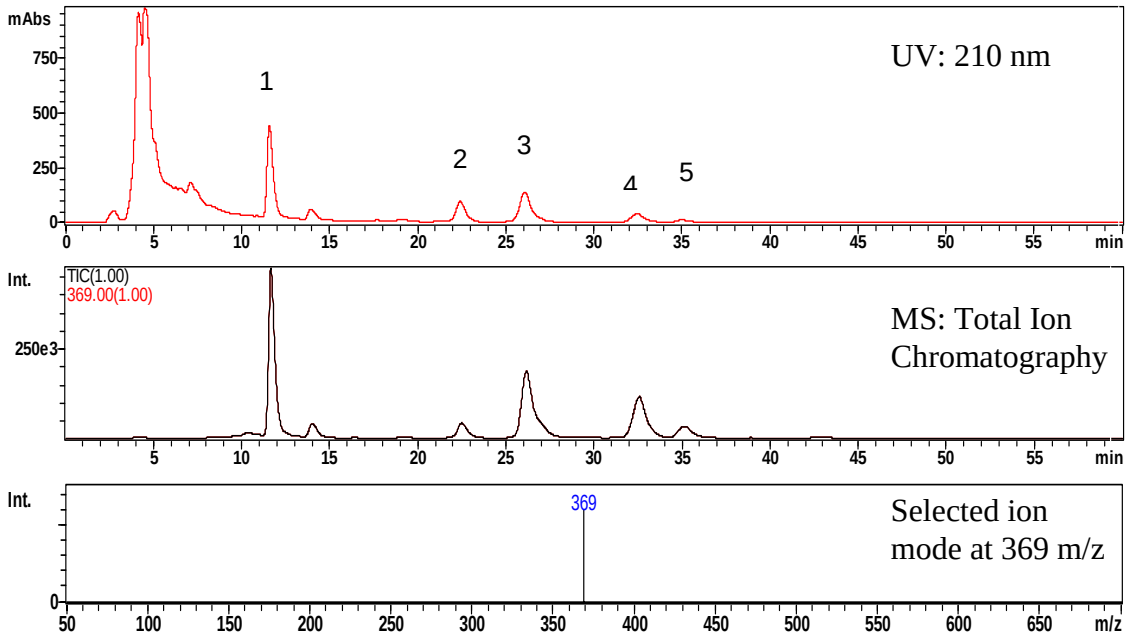

Injection: 10 µL
Peaks: 1. Cholesterol: 2. Linolenate: 3. Linoleate: 4. Oleate: 5. Palmitate

Sample 12 62 year old male Aorta Extract 175-92

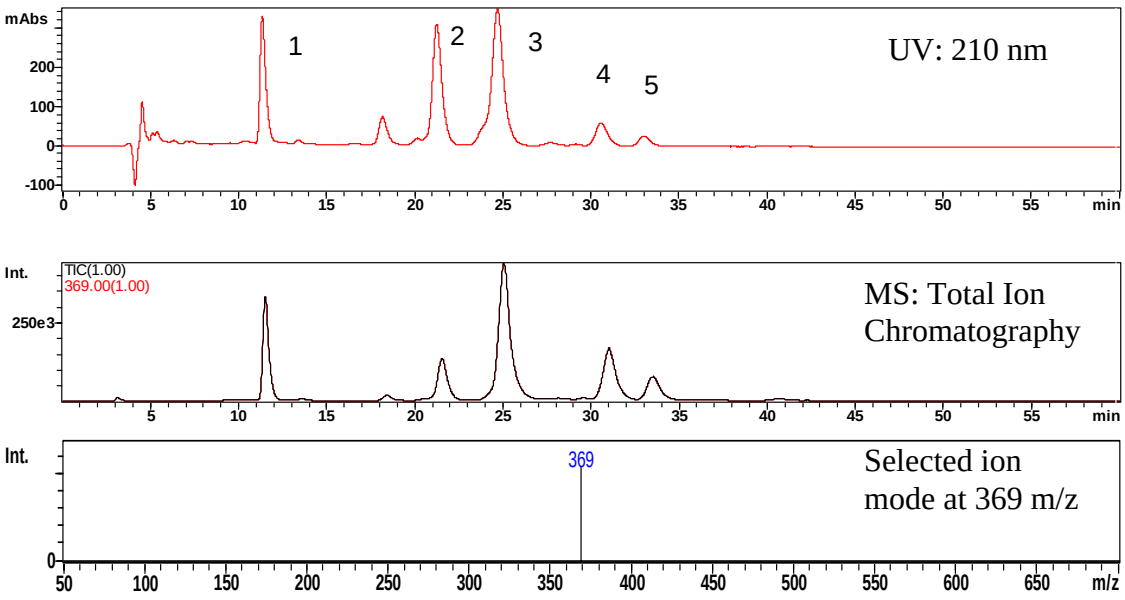

Injection: 10 µL
Peaks: 1. Cholesterol: 2. Linolenate: 3. Linoleate: 4. Oleate: 5. Palmitate

Sample 13 68 year old male Aorta Extract 175-87

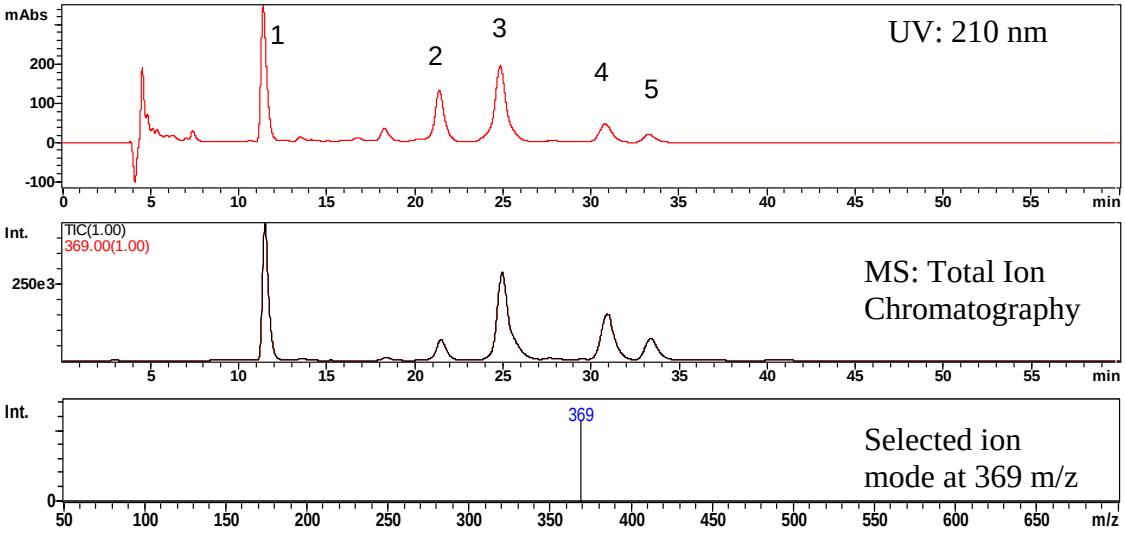

Injection: 10 µL
Peaks: 1. Cholesterol: 2. Linolenate: 3. Linoleate: 4. Oleate: 5. Palmitate

Sample 14 81 year old male aorta plaque intima-media extract 175-7

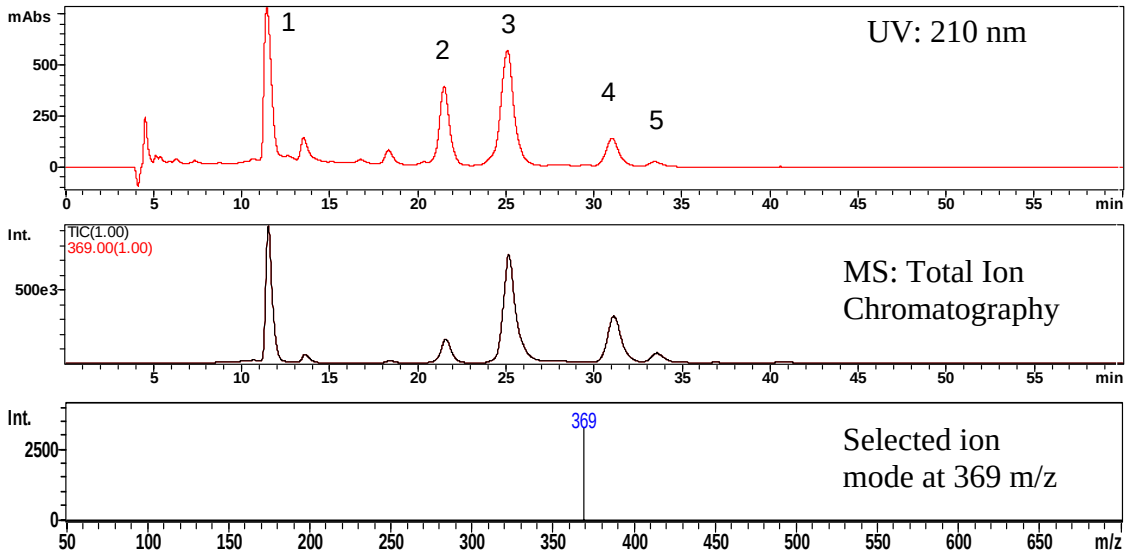

Injection: 10 µL
Peaks: 1. Cholesterol: 2. Linolenate: 3. Linoleate: 4. Oleate: 5. Palmitate

Sample 15 56 year old male aorta extract 175-35

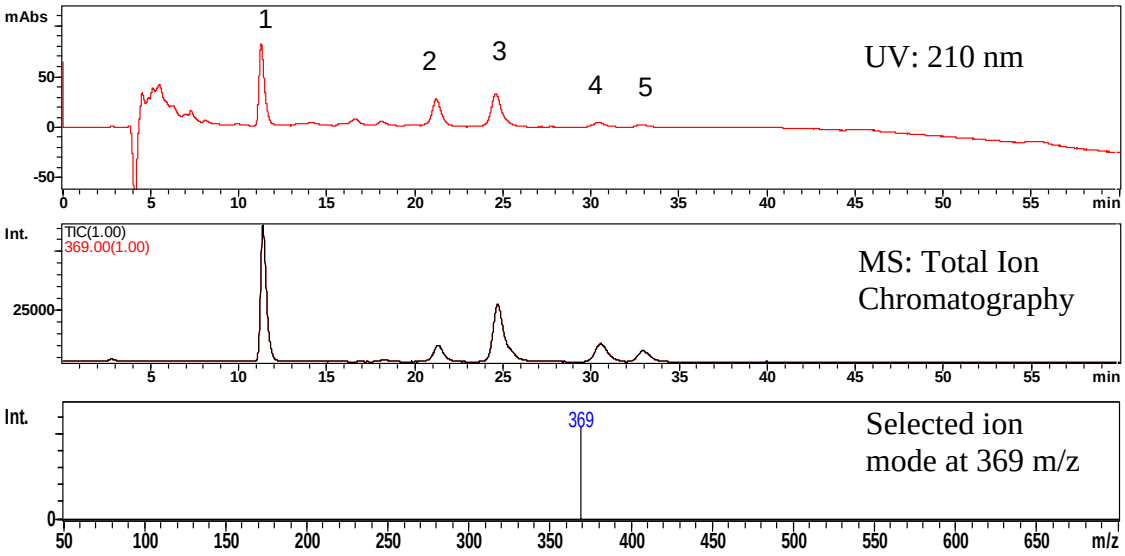

Injection: 10 µL
Peaks: 1. Cholesterol: 2. Linolenate: 3. Linoleate: 4. Oleate: 5. Palmitate

Sample 16 64 year old male aorta extract 175-20

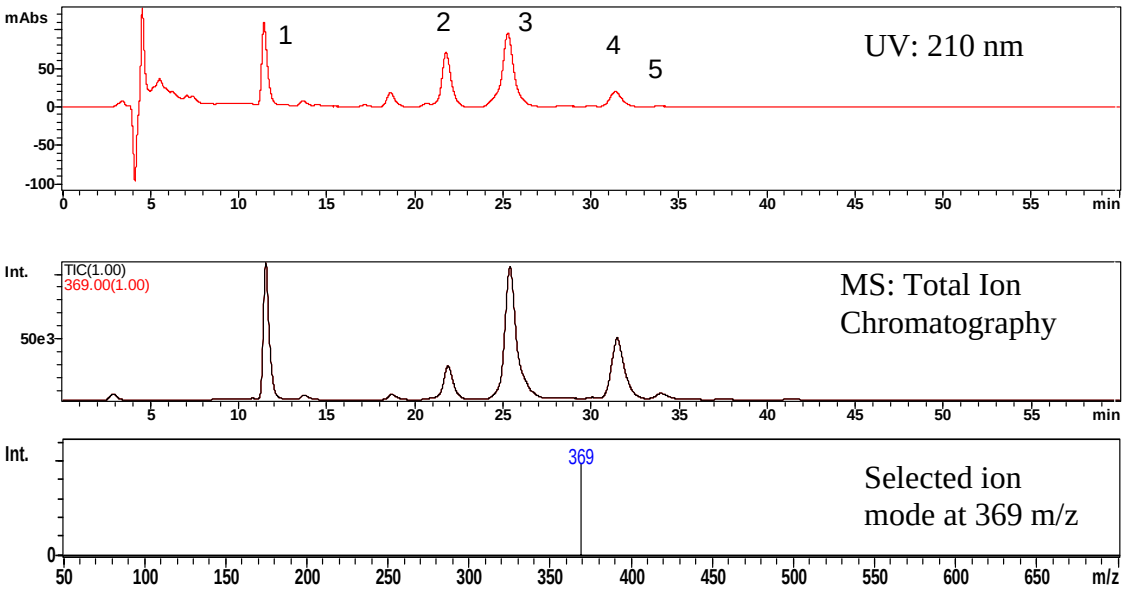

Injection: 10 µL
Peaks: 1. Cholesterol: 2. Linolenate: 3. Linoleate: 4. Oleate: 5. Palmitate

Sample 17 81 year old male aorta extract 175-7

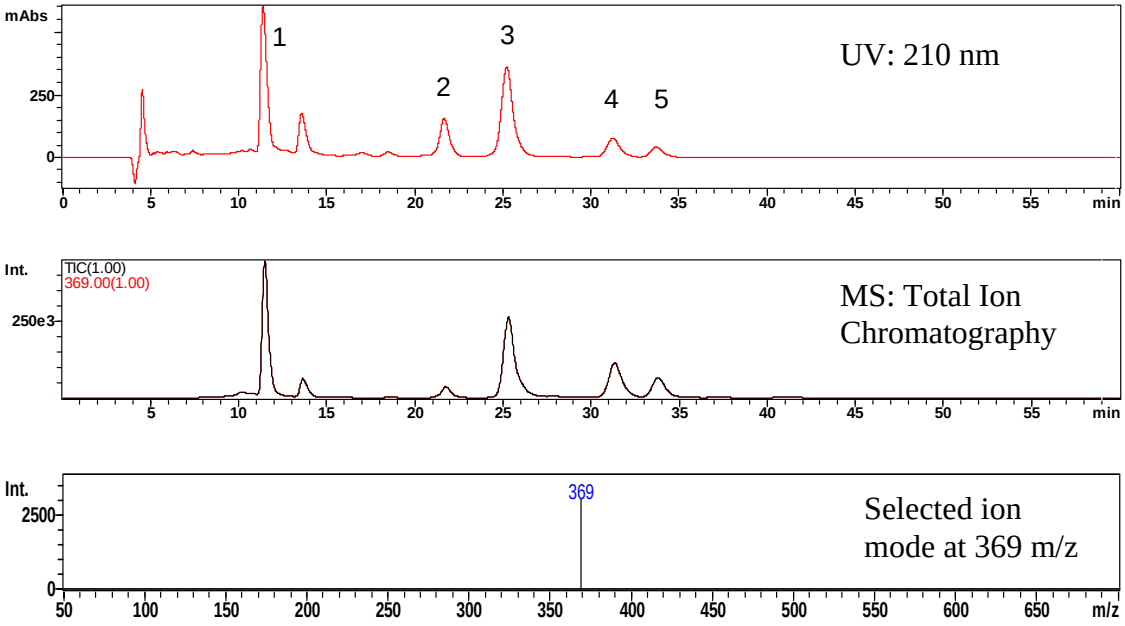

Injection: 10 µL
Peaks: 1. Cholesterol: 2. Linolenate: 3. Linoleate: 4. Oleate: 5. Palmitate

Sample 18 54 year old male aorta extract 175-30

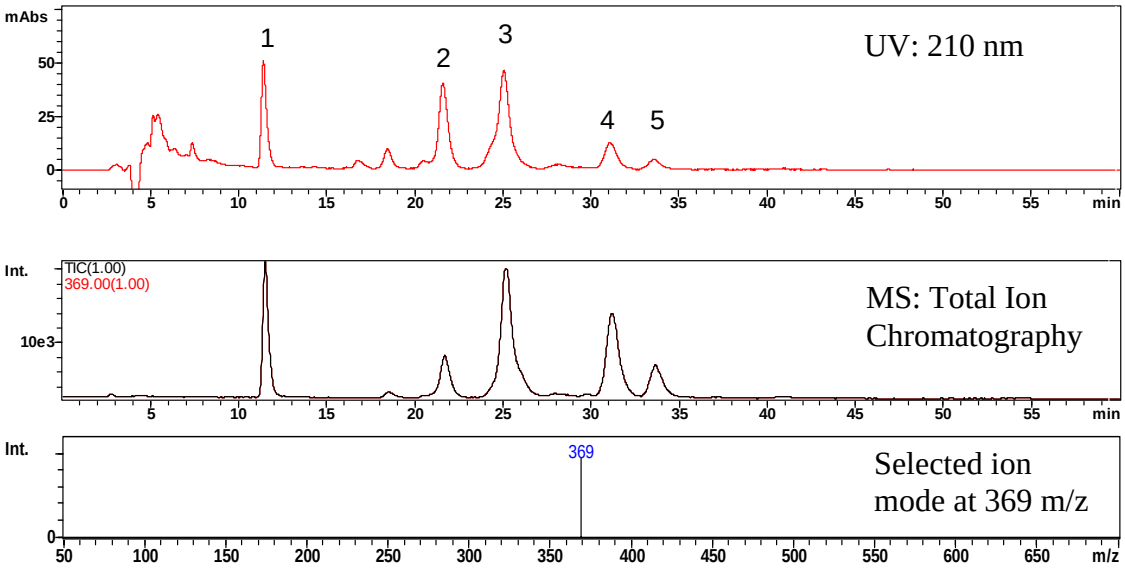

Injection: 10 µL
Peaks: 1. Cholesterol: 2. Linolenate: 3. Linoleate: 4. Oleate: 5. Palmitate

Sample 19 56 year old male aorta extract 175-29

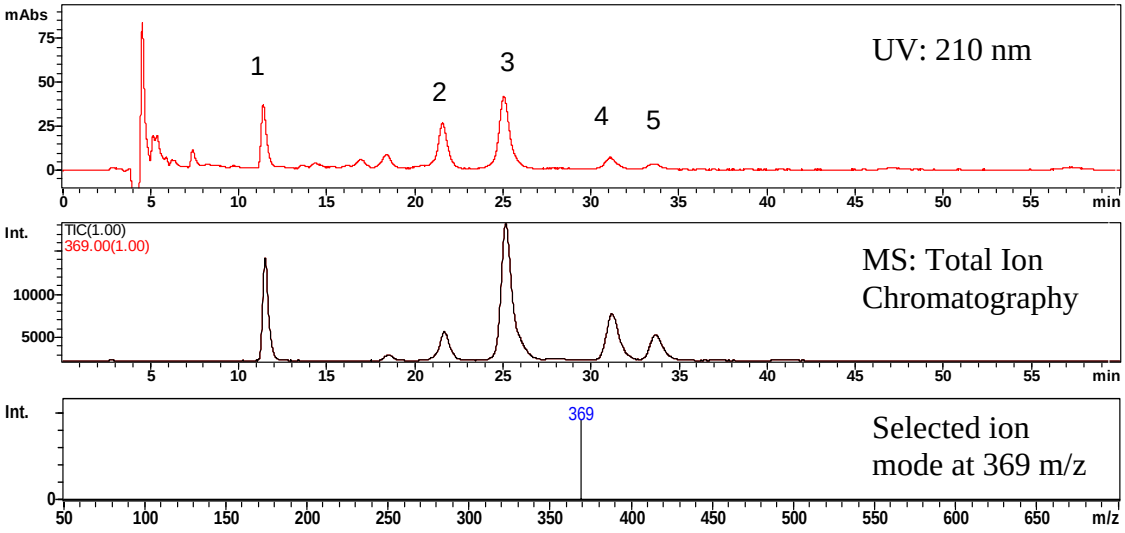

Injection: 10 µL
Peaks: 1. Cholesterol: 2. Linolenate: 3. Linoleate: 4. Oleate: 5. Palmitate

Sample 20 56 year old male aorta extract 175-5

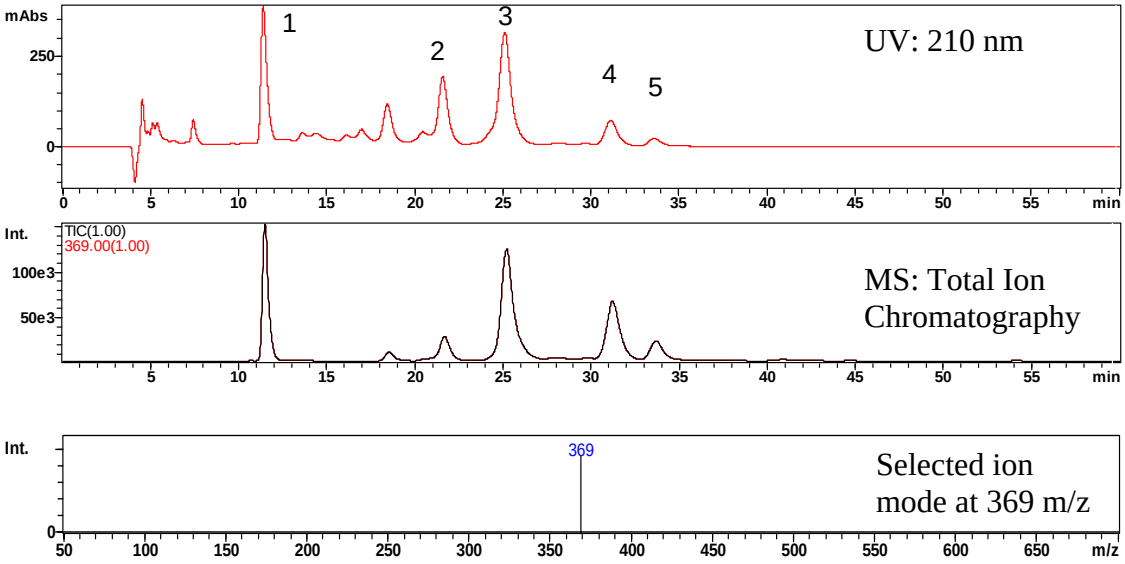

Injection: 10 µL
Peaks: 1. Cholesterol: 2. Linolenate: 3. Linoleate: 4. Oleate: 5. Palmitate

Sample 21 57 year old male aorta extract 175-34

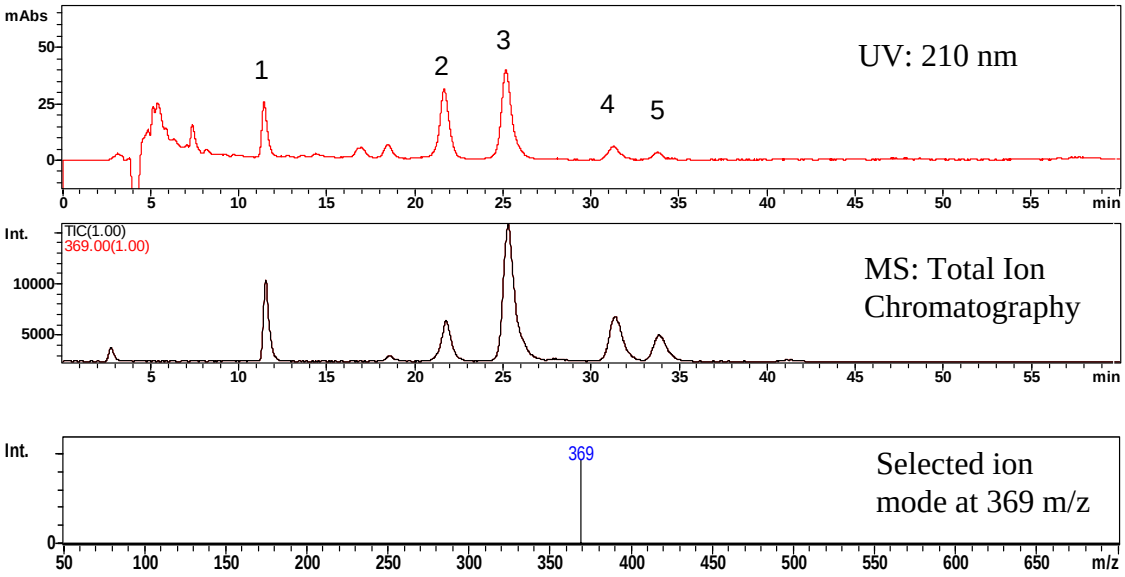

Injection: 10 µL
Peaks: 1. Cholesterol: 2. Linolenate: 3. Linoleate: 4. Oleate: 5. Palmitate

Sample 22 61 year old male aorta extract 175-19

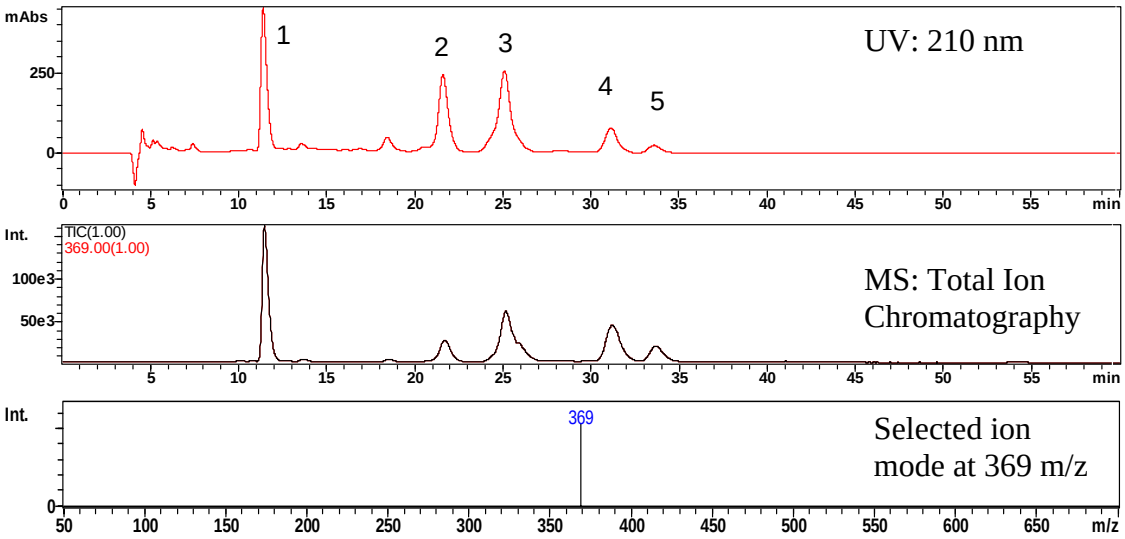

Injection: 10 µL
Peaks: 1. Cholesterol: 2. Linolenate: 3. Linoleate: 4. Oleate: 5. Palmitate

Sample 23 69 year old male aorta extract 175-28

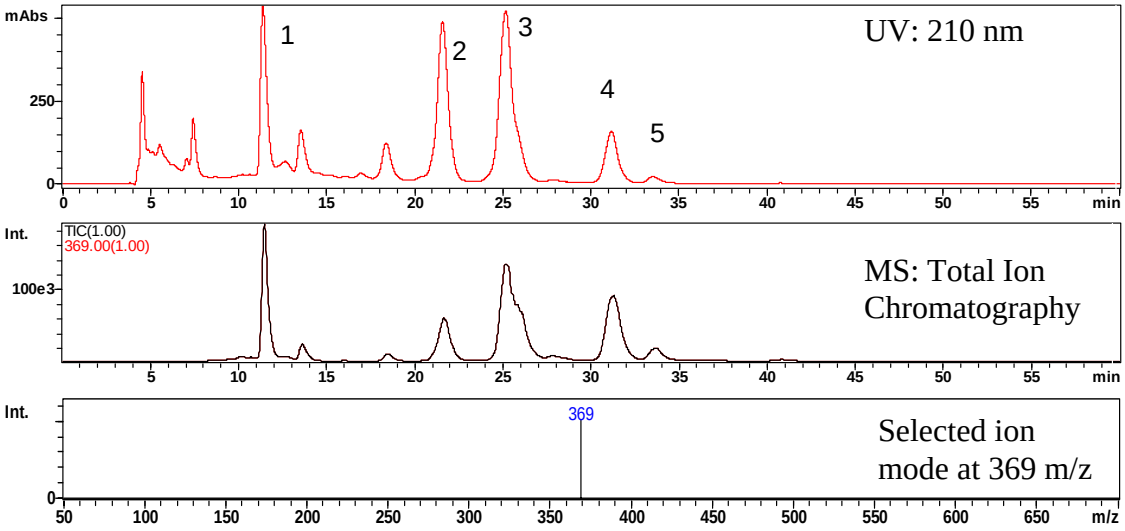

Injection: 10 µL
Peaks: 1. Cholesterol: 2. Linolenate: 3. Linoleate: 4. Oleate: 5. Palmitate

Sample 24 36 year old male aorta extract 175-42

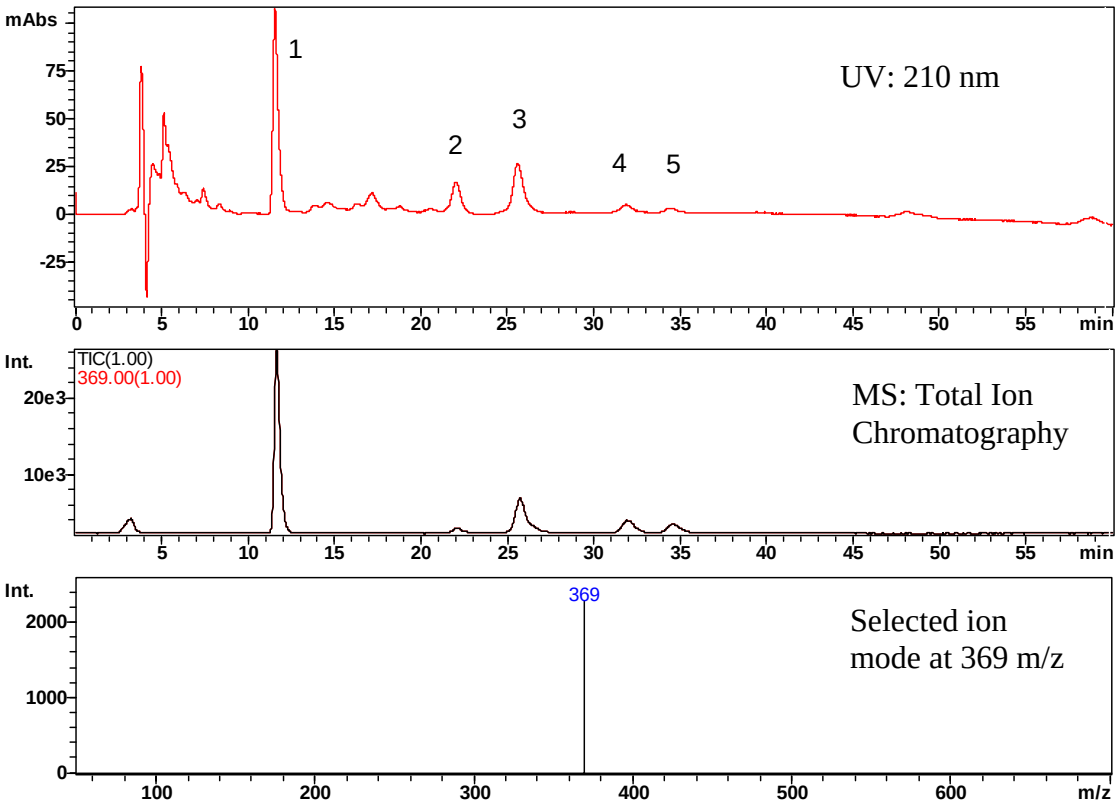

Injection: 10 µL
Peaks: 1. Cholesterol: 2. Linolenate: 3. Linoleate: 4. Oleate: 5. Palmitate

Sample 25 53 year old female aorta extract 175-94

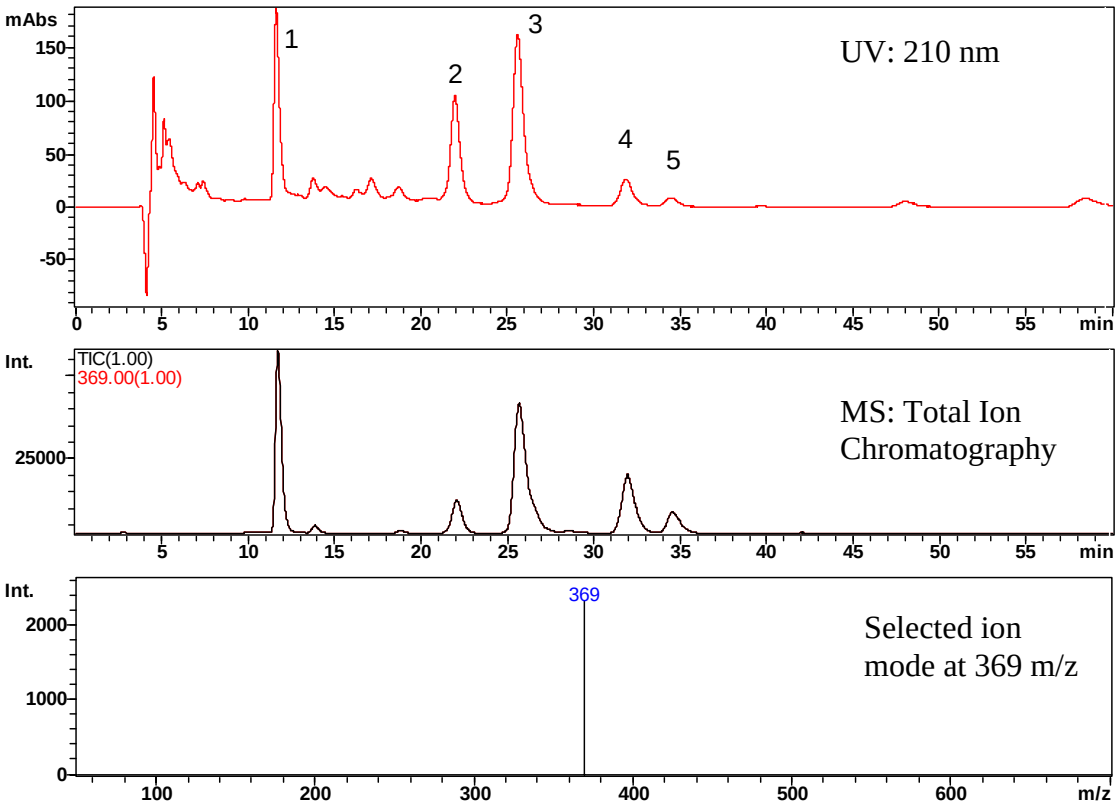

Injection: 10 µL

Peaks: 1. Cholesterol; 2. Linolenate; 3. Linoleate; 4. Oleate; 5. Palmitate

Sample 26 59 year old male aorta extract 175-58

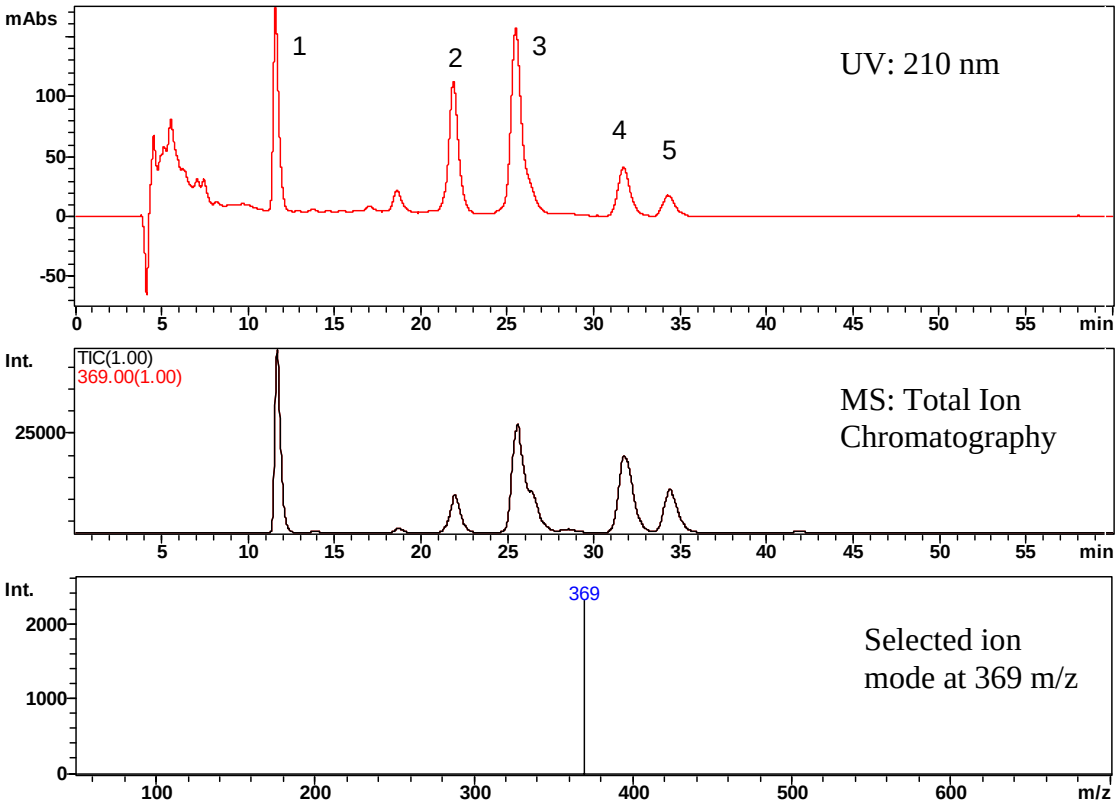

Injection: 10 µL
Peaks: 1. Cholesterol; 2. Linolenate; 3. Linoleate; 4. Oleate; 5. Palmitate

Sample 27 60 year old male aorta extract 175-75

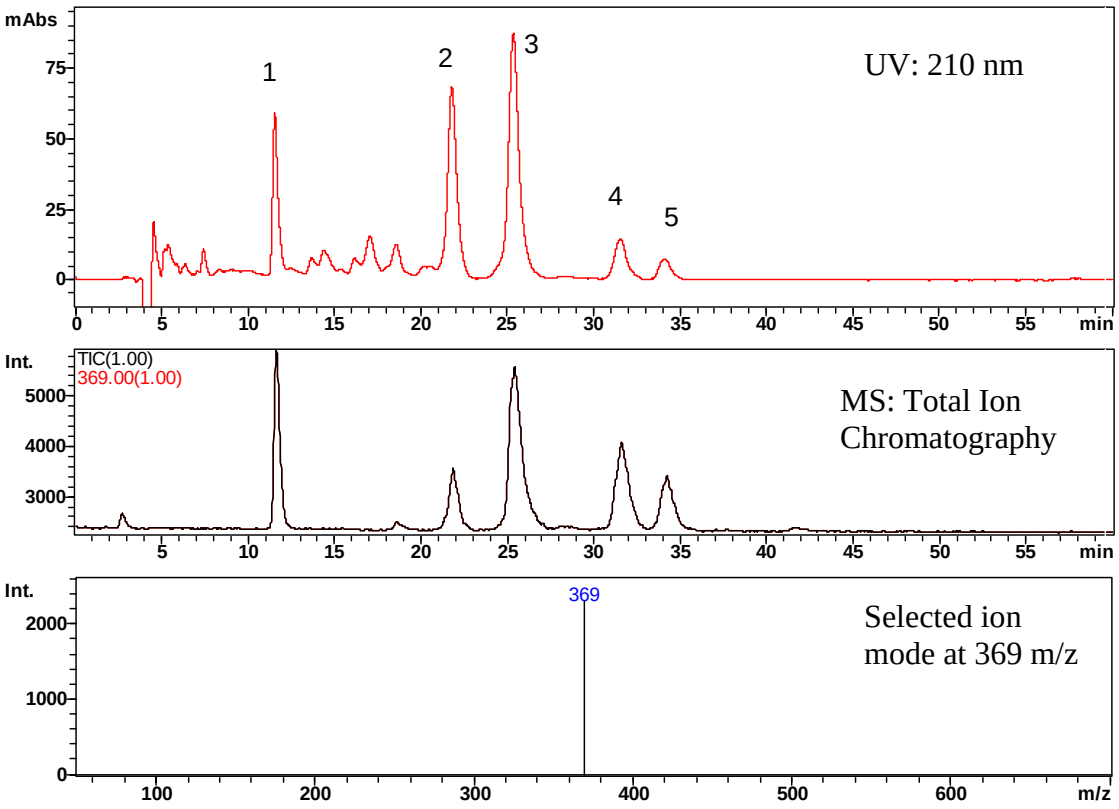

Injection: 10 µL
Peaks: 1. Cholesterol; 2. Linolenate; 3. Linoleate; 4. Oleate; 5. Palmitate

Sample 28 66 year old female aorta extract 175-45

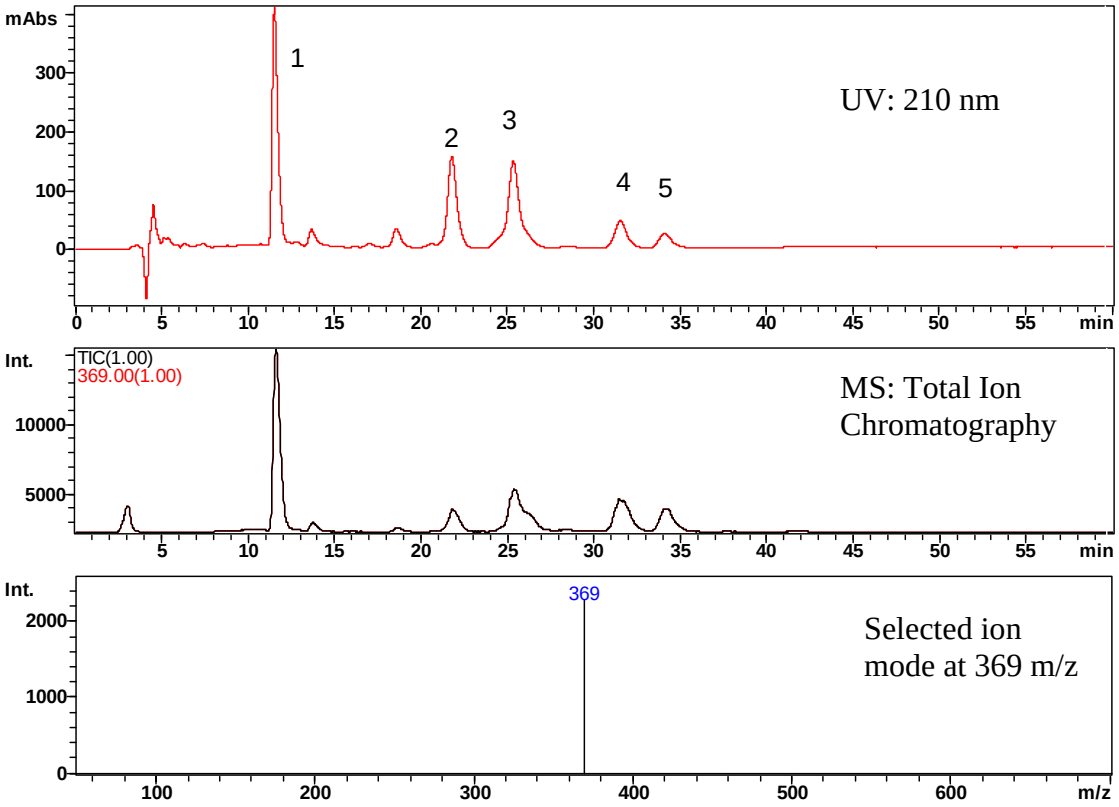

Injection: 10 µL

Peaks: 1. Cholesterol; 2. Linolenate; 3. Linoleate; 4. Oleate; 5. Palmitate

Sample 29 86 year old male aorta extract 175-74

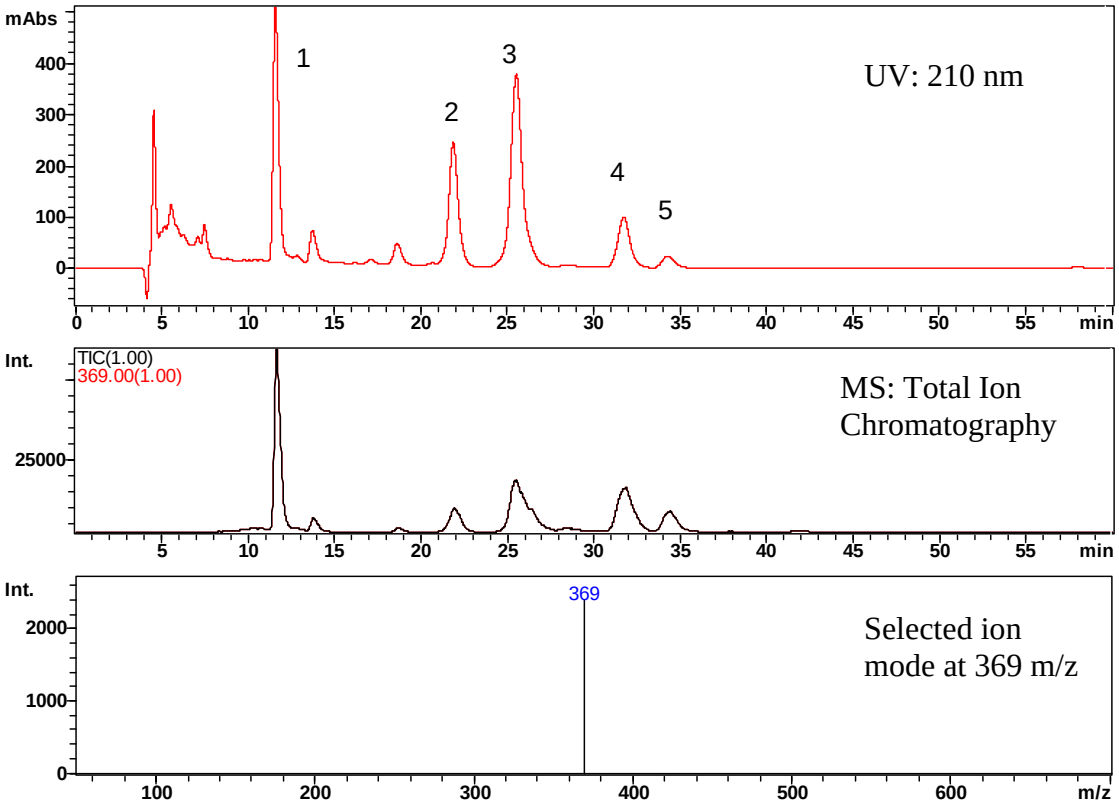

Injection: 10 µL
Peaks: 1. Cholesterol; 2. Linolenate; 3. Linoleate; 4. Oleate; 5. Palmitate

Sample 30 47 year old female aorta extract 175-24

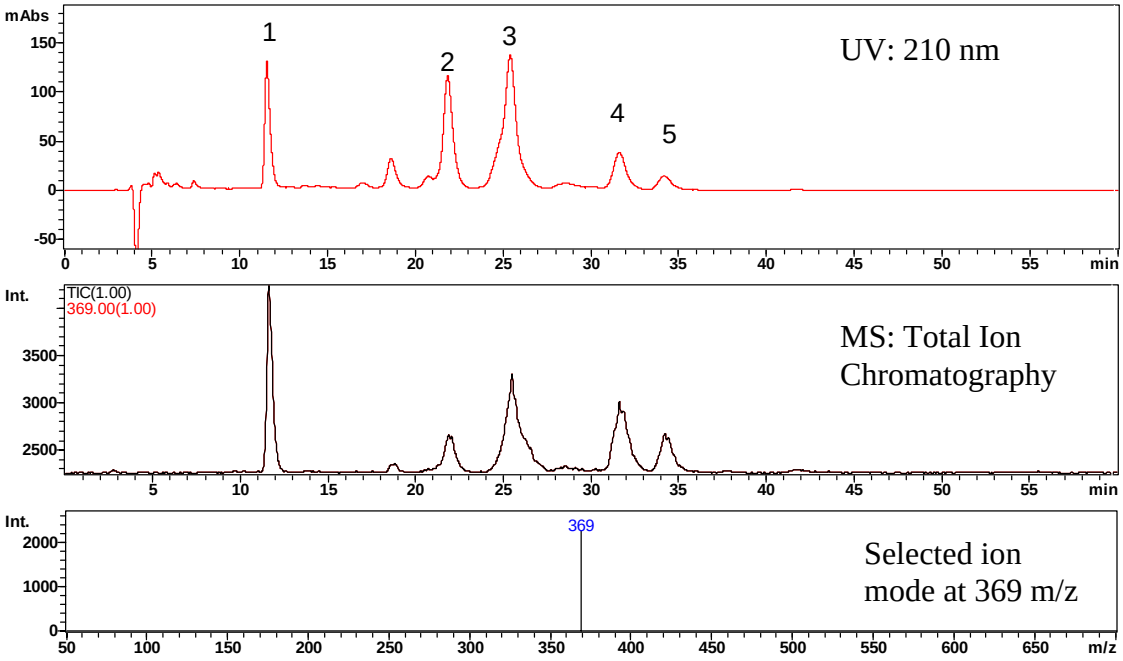

Injection: 10 µL

Peaks: 1. Cholesterol; 2. Linolenate; 3. Linoleate; 4. Oleate; 5. Palmitate

Sample 31 52 year old male aorta extract 175-32

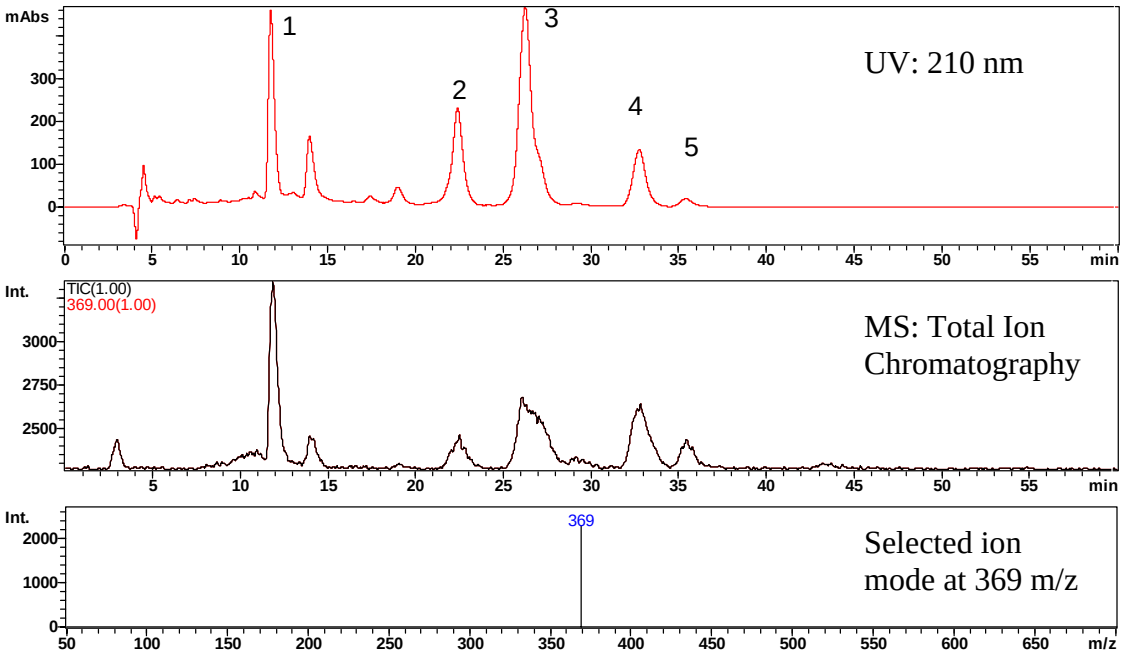

Injection: 10 µL
Peaks: 1. Cholesterol: 2. Linolenate: 3. Linoleate: 4. Oleate: 5. Palmitate

Sample 32 53 year old female aorta extract 175-2

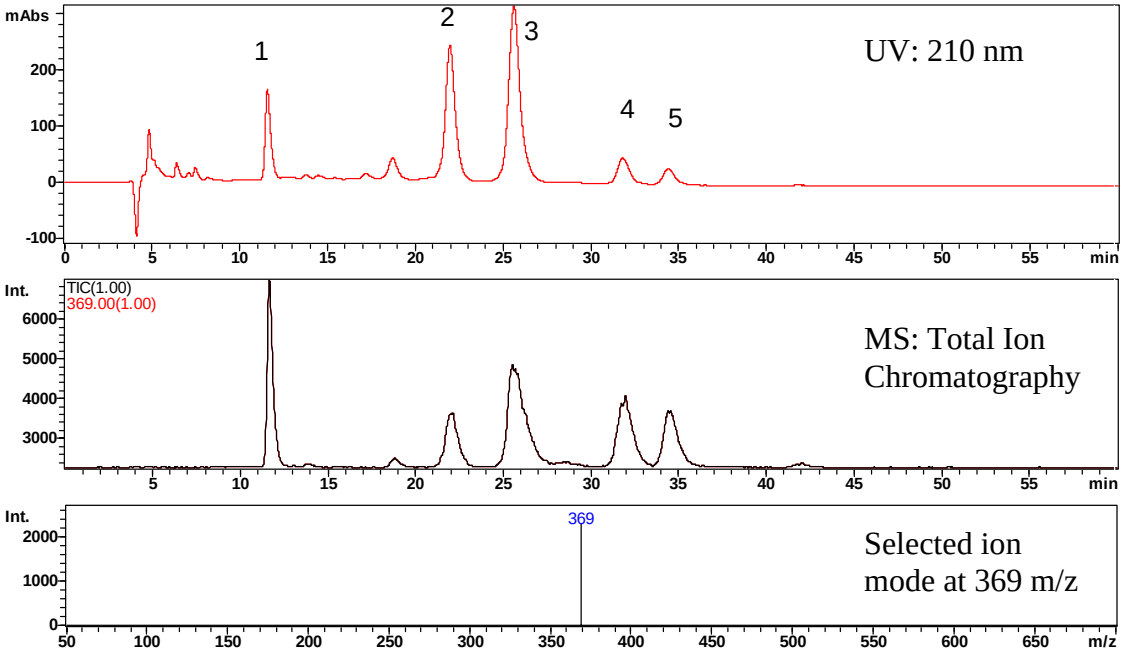

Injection: 10 µL
Peaks: 1. Cholesterol: 2. Linolenate: 3. Linoleate: 4. Oleate: 5. Palmitate

Sample 33 54 year old male aorta extract 175-69

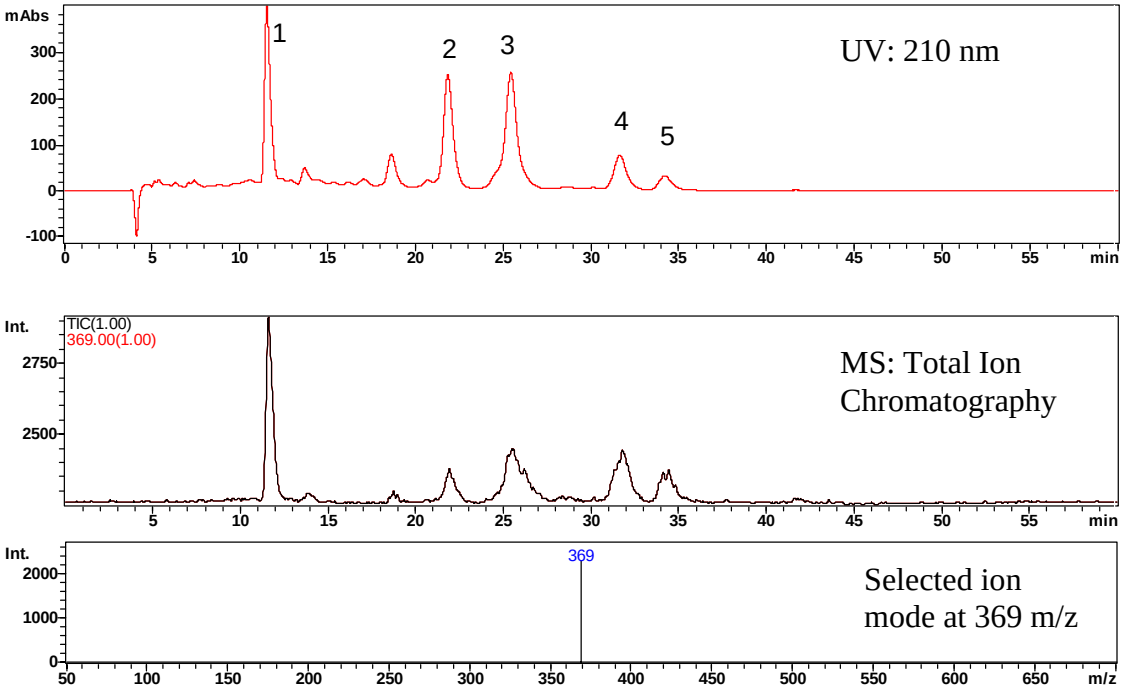

Injection: 10 µL
Peaks: 1. Cholesterol: 2. Linolenate: 3. Linoleate: 4. Oleate: 5. Palmitate

Sample 34 34 year old male aorta extract 175-40

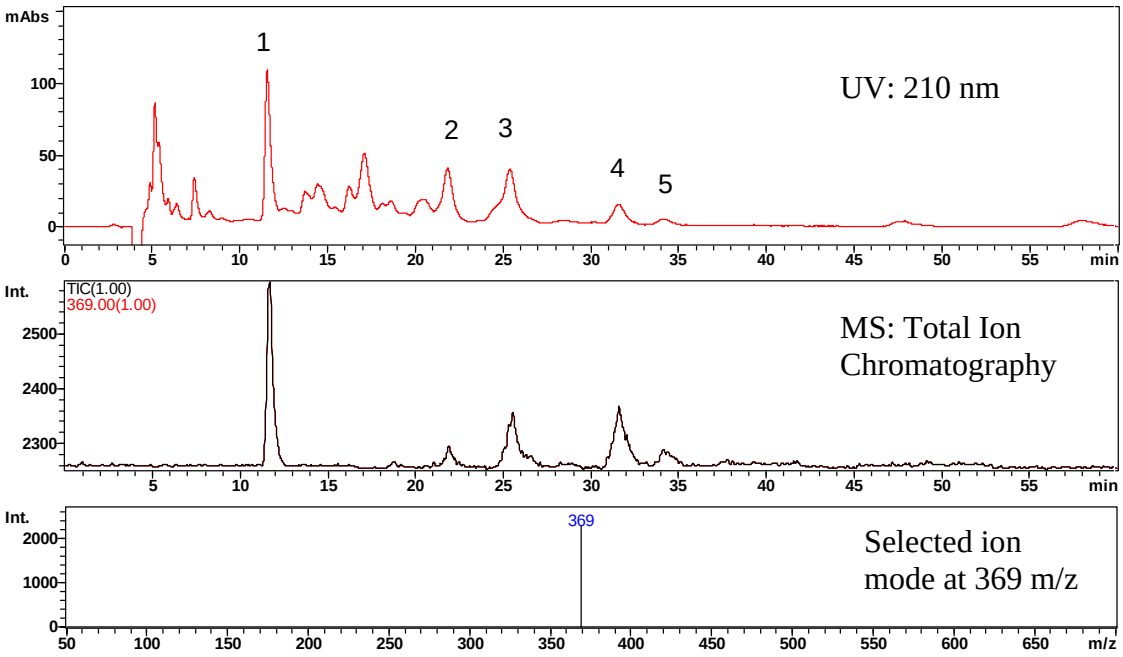

Injection: 10 µL
Peaks: 1. Cholesterol: 2. Linolenate: 3. Linoleate: 4. Oleate: 5. Palmitate

Sample 35 20 year old male aorta extract 175-31

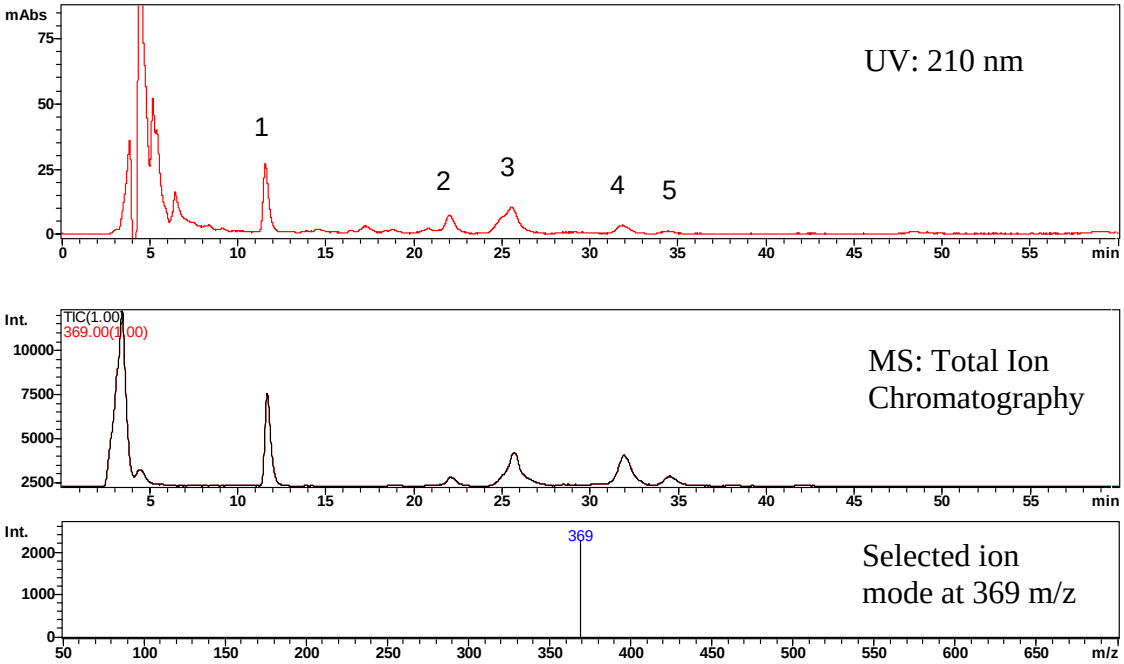

Injection: 20 µL
Peaks: 1. Cholesterol: 2. Linolenate: 3. Linoleate: 4. Oleate: 5. Palmitate

VITA

Samuel Jean Washington was born in Monroe, Louisiana, on April 16, 1952, to J.D. and Ruby Washington. He attended primary school at Franklin High School in Winnsboro, Louisiana. After receiving his high school diploma in 1970, he attended Northeast Louisiana University and graduated with a Bachelor of Science degree in chemistry in 1973. In 1973, he attended the University of Nebraska-Lincoln under the guidance of Professor Desmond Wheeler. He received his Master of Science degree in 1978.

Samuel has been at Southern University since 1996. Samuel initiated the Department of Defense Mentor-Protégé Program and Student Mentor-Protégé at Southern University. His experience with Mentor-Protégé programs at Southern allowed him to provide oversight, coordination, and guidance to task managers and staff support at Southern involved with various projects. Prior to his work at Southern, Samuel was employed for 20 years in the research and development area at Dow Chemical Company in Plaquemine, Louisiana.

In the fall of 1999, Samuel was admitted to Louisiana State University to pursue graduate studies in the Department of Chemistry under the guidance of Professor Isaiah Warner and Professor Patrick Limbach. His dissertation focuses on the separation and identification of proteins associated with the formation of atherosclerotic plaques using two dimensional gel electrophoresis and mass spectrometry.